

UNIVERSITÉ CLERMONT AUVERGNE
ÉCOLE DOCTORALE
SCIENCES POUR L'INGÉNIEUR DE CLERMONT-FERRAND

UNIVERSITÉ DE SOUSSE
ÉCOLE NATIONALE D'INGÉNIEURS DE SOUSSE (ENISO)

THÈSE

Présentée par

NADHIR MANSOUR BEN LAKHAL

Ingénieur en Génie Electronique Industrielle (ENISO)

Mastère Systèmes Intelligents et Communicants (ENISO)

pour obtenir le grade de

Docteur d'Université

Spécialités : **Electronique et Systèmes; Génie Electrique**

Risk Assessment and Management based on Interval Analysis for Safe and Reliable Navigation of Intelligent Vehicles

Soutenue publiquement le 2021 devant le Jury composé de :

JAWHAR GHOMMAM	Rapporteur	Professeur, Université de Carthage
NACIM RAMDANI	Rapporteur	Professeur, Université d'Orléans
LYDIE NOUVELIERE	Examinateuse	Maître de conférences-HDR, Université d'Evry
YOUSSEF MEZOUAR	Examinateur	Professeur, SIGMA Clermont Auvergne
LOUNIS ADOUANE	Directeur de thèse	Professeur, Université de Technologie de Compiègne, Associé à l'Institut Pascal/UCA
JALELEDDINE BEN HADJ SLAMA	Directeur de thèse	Professeur, Université de Sousse
OTHMAN NASRI	Co-encadrant	Maître de conférences, Université de Sousse

ACKNOWLEDGEMENTS

ABSTRACT

Huge advancements have been witnessed recently in the field of Intelligent Transportation Systems (ITSs). In particular, a special focus has been dedicated to ensure the safe and reliable operation of Intelligent Vehicles (IVs). This issue is very challenging due to the considerable environmental uncertainties impacting IVs. Besides, the sophisticated architectures of modern IVs have brought new complications and uncertainty sources, such as failures, communication latencies, etc. This Ph.D thesis aims to provide guaranteed navigation strategies i.e., approaches that consider all potential uncertainty states. To meet this goal, the interval analysis is employed. The principle part of this Ph.D contribution concerns the IV architectures and control aspects. First, a reliable reachability scheme is proposed to present strong safety guarantees for a flexible Navigation Strategy based on Sequential Waypoint Reaching (NSbSWR). The risk management proposed for the NSbSWR reveals the vehicle reachable space, while explicitly considering different uncertainties in modelling and/or perception, etc. The reachability analysis is proceeded via an interval Taylor series expansion method. It uses also the system historical features to improve accuracy of the navigation system reachable space. Once a collision risk is detected, the risk management acts on the control parameters to master the critical situation. Then, this thesis tackles the establishment of risk management solutions for a car-following scenario, which is performed by an Adaptive Cruise Control (ACC) system. Instead of an uncertain probabilistic prediction of threats, the suggested solution has recourse to an interval-based conjoint modeling/data-driven characterization of uncertainties. Hence, a novel extension of the Time-To-Collision (TTC) indicator is introduced to carry out the in-road risk assessment with a comprehensive consideration of uncertainties and material constraints. This extension of TTC is improved later by combining the interval-based computation with a stochastic approach for optimality purposes. The second part of this thesis contributions addresses the tight link between the high-level control aspect and hardware one of IVs. To enhance the risk management robustness to the IV material constraints, relevant techniques to quantify intervals of the inter/intra-vehicular communication latencies are presented. These techniques may avoid any inappropriate and slow reactions of the IV risk management to the in-road threats. Even more, an interval-based extension is proposed for the Principle Component Analysis (PCA) diagnosis method to overcome impacts of failures on IVs. The interval-based PCA is integrated into an ACC architecture to provide a fault-aware risk management level. The sensitivity to faults is increased and the system is monitored in respect to the uncertainty worst cases. The mutuality between the interval-based diagnosis and uncertainty handling approaches enabled to simultaneously detect failures and master all uncertainties. Finally, all the interval-based solutions suggested in this thesis have been validated through extensive simulation work and experiments.

Keywords: Intelligent transportation system, Intelligent vehicle, Risk assessment/management, Interval analysis, Intelligent vehicles, Reachability analysis, System statistical features, Material constraints, Interval-based diagnosis.

RÉSUMÉ

Le domaine de développement des Systèmes de Transport Intelligents (STIs) a été ces dernières décennies une source de multiples évolutions marquantes. En revanche, il est primordial d'améliorer davantage la fiabilité et la sûreté des systèmes autonomes de navigation ainsi que la sécurité routière. Ceci représente un grand défi vu les considérables incertitudes liées à environnement d'évolution des Véhicules Intelligents (VIs). Ces problématiques de fiabilité sont accentuées en raison de la complexité des architectures modernes des VIs. Ainsi, les VIs sont à présent de plus en plus soumis aux défauts, aux latences de communication, etc. Cette thèse de doctorat cherche à présenter des stratégies garanties de navigation (approches qui sont censées tenir compte de toutes les sources d'incertitudes potentielles). Pour ce faire, l'analyse par intervalle est adoptée pour assurer un fonctionnement fiable des VIs. Cette thèse présente deux catégories de contributions. La principale partie des travaux est liée aux architectures de contrôle des VIs. En premier lieu, une méthode d'estimation de l'espace d'atteignabilité des VIs est proposée pour vérifier la sûreté d'une méthode de navigation nommée NSbSWR (pour Navigation Strategy based on Sequential Waypoint Reaching). Le management des risques proposé pour la NSbSWR prédit l'espace atteignable de véhicule en considérant notamment des incertitudes de modélisation ainsi que de perception. L'étude d'atteignabilité est abordée en utilisant les développements de Taylor par intervalles. L'historique de la propagation des incertitudes au sein du système de navigation est exploité afin d'optimiser la précision de l'atteignabilité. Si un danger de collision est détecté en observant l'Espace Atteignable (EA), la méthode proposée agit sur les paramètres de la loi de commande pour éviter les situations critiques. Les travaux de thèse ont portés par la suite sur le développement des solutions du management des risques pour un scenario de suivi des véhicules assuré par un Système de Régulation Adaptative de la Vitesse (SRAV). La solution adoptée rejoint l'arithmétique par intervalles et l'analyse des données. Dans cette optique, une nouvelle extension de l'indicateur de risque TTC (pour Time-To-Collision) est introduite. L'évaluation des risques se manifeste ainsi en considérant plusieurs incertitudes et contraintes matérielles. L'extension ensembliste de la TTC est améliorée ultérieurement en combinant le calcul par intervalles avec une approche stochastique à des fins d'optimisation. Le deuxième volet des contributions de cette thèse vise à renforcer le lien entre l'aspect de commande et l'aspect matériel des VIs. Pour faire face aux contraintes matérielles des STIs, des approches de quantification des intervalles des latences de communication inter/intra-véhiculaire sont proposées. En outre, une extension par intervalles de la méthode de diagnostic par Analyse en Composantes Principales (ACP) est développée pour détecter les défauts affectant un SRAV. La sensibilité aux défauts est améliorée en prenant compte des pires cas d'incertitudes. La mutualité entre les approches de diagnostic et du management des risques permet de détecter simultanément les défauts et d'éliminer les risques liés aux incertitudes. Au final, un travail extensif de simulations et d'expérimentation est abordé pour valider les travaux de cette thèse.

Mots-clés : Systèmes intelligents de transport, Véhicule intelligent, Evaluation/management des risques, Analyse par intervalles, Atteignabilité, Caractéristiques statistiques du système, Contraintes matérielles, Diagnostic par intervalles.

CONTENTS

General introduction	7
I Context and state of the art	11
1 Autonomous navigation: reliability/safety prospects	13
1.1 Intelligent navigation systems evolution	14
1.1.1 IV reactive architecture	14
1.1.2 IV multi-controller behavioral architecture	15
1.1.3 IV increased safety/autonomy distributed architecture	17
1.1.3.1 Modern automotive embedded systems composition	17
1.1.3.2 Driving tasks deployment into automotive NCSs	18
1.1.3.3 Safety enhancements for IV distributed architecture	19
1.1.3.4 Responsibility-sensitive-safety concept example	21
1.2 Modern IV architecture complexity-issued challenges	23
1.3 Uncertainty prediction for autonomous navigation	24
1.3.1 Probabilistic uncertainty handling approaches	25
1.3.2 Non-probabilistic uncertainty handling approaches	28
1.3.3 Reachability Analysis (RA) for long-term horizon prediction	29
1.4 Requirements of modern navigation systems	30
1.4.1 Flexibility	30
1.4.2 Awareness about material constraints	31
1.4.3 Guaranteed uncertainty prediction	31
1.5 Conclusion	32
2 Interval analysis enhancements for IV reliability	33
2.1 Interval arithmetic: Preliminaries	34
2.1.1 Interval arithmetic principle	34
2.1.2 Classical mathematical operators for intervals	35
2.1.3 Interval vectors/matrices	35

2.1.4	Set operations for intervals	35
2.1.5	Inclusion functions	36
2.2	Model-based vs. data-driven approaches for IVs	37
2.2.1	Model-driven approaches for IVs	37
2.2.2	Data-driven approaches for IVs	40
2.3	Interval-based approaches related work	41
2.3.1	Interval-based model processes	42
2.3.2	Interval-based data analysis	44
2.3.3	Discussion	45
2.4	Pessimism impacting interval-based methods	46
2.5	Conclusion	47
II	Safe and reliable navigation	48
3	Reachability analysis for adaptive autonomous navigation based on sequential waypoints	50
3.1	Navigation based on waypoints (general context)	51
3.1.1	Control law	52
3.1.2	Sequential target assignment	54
3.1.3	Safety guarantees for target reaching	56
3.2	Reachable sets computation strategy for NSbSWR	56
3.3	ITbCCRA method for safe waypoint reaching	61
3.3.1	Standard interval Taylor expansion series	62
3.3.2	Correlation-based optimization for interval Taylor method	63
3.3.3	Offline library of the correlation evolution	65
3.3.3.1	Correlation computation for interval-valued variables	66
3.3.3.2	Complexity analysis	69
3.3.4	ITbCCRA simulation-based validation work	70
3.3.4.1	Prediction horizon of the proposed ITbCCRA method	71
3.3.4.2	Consistency of the proposed ITbCCRA method	75
3.4	ITbCCRA-based risk assessment and management	81
3.4.1	Risk management algorithm for NSbSWR	82
3.4.2	Simulation setups and results	84
3.5	Conclusion	91
4	Reliable risk management for safe navigation: Application to an adaptive	

cruise control	92
4.1 Novel TTC over-approximation for a car following scenario	93
4.1.1 Problem statement	93
4.1.2 Set-membership TTC formalization and error quantification strategy	94
4.1.3 Material constraints-issued uncertainties	96
4.1.3.1 Inter-vehicular communication related latency	96
4.1.3.2 Intra-vehicular communication related latency	97
4.1.4 Interval-based/data-driven TTC	98
4.1.5 Interval-based risk management deployment into ACC	100
4.1.6 Simulation setups and results	101
4.2 Enhanced correlation estimation for interval-data	104
4.2.1 Samples update	105
4.2.2 Sample matrix centering	105
4.2.3 Robust evaluation of covariance matrix	106
4.3 Second-order vs. first order interval TTC	108
4.3.1 Second order interval-based TTC formalization	109
4.3.2 Solving quadratic interval polynomial	110
4.3.3 Simulation results and discussion	113
4.4 Combination of interval analysis/stochastic results	114
4.4.1 Main motivations	115
4.4.2 Confidence metrics for merging interval-based and stochastic results	116
4.4.2.1 Cumulative distribution-based confidence assessment . . .	116
4.4.2.2 Redundant modeling-based confidence assessment . . .	117
4.4.3 Interval-based/Stochastic risk management for ACC system . . .	118
4.4.4 Simulation results	120
4.5 Conclusion	122
5 Material constraints-related reliability issues: faults and on-board communication delays	123
5.1 Interval-based diagnosis for reliable IVs	124
5.1.1 Diagnosis-related work	124
5.1.2 Vertices Principle Component Analysis (VPCA) diagnosis	126
5.1.2.1 VPCA implicit model and dimensionality reduction step .	126
5.1.2.2 VPCA statistical/threshold-based fault detection step . .	128
5.1.2.3 VPCA fault isolation step	129

5.1.3	VPCA-based diagnosis integration into Adaptive Cruise Control (ACC) architecture	130
5.1.4	Diagnosis results	131
5.2	RTA for intra-vehicular latency characterization	133
5.2.1	RTA principle and related work	133
5.2.2	RTA model for interval time of CAN responses	134
5.2.3	Proof of concept: application on Smart Distance Keeping (SDK) system	138
5.2.4	Experimental conditions and emulation environment	142
5.3	Conclusion	145
General conclusion and future work		146
III	Annexes	150
A	Stability proof of control law for static/dynamic target reaching	152
B	Analytical guarantees for safe target reaching	156
Bibliography		159

LIST OF FIGURES

1	Manuscript outline.	10
1.1	Commercialized/under-test intelligent navigation systems.	13
1.2	Examples of intelligent vehicles' incidents in public roads.	14
1.3	Reactive architecture-based navigation systems.	15
1.4	Multi-controller architecture implemented on VIPLAB vehicles for collaborative navigation [301].	16
1.5	Typical architecture of automotive NCS.	18
1.6	Decentralized diagnosis architecture.	21
1.7	Distributed diagnosis architecture.	21
1.8	Critical navigation scenarios treated by RSS model for safety guarantees. .	22
1.9	Evolution of autonomous navigation systems architectures and capacities. .	22
1.10	Requirements to reach full autonomy, reliability and safety of modern IVs (scheme inspired from [19]).	32
2.1	Examples of inclusion functions.	36
2.2	Main components of reliable modeling for IVs.	39
2.3	Interval process model.	42
2.4	Pessimism related to the wrapping effect.	47
3.1	NSbSWR framework architecture.	52
3.2	Vehicle/target configurations and control variables.	54
3.3	Description of NSbSWR target assignment strategy [297].	55
3.4	Geometrical representation of reachable sets in the space domain.	60
3.5	Reachable space bounding through convex hull enclosure.	61
3.6	Flow chart of the proposed RA process for reaching a given waypoint. . .	62
3.7	Vertices technique in dimensions 2 and 3 for number of observations $N = 1$. .	67
3.8	Reachability computation via ITbCCRA for NSbSWR.	69
3.9	Prediction horizon characterization of ITbCCRA method.	72
3.10	Reachable space behavior according to e_{θ_0}	72
3.11	$d_{ITbCCRA}$ calculation.	73

3.12 Horizon prediction relatively to uncertainty in position and e_{θ_0}	74
3.13 Horizon prediction relatively to uncertainty in θ_V and e_{θ_0}	75
3.14 Batch simulation principle.	76
3.15 First scenario batch simulation results representation in 2D space.	77
3.16 Evolution of x_V compared to bounds of the reachable space with/without narrowing (scenario 1).	77
3.17 Evolution of y_V compared to bounds of the reachable space with/without narrowing with/without narrowing (scenario 1).	78
3.18 Evolution of θ_V compared to bounds of reachable space with/without narrowing (scenario 1).	78
3.19 Second scenario batch simulation results representation in 2D space.	79
3.20 Evolution of x_V compared to bounds of the reachable space with/without narrowing (scenario 2).	80
3.21 Evolution of y_V compared to bounds of the reachable space with/without narrowing (scenario 2).	80
3.22 Evolution of θ_V compared to bounds of reachable space with/without narrowing (scenario 2).	81
3.23 ITbCCRA-based risk management principle.	81
3.24 Orientation of the bounded reachable space.	82
3.25 θ_R estimation method.	83
3.26 Simulation test-scene.	85
3.27 NSbSWR simulation results within nominal control parameters.	87
3.28 Lyapunov function evolution based on proposed control law for NSbSWR. .	87
3.29 Evolution of distance/angular errors.	88
3.30 NSbSWR simulation results within ITbCCRA-based risk management.	89
3.31 Lyapunov function evolution after acting on control parameters.	89
3.32 Evolution of distance/angular errors with adapted control parameters.	90
4.1 Car-following via interval-based ACC system.	94
4.2 Uncertainty assessment strategy for interval-based TTC.	98
4.3 Architecture of proposed interval analysis-based ACC.	101
4.4 Interval-based/data-driven TTC enclosures.	103
4.5 Interval-based TTC results with high uncertainty injection.	104
4.6 Correlation assessment for interval variables $[V_i]$ and $[V_j]$	108
4.7 Examples of quadratic interval polynomials.	111
4.8 $[TTC_{O1}]$ and $[TTC_{O2}]$ evolution before/after narrowing.	113
4.9 TTC_{O1} and TTC_{O2} enclosures compared with exact results.	114

4.10 Reliability check for EKF modeling performances.	117
4.11 Suggested ACC principle.	119
4.12 Flowchart of target set-point generation strategy.	119
4.13 Set-membership/stochastic ACC architecture.	120
4.14 d_{ref} evolution.	120
4.15 d_{ref} evolution for EKF correct behavior.	121
4.16 d_{ref} evolution for EKF imperfect behavior.	121
5.1 VPCA-based run-time fault detection principle.	129
5.2 Interval-based ACC fault aware control architecture.	130
5.3 Number of principle components-based on VRE method.	131
5.4 SPE index-based fault detection.	132
5.5 Fault localisation.	132
5.6 Node modeling for RTA purposes.	135
5.7 Data flows modeling.	136
5.8 SDK capacities in truck drivers assistance.	139
5.9 SDK data flows.	141
5.10 HIL platform for realistic experimentations.	143
6.1 Overall view of interval-based reasoning for risk assessment and management of multi-control architecture.	149
A.1 Vehicle/target parameters used for control law proof of stability.	153
B.1 Analytical method for safe reaching of waypoints [297].	158

LIST OF TABLES

1.1	Different categories of ADASs	19
1.2	Comparison between uncertainty prediction approaches for IVs	30
2.1	Classical mathematical operators for interval data	35
2.2	Classical set operations for intervals	36
3.1	First scenario of batch simulation setups for Gaussian uncertainty injection	76
3.2	Second scenario of batch simulation setups for Gaussian uncertainty injection	79
3.3	Waypoints configurations	85
3.4	Interval-type uncertainty injection setups	86
3.5	Simulation setups of Gaussian uncertainty injection	86
3.6	Risk management modifications in control parameters	89
4.1	DSRC delays within different speeds	97
4.2	DSRC delays within distinct number of vicinity vehicles	97
4.3	Simulation setups	102
4.4	Error impacting d_{ref}	104
4.5	$P([x])$ interval roots relatively to n	112
4.6	Error impacting d_{ref}	122
5.1	PCA-based fault detection step: indexes/thresholds	128
5.2	Minimum and maximum response times of elements in flow φ_1	144
5.3	Minimum and maximum response times of elements in flow φ_2	144
5.4	Minimum and maximum response times of elements in flow φ_3	144
5.5	Experimental results	144

GLOSSARY

- **ABS:** Anti-lock Braking System.
- **ACC:** Adaptive Cruise Control.
- **ADAS:** Advanced Drive Assistance System.
- **ASFA:** Association des sociétés françaises d'autoroutes.
- **CAN:** Controller Area Network.
- **CDF:** Cumulative Distribution Function.
- **CPS:** Cyber Physical System.
- **DI:** Differential Inequalities.
- **DSRC:** Dedicated Short Range Communications.
- **ECU:** Electronic Control Unit.
- **EKF:** Extended Kalman Filter.
- **EMI:** Electromagnetic Interference.
- **HIL:** Hardware-In-the-Loop.
- **HMI:** Human Machine Interface.
- **ICA:** Independent Component Analysis.
- **ITbCCRA:** Interval Taylor-based Correlation Constrained Reachability Analysis.
- **IV:** Intelligent Vehicle.
- **LD:** Lower Distance.
- **LIN:** Local Interconnect Network.
- **MRT:** Mean Response Time.
- **NCS:** Networked Control System.
- **NSbSWR:** Navigation Strategy based on Sequential Waypoint Reaching.
- **ODE:** Ordinary Differential Equation.

- **PAVIN:** Plate-forme d'Auvergne pour Véhicules INtelligents.
- **PCA:** Principle Component Analysis.
- **PDF:** Probability Distribution Function.
- **RA:** Reachability Analysis.
- **RSS:** Responsibility Sensitive Safety.
- **RTA:** Response Time Analysis.
- **SCM:** Sample Covariance Matrix.
- **SDK:** Smart Distance Keeping.
- **SEA:** Society for Automobile Engineers.
- **SPE:** Squared Prediction Error.
- **TTC:** Time-To-Collision.
- **USART:** Univer-sal Synchronous/Asynchronous Receiver/Transmitter.
- **V2I:** Vehicle-to-Infrastructure.
- **V2P:** Vehicle-to-Pedestrian.
- **V2V:** Vehicle-to-Vehicle.
- **VIPALAB:** Véhicule Individuel Public et Autonome.
- **VPCA:** Vertices Principle Component Analysis.
- **VT:** Vertices Transformation.
- **WCRT:** Worst Case Response Time.

GENERAL INTRODUCTION

“Uncertainty is the only certainty there is, and knowing how to live with insecurity is the only security.”

John Allen Paulos (born July 4, 1945)
An american renowned mathematician

Thanks to applied science, new horizons have been created in terms of technical maturity and powerful supplied services of autonomous systems. Nowadays, autonomous/semi-autonomous systems are omnipresent in human life in various areas. Yet, several overlapping aspects related to the autonomous systems are still under investigation. Hence, recent advances in decision support development, control theories and modeling/design trend of autonomous systems were reviewed in [207].

In particular, the development of Intelligent Navigation Systems (IVs) is attracting a great deal of attention lately. There can be no denying that autonomous vehicles are the future of mobility. Since the increased autonomy puts forth the safety requirement, IVs are expected to drastically decrease the number of occurring accidents in public roads. With this respect, various metrics have been defined in the literature to assess and describe navigation systems abilities in acting without any human intervention. The three-level-scaled autonomy measure, prescribed in [296], is among these proposals. However, the different degrees of autonomy, which are introduced by the international Society for Automobile Engineers (SEA), represent probably the most common and relevant taxonomy for IVs [286]. Roughly, all the existing taxonomies agree that the autonomy levels vary from a reduced or partial automation to a complete autonomous responsiveness to the environmental changes and to the requested task to achieve.

In a narrower sense, the autonomous navigation should be conducted through sound and reliable approaches to be trusted by the community and to lead finally to as safest IVs as possible. According to [194], the autonomy construction, especially for IVs, may be conducted through distinct manners. For instance, the rule-based autonomy can be built via empirically-induced policies or the system designer preferences. In the case of the model-based autonomy construction, the system autonomy-level is reinforced thanks to mathematical-driven decision analysis schema. Through the utility-based autonomy, autonomous decisions are made depending only on the system actual goals. Differently, the learning-based autonomy relies on a continuous optimization of the system supplied functionalities by examining its performance patterns. Finally, another way to increase the autonomy of IVs is while using a context-based paradigm, where several improvised process re-configurations are achieved according to the system run-time temporal and operational context.

Thanks to the acquired autonomy, IVs are expected to afford a risk free navigation. They also should optimize as much as possible the mission elementary tasks. Unless the autonomous navigation is undertaken in a static and known environment, the safety and

optimality requirements (in terms of several criteria such as traveled distance, navigation smoothness, etc.) cannot be warranted without mission planning and risk management units. Consequently, the aforementioned autonomy construction methods for IVs should be enhanced with a hierarchical layer to provide a simultaneous increased autonomy and safety. This layer main role is to manage the situational responsiveness to hazards and more importantly to ensure verifiable self-aware navigation decisions.

On the one hand, it is important to pick up a range of navigation techniques with feasible and resilient verification capacities. For instance, it is quite complicated to use probabilistic approaches for safety verification purposes. Checking all the potential probable future behaviors for vehicles appears as costly and unfeasible [6], [27]. On the other hand, the risk management and safety verification must imperatively be effective in coping with unforeseen disturbances and uncertainties. Due to the lack in the anticipatory capabilities about the uncertainty evolution that may impact the IV in short and/or long time horizon, it is highly challenging to make relevant decisions. To face such a problem, the Intelligent Transportation System (ITS) community has recourse currently to the human-in-the-loop concept i.e., relying on a human driver back-up and interventions. Despite its efficiency in risks/uncertainty management, the employment of the human-in-the-loop concept is completely a different vision to deal with IVs, and is in certain way another point of view which does not target fully autonomous vehicles. Such a direction may be the main reason that only vehicles of level-two of autonomy (according to the SAE standard) are up to now promoted in the market [286].

As clear, dealing with uncertainties¹ and handling complex driving situations in unknown navigation environments are the principle barriers for a wider use of IVs with higher autonomy in roads. Conventionally, succeeding a decision making layout is tightly linked to the accuracy and consistency of the knowledge about the current situation. The less accurate and precise was the management of the situation, the less likely an IV is able to make relevant decisions. Nevertheless, one of the greatest challenges about IVs is how to verify whether the instantaneous knowledge about the system is enough certain to guarantee the operational safety. Indeed, many fundamental questions should find answers in this context. What would happen if the required level of certainty could never be reached? Mitigating uncertainties might be not trivial due to the strong environment variability. How to construct then a navigation strategy that even without enough accurate knowledge may be effective? How to turn objectively uncertain information to knowledge, and knowledge to wise decisions?

PH.D THESIS CONTEXT AND GOALS

This Ph.D thesis is a joint program between the “Institut Pascal-Clermont Auvergne University” from France and “LATIS Laboratory-University of Sousse” from Tunisia. From one side, such a collaboration permits to exploit the LATIS laboratory knowhow in terms of formal verification techniques for complex systems. It tends also to take advantage of the large expertise of the Institut Pascal in autonomous vehicles field, notably in terms of control architectures, risk assessment/management, and innovative techniques for autonomous navigation. In this context, the present Ph.D addresses the reliability and safety of intelligent navigation systems. As already discussed, uncertainty is the most influenc-

¹Uncertainties issued from: measurements, anticipatory capabilities, decision making models, etc.

ing factor that rules the reliability/safety concerns related to the autonomous navigation systems. Thus, this work intends to analyze elements that may reduce the reliability of uncertainty characterization and handling. Within this scope, this thesis has as objective to develop a range of navigation solutions, where all the uncertainty sources are well-encountered to guarantee a safe and reliable functioning of IVs. Not only the different uncertainties should be handled through the approaches introduced all along this thesis contributions, but also an optimal behavior of autonomous navigation should be assured. At the end, this thesis looks forward constructing novel IV architecture that includes safety verification layers of guaranteed performances and great capacities to overstep any potential risk.

MANUSCRIPT OUTLINE

The first part of this manuscript is devoted to analyze the state-of-the-art as well as the state-of-the-practice, which are related to the IV reliability and the in-road safety. This is essential to explain the choice of the navigation approaches developed in this thesis.

- **Chapter 1 - Autonomous navigation: Reliability/Safety prospects**

In an effort to more clarify this thesis general context, this chapter highlights the urgent need to enhance performances of modern navigation systems, especially from reliability/safety perspectives. More precisely, it aims to reveal the new reliability requirements of autonomous vehicles through a broad analysis of the state-of-the-art. A comprehensive overview and comparative studies between the existing methodologies, used to ensure a safe autonomous navigation, are depicted.

- **Chapter 2 - Interval analysis enhancements for IV reliability**

The literature review has put the stress on advantages of the set-membership approaches in handling uncertainties that may propagate through the navigation process. Accordingly, this chapter aims to justify the deep interest of the interval analysis to deal with different uncertainty-issued in-road risks. Thus, more details about the interval arithmetic pros and cons are delivered. For a better use of the interval analysis in the benefit of IVs, the different interval-based methodologies applied to enhance systems' reliability and accuracy are overseen.

Based on findings of the state-of-the-art analysis, several interval-based contributions, in the context of ensuring a safe autonomous navigation, are presented in this Ph.D. These latter can be classified into two key categories. The first one is linked to the autonomous navigation architectures and control issues in regard to safety assurance. As this thesis principle scope, the IV control-related contributions are presented as follows:

- **Chapter 3 - Reachability analysis for adaptive autonomous navigation based on sequential waypoints**

The goal of this chapter is to provide highly flexible and safe navigation approach. In this context, interest is given to a sequential waypoint-based navigation strategy. Thus, a relevant risk assessment technique for this navigation strategy is inspected via an interval-based reachability analysis scheme. In brief, this chapter tends to draw a reliable methodology allowing: (i) to derive confidante and sharp reachable space for IVs, and (ii) to establish a back-up strategy by acting on the control parameters to avoid hazards once a probable collision is detected at an early phase.

- **Chapter 4 - Reliable risk management for safe navigation: Application to an adaptive cruise control**

This chapter deals with issues related to performances of intelligent vehicles during a car-following scenario. In particular, an interval analysis-based risk assessment and management strategies that fit well this driving maneuver is developed. Afterwards, several enhancements are integrated into the introduced risk management in order to compromise between this approach performances in terms of accuracy, simplicity, computational demands and behavioural optimality. This chapter also depicts a proof of concept of the suggested risk management through simulations undertaken on an Adaptive Cruise Control (ACC) system.

In a second place, the IV reliability is not attainable without addressing the material constraint issues. Accordingly, this thesis contributions count even on enhancing the link between the Software aspect and Hardware one of IVs. This direction aims to finally provide material constraint aware-risk management techniques for IVs.

- **Chapter 5 - Material constraints-related reliability issues: Faults and onboard communication delays**

This chapter is dedicated to propose efficient solutions for sever material constraints that may invoke risks issued from the in-vehicular composition of navigation systems. Mainly, the addressed constraints are system failures and in-vehicular communication delays. The introduced solutions have actually great compatibility with the interval-based navigation frameworks that were proposed in previous chapters.

The manuscript is ended with a general conclusion recapitulating this thesis contributions and perspectives. For more details, Figure 1 illustrates the whole manuscript outline.

Part I: state-of-the-art analysis

Chapter 1

- Evolution of IVs
- New requirements of modern IVs
 - Flexibility
 - Guaranteed uncertainty prediction
 - Awareness about material constraints: faults and latencies

Chapter 2

- Generalities about interval analysis
- Interval analysis enhancements
 - Interval-based modeling
 - Interval-based data analysis
- Interval analysis pessimism

Part II: contributions

Chapter 5

- Interval-based diagnosis
 - System characterization
 - Fault detection
 - Fault isolation
- Uncertainty/fault-aware IV
- In-vehicular delay-aware IV

Chapter 4

- Interval-based risk evaluation
- Analysis of interval modeling performances
- Robust interval statics for risk assessment
- Combined stochastic/interval based risk management

Chapter 3

- Waypoint-based navigation
- Interval-based reachability
 - Interval Taylor expansion
 - Correlation constrained reachability
- Risk management via interval-based reachability

Figure 1: Manuscript outline.



CONTEXT AND STATE OF THE ART

AUTONOMOUS NAVIGATION: RELIABILITY/SAFETY PROSPECTS

This chapter presents a comprehensive coverage of the state-of-the-art/state-of-the-practice related to the mobile autonomous navigation systems. A special focus is given to investigate the reliability and safety considerations related to today's Intelligent Vehicles (IVs). Based on the reviewed literature, requirements of modern navigation systems are highlighted and components that stand behind the safe and reliable navigation are analyzed.

Over time, huge efforts have been spent by the IV community to increase transportation systems autonomy [65]. Nowadays, several modern vehicles with great autonomy capacities are put in practice thanks to the academical and industrial tight collaboration. Hence, a new wave of autonomous vehicles are currently tested or commercialized for use in highway-roads or for urban public transportation (cf. Figure 1.1) [217]. The ultimate purpose behind the public use of autonomous vehicles is to provide safer roadways via efficient crash avoidance processes. Besides, it reduces the need for human driving tasks and improves passengers comfort and safety. IVs contribute also in enhancing mobility by increasing navigation systems efficiency. Accordingly, many beneficial environmental impacts, such as managing traffic flows and avoiding congestion, can be easily met.

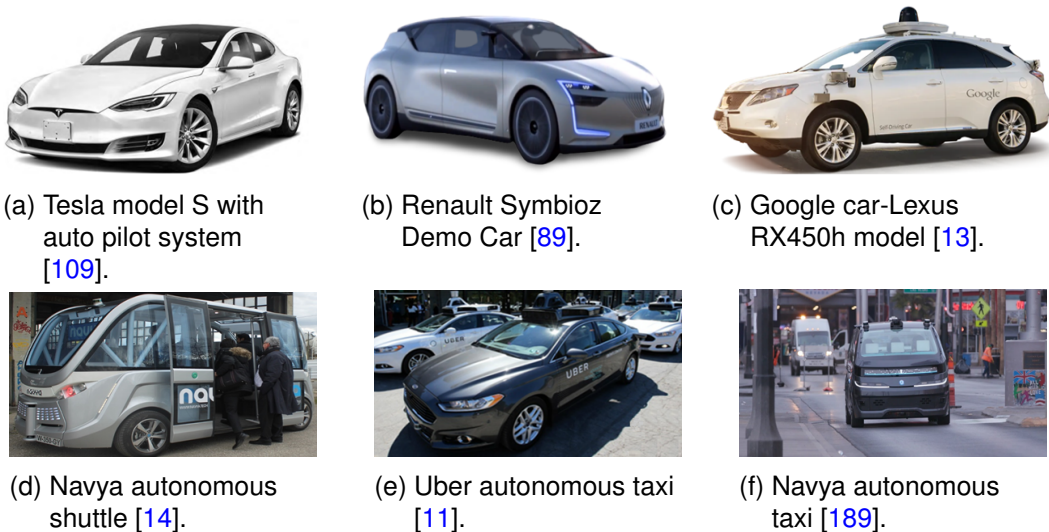


Figure 1.1: Commercialized/under-test intelligent navigation systems.



(a) Tesla model X crash, California, March 2018 [12].



(b) Navya shuttle crash, Las Vegas, November 2017 [173].

Figure 1.2: Examples of intelligent vehicles' incidents in public roads.

Although the new generation of IVs are equipped with the most advanced automotive technologies, their reliability is for yet controversial. It is worth mentioning that the reliability in the autonomous navigation context means the capacity to proceed the navigation tasks as expected while guaranteeing the in-road safety [19]. Intuitively, the strong relation between the IVs reliability and the in-road safety is evident. As shown in Figure 1.2, numerous incidents have been witnessed in public roads due to technical failures or wrong decisions made by IVs. Certainly, these crashes invoked a deep impact on the society and raised trust gaps on self-driving vehicles [82], [270]. As a consequence, the IVs reliability issues and the in-road risk management have become research fields of utmost importance.

In order to reveal the IVs-related reliability/safety issues, the evolution of the autonomous navigation systems over time is detailed in the following. It permits to figure out and establish the link between the complexity aspects characterizing today's modern transportation systems and the reliability challenges.

1.1/ INTELLIGENT NAVIGATION SYSTEMS EVOLUTION

Due to the increasing interest in improving mobility, the IV structure has known a rapid evolution during the last few decades. In this thesis, it is assumed that the evolution of the IV architectures can be summarized in three main hierarchical structures. Specifications of these latter ones are briefly discussed in the sequel. More specifically, changes implied by these architectures on the reliability/safety notions are pinpointed.

1.1.1/ IV REACTIVE ARCHITECTURE

Since 1949, the concept of intelligent navigation system has emerged with the development of first autonomous robots [36]. After acquiring data from the environment by a set of simple sensing tools, the autonomous robot motions were managed by means of an on-board control unit [43]. Decisions made by this latter serve to govern the system operative part, including actuators and the robot mechanical composition. Accordingly, this simple architecture of first autonomous navigation systems was characterized by a very limited computational performances enabling basic tasks such as indoor navigation. Due to their undeveloped sensing, planning and computational capacities, these processes could not handle huge amounts of data that may provide a prior knowledge of the navi-

gation environment. Hence, this category of IVs can be classified as reactive, since they exploit the locally issued sensorial data to react to the environment stimulus [17].

Clearly, the reactive architectures are dedicated only to ensure slow motion navigation in static environments. In addition, the unicycle robot kinematic model has been often adapted for the reactive architecture-based navigation. This model simple kinematic properties were relevant to fit control units with limited computational capacities [281].

The first concern of the research community to improve the reactive navigation architecture was to integrate more and more advanced sensors into the robot composition. Improving the robot sensing level aimed to provide more efficient cognitive navigation [31]. More cognitive knowledge was mandatory, since robots abilities in reacting to changes in the navigation environment were poor. Otherwise, another part from the robotic community focused in enhancing the kinematic/dynamic modeling for mobile robots and introducing appropriate control strategies [108]. The stability of the suggested control could be demonstrated through a Lyapunov function-based analysis [40].

For the reactive architecture, the navigation safety was totally related to obstacle avoidance via the robot low sensing abilities. As already stated, IVs with reactive architectures were dedicated to navigate static and uncrowded environments. Correspondingly, the reliability concerns for this architecture were rarely studied. There were no strict reliability constraints to be considered in practice.



(a) G. Walter turtle-like robot [43]. (b) Shakey robot [274]. (c) Hilare robot [170].

Figure 1.3: Reactive architecture-based navigation systems.

1.1.2/ IV MULTI-CONTROLLER BEHAVIORAL ARCHITECTURE

With time, the technological progress has evolved the concept of navigation systems from robots to car-like vehicles. The first test of a driver-less car in empty highways was realized in 1987 [38]. Since that date, many similar pioneer projects have been tackled. In this context, a comprehensive overview about first attempts to develop autonomous cars can be found in [19]. Step by step, advances in the Hardware and Software co-design has permitted the deployment of more and more functionalities into one navigation architecture [152]. As a matter of fact, the early discussed reactive architecture cannot support the expanding complexity of these tasks. As an alternative, the algorithm of every navigation task was implemented on a single controller to overcome the complexity issue. This direction helped to turns the navigation architecture to a behavioral one, where a hierarchical coordination between several tasks takes place [21]. Indeed, the ability of accomplishing more complicated behaviors, such as avoiding static/dynamic obstacles, following a leader vehicle, etc., enhanced the navigation systems chances to be safer.

Thus, autonomous vehicles were able to navigate in more challenging environments. The radical architectural improvements practiced on the autonomous vehicles brought many advantageous reflections on the IV-related research work, which are as follows:

- As already stated, the multi-behavioral hierarchy permitted to apply more computationally demanding navigation algorithms. Therefore, tremendous efforts to improve the early existing navigation methods or even to introduce novel techniques have been noticed in the literature. These methods have been used towards target reaching from a specific trajectory/path. Aside from the path planning task, they should prohibit collision with stationary or dynamic objects. According to the navigation conditions and the vehicle capabilities (kinematic and dynamical properties), the navigation algorithms have as a fundamental mission to generate/regenerate feasible collision-free trajectory. On the one hand, the potential fields, Voronoï diagrams, visibility graphs and rapidly-exploring random tree are among the most whispered approaches in the literature [20], [231]. On the other hand, the new mapping technologies have contributed in the appearance of several road-map heuristics search algorithms and cell decomposition-based navigation strategies [306], [348].
- Furthermore, the navigation of a unique vehicle has been extended to multi-agent navigation systems thanks to the multitude of permitted behaviors by IVs. As a result, the collaborative navigation, platoon formation/optimized control and intersection management have become among the most interesting navigation scenarios, which are studied in the literature [158, 192, 223, 299].



(a) Convoy of VIPLAB vehicles.



(b) Group formation of VIPLAB vehicles.

Figure 1.4: Multi-controller architecture implemented on VIPLAB vehicles for collaborative navigation [301].

- The multi-controller behavioral architecture has definitely contributed in providing more mature navigation systems. At this stage, several optimality metrics evaluating navigation performances have been introduced (trajectory smoothness, traveling time, traveled distance, energy consumption, etc.) [19], [77]. Henceforth, the navigation systems are required not only to perform diverse navigation tasks, but also they should meet a set of optimization goals.
- Intuitively, the common study of the control stability should be adapted to the nature of the multi-controller architecture. Stability can be lost at the switching instants between the different tasks. To overcome this matter, the Lyapunov synthesis have been extended to multi-Lyapunov function based-proofs of stability [39].

Indeed, the main reliability and safety issues, which were studied relatively to this architecture consist of the good timing to activate the appropriate controller. For instance,

delays in activating the obstacle avoidance controller, especially after detecting a fast motion dynamic obstacle in the vehicle proximity, may endanger the navigation safety.

1.1.3/ IV INCREASED SAFETY/AUTONOMY DISTRIBUTED ARCHITECTURE

Up to now, the possible navigation behaviors, which may be accomplished thanks to the multi-controller-based architecture have been extremely enlarged. As a step forward towards the IVs full autonomy, the developed autonomous driving behaviors need to be integrated into modern embedded automotive systems. This trend will gradually make IVs able to achieve all driving tasks ensured conventionally by human drivers.

This section aims to explore features of the latest generation of intelligent navigation systems to analyze later the IV complexity impacts on the navigation reliability/safety (cf. section 1.2). To meet this purpose, subsection 1.1.3.1 oversees the modern IVs specifications. A brief background about the structure of present-day automotive embedded systems (distribution of the IV components) is presented. Further, subsection 1.1.3.2 investigates the nature of tasks integrated into modern IV components. In this context, systems deployed into todays' IVs to increase their autonomy are reviewed. Besides, the full autonomy and the navigation in more complicated environments emphasize the IV safety challenges. Correspondingly, subsection 1.1.3.3 highlights the hierarchical changes applied on IVs to comply with the reliability and safety new emergent requirements. With accordance to the discussed issues in this section, subsection 1.1.3.4 presents finally an example of a new industrial paradigm ensuring safety assurance for modern IVs.

1.1.3.1/ MODERN AUTOMOTIVE EMBEDDED SYSTEMS COMPOSITION

The upgrade of the vehicular structure from simple assembled mechanical components to its current sophisticated structure has been realized thanks to Cyber Physical Systems (CPSs) concept and the IVs electrification trend. CPSs are actually a set of computational physical entities. These latter ones offer a high autonomy degree to IVs through the high interaction between Hardware/Software components, which permits to warrant more powerful automotive functionalities [336]. Important facilities such as processing sensors-issued data and controlling actuators are ensured by means of CPSs [116]. Technically speaking, the Electronic Control Unit (ECU) represents the elementary computational component in the in-vehicular system. Numerous embedded functions may be distributed on distinct ECUs e.g., the engine control, the battery management, etc.

Assembling CPSs/ECUs over a distributed architecture turns the automotive embedded system to an expanded Networked Control System (NCS) [285]. In fact, an NCS consists of a large control system, which incorporates a great number of CPSs and several communication protocols to ensure a feedback loop between all the integrated CPSs [51].

Otherwise, the in-vehicular NCS must include a communication layer to manage the overall data traffic between components. This layer may be constructed based on a single in-vehicular communication protocols. Controller Area Network (CAN), Local Interconnect Network (LIN), FlexRay and Ethernet are currently the mostly used protocols in the automotive industry [2], [176]. Differently, the in-vehicular communication layer may incorporate multiple protocols side-by-side to convene their distinct strengths [171]. Finally, Figure 1.5 depicts a typical example of an automotive NCS and its different components.

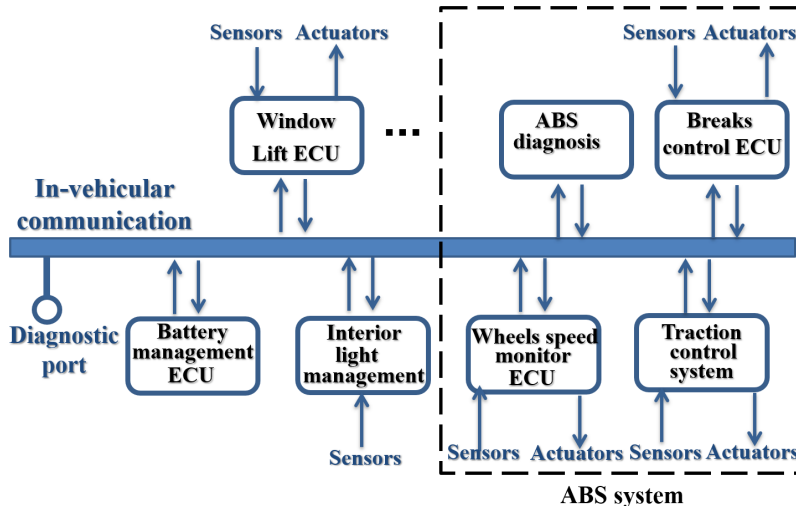


Figure 1.5: Typical architecture of automotive NCS.

1.1.3.2/ DRIVING TASKS DEPLOYMENT INTO AUTOMOTIVE NCSs

As already explained, the worldwide competition between automotive manufacturers has motivated the heading towards promoting more intelligent/autonomous vehicles. However, customers must not only be comfortable at wheels, but they should more importantly feel secure and confident. In that respect, a large scale of driver comfort and safety-oriented processes are currently being integrated into the automotive NCSs. These mechanisms are generally known as Advanced Drive Assistance Systems (ADASs) [134]. Thus, ADASs are progressively becoming among the standard vehicular equipment.

Each ADAS offers a given degree of autonomy to the navigation system relatively to its supplied services. These services vary between delivering warnings and taking important control decisions. In such a way, several ADASs may be implemented in a distributed manner over the backbone automotive NCS. In the hierarchical level, the resulting IV structure consists of a distributed increased safety/autonomy navigation architecture.

Undoubtedly, ADASs require a high connectivity between the navigation system and the environment. For this reason, a multitude of advanced perception tools are mounted on today's transportation systems. These perception tools involve LiDar systems, radars, cameras, etc. [293]. As soon as the perception layer acquires the necessary data, useful information are extracted through the artificial intelligence and computer vision-based approaches to deal correctly with any situation. Video/image processing, street scene analysis, visual tracking and object detection are frequently used in this context [15].

ADASs also exploit the communication protocols dedicated for automotive platforms to guarantee an appropriate automatic maneuverability. Nowadays, the Dedicated Short Range Communications (DSRC) and cellular technologies are essential for connected and automated vehicles. All existing wireless technologies for vehicular embedded platforms, including Vehicle-to-Vehicle (V2V), Vehicle-to-Infrastructure (V2I), Vehicle-to-Pedestrian (V2P), etc., are denoted now as Vehicle-to-everything (V2X) communication [276]. This fact pinpoints the trend to make modern IVs more connected to the environ-

ment and other road-participants. According to [97], standardizing the use of the V2V/V2I communication in public roads may diminish about 80% of potential incidents. Finally, Table 1.1 presents examples of the commercialized ADASs by the automotive industry.

Table 1.1: Different categories of ADASs

System	Assigned task	Ref
Adaptive Cruise Control (ACC)	-Perform regular control of velocity to ensure driver comfort -Maintain a safety distance from an in-front car	[71], [193]
Enhanced driver visibility system	-Assist driver to overcome day/night-time visibility troubles -Provide warnings about driving zones affected by fog	[162], [229]
Pedestrian recognition system	-Detect road crossing persons and deliver warnings to driver -Anticipate pedestrian behaviors to capture collision risks	[57]
Road sign recognizing	-Enhance driver awareness about road signalization	[280]
Driver distraction detection systems	-Inspect the driver vigilance -Monitor the driver eyes or head movements	[23]
Smart lane departure warning	-Warn driver in case of departure from the driving lanes -Manage position estimation for several road models	[112]
Self-parking/parking assistance	-Help drivers in finding vacant parking location -Track a smooth path towards a vacant spot	[112], [260]
Co-pilot/autopilot system	-Ensure autonomous driving via human-like vehicle control -Alleviate consequences of drivers slow reactions to threats	[22]
Blind spot detection	-Object detection in blind spot -Side rear blind spot warning for parking lots	[174]
Anti-lock Braking System (ABS)	-Prohibit wheels from sliding during hard braking -Monitor the contact between wheels and road surface	[302]

1.1.3.3/ SAFETY ENHANCEMENTS FOR IV DISTRIBUTED ARCHITECTURE

As already mentioned, modern autonomous vehicles should be ready to navigate in highly threatening and interactive environments. The need to take into account the safety critical context is emphasized especially for fast motion navigation including dangerous maneuvers (lane changing, over-taking, etc.) [341]. As a result, IVs makers are developing more efficient solutions for safety assurance. Regarding their importance, these solutions are appreciated as fundamental layers from the navigation hierarchy. Indeed, these key automotive components can be classified as follows:

- **The risk management level for explicit safety assurance:** This layer from the navigation system structure is explicitly dedicated to deal with safety assurance purposes and the in-road hazards. The definition of a sound risk management policy to ensure the in-road safety is nowadays crucial. The risk management process includes in fact two distinct steps: risk assessment and reaction against risks.

At first, the risk assessment task consists in identifying in real-time the potential in-road hazards through a deep situational awareness of risk. The required awareness about threats is imperatively obtained by analyzing the environmental data. Risks may be directly captured based on several vision systems co-joined with scene analysis methods. The collected images/videos are processed and analyzed to verify/validate the vehicle safety [15]. However, these methods are computationally demanding and not always suitable for real-time safety critical applications. Besides, problems such as shadowing and occlusion may render results of the scene analysis incredible [340].

As an alternative, it is preferable to rely on more simple physical parameters describing vehicle motions, such as inter-vehicle distances, velocities and accelerations, to interpret the risk assigned to a given situation. According to this understanding, the IV community has focused in introducing various analytical risk indicators, which are calculated through real measurements of the stated parameters. These indicators use physical-based models to make the risk identification closest to reality. In such a way, the risk assessment efficiency is related to these indicator accuracy. The indicators analytical formalizations are in charge of detecting potential future collisions. For instance, the Time To Collision (TTC) and the distance to collision are widely used as collision indicators due to their consistency in anticipating crashes [56], [349]. Other risk indicators can predict other drivers behaviors or the navigation system reactions to sudden events e.g., time to stop, time to steer and time to react [159]. The employment of multiple formalizations for every adopted indicator is possible. In a sequential manner, the most adequate analytical formalization for the current situation should be picked up [349].

Once a potential hazard is identified, the risk must be mastered by acting on the decisional level. The hazard can be avoided simply by acting directly on the control parameters i.e., adapting the vehicle lateral or angular velocity. Collisions may be also prohibited by switching from a behavior to another as the case of an over-taking a vehicle. Reacting to such threats may take place through a dedicated decisional model [9], [246]. Differently, behavioral risk management approaches based on the multi-level Bayesian decision making or neural networks can be adopted [150].

- **Diagnosis functions for implicit safety assurance:** As explained above, a safe navigation process is able to assess risks and to react always quickly. As clear, an appropriate risk assessment requires an accurate sensing of the navigation system proximity. According to the perceived data, a planning scheme defined by a comprehensive decisional model is applied while taking into account any risk or collision probability imposed by the current situation. Then, decisions made by the planning/risk management layers are transformed to actions thanks to controls provided to actuators. Eventually, the IV operational safety is tightly linked to the reliable functioning of the sensing, planning, decision making and control layers. Failures that might cause fatal crashes can stem from any layer from the navigation system. It makes no sense to look for safety guarantees, when the system is prone to fault occurrence. Hence, the system ability to react against faults is implicitly related to the navigation system safety. For the sake of safety, numerous universal standards have been prescribed over the last decades to map efficient diagnosis deployment schema for car makers. For instance, standards as ISO 26262, ISO 15031-4, ISO 22901, ISO 15765-4 and Autosar have been specified to deal with the automotive embedded system failures [135], [137].

To detect faults and localize their sources, a sound diagnosis strategy must be assigned to the already described modern distributed IV architecture. From a hierarchical point of view, there are three distinct manners to implement the on-board diagnosis functions. First, it is possible to devote a unique global diagnosis unit to monitor the overall automotive system [172]. However, the centralized diagnosis is not suitable for large scale automotive NCSs. Real time issues will raise since an important amount of data must be proceeded by the central monitoring unit.

Alternatively, the diagnosis layer can be decentralized over the navigation system architecture [10]. A particular local diagnosis function can be allocated to every ve-

hicular module from the automotive NCS (see Figure 1.6). Thereafter, a supervisor block is responsible of solving conflicts between the locally made diagnosis reports. Roughly speaking, the supervisor final decision about whether to abort the IV operation or to carry on with reduced capacities is made via a predefined fault-tolerant control strategy.

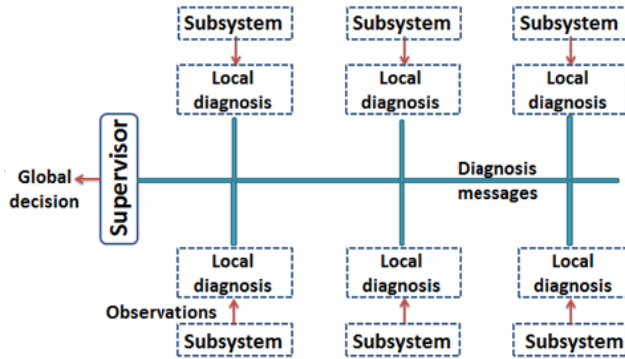


Figure 1.6: Decentralized diagnosis architecture.

Finally, instead of allocating a supervision unit, a collaboration is created via the communication between the local diagnosers [208]. Evidently, this distributed diagnosis may raise the data exchange between the sub-diagnosers (see Figure 1.7).

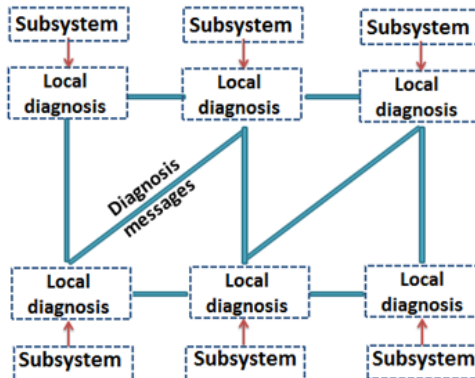


Figure 1.7: Distributed diagnosis architecture.

1.1.3.4/ RESPONSIBILITY-SENSITIVE-SAFETY CONCEPT EXAMPLE

Recently, Mobileye (an Intel company) has promoted for a new safety concept for autonomous navigation systems [262]. This project consists in developing and improving an operational safety verification model, called Responsibility Sensitive Safety (RSS). It provides an safety-oriented open source executable algorithms in order to implement provable and verifiable navigation behaviors [117]. RSS should be considered as a design guidance for navigation strategies to evoke a completely safe decision making for critical situations. Even more, Mobileye has expanded the understanding of safe intelligent navigation according to the RSS terminology. RSS-based navigation algorithms allow not only to take precautions of risks caused by other road participants, but it prohibits

performing any act that may evoke hazards. Hence, RSS defines a set of mathematical models to formalize and put into practice this particular interpretation of safety. Figure 1.8 presents several complicated navigation scenarios, where RSS specifies mathematical safety guarantees. It turns the initial navigation approach to a safety constrained navigation strategy. These constraints include how to respond to risks implied by other agents (proximity vehicles, pedestrians, etc.) and how to avoid initiating critical situations.



Figure 1.8: Critical navigation scenarios treated by RSS model for safety guarantees.

For instance, the study reported in [52] presented a proof of concept of embedding RSS into an ACC for functional safety aims. Noticeable improvements in terms of safety were marked in the ACC performances with the RSS model. According to this understanding, the RSS concept fits perfectly the distributed nature of modern navigation systems architectures, where several ADASs are implemented. Correspondingly, RSS chances to play as powerful tool to develop large range of navigation test scenarios for operational safety purposes in the near future are strong. To recapitulate the discussed issues in this section, Figure 1.9 illustrates the witnessed changes in the autonomous navigation system.

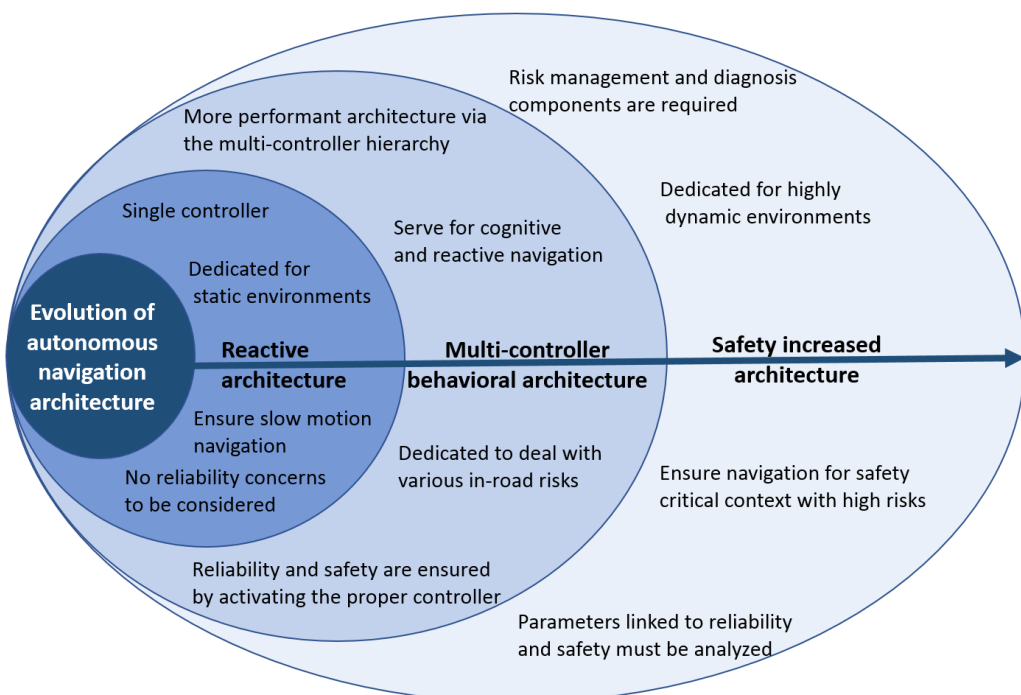


Figure 1.9: Evolution of autonomous navigation systems architectures and capacities.

1.2/ MODERN IV ARCHITECTURE COMPLEXITY-ISSUED CHALLENGES

As detailed in the previous section, the architecture of modern IVs have known lately many changes. This architecture depicts boundless proofs of complexity. Nonetheless, the link between the complexity consequences and the navigation safety has been rarely analyzed. Accordingly, this section highlights the IV complexity-issued challenges. The impact of these challenges on the intelligent navigation safety is interpreted. In this sense, a classification of complexity issued concerns is proposed as follows:

- **Large scale NCSs with integrated components/functionalities:** More ECUs and entirely new layers as the diagnosis and risk management levels are incorporated into today's IVs. Especially for IVs with cumbersome navigation algorithms, the evasive integration of supplementary components and functionalities brings additional complications. The proper functioning of a given IV requires a continuous and tight interaction between Software functions and Hardware entities, which is really challenging for a large scale embedded system [94]. Concerns such as resource planning and Hardware concurrency may make the IV less quick, less reactive and consequently less reliable [54], [95].
- **Data proliferation:** The data proliferation into the automotive systems is another complexity source of modern IVs. The convergence between the artificial applied sciences and the big data trend is unavoidable for the automation of the transportation means. On the one hand, a large range of sensor-issued data is proceeded by IVs to sense the environment and perform a safe navigation [72]. On the other hand, the data proliferation issue is accentuated due to some trends followed by car makers. To entertain and satisfy clients, modern transportation means afford several interactive and infotainment services. The promoted automotive infotainment mechanisms, including vocal control systems and television band receivers, handle conventionally huge amounts of audio-visual media [125]. Indeed, the capacity of the in-vehicular embedded systems to support such a high transmission rate is questionable. Predefined time constraints may be violated due to extra-loaded communication. To not slow-down the automotive NCS, keeping the intelligent navigation system up-to-date with the data proliferation trend is necessary. Accordingly, many solutions have been proposed to overcome side effects of the overloaded in-vehicular traffic data to guarantee the IV reliability [237, 265, 347]. Due to the safety critical context, it should be noted that risks related to the data proliferation are higher for information interchanged with the diagnosis or the risk management layout. Taking quick countermeasures against menaces and failures is vital for the in-road safety.
- **In-vehicular network-induced imperfections:** Abundant number of components with completely distinct timing features are incorporated into modern IVs e.g., powertrain, breaking system, etc. The time-constrained communication between these components within a fixed global time-sampling step may implicate non-negligible network-induced imperfections. An arbitrary loss or disorder in the communication packets can happen and may lead to a hazardous irregularity/discontinuity in the IV behavior [73], [319]. This issue is emphasized by the new structure of the heterogeneous automotive NCSs including multiple communication protocols of different

scheduability features [171]. Due to its tight relation with the IV reliability, timing-features should be carefully verified, especially for delay-sensitive components. As already mentioned, modern IVs are equipped with a large range of critical safety applications and driver assistance systems. These systems impose additional material constraints and resource availability concerns. Network-induced imperfections, communication delays, errors in data transmission are destructive for these processes and respectively the overall navigation safety [44], [307].

- **Extra connectivity:** To perceive appropriately the environment and its over-changing dynamics, the number of sensing and communication devices mounted on IV is drastically increasing. Moreover, novel sensing technologies such as wirelessly interconnected sensors are currently substituting the conventional ones for a better perception quality and accuracy. Even though these technologies are more powerful, they have brought new reliability challenges for IVs such as the connectivity, sensing delays and scalability issues [290], [330]. Evidently, integrating sensing tools into IVs is one step from the full electrification of navigation systems. Due to their electrical and/or electromagnetic nature, the sensing devices receive and generate a great amount of electromagnetic disturbances. These disturbances can propagate from the sensing layer to the remaining parts of the automotive NCS in the form of radiated or conducted Electromagnetic Interference (EMI) [113]. Under these interferences, accuracy of measurements provided by the sensing layer may be affected. Even more, probability of failure occurrence becomes stronger due the EMI propagation through the whole IV.

The autonomous navigation systems are among the most complicated and safety-critical processes. Plenty of uncertainty sources may endanger the IV safety. IVs must deal with highly interactive and uncertain environments, where it is difficult to predict behaviors of other road participants. Numerous additional factors may emphasize the uncertainty impacts such as the influence of bad weather conditions on the sensing quality and the navigation through dense traffic flows. Apart of these uncertainty sources, the discussed complexity aspect characterizing the architecture of modern IVs invoke other new challenges and uncertainty origins. Underneath the discussed issues in this section, latency effects on today's navigation systems are much important. Due to their complex structures, the IVs responses to risks are quite indeterminate. IVs are currently sensitive more than ever to faults because of their extreme sophistication.

Indeed, there is a clear coupling between the IV reliability (including robustness against latency, uncertainty and failures) and the in-road safety. The navigation safety is turning into an overlapping issues, where reacting to risky situations is no more sufficient. Mastering the reliability-related challenges issued from the IV complex architecture is indispensable.

1.3/ UNCERTAINTY PREDICTION FOR AUTONOMOUS NAVIGATION

As a matter of fact, IVs are prone to enormous uncertainties, especially when navigating side by side with other agents of unpredictable behaviors. Furthermore, the complexity of modern navigation systems engender more uncertainties due to communication/perception latencies and interferences, etc. Consequently, uncertainty handling is

not restrained for measurement filtering and data fusion in the case of autonomous driving. It includes also states estimation, events prediction, forecasting road participant behaviors, decision making, etc. In this regard, uncertainty propagation into the different layers of the navigation system needs to be characterized in a holistic manner. To fill the massive need for safety guarantees and to provide reliable criticality measures, the IV community has continuously attempted to introduce more efficient uncertainty characterization approaches for both long and short time horizon. The rest of this section oversees and classifies the uncertainty handling related work to discuss each class of methods pros and cons. Moreover, relevance of each investigated method for autonomous transportation systems is analyzed.

1.3.1/ PROBABILISTIC UNCERTAINTY HANDLING APPROACHES

The prediction of the uncertainty propagation into the navigation system has been largely studied via classical stochastically-driven approaches [313]. This class of methods is generally based on the use of Bayesian inference theories to ensure the probabilistic estimation. In general, consistency of the probabilistic estimation is also reinforced through a model-based description of the transition in the system states. Therefore, a profound knowledge of the system behavioral aspects and its dynamical/kinematic constraints is essential to succeed the prediction. At the same time, the system noise characteristics are then involved in the established model. Hence, the progression of uncertainty into the model dynamics is predicted via a predefined Probability Distribution Function (PDF) [224] e.g., Gaussian, likelihood distribution, etc. It is important to notice that the stochastic approaches are generally outlined in the literature as linear-based abstraction methods. The linearization of the model describing the system states is mandatory to make sure that the noise process is still always governed by the Gaussian law. Nonetheless, the linearization errors prohibit the employment of the stochastic filtering for long term horizon [308]. The stochastic uncertainty evaluation is also non-deterministic since the elaborated probabilistic estimations may mismatch the reality. Assuming that the noise features are given by a particular PDF does not always hold, and modifications in noise properties may happen [244]. The environmental impairments entailed from harsh weather conditions may be taken as potential reasons for changes in sensor noise features. In this context, a study was tackled in [138] to explore LiDAR sensor behaviors under various environmental conditions and to mitigate impacts of any probable sensing degradation on the data fusion process.

Several extensions of Kalman filters introduced in the literature are classical examples of the stochastic prediction approaches [139]. Actually, performances of these filters depend on the accurate knowledge of the system initial states. When the filter is not properly conditioned, it diverges to faulty estimations [221]. Accordingly, more attention is paid currently to formulate Bayesian inference based filtering techniques, which are not relying on the prior availability of the statistical features of sensors. To this end, the filtering technique introduced in [228] admitted the manifestation of the worst-case of disturbances into the system instead of the common use of Gaussian distribution. By referring to ground truth observations, the estimation accuracy was improved compared to Kalman filters. However, the full accuracy of estimates was not reached, since around of 3.51% as a mean error in prediction was found.

The aforementioned stochastic methods are able to estimate easily the probability of a

given assumption. Nonetheless, they ignore any available evidence while predicting uncertainty evolution. Contrary to classical methods, the belief theory method considers the available evidences as an effective opportunity to improve the uncertainty characterization by exploiting the evidence-based additional statistical support. After considering all the existing evidences that may originate from distinct sources, a degree of belief is attributed to every made prediction. Since it evaluates the credibility and reliability of the proceeded uncertainty estimation, the belief theory is quite relevant to conduct uncertainty characterization for IVs. For instance, the work depicted in [214] proposed a belief theory-based scheme to distinguish between faulty and consistent data issued from the navigation environment.

In order to enhance the stochastic methods consistency and credibility, an increased interest is attributed lately to the multi-simulation approaches for uncertainty estimation and motion prediction. The application of the Monte Carlo approach in this context is mainstream due to its aptitude in accomplishing a more relevant probabilistic forecasting [111]. Instead of relying on a unique cycle of uncertainty estimation, the Monte Carlo method executes a large number of simulations in a simultaneous manner. It allows to address all potential states of the navigation system and the variability in its inputs [145]. Afterwards, a much reliable final prediction is derived according to the density of the proceeded simulation results. Intuitively, the probability to obtain a prediction much more closer to the reality is stronger. The huge number of executed simulations makes the Monte Carlo approach among the most computationally demanding prediction methods. Most importantly, findings of the Monte Carlo method vary from an execution to another, even though the same simulation setups are used. To conclude, the multi-simulation uncertainty handling approaches are time consuming, non-deterministic and sensitive to linearization.

Indeed, the multi-simulation techniques are generally joined with a occupancy grid-based technique. The navigation scene is decomposed into different cells. Cells, which may be occupied by the vehicle in the near future, are identified by turning the density of probabilities obtained via the multi-simulations to a binary data [271]. The major drawback presented by the occupancy grids is the expended number of cells to be verified. This matter arises from the additional degree of freedom in potential vehicle motions because of the multitude maneuvers that may be performed.

Despite its high computational cost, the multi-simulation methods may serve to validate results of other prediction techniques. Due to its capacity in considering the variance in the input data, such approaches have great offline utilities, especially when ground truth reference measurements are unavailable.

To avoid the inaccuracy entailed by linearization, another line of research work has recourse to a several learning-based prediction approaches. Hidden Markov models, artificial neural networks and Bayesian networks have been largely adopted to predict driving behaviors and uncertain events [56, 129, 149].

From a theoretical standpoint, the learning-based techniques handle two uncertainty types. Similarly to classical techniques, they characterize the aleatoric uncertainties originating mainly from sensor noises described by a PDF that fits the studied system. Aside of the aleatoric disturbances, the learning methods take advantage from their capacities in dealing with the epistemic uncertainties, which are in relation with some systematic imperfections such as modeling and training errors [312]. This is done by enlarging the acquired knowledge during the training phase by estimating the predictions consistency

during run-time. In addition, the learning-based methods open the possibility to estimate the uncertainty propagation even with complicated cases of missed measurements. Such situations are frequent due to occluded observations or intermittent sensing failures [37].

Technically speaking, the greatest part from the learning-based approaches are multi-layers graphical models, where the Bayesian inference-based probability theory is applied to fuse uncertainties in the model inputs, weights and outputs [213]. Thus, the main difficulty while developing such approaches is how to define an appropriate architecture of the learning system. For yet, there is no known methodological manner to reach explicitly the optimal architecture of such models. The layout of the learning model is often defined randomly or empirically. In [105], an artificial neural network was in charge of estimating uncertainty evolution for a vehicular LiDAR sensor. To optimize the architectural performances of the uncertainty handling network, a second learning stage was integrated into the neuronal model to distinguish between relevant and noisy inputs provided to the first stage.

Roughly, the uncertainty affecting the system outputs is assessed through sampling data from a particular learned probability distribution. Hence, establishing a sound link between the estimates evolution and factors that rule the variation among samples appears necessary. From this perspective, IV state transitions is extremely coupled with behaviors of other road participants. Unlike the classical uncertainty handling techniques, which consider the navigation process as a separated system, the learning-based techniques may integrate all interactions with other vehicles into the uncertainty assessment phase [147]. As they take into account the surrounding context, much more accurate estimates are obtained within a longer prediction horizon time. For each traffic scenario, particular knowledge-based transitional models for the inter-vehicles interactions are used to boost the prediction quality. In addition, accuracy of the uncertainty assessment depends on the modeling methodology of all possible interactions between vehicles. These interactions may be modeled through two distinct ways. First, it is possible to use standard homogeneous learning models, where all the behavioral, kinematic and dynamic features of vehicles are assumed identical. Although homogeneous models are simple and computationally reasonable, they are inaccurate and poorly efficient. Additional struggle to adapt these models to each vehicle features and to recover the individual dissimilarities is needed for a better prediction. Hence, heterogeneous modeling of the inter-vehicle interactions is constructed via adaptive multi-modal techniques. For more details about this topic, several examples of adaptation algorithms were proposed and tested in [267]. Using real experimental data to perform the training phase appears as a reliable practice to improve performances of the learning-based approaches. However, erroneous uncertainty estimation occurs especially in case of unpredicted driving situations. Such situations are difficult to be captured in reality. Especially for the risk assessment, experimentally collected training data can never be issued from real dangerous situations as collisions [167]. Alternatively, the ignored/rare events and driving situations can be easily predicted through synthetic training data-sets [75].

As most of the probabilistic methods, the main weakness presented by the learning-based techniques is their heuristic nature. Accordingly, the machine learning research community have attempted to overstep this drawback. To overcome the heuristic aspect characterizing the neural networks used for trajectory forecast, the authors in [338] employed two different probability distributions of the uncertain estimates. Hereby, the comparison between the estimates resulting from each distribution by several statistical means improved the uncertainty prediction consistency.

In other respects, efficiency of the learning-based techniques depends drastically on parameters defined during the training and learning phases. A minor variation in these parameters may alter the overall behavior of the prediction system. For example, the Markov decision process principle consists in discretizing the system states in order to determine the system future states based on transition probability functions [234], [259]. The study reported in [349] revealed the discretization effects on the precision of the Markov process outcomes in a collision prediction context. Avoiding discretization errors and selecting an appropriate sampling step are necessary to neither under-estimate nor to over-evaluate the uncertainty states. Otherwise, the learning-based class of uncertainty assessment techniques are considered as black boxes with unpredictable behaviors. The absence of analytical models that describe such approaches makes them unverifiable.

To overcome the early outpointed limitations of the probabilistic techniques, the cooperative handling of uncertainties is a promising research direction. Evidently, vehicles navigating in the same area must perceive each other. By collecting observation of each vehicle, the redundancy in data may refine remarkably the uncertainty estimation performances. From this point of view, a cooperative perception strategy was introduced in [47] and [320] for more accurate positioning. Even more, recognizing vehicles, which are in a better situation to localize other road participants, reduced the uncertainty estimation errors [148]. Nonetheless, the cooperative perception can be applied only in navigation scenarios where all the vehicles are assumed to be connected cars.

1.3.2/ NON-PROBABILISTIC UNCERTAINTY HANDLING APPROACHES

As a cut off with the unwarranted stochastic uncertainty estimation, a new wave of set-membership non-probabilistic methods have been emerged. This class of methods relies on the geometrical extrapolation of the system future states. First, data describing the system (states, inputs and parameters) are enclosed into particular geometrical shapes to consider the uncertainty e.g., ellipsoids, zonotopes, polytopes, etc. Afterwards, the uncertain states are iteratively propagated through a specific mathematical model describing the studied process to characterize the uncertainty progression. It is worth mentioning that a careful selection of the enclosure shape is indispensable. Predicting the uncertainty propagation into the IV system with a complex set-representation of data requires a strong theoretical background about the computational geometry. It also may invoke considerable computational costs. Although some enclosure forms are more compact than others (such as zonotopes and ellipsoids), there is not enough available advanced computation processes within these sets [219].

Rather, an extensive research work has focalized the light on the interval analysis. As a simple closed form, the interval shape is easily handled in a natural way by equations. Correspondingly, fundamental basis of the interval arithmetic have been rapidly developed [154], [202]. Then, the interval arithmetic has helped to enclose all possible solutions of several uncertain problems such as numeric integration, derivation and solving systems of non-linear equations. The set-membership computation is assumed as guaranteed and reliable since the exact value of data is enclosed inside the resulting interval bounds.

For the sake of accuracy, various interval-based filtering approaches, including a “prediction-correction” steps, have been suggested in the literature [29]. A guaranteed state prediction for IVs is realized through these estimators without relying on probabil-

ties. Instead, these filters use for instance the system observability and numeric set-inversion techniques to refine the uncertainty estimation [200]. In general, the existing interval-based approaches may be classified into two different categories. On the one hand, a great part from these methods incorporate explicitly the prior knowledge of the uncertainty extents into the prediction process. This knowledge is roughly acquired through studying features of the IV system sensor's [27]. These uncertainty handling approaches are specially suitable for the automotive diagnosis processes. Performing the diagnosis within a bounded error context increases the sensitivity to faults [55], [66]. This latter minimizes false alarms and leads to a high fault-awareness for IVs.

One more class of interval-based approaches play as numeric “branch and bound” calculation tools [80]. By proceeding in an recursive manner, these approaches select an initial set from the data space domain. Then, several set-inversion operations take place to finally find and bound the exact solutions of the studied problem. Unfortunately, although these approaches are extremely accurate, they have an unpredictable computation time.

1.3.3/ REACHABILITY ANALYSIS (RA) FOR LONG-TERM HORIZON PREDICTION

To explore any risk entailed from a particular decision, there is a crucial need to perform the prediction for a long-term horizon. This is known in the literature as the RA concept. Over the last decade, the considerable literature on RA has turned this research field into a very active one [126]. Despite the already existing solutions, RA remains a subject of intensive ongoing research.

To start with, the system reachable sets may be extrapolated by incorporating uncertainties into a stochastic/Bayesian inference-based model. Similar to the short time horizon stochastic methods, stochastic RA may only produce approximate and low-confident reachable sets of the studied system. To solve such an issue, several data-driven characterization techniques of the system have been exploited to provide knowledge-based enhancements for the stochastic RA reliability in [127]. The work reported in [90], has employed human-like driving models and empirical data to enhance the confidence-level of the vehicle estimated reachable space. Nevertheless, the correct prediction rate of these methods remains too low, even with the aforementioned improvements.

As an alternative, the use of the set-membership modeling was frequent to apply the RA schema. The employment of complicated sets to compute the system reachable states implies always a linearization phase for non-linear systems. Hence, the RA process may suffer from sever linearization errors. In this regard, deterministic RA approaches that combine Hamilton-Jacobi equations with convex programming and set-level methods have been largely used to ensure conservative abstractions [322]. However, the algorithmic complexity expansion of these methods is linked to the number of the system state variables. In case of high scalable systems, additional struggles to decrease the high dimensionality side effects by decomposing the initial system are unavoidable [59].

For its simplicity, the interval analysis has contributed also in shaping several RA processes. More precisely, the reachable sets have been defined by rephrasing the RA context to a constraint satisfaction problem while using branch and brought interval-based algorithms [250]. Findings of these latter ones are highly accurate and confident, but computationally expensive. The iterative use of numerical inclusion tests entails an unpredictable execution time for these algorithms. Another class from the interval-based solutions relies on the Differential Inequalities (DI) theory. Numerous researches have prof-

ited from characteristics of the monotonous and cooperative systems, which are featured with natural prior enclosures of their states [204]. As a result, extremely tight bounds for the system reachable sets can be determined. Respectively, several attempts have been carried out to generalize the DI application. Different discretization and/or hybridization processes of the initial system into locally monotonous subsystems have been proposed [240], [329]. Nonetheless, the design of such processes is not always evident. Even more, complexity of the RA problem depend exponentially to the derived subsystems number.

Only few exceptions from the interval-based approaches can study systems' reachability by dealing with whole regions of initial states. An interval extension of the well-known Taylor series expansion has succeeded the over-approximation of the reachable space [181]. The upper/lower bounds of Taylor-based approaches are conceived without any need for a mathematical transformation for the studied system or partitioning its initial states. Instead, set-valued solvers for the uncertain Ordinary Differential Equation (ODE) that describes the system evolution are used.

In accordance with the above undertaken debate, a comparison between the reviewed uncertainty prediction techniques is derived in Table 1.2. Obviously, the interval-based approaches opportunities in coping with limitations raised from the heuristic nature of the probabilistic methods are quite promising.

Table 1.2: Comparison between uncertainty prediction approaches for IVs

Navigation requirement	Accuracy	Handling modeling imperfection	Low computational complexity	Long-term horizon prediction
Classical stochastic approaches	--	--	++	---
Multi-simulation approaches	-	-	---	--
Learning-based approaches	--	++	+	--
Branch and bound interval-based approaches	+++	+++	---	++
Uncertainty prior knowledge interval approaches	++	++	-	+
Stochastic RA approaches	--	---	++	--
Linearization-based set-membership RA approaches	++	--	--	++
Numeric set inversion interval-based RA approaches	+++	+++	---	+++
DI-based RA approaches	+++	++	+	+++
Full interval-based RA approaches	+++	++	+	++

1.4/ REQUIREMENTS OF MODERN NAVIGATION SYSTEMS

Previously in this chapter, challenges imposed by the new generation of autonomous navigation technologies have been briefly reviewed. In the light of these challenges, new requirements related to the reliability/safety concerns should be taken into consideration to solve complications entailed by todays' intelligent/autonomous vehicles. Without fulfilling these requirements, reaching a full satisfactory level of reliability/safety for autonomous navigation systems is still far away from reality. In the sequel, the new reliability/safety requirements for IVs are recapitulated.

1.4.1/ FLEXIBILITY

For a long time, IVs proper operation was judged by their ability to accomplish their designated tasks while pursuing accurately a predetermined navigation policy. Any deviation

from the preconceived navigation guidelines is assumed as a threatening violation for the safety constraints. However, to reach the full autonomy, IVs must be ready to face all sorts of unexpected events and master all types of uncertainties. As noticed in previous sections, the surrounding/in-vehicular uncertainty sources are becoming abundant and unrestricted. From this scope, a relevant question arises systematically concerning the IVs safety: Can modern IVs achieve their missions precisely as expected under the stated important uncertainty origins? For instance, the navigation system ability to track precisely a given trajectory in crowded highway areas is absolutely doubtful.

Indeed, offering IVs a more degree of freedom may be the key solution to face uncertainties and safety challenges. Allowing modern navigation systems to act in several possible manners (choose another path, change current waypoint location, etc.) can provide multiple backup/recovery solutions for critical situations.

Accordingly, flexibility is now needed as never before for modern IVs. To address adequately this challenge, there is for instance an increasing trend to substitute the existing trajectory planners by waypoint assignment strategies [53, 298, 309]. Following particular points from a discretized path simplifies drastically the navigation mission. Instead of the rigorous and arduous path following, few series of waypoints must be properly arranged to guide the vehicle. Contrarily to former approaches, the navigation system moves freely between the assigned waypoints until reaching a final desired destination (cf. chapter 3).

1.4.2/ AWARENESS ABOUT MATERIAL CONSTRAINTS

To master all reliability and safety problems resulting from vehicle automation, uncertainty and failure probabilities must be included at the decision making level (to ensure vehicle navigation safety). The future directions are making the vehicle isolated control units aware of Networked Control System (NCS) material constraints. Now, transportation risk management strategies are investigating only the in-road hazards. In contrast, vehicular navigation is not safe without solving issues related to NCS capacities in reacting appropriately to environmental events. Intra/in-vehicle communication latencies may increase in an unpredictable way a given in-road situation criticality. From this scope, risk management strategies should focus on integrating the material constraints into the hazard identification phase. Adaptive and material constraint-aware control will be the best solution to overcome NCS-induced risks and guarantee the safety of next-generation vehicles.

1.4.3/ GUARANTEED UNCERTAINTY PREDICTION

Especially for the risk management and diagnosis levels, uncertainties may lead to erroneous decisions. In that case, the navigation system is no more reliable and safety will be menaced. Therefore, much more interest should be paid to improve accuracy of the uncertainty prediction methods. More interestingly, the verification of all probable predicted events/states is in general not feasible. Then, alternative approaches to substitute the probabilistic estimation of uncertainty are recommended. All uncertainty types (especially uncertainties imposed by the material constraints) should be considered. Methodological ways permitting taking precautions about the sensing minimum/maximum errors, without any probabilistic reasoning are interesting in this context. IVs guaranteed performances can only be met with methods handling all possible states of uncertainty. Noticeably,

since all possible states of uncertainty should be considered, such methods can be time consuming. Nevertheless, the respect of the real-time constraints is also essential.

On the basis of the above discussed safe navigation new requirements, Figure 1.10 illustrates how to satisfy the reliability/safety constraints for modern IVs. Adopting flexible navigation approaches and guaranteeing the IV ability to handle uncertainties/faults are essential to develop highly reliable navigation systems. In addition, neglecting the IV material constraints, imposed by its embedded composition, will certainly limit its capacities in dealing with risks.

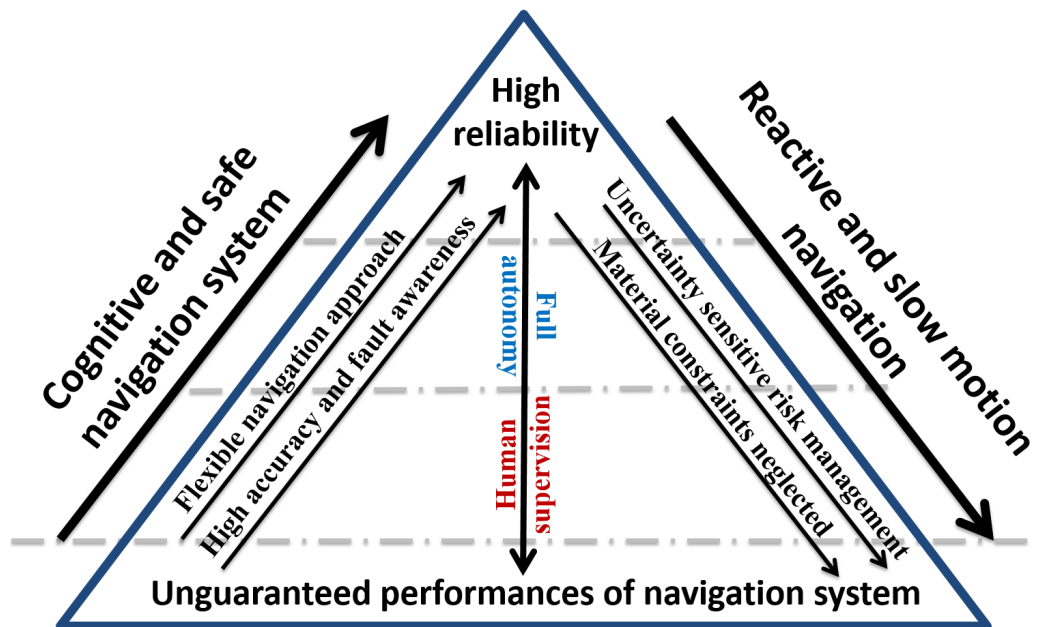


Figure 1.10: Requirements to reach full autonomy, reliability and safety of modern IVs (scheme inspired from [19]).

1.5/ CONCLUSION

This chapter presented a comprehensive overview about the mobile intelligent navigation systems. The light was focused on the reliability/safety prospects. Through the in-depth analysis of the state-of-the-art, features of modern autonomous/intelligent navigation processes were highlighted. Afterwards, challenges raised from the complex and sophisticated shape of modern Intelligent Vehicles (IVs) were identified. The relation between the IV reliability and the in-road safety has been largely studied. Eventually, the basic new requirements in order to reach a satisfactory level of navigation reliability/safety were deduced. In accordance with these requirements, several contributions in the context of safe/reliable navigation will be introduced in this thesis. Solution suggesting safe and flexible navigation strategies, reliable uncertainty estimation approaches and increased sensitivity to faults will be detailed in chapters 3, 4 and 5.

2

INTERVAL ANALYSIS ENHANCEMENTS FOR IV RELIABILITY

As stated in the previous chapter, the uncertainty sources encountering modern Intelligent Vehicles (IVs) have been multiplied. These uncertainties may be sufficiently enormous to prevent the IV from achieving its tasks. In this view, some recent studies have lately linked the autonomy level of a given system to its robustness to uncertainty [30]. The greater the amount of uncertainties the process can cope with, the more considerable its autonomy. To confront the uncertainty-induced risks, large varieties of probabilistic/stochastic approaches are frequently used for IVs. However, probabilities may mismatch the reality.

On this basis, numerous interval-based accomplishments have been proposed in the literature to render the IV performances guaranteed and immune against the uncertainty harmful impacts. At present, the interval analysis is playing more valuable role in optimal trajectory computation, safe obstacle avoidance, precise localization, emergency management systems, state estimation, fault detection, etc. [240, 303, 304].

Stating that a solution is guaranteed is too vague. Concretely, the terminology of guaranteed approaches refers to methods able to outcome certain results throughout a bounded computation. Solutions of the interval-based approaches enclose the exact outcomes, which correspond to the reality. Bounds of the resulting interval findings report all possible scenarios of the uncertainty propagation into the studied process. The characterization of the uncertainty propagation into autonomous systems via the interval analysis is easier than the rest of the set-membership methods. Due to its simple wrapping shape, the interval analysis extends easily the standard arithmetic theories to handle intervals. Despite the immersive interest in guaranteed methods, advantages presented by the interval-based developments for IVs have never been deeply prospected. The design of interval-based navigation methods requires further exploration.

In the remainder of this chapter, bases and fundamental notions to proceed through the interval arithmetic are summarized in section 2.1. Afterwards, enhancements for the intelligent navigation systems that may be conquered via interval analysis are revealed in section 2.3. To be comprehensive, improvements brought by the interval-based computation are divided respectively into two parts: enhancements for the model-based and data-driven navigation approaches (cf. subsections 2.3.1 and 2.3.2). As any methodology, the interval analysis has also few limitations, which may damage the IV performances. The different root causes of such limitations that may constrain the development of guaranteed solutions for IVs are discussed in section 2.4.

2.1/ INTERVAL ARITHMETIC: PRELIMINARIES

At first, the interval arithmetic was used in the aim of providing a remedy for the imprecision related to the numeric computation. Especially after the raise of computer sciences, the interval representation of numbers was efficient to avoid truncation and rounding errors. The propagation and accumulation of such errors throughout large scale computation algorithms emphasize the calculation inaccuracy. Correspondingly, the interval arithmetic was regarded as a powerful tool enabling reliable calculation for problems where precision is a central component. The interval analysis is also useful in dealing with the uncertainty reproduced by several indirect analytical computation operations, including linear or polynomial approximation/expansion of a function. In that case, the representation of the remainder error in the form of interval is very popular, which justifies the employment of the interval analysis.

Rapidly, the interval analysis has been developed from a simple tool used to refine the computation quality to an advanced uncertainty characterization method. The foremost reason behind using the interval analysis in this context is to recognize all potential behavioral trajectories of the system under uncertainty. Before proceeding further, let introduce some fundamental notions about how the interval analysis can provide a reliable estimation of the uncertainty states. To be concise, focus will be given exclusively for interval-based mathematical operations and procedures required for the different contributions suggested in the present thesis.

2.1.1/ INTERVAL ARITHMETIC PRINCIPLE

The concept of interval arithmetic relies on transforming a standard variable x , which is quantified in general through punctual scalars or single-valued numbers, to an interval-valued variable. A simple definition of an interval, denoted $[x]$, consists of a close set of real numbers. Points belonging to the interval are naturally framed between two endpoints i.e., single values representing the worst cases of uncertainty extents. Intuitively, the interval endpoints assume the role of boundary wrappers for the interval content. As a notation, $[x] = [\underline{x}, \bar{x}]$ refers to the interval designated to describe the uncertain variable x , where \underline{x} and \bar{x} are respectively the interval lower and upper endpoints. Generally, $\underline{x} < \bar{x}$, but certain data may be represented through a degenerate interval by assuming $\underline{x} = \bar{x}$. Although an interval is a closed set of points, both or one of the interval bounds may be infinite (such as $[-\infty, 0]$, $[0, +\infty]$ and $[-\infty, +\infty]$). Otherwise, two additional characteristics of $[x]$ can be derived through out its endpoints \underline{x} and \bar{x} :

- The interval midpoint, noted $mid([x])$, represents the centre of the interval extent. In the data representation space, the uncertainty is distributed over this central point. Evidently, $mid([x])$ is expressed as follows:

$$mid([x]) = (\underline{x} + \bar{x})/2 \quad (2.1)$$

- The interval width $wid([x])$ quantifies the uncertainty amount impacting the interval-valued data. $wid([x])$ is given by the expression below:

$$wid([x]) = \bar{x} - \underline{x} \quad (2.2)$$

2.1.2/ CLASSICAL MATHEMATICAL OPERATORS FOR INTERVALS

Indeed, the interval arithmetic specifies the appropriate instructions and computation procedures that are convenient to the interval-type data. These procedures include mainly the fundamental formula and guidelines to extend the mathematical operators to intervals [49], [154]. For more details, the required expressions to apply the set of classical operators (+, -, ×, /) for intervals are given in Table 2.1.

Table 2.1: Classical mathematical operators for interval data

Operator	Formula
Addition	$[x] + [y] = [\underline{x} + \underline{y}, \bar{x} + \bar{y}]$
Subs-traction	$[x] - [y] = [\underline{x} - \underline{y}, \bar{x} - \bar{y}]$
Multiplication	$[x] \times [y] = [\min(\underline{x} \times \underline{y}, \underline{x} \times \bar{y}, \bar{x} \times \underline{y}, \bar{x} \times \bar{y}), \max(\underline{x} \times \underline{y}, \underline{x} \times \bar{y}, \bar{x} \times \underline{y}, \bar{x} \times \bar{y})]$
Division (for $0 \notin [y]$) ¹	$[x]/[y] = [\min(\underline{x}/\underline{y}, \underline{x}/\bar{y}, \bar{x}/\underline{y}, \bar{x}/\bar{y}), \max(x/\underline{y}, \underline{x}/\bar{y}, \bar{x}/\underline{y}, \bar{x}/\bar{y})]$

2.1.3/ INTERVAL VECTORS/MATRICES

Similar to the real arithmetic, the standard mathematical operations can be also applied on interval vectors and matrices. In n -dimensional space, an interval vector, known also in the literature as an axis-aligned box, is often defined as the Cartesian product of n interval components:

$$[x] = [x_1] \times [x_2] \times \cdots \times [x_n] \quad (2.3)$$

Likewise, an interval matrix $[A]$ of n rows and m columns refers formally to a Cartesian product of $n \times m$ real interval elements:

$$[A] = \begin{pmatrix} [\underline{a}_{1,1}, \bar{a}_{1,1}] & \cdots & [\underline{a}_{m,1}, \bar{a}_{m,1}] \\ \vdots & \ddots & \vdots \\ [\underline{a}_{n,1}, \bar{a}_{n,1}] & \cdots & [\underline{a}_{n,m}, \bar{a}_{n,m}] \end{pmatrix} \quad (2.4)$$

It is worth noting that the width of a vector or matrix is the maximum width of their interval components. Thanks to the interval analysis, the elementary algebra and standard simple logic are straightly applied on interval vectors and matrices conforming to the real arithmetic. Unlike standard computation schema, the interval vector/matrix calculation permits the consideration of the uncertainty propagation all along any algorithm.

2.1.4/ SET OPERATIONS FOR INTERVALS

As the case for the majority of set theories, the inclusion operations are quite important to compare interval-type data and underline relations between subsets. Since they are represented only by two simple real numbers (endpoints), it is easy to define regions resulting from the intersection/union between interval-sets or to realize inclusion tests. Let consider the following interval vectors of dimension n : $[X]$, $[Y]$ and $[Z]$. Then, the interpretation of the set operations are illustrated in Table 2.2.

¹For the sake of brevity, expressions where $0 \in [y]$ can be found in [199].

Table 2.2: Classical set operations for intervals

Set operation	Interpretation
Inclusion $[X] \subseteq [Y]$	$\forall i \leq n, \underline{X}_i \geq \underline{Y}_i \wedge \bar{X}_i \geq \bar{Y}_i$
Intersection $[Z] = [X] \cap [Y]$	If $\underline{X}_i \leq \underline{Y}_i \vee \bar{Y}_i \leq \underline{X}_i$ Then $[Z_i] = \emptyset$ Else $[Z_i] = [\max(\underline{X}_i, \underline{Y}_i), \min(\bar{X}_i, \bar{Y}_i)]$
Union $[Z] = [X] \cup [Y]$	$\forall i \leq n, [Z_i] = [\min(\underline{X}_i, \underline{Y}_i), \max(\bar{X}_i, \bar{Y}_i)]$

2.1.5/ INCLUSION FUNCTIONS

After enabling the computation via interval vectors/matrices within the standard operations, it remains to extend functions (1-dimensional or vector-valued functions) to handle arguments in form of axis-aligned boxes to build full interval-based calculation platforms. As a matter of reality, a function is roughly defined as a transformation of a set of inputs from an initial data representation space to another one based on predefined analytical expressions. These latter are composed basically from constants, variables and elementary functions ($\sin, \cos, \log, \text{etc.}$), which are related analytically with standard mathematical operations. Intuitively, looking for the image of every point from the input intervals via a given function is a bit absurd. Herein, determining images of the interval inputs through an interval function implies to seek and bound sets including each possible output originating from the interval expression presented by the function. This understanding has introduced the notion of inclusion functions. Let denote by $[f([x])]$ the inclusion function associated to $f([x])$. In accordance with the interval arithmetic, the inclusion frame used to represent $[f([x])]$ is an aligned-axis box, which always satisfies $f([x]) \subset [f([x])]$.

Substituting every real variable by its interval value is the easiest manner to build inclusion functions. This method is efficient especially for monotonous interval functions where the natural inclusion function are spontaneously optimal and too tight [202]. However, for non-monotonous functions, obtaining the smallest possible enclosures for the inclusion function results is not always guaranteed (cf. Figure 2.1).

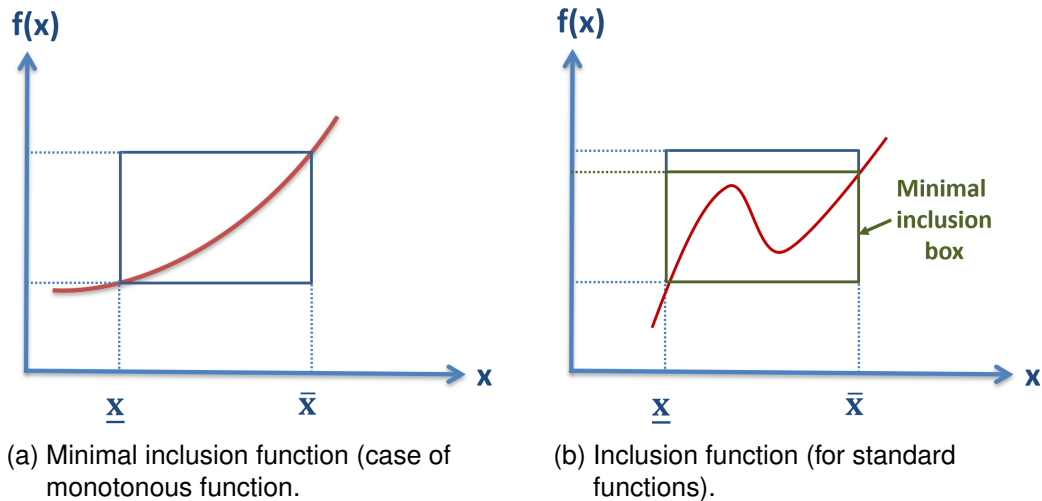


Figure 2.1: Examples of inclusion functions.

Indeed, the natural inclusion function may be too large due to the dependency effect (this issue will be detailed in section 2.4). To resolve this shortcoming, sharper enclosures are provided thanks to various polynomial and Taylor series-based inclusion functions [78], [314]. Another option to address inclusion function estimation is through numeric algorithms that employ intensively inclusion tests to contract and explore the smallest sets enclosing $f([x])$ [154]. In summary, distinct inclusion functions can be assigned to a given $f([x])$. To avoid making the interval computation cumbersome, a trade off between simplicity and quality of the inclusion function should be maintained.

2.2/ MODEL-BASED VS. DATA-DRIVEN APPROACHES FOR IVs

In an effort to clarify later how the interval analysis may be used in the benefit of the intelligent navigation strategies, the required approaches to perform the autonomous navigation task are classified into two bunches: model-based and data-driven methods². The model-based methods rely mainly on an analytical representation of the concerned system expected behavior through mathematical models [9]. In such a manner, outputs of the established model are exploited in real-time to control and/or monitor the real system performances. In contrast, the data-driven methods skip the modeling phase. Instead of modeling the system behavior and its outputs under several conditions, more attention is given to extract the system properties [150]. This may be undertaken based on learning approaches, statistics, etc. For sure, every class of methods has particular weaknesses and advantages. In that respect, the employment of the interval analysis to improve performances of each class of approaches may have different prospects and practical purposes. Accordingly, features of modeling practices for IVs and the data analysis procedures are discussed below.

2.2.1/ MODEL-DRIVEN APPROACHES FOR IVs

Through theory and experiments, model-based development is a valuable mean to monitor mechanisms and gain a deep knowledge about their behaviors. In particular, the realized range of models for IVs cover practically all essential components of the stand-alone navigation systems. For instance, state-space representation for IV is not feasible without specifying a motion model to facilitate studying the system evolution. For their simplicity and linearity, the constant velocity/acceleration motion models have a broad application in practice [177]. Other models address the vehicle orientation to refine the estimation process [256]. Furthermore, several complicated motion models such as the constant turn rate/velocity and constant turn rate/acceleration take into account the heading direction angle of the vehicle to be more comprehensive [25].

Differently, the IV control layer consists principally of a set of mathematical models that guarantee the convergence towards a given target or ensuring a stable tracking of a predefined trajectory [268]. On top of that, the kinematic and dynamic constraints of navigation systems must be accurately defined by models to find out the vehicle realistic responses to controls [67].

²This issue was detailed during the workshop “Formal Methods vs. Machine Learning approaches for Reliable Navigation” (FRCA-IAV) of the 2019 IEEE Intelligent Vehicles Symposium (IV 2019), available at: <https://iv2019.org/workshops/>.

As can be seen from [20] and [269], much modeling work has been dedicated also to represent obstacles by boxes, circular or elliptic orbital shapes, etc. Through this geometric representation of obstacles, plenty of model-based approaches, such as the limit cycle, are then used to derive obstacle-free trajectories [45]. More complicated models permit avoiding moving obstacles by analyzing the variance in their positions [179]. Moreover, a huge part from the in-road emergency management strategies are conducted on the basis of formal model checking approaches [16], [141]. The overall navigation process is described via a finite-state model and the system safety is verified at every transition from a state to another. Similarly, the use of model-driven techniques for diagnosis objectives is common. Several quantitative behavioral models are put in charge of characterizing the navigation system nominal operation [168]. Captured deviations between reality and these models outcomes help to detect faults. As clear, modeling is omnipresent in the different components of the navigation system. At this stage, it is reasonable to explore factors ruling the modeling reliability and precision for IVs. Cost and feasibility of the model development also should be analyzed.

First of all, the high complexity and non-linearity are among conventional aspects of models. Both the quantitative/qualitative as well as continuous/discrete features of the modeled aspects must be thoroughly mastered. Even more, modeled parts or aspects from IVs cannot be considered separately. As already stated, the autonomous navigation systems are large scale processes that are composed of highly interacting sub-entities. Neglecting any part of the IV subsystem may degrade the whole model precision. Involving the overall subsystems and integrating all the intervening parameters into the modeling phase is the key to reach high fidelity. In such a way, IVs should be described by holistic and heterogeneous models, where each modeled sub-entity has a specific time scale, architecture, etc. Therefore, dissimilarities between the sub-models and the uncertainty associated to their interactions should be attentively considered.

More importantly, it is imperative to gain a deep knowledge about all aspects related to the concerned system to succeed the modeling phase. The more detailed the model description, the more accurate its outcomes. Prototypes of models can be simple with low dynamics, where only linear theories are applied. However, to have a deeper insight of the modeled process responses, complex prototypes utilize more sophisticated non-linear models [233]. The most prominent intervening phenomena should be studied and involved into the model development process. Respectively, modeling for IVs is turning progressively into a multi-aspect-aware design. Actuator modeling is a clear evidence that proves this fact. It is worth reminding that actuators are the common operative part from IVs. The actuator electrical aspects, the effects of coupling between electrostatic forces, the inertia properties and the friction are among elements that must be well-examined to reach a satisfactory modeling performances for actuators [92], [100].

Otherwise, accurate models consider also events of realistic circumstances, where the navigation system is prone to various disturbances, parameter variation and electrical noises. In this respect, the study reported in [180] proved that aside of the non-linearity and the hysteresis effect, the luminosity or/and the temperature are the most decisive elements when modeling certain sensors.

Due to the safety critical context, ensuring accurate and reliable modeling for IVs is a priority. For that reason, few modeling engineering practices are widespread in the autonomous navigation area. First, it is strongly recommended to determine the modeled system responses produced by a wide range of potential configurations to enhance the

model accuracy. Another efficient technique to meet accuracy is comparing findings of the established model with experimental results in both time and frequency domains. Sensitivity analysis can also help in distinguishing the most important parameters ruling the modeled process. Thereby, the analytical formalization of the model may be built based on the most significant parameters. For practical reasons as decreasing the model complexity, simplifications can include the less influencing elements.

Within all the struggle made to improve accuracy of IVs' modeling, anxiousness about modeling errors remains existent for yet. Even more, the assessment of the model credibility is more challenging when the model complexity rises. Actually, modeling errors are among main reasons that complicate the validation phase of IVs. The definition and validation of the model and its parameters usually necessitate specially designed experiments and statistical approaches. Thus, a huge number of realistic testing scenarios and hundreds of millions of miles must be driven to demonstrate the autonomous vehicle reliability [157], [212]. According to the undertaken discussion above, Figure 2.2 summarizes the engineering practices leading to a reliable modeling for IVs.

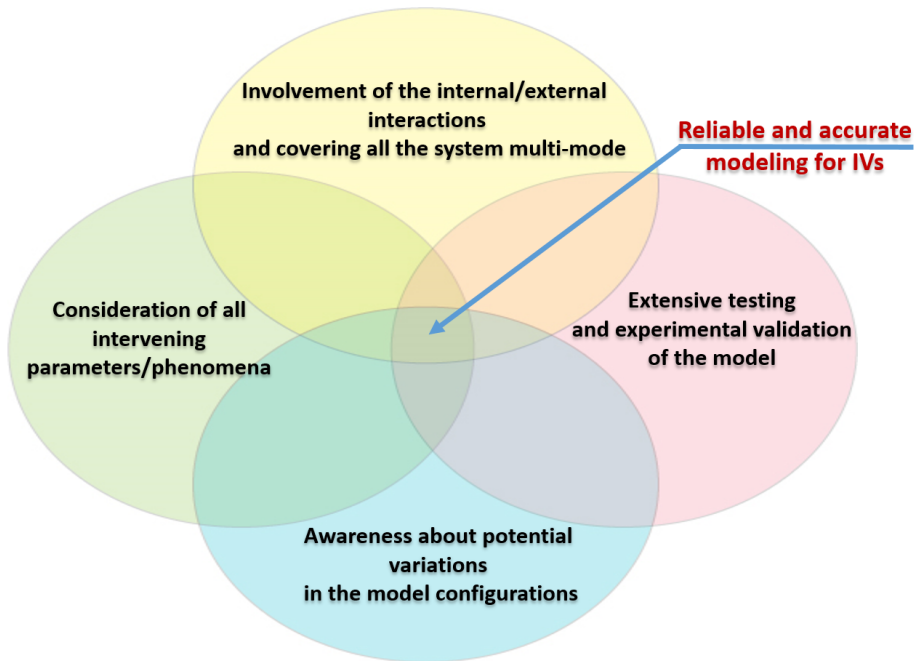


Figure 2.2: Main components of reliable modeling for IVs.

To conclude, two important questions raise at this level: (i) Is it possible to develop comprehensive models that may capture the system behavior according to its different operational modes? and (ii) If so, is it judicious to waste efforts and time to establish such complicated models?

As an answer to the questions above, a part from the research community admits that relying only on models is not conducive to the development of complex man-made engineering systems. Especially for large scale systems, modeling is pointless and inefficient in replicating behaviors of multi-modal processes. Beyond that, the usage of data-driven approaches is seen lately as a cut-off with modeling [163]. Motivated by the irrelevant cost of model development in terms of time and effort, data analysis is an adequate methodology to ensure IV operational efficiency. Principle of the data-driven approaches and their application for the benefits of IVs is tackled hereafter.

2.2.2/ DATA-DRIVEN APPROACHES FOR IVs

Nowadays, no one can deny that data is a potent source of knowledge. The application of data-driven approaches for IVs is relevant whenever their practical and operational cost is low and data is accessible (the IV system is observable). As outlined in [201], data collections involved into the model-free approaches can be divided according to the time-line level into three categories: historical, current and predictive data. These collections (especially the historical data) may be processed, interpreted and exploited in the decision making for IVs instead of models. Indeed, the data-driven approaches are almost statistical techniques attempting to extract qualitative and informative useful deductions from the data structure and distribution in the temporal and spatial domains. To reveal the required deductions, a set of quantitative relations ruling variables are taken as principal descriptive characteristics of the system. Foremost, the system features are roughly marked via the hidden auto-correlation and cross-correlation properties estimated through samples of the variable attributes [343].

Mainly, the data-driven approaches are constructed through two general steps. The first one can be identified as the offline phase. During this stage, the system variables, inputs and outputs that may play an important instructional role and describe in the best way the studied system are selected. Samples of data flows associated to the selected variables are collected in a passive manner. Instead of modeling directly the system behavior, an implicit model that targets the statistical relations between variables corresponding to the recorded samples is then built to reach the desired cognitive knowledge about the system. The implicit model can be obtained through a training technique thanks to a learning mechanism. It can be also constructed via the explicit use of statistical indexes employed for data analysis [343]. In the online phase, the implicit model exhibiting the system historical properties is taken as a reference description for the system nominal operation. The online data samples are monitored and the acquired knowledge during the offline phase is exploited to facilitate the prediction or the decision making.

The appearance of some powerful conceptual frameworks dedicated for data extrapolation in the worldwide markets has motivated the use of the data driven approaches. In this context, the Cloud framework has become a common computing framework for robotic applications. As a matter of fact, the IV community has largely taken advantage of the Cloud huge capacities in terms of rapid computation and data storage [160].

As clear, the model-driven approaches are conducted in a way quite differing from that in use for the data-driven techniques. In the sequel, additional dissimilarities between both methodologies are highlighted:

- A significant difference between the data-driven methods and the model-based ones consists of the provided accuracy-level. Frequently, model-based approaches are less accurate because of the modeling simplifications made for technical purposes especially for non-linear behaviors.
- Unlike the model-driven approaches that their complexity increases relatively to the number of involved variables, the big data concept witnessed in the IV field may be beneficial for the data-driven methods. The extra number of sensors implemented into IVs contributes in capturing more comprehensive features. The availability of multiple and distinct sources of information would underline more redundancy and dependency between variables. Thus, better quality and accuracy of the data structural analysis are reached.

- As the model-driven approaches, some data-driven methods are sensitive to non-linearities. Nonetheless, this limitation has been eliminated thanks to the data analysis flexibility. In this context, the kernel-based method has been introduced to permit a broader application of data analysis on non-linear systems [136]. Thanks to a mathematical kernel function, data are transformed to a new dimensional space, where the system can be described through linear relations.

It is noteworthy that the employment of the data-driven analysis without guarantying at first the data availability may be troublesome. It is meant by data availability the precautions taken in to prevent the loss of sensor-issued data [332]. Consequences linked to the loss of data even temporarily due to intermittent failures will unavoidably propagate to the data analysis level, which leads to improper interpretations [227]. Not only the information availability is required, but the freshness of the run-time data is also responsible of correctness and exactness of the established analytics. Indeed, the verification of the data freshness aims to inspect the data validity in the time space. All along the IV functional lifetime, using expired samples not corresponding to the current real-time sampling step must be strictly avoided. In this context, recent studies about recognizing the data validity interval time acquire special relevancy [110].

Another important issue concerning the efficiency of the data-driven approaches is related to the cognitive knowledge, which may be extracted from data. Developers of the data-driven analytics should verify in prior whether the knowledge-derived from the data structure is sufficient or not to report all the system behavioral aspects even under uncertainty. Most notably, a low value density data used to characterize the studied system does not lead necessarily to insufficient or not entirely matched knowledge. Extracting the required relevant information is tightly linked to the nature/quality of data. In other words, an appropriate feature extraction depends the most on the diversity of the gathered range of data. A large amount of correlated historical data can be useless, whereas low density data may cover all the system multi-mode.

Furthermore, in order to facilitate the feature extraction and avoid the usage of large scale data amounts, several data-driven approaches are conventionally adopted to mitigate and alleviate the massive quantity of initial data amounts. Methods such as principle component analysis, independent component analysis and support vector machine have the capacity to identify the significant data and derive conducive information during the system characterization phase [155].

Finally, the biggest problem witnessed with the data-driven approaches is being vulnerable against uncertainty. The historical properties of the system can be misused if the online data are uncertain. Even a slight deviation in data attributes compared to reality can lead to misleading interpretation of the data content and structure. For this reason, the improvement of the data-driven analysis in terms of robustness against uncertainty is still an open research topic.

2.3/ INTERVAL-BASED APPROACHES RELATED WORK

Potential limitations that may be faced for IV system designers whether through model-driven and data-driven methods have been reviewed and analyzed. Hence, the current section aims to explore the interval analysis strengths that may put in the favor of modern

IVs. Actually, the interval-based contributions have never been comprehensively classified and examined while taking into account separately specifications of the model-based and data-driven methods. In the sequel, the theoretical and practical advancements proposed to reinforce the interval set-membership modeling and data analysis are summarized regardless to a particular application area.

2.3.1/ INTERVAL-BASED MODEL PROCESSES

The development of interval computing models are becoming a common reliability design practice with a wide application in all engineering fields [50, 187, 284]. Augmented accuracy models have been ensured due to the set-theory [101]. This direction has accelerated the diffusion of paradigms of interval process model or interval system [64], [288]. The notion of interval process model is of utmost utility especially for reliability critical applications, where the scarcity of data samples prohibits the utilization of the probabilistic modeling or the data-driven analysis.

The full-interval based models exclude any probabilistic or stochastic calculation to obtain guaranteed findings. Instead probabilities, a methodological strategy is generally selected to proceed a realistic and reasonable transformation of data to intervals. This step can be undertaken with the help of a statistical support, including the system historical properties or by creating a kind of link between the system parameters and the uncertainty influencing factors (cf. Figure 2.3). Then, guaranteed findings of the model are estimated thanks to the concept of the interval-valued functions and notions reviewed in section 2.1. Let consider an interval system of n inputs and m outputs, denoted respectively by $x_{i=1..n}$ and $y_{j=1..m}$. The general layout of such a system is illustrated by Figure 2.3.

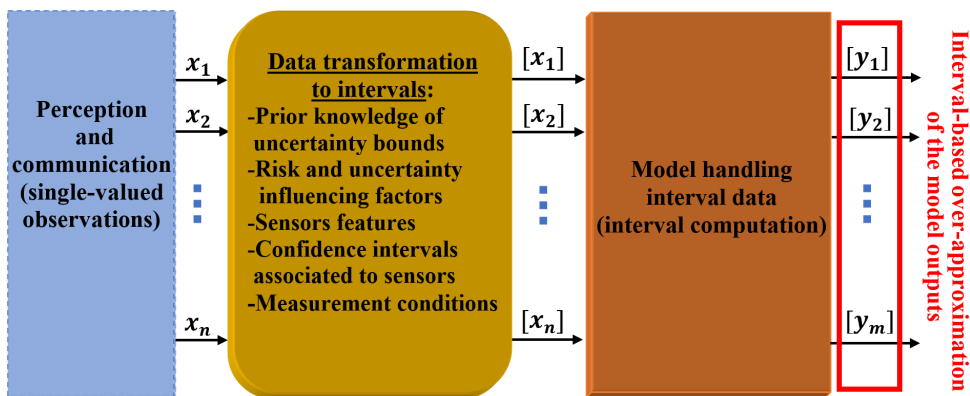


Figure 2.3: Interval process model.

In order to give interval models a more potent role in studying uncertainty propagation into systems and enlarge their field of application, numerous researchers in the reliable computing area of expertise have focused in extending several advanced algebraic computation systems and optimization processes to handle intervals. Accordingly, plenty of contributions have discussed theories and properties related to the existence/uniqueness of solutions associated to various analytical interval-based problems. Algorithms to ensure a systematic and quick convergence towards solutions of systems of nonlinear interval equations have been tremendously suggested in the literature [24]. Since several models are based on the representation of the studied problem in form of a polynomial equation, attention has been paid to methods of finding roots of polynomials with interval

coefficients [339]. Much research work has been also tackled to formalize approaches to proceed numerical integration and derivative computation for interval functions. This fact contributed also to define efficient approaches dedicated to solve sets of differential interval inequalities [334]. In particular, the recursive evaluation of derivatives in a bounded context has lead to the emergence of the automatic differentiation [239].

Apparently, there is an ongoing struggle and an extensive research work to evolve the interval-set theories to cover all the mathematical issues dealt usually with the real arithmetic. The novel interval extension of the finite element method is an illustrative example of the continuous work to enlarge the interval mathematical use-cases [220]. Thanks to the theoretical advances involved into this extension, it is possible to solve a large range of engineering problems and perform a space discretization with uncertain parameters.

Aside from the full interval-based models, the interval analysis is commonly used to boost the quantification of probabilistic uncertainty. According to the authors in [62, 305, 342], joining together the interval-based and probabilistic modeling of the uncertainty evolution into processes allows the consideration of wider varieties of uncertainty types (aleatory/epistemic uncertainties) and increases the model determinism. For such combined models, the interval analysis has as a principle role to validate the estimated probabilities once the convergence between both methodologies is confirmed.

Instead of co-joining the probabilistic and the interval-based reasoning, it is also possible to construct full-interval probabilistic models [104], [146]. The interval analysis in this case is efficient in overcoming the shortcoming related to imprecise probability distribution [324]. Such an imprecision is caused generally by an imperfect and incomplete knowledge about sensor features. To overstep these problems, interval probabilities are estimated through Probability Distribution Function (PDF) via bounded convex sets. In [331], both the belief theory and the interval analysis have been used in conjunction to perform more reliable characterization of uncertainties.

In the literature, hybrid interval models do not include only the interval-based/probabilistic uncertainty quantification frameworks. Instead of being the main component from the established model, the interval analysis may be used to reinforce the reliability of other heuristic models. Side by side with these heuristics, the interval analysis permits the consideration of the variance in the original model parameters. In such a context, the interval analysis has been joined with a fuzzy system where the fuzzy rules were defined as interval-sets [35], [188]. The development of similar interval fuzzy systems has been tackled in details in [183]. In the same manner, interval neural networks have been presented in [121], where the hidden input weights were intervals. Based on the examined literature above, there is an obvious intention to unify the interval analysis with other uncertainty assessment techniques. This direction aims to reach full operational reliability and accuracy of model based systems. Relying on several methodologies of different nature is definitely beneficial for reliability.

Otherwise, sensitivity analysis can be used as a qualitative enhancement for model establishment by interpreting the analytical formalization of the interval process via examining the uncertainty impacting the model inputs and revealing these uncertainty influence on the corresponding outcomes. The study reported in [283] presents an example of the sensitivity-based improvement for the interval-based plants. The work of [254] is another case of study where a sensitivity analysis-based method has been utilized to study the variation in parameters of the interval model process. It helped to properly define end-points of interval-valued attributes.

2.3.2/ INTERVAL-BASED DATA ANALYSIS

The development of interval-based data-driven methods to characterize the uncertainty impacts into systems is less common relatively to the interval-based modeling. On the one hand, the practice of such methods requires a strong background about statistics, exploratory analysis and the interval arithmetic. On the other hand, the interval data-driven approaches are convenient when there are no reasonable assumptions to be made about the uncertainty evolution. In such a case, the typical solution followed in the literature to overcome this limitation is to augment the system observability by adding sensors, which is not cost-effective.

According to this understanding, the application of the data-driven approaches combined with the interval analysis was mostly for diagnosis purposes [83, 122, 132]. When the system is under potential faults, the predefined assumptions about the uncertainty evolution cannot hold true. Even more, it is difficult to solve conflicts between redundant sensor measurements. In this sense, large varieties of diagnosis strategies belong to the data-driven class of methods. Whether during the offline feature extraction phase or in the run-time system operation, analysis proceeded on uncertain data is ineffective and can provide a misleading decision support. For that reason, enhancing the data-driven diagnosis robustness against uncertainties through a guaranteed interval-based computation was a relevant research line.

It is quite evident that matrices are the natural data support to store and arrange systematically the gathered samples and observations of the system. Without doubt, matrix computation is essential for the data-driven approaches. Unlike the standard ones, the interval matrices are more convenient to account for the uncertainty impacting values of the stored quantities. In spite of their apparent advantages, some algebraic problems are difficult to proceed with interval matrices. For instance, proving that an interval matrix is invertible and finding its inverse are not feasible in a straightforward manner as the case for the real arithmetic [222]. Theoretical demonstrations as well as practical algorithms to define elements of the inverse matrix are available in [248]. In addition, the interval matrix decomposition by determining the interval eigen values/vectors is among the most discussed algebraic properties in relation to the interval data-driven analysis [79], [249]. As a fact of reality, the eigen values/vectors are largely involved in the resolution of linear interval equations. As well, several statistical indexes in the literature are formulated in function of the eigenvalues associated to the initial system [218].

The determination of the inclusion sets for interval eigenvalues was tackled in [142] and [143] based on theories devoted to symmetric interval matrices. Indeed, matrix symmetry invokes extra-dependencies between the matrix components, which complicates the interval eigenvalues computation. Accordingly, the authors in [142] and [143] provided algorithms to calculate the eigenvalues for both unsymmetric/symmetric interval matrix. Similarly in [61], solutions and numerical examples of the interval eigenvalue analysis were proposed based on some simplifications made on the matrix components to balance between the complexity and accuracy of the interval algebraic eigenvalue problem.

As key features of systems, the computation of the variance, covariance and correlation is the backbone part from most of the data-driven exploratory analysis. Hence, introducing computationally low-cost algorithms to calculate these statistical metrics for interval data was an issue of top priority to build practical interval data-driven frameworks. In [107], the lower and upper endpoints of the variance interval value were estimated separately.

Nevertheless, the suggested algorithms were restricted to some situations and cannot be generalized for all cases of interval samples. A similar work was presented in [153] to estimate respectively the inferior and superior bounds of the correlation under interval uncertainty. The authors in [318] presented more generic algorithms to compute several statistical metrics for interval data, including the variance parameter. Recently, less computationally demanding approaches, which are based on the use of interval power iterations and linear matrix inequalities, were proposed to extract tight intervals of the variance, covariance and correlation starting from interval data samples [166].

As obvious, the computation of the aforementioned statistics under interval uncertainty is quite challenging. Even more, the computational demands of the proposed algorithms dedicated for this purpose should be carefully examined. One more alternative methodology to derive reliable statistics for intervals consists in the interpretation of the geometrical distribution of the data structure in the n -dimensional space. Instead of the exact calculation through full interval sets, some computational tricks used the symbolic spatial representation of data to ensure that the exact results of the statistics are reached while considering the minimum/maximum sample values [87], [123].

As mentioned before, one major utility of the sensitivity analysis is improving the modeling quality. Nonetheless, the employment of the interval data-driven processes to perform sensitivity analysis appears as very promising. This direction is quite reasonable since the study of sensitivity may be carried out through statistics. Compared to other conventional approaches, the interval-based/data-driven sensitivity analysis method proposed in [236] has shown better performances due the ability in dealing with the aleatory and epistemic uncertainties in same time. This privilege makes from the interval data-driven sensitivity analysis suitable for uncertain large scale dynamic systems.

2.3.3/ DISCUSSION

Underneath the debate that has been undertaken in section 2.2, neither the model-based approaches nor the data analysis techniques seem to be fully infallible. Each class of methods has particular pros and cons. Hence, the design of navigation strategies and approaches must be well-tailored regarding to the nature of the particular task achieved by the IV. Within a cost/efficiency-aware design policy, the system specifications should be examined to finally select the most appropriate methodology.

As early explained, the interval analysis may in a way or another compensate inaccuracies of both model-based and model-free approaches. It intervenes to turns these approaches to guaranteed. Already used to deal with modeling errors, the interval analysis permits to account simultaneously for several uncertainties including but not limited to inaccuracy related either to external disturbances or interactions between the model sub-entities, non-linearity, etc. In a completely easy manner, configurations with large range of variation are tested via the interval arithmetic to evaluate how models act. Consequently, interval analysis may be regarded as a valuable mean to develop and validate models without wasting time and efforts.

In addition, the data-driven approaches may take advantages from the interval-based computation to provide uncertainty-aware statistics. By counting on the set-representation of data, the interval analysis may be an efficient remake for technically-related uncertainty sources for IVs, such as data validity in the time horizon, incomplete scenarios for the feature extraction phase, etc.

Moreover, according to the above revised related work, the interval analysis-based approaches may be developed and implemented flexibly in several distinct ways. Foremost, for each problem studied via the interval analysis, there are a rich literature and large propositions that lead to guaranteed solutions for the problem through different policies. In respect to the interval-based reasoning, when the explicit theoretical-based algorithms are cumbersome and complicated, it is possible to exploit the geometrical and spatial distribution of data to characterize uncertainty all along the decision support process.

Finally, both the model-driven and the data-driven interval methods may reciprocally complement each other. For instance, the authors in [84] have extracted the system statistical properties via data-driven interval-based approaches. Later, these properties have been exploited to increase the model accuracy while using less samples for deriving the probability function of the uncertainty distribution.

2.4/ PESSIMISM IMPACTING INTERVAL-BASED METHODS

The main problem that disallowed a wider application of the interval-based guaranteed methods is the interval arithmetic conservatism. For every step from the computation process, the range of accumulated uncertainty attributed to interval results due to the pessimism becomes larger. Especially for the autonomous navigation, the pessimism can be disturbing. It is quite difficult to take an appropriate decision when the navigation parameters are enormously uncertain. Moreover, precautions against the uncertainty worst cases should be taken for safety assurance. Hence, over-conservative safety countermeasures may be selected. Such a behavior is not optimal and may degrade the navigation performances. In the following, the main pessimism sources are identified and classified into three main origins.

- **Dependency effect:** The pessimism may arise from the memory less-nature of the interval-based computation. To reach guaranteed results, the interval arithmetic over-estimates variables in exaggerated way. In such a manner, variables occurring several times in one expression are assumed as independently varying over their enclosures. This side effect from the interval computation is known in the literature by the “dependency effect”. It can be easily illustrated by the example demonstrated in equation (2.5), where $[x] = [-1, 3]$. Although it is evident that $x^2 + x = (x + \frac{1}{2})^2 - \frac{1}{4}$, $[x]^2 + [x]$ is a pessimistic over-approximation of $([x] + \frac{1}{2})^2 - \frac{1}{4}$:

$$\begin{cases} [x]^2 + [x] = [-1, 2]^2 + [-1, 2] = [0, 4] + [-1, 2] = [-1, 6] \\ ([x] + \frac{1}{2})^2 - \frac{1}{4} = [-\frac{1}{2}, \frac{5}{2}]^2 - \frac{1}{4} = [0, \frac{25}{4}] - \frac{1}{4} = [-\frac{1}{4}, 6] \end{cases} \quad (2.5)$$

- **Wrapping effect:** Aside from the “dependency effect”, the pessimism is drastically emphasized through the “wrapping effect” phenomenon. Due to the non-compact form of interval wrappers, exact sets resulting from a given interval mathematical operation are systematically over-approximated. A typical example depicting clearly the wrapping effect resides in the matrix multiplication (example inspired from [154]). According to the interval arithmetic, the product of two matrices A and $[x]$ is given below:

$$A = \begin{pmatrix} 1 & 1 \\ 0 & 1 \end{pmatrix}, [x] = \begin{pmatrix} [-1, 0] \\ [1, 2] \end{pmatrix} \implies A.[x] = \begin{pmatrix} [0, 2] \\ [1, 2] \end{pmatrix} \quad (2.6)$$

However, the real set resulting from the product of both matrices is defined as $B = \{A \cdot x \mid x \in [x]\}$. The non-optimality of the interval computation, which is mainly caused by the “wrapping effect”, is obvious in Figure 2.4.

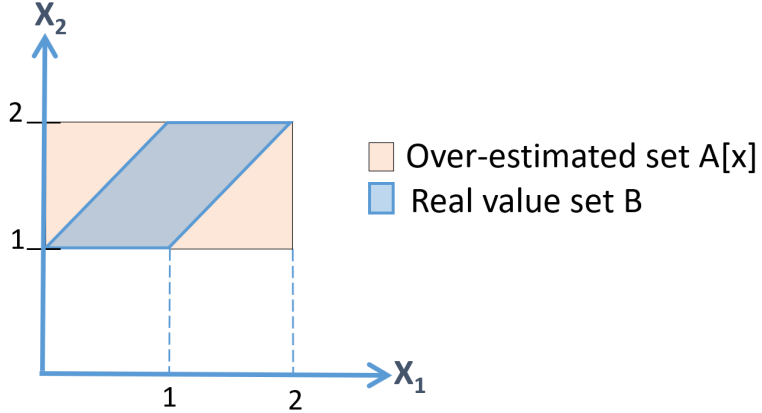


Figure 2.4: Pessimism related to the wrapping effect.

- **Pessimism non related to interval arithmetic:** An additional important source of pessimism, which has no explicit connection with the interval analysis, is linked to the initial exaggerated uncertainty assignment for interval data. In general, a prior knowledge of the uncertainty bounds is assumed to transform data from its single value to interval. However, there is no clear strategy to fix each interval minimum/maximum uncertainty bounds. Even more, these boundary values can change relatively to the run-time circumstances. To avoid such a problem, interval bounds are generally selected while admitting arbitrary excessive amounts of uncertainties.

2.5/ CONCLUSION

This chapter presented a deeper insight into the interval analysis different aspects. Not only the interval arithmetic fundamentals were detailed, but also the various possible methodologies to use the interval set-membership reasoning for a better uncertainty characterization. To be more comprehensive, the light was focused on the interval-based modeling and data-driven analysis advantages. In the remaining chapters, several interval-based solutions for autonomous navigation are proposed. These contributions count on the interval analysis to deal with the already discussed Intelligent Vehicle (IV) complexity-issued problems witnessed currently in the literature. Besides, a particular interest will be devoted to overcome the interval arithmetic pessimism for optimality purposes. Accordingly, the proposed contributions for reliable autonomous navigation are an alliance between a set of interval data-driven and model-based methods.



SAFE AND RELIABLE NAVIGATION

3

REACHABILITY ANALYSIS FOR ADAPTIVE AUTONOMOUS NAVIGATION BASED ON SEQUENTIAL WAYPOINTS

Flexible autonomous navigation approaches open opportunities for more efficient risk management back-up solutions. Navigation strategies based on waypoints reaching are one way to meet the flexibility requirement (cf. subsection 1.4.1, page 30). Nonetheless, only few novel waypoint selection approaches have been proposed in the literature [53, 298, 309]. Besides, the current related-work to this topic is mainly focusing on optimizing this approach in terms of stability, traveling time and path smoothness [140], [242]. More importantly, safety assurance methods, devoted to the waypoint-based navigation, are up to now restricted to obstacle avoidance [275].

Obviously, safety of the waypoint-based navigation needs to be studied from broader prospects. Despite its huge importance, the appropriate and guaranteed reaching of next waypoints under uncertainty is insufficiently investigated. Trajectory re-planning methods with the use of interim targets were used in this context in [63]. An error feedback controller was employed to minimize waypoint tracking errors in [120]. Nevertheless, consistency of the adopted error model was not proven. With a posterior knowledge of the navigation environment, a view-matching vision-based approach was utilized to cross the selected waypoints in [226]. Differently in [333], the number and size of waypoints were reconfigured via a genetic algorithm to reduce the path following errors. According to the Software verification concept, the authors in [185] developed a risk management that checks the temporal and logic behavioral aspects from the navigation process. Needless to say, Software checking approaches may monitor a limited number of inputs, but cannot deal with the high uncertainty of the navigation dynamics. As a matter of reality, the lack of reliable safety guarantees for the waypoint-based navigation has a profound impact on its perspectives. Without the required warranties, it remains restricted for slow-motion navigation systems and environments without severe risks.

As an efficient predictability technique, Reachability Analysis (RA) has been recently exploited to solve several IVs-related problems. Path parametrization, optimal control, vehicular communication security, stochastic filtering and risk identification are among the RA use-cases [69, 70, 114, 169, 273]. In this chapter, a specific RA scheme is developed to perform safety verification for an already proposed flexible Navigation Strategy based on Sequential Waypoint Reaching (NSbSWR) framework [297], [298]. In the following, the overall NSbSWR navigation approach is detailed. Then, a novel interval RA-based

risk management for NSbSWR is introduced. The proposed approach is based on the already discussed interval-based modeling (cf. subsection 2.3.1, page 42). It includes also a set-membership data analysis step to deal with the interval arithmetic pessimism (cf. section 2.4, page 46). The RA-issued results are exploited then to re-configure the navigation parameters in order to guarantee the appropriate reaching of waypoints under uncertainty.

3.1/ NAVIGATION BASED ON WAYPOINTS (GENERAL CONTEXT)

This section presents the adopted NSbSWR framework for flexible and safe navigation through waypoints. The simplest way to determine these waypoints is to pick up few set-points from an already available trajectory [151]. The expanding tree and grid map-based approaches were also used for the same aim [279].

In this chapter, the tackled NSbSWR framework corresponds to the one introduced in [297, 298]. More precisely, the previous work reported in [297] explained the suggested NSbSWR principle as well as the applied target assignment method (selection of a particular target to be reached from a set of sequential waypoints). Meanwhile, the optimal selection of the sequential waypoints' configurations, i.e., each waypoint's position, orientation and velocity, is detailed in [297, 298]. Hence, this chapter proposes a reliable risk assessment and management strategy of NSbSWR under high uncertainties (in terms of perception and modeling). Therefore, there is no intention to detail here the selection of the waypoint configurations. A high level-planning task is devoted to accomplish this objective [298]. Correspondingly, the waypoints' configurations are modified in run-time depending on the environmental changes. The waypoint selection task includes also a limit cycle-based obstacle avoidance approach [18], [300]. In such a manner, the generated waypoints ensure a free-collision navigation. The rest of this section describes the proposed NSbSWR navigation system architecture. A general overview of the navigation based on waypoints as shown in [297, 298] is given below. The aim is to understand the main elements composing this kind of navigation in order to make after the focus on the main proposed components in this chapter.

At first, the overall control architecture dedicated to deal with such a navigation strategy is illustrated in Figure 3.1. This architecture includes the required blocks to simultaneously maintain a high level of flexibility and perform a navigation with provable safety. The main blocks of the proposed NSbSWR architecture are listed below:

- The “Waypoint disposition high level-planning task”, as already stated, provides the waypoints' convenient configurations [298].
- The “Control law” block guarantees an asymptotically stable reaching of the currently assigned waypoint (cf. subsection 3.1.1).
- The “Target assignment” block selects at every sample time the appropriate target to reach from the set of sequential waypoints (cf. subsection 3.1.2).
- The “Analytical analysis for safe waypoint reaching” block indicates the suitable conditions required for a safe reaching of every assigned target as shown in [297] (cf. subsection 3.1.3).

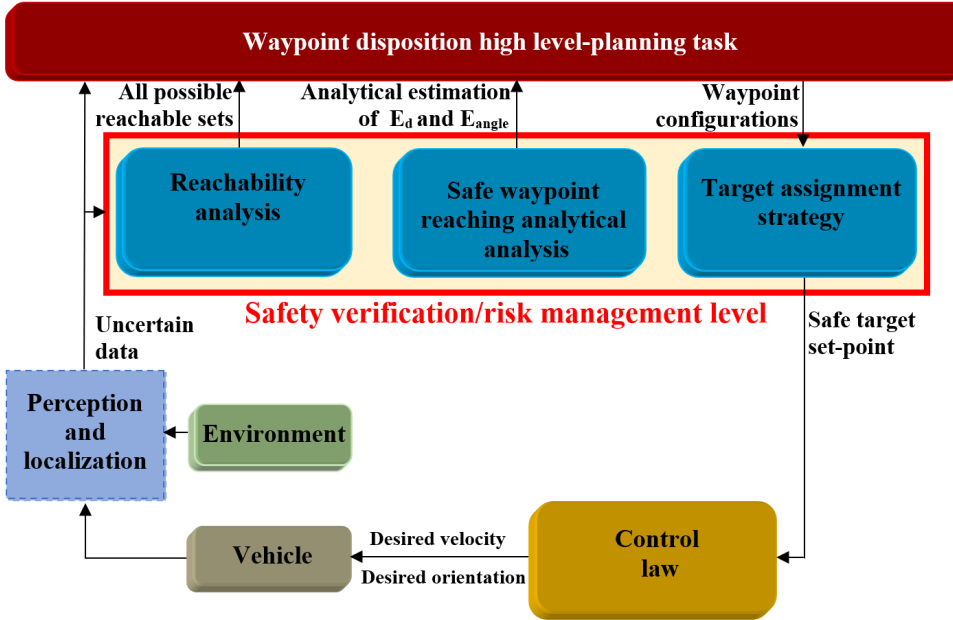


Figure 3.1: NSbSWR framework architecture.

- The “Reachability analysis” block is responsible of the risk assessment and management for the NSbSWR framework (cf. sections 3.2, 3.3 and 3.4).

The different components of the NSbSWR architecture are explained in the current chapter remaining parts.

3.1.1/ CONTROL LAW

The waypoints consist of a sequential set of static targets located in the navigation space. Correspondingly, any stable control law permitting to reach asymptotically the targets can be used in order to achieve the NSbSWR-based navigation task. The control law which is chosen for the NSbSWR in this thesis is detailed in the sequel.

Let (x_V, y_V, θ_V) denote the vehicle pose with respect to a global frame (O_G, X_G, Y_G) . Then, a typical tricycle kinematic model is used to describe the vehicle motion:

$$\begin{cases} \dot{x}_V = V \cos(\theta_V) \\ \dot{y}_V = V \sin(\theta_V) \\ \dot{\theta}_V = V \tan(\gamma_V)/l_b \end{cases} \quad (3.1)$$

Where V is the vehicle linear velocity and γ_V is its front wheel orientation. l_b indicates the vehicle's wheelbase. As can be seen from Figure 3.2, I_{cc} is the center of curvature characterizing the vehicle's trajectory. The curvature and the radius of curvature, which are respectively noted c_c and r_c , obey to:

$$\begin{cases} r_c = l_b / \tan(\gamma_V) \\ c_c = 1/r_c \end{cases} \quad (3.2)$$

At every sampling time, the adopted control approach acts on the relative pose between the vehicle and the target. For sake of simplicity, the adopted controller is supposed to

lead the navigation system towards targets with non-holonomic constraints (cf. Figure 3.2). Correspondingly, convenient values of V and γ_V are provided to drop steadily the relative pose to zero. Unlike other approaches that require full details about the tracked trajectory, the adopted control approach uses only the target pose (x_T, y_T, θ_T) and its velocity V_T . Either static or dynamic targets can be accurately reached with a desired orientation and velocity. Let us assume the following kinematic model for the target:

$$\begin{cases} \dot{x}_T = V_T \cos(\theta_T) \\ \dot{y}_T = V_T \sin(\theta_T) \\ \dot{\theta}_T = \omega_T \end{cases} \quad (3.3)$$

It is worth pointing that the following kinematic properties must be respected to successfully reach the target: $V_T \leq V_{max}$ and $r_{c_T} \geq r_{c_{min}}$. Notably, V_{max} is the vehicle maximum velocity and $r_{c_{min}}$ is its minimum radius of curvature ($r_{c_{min}} = l_b / \tan(\gamma_{V_{max}})$).

As previously stated, the control law objective is to make the relative pose between the vehicle and the target converge to zero. In this sense, consider the following navigation error states (e_x , e_y , e_θ) with regard to a local frame (O_L , X_L , Y_L):

$$\begin{bmatrix} e_x \\ e_y \\ e_\theta \end{bmatrix} = \begin{bmatrix} \cos(\theta_V) & \sin(\theta_V) & 0 \\ -\sin(\theta_V) & \cos(\theta_V) & 0 \\ 0 & 0 & 1 \end{bmatrix} \begin{bmatrix} x_T - x_V \\ y_T - y_V \\ \theta_T - \theta_V \end{bmatrix} \quad (3.4)$$

Similarly, d and θ_{VT} indicate respectively the distance and the angle between the position of the vehicle and the target:

$$d = \sqrt{(x_T - x_V)^2 + (y_T - y_V)^2} \quad (3.5)$$

$$\begin{cases} \theta_{VT} = \arctan\left(\frac{y_T - y_V}{x_T - x_V}\right) & \text{if } d > \xi \\ \theta_{VT} = \theta_T & \text{if } d \leq \xi \end{cases} \quad (3.6)$$

where ξ is a small positive value ($\xi \approx 0$). Otherwise, e_{VT} is an error variable that identifies implicitly the vehicle position-related error while considering the target orientation θ_T :

$$e_{VT} = \theta_T - \theta_{VT} \quad (3.7)$$

e_{VT} can be written in terms of e_x , e_y and e_θ as (cf. Figure 3.2):

$$\begin{aligned} \tan(e_{VT}) &= \tan(e_\theta - (\theta_{VT} - \theta_V)) \\ &= \frac{\tan(e_\theta) - e_y e_x^{-1}}{1 + \tan(e_\theta) e_y e_x^{-1}} \\ &= \frac{e_x \tan(e_\theta) - e_y}{e_x + \tan(e_\theta) e_y} \end{aligned} \quad (3.8)$$

Thus, e_{VT} is another error variable derived from (e_x, e_y, e_θ) . Finally, all errors are stabilized with the below expressions:

$$V = V_T \cos(e_\theta) + v_b \quad (3.9)$$

$$\gamma_V = \arctan(l_b c_c) \quad (3.10)$$

where equations (3.11) and (3.12) define v_b and c_c through a set of fixed positive constants $\mathbf{K} = (K_d, K_l, K_o, K_x, K_{VT}, K_\theta)$:

$$v_b = K_x [K_d e_x + K_l d \sin(e_{VT}) \sin(e_\theta) + K_o \sin(e_\theta) c_c] \quad (3.11)$$

$$c_c = \frac{1}{r_{c_T} \cos(e_\theta)} + \frac{d^2 K_l \sin(e_{VT}) \cos(e_{VT})}{r_{c_T} K_o \sin(e_\theta) \cos(e_\theta)} + K_\theta \tan(e_\theta) + \frac{K_d e_y - K_l d \sin(e_{VT}) \cos(e_\theta)}{K_o \cos(e_\theta)} + \frac{K_{VT} \sin^2(e_{VT})}{\sin(e_\theta) \cos(e_\theta)} \quad (3.12)$$

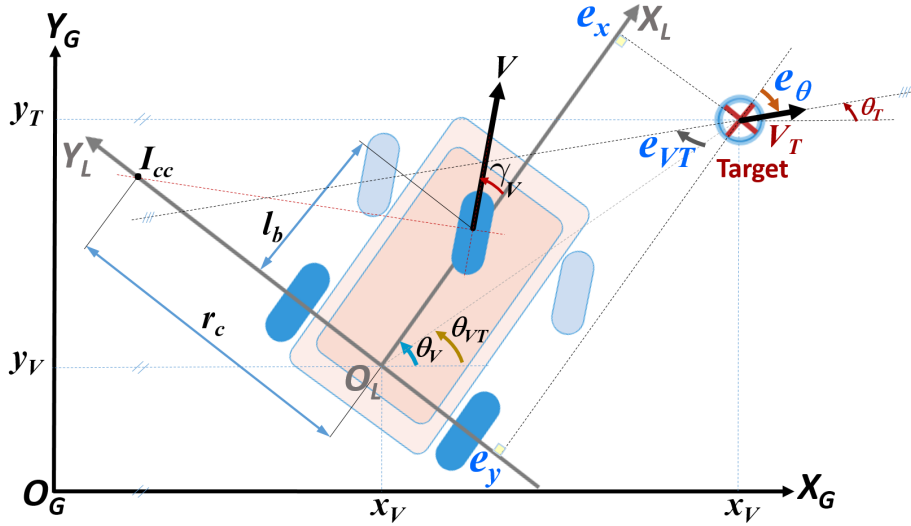


Figure 3.2: Vehicle/target configurations and control variables.

The complete proof of stability of the adopted control law is detailed in [297] and summarized in Appendix A. Otherwise, the evaluation of this latter in terms of smoothness, accuracy and flexibility was discussed in [19]. Regarding to its efficiency, the adopted controller has already shown very interesting performances in different applications such as car-following and multi-vehicle formations [9], [299].

3.1.2/ SEQUENTIAL TARGET ASSIGNMENT

Without a doubt, it is crucial to define a reliable strategy to switch between the different waypoints located in the environment. The NSbSWR is carried out thorough a quite simple target assignment strategy [297]. This latter is valid for any navigation context (slow/fast-motion, urban or highway roads, etc.). Henceforward, the currently followed waypoint is called target. At every sample time, the relative pose between the vehicle and the target is checked. Then, a decision about whether to keep moving ahead the current target or to shift towards the next waypoint is made. Let consider a set of sorted waypoints (see Figure 3.3). Every pair of successive waypoints P_{i-1} and P_i are separated by a distance denoted d_i . The orientation of P_i , named θ_{P_i} , is evaluated using coordinates of P_{i+1} . In this way, θ_{P_i} is compliant with the direction of the pre-selected path (orientation of the line joining P_i and P_{i+1}):

$$\theta_{P_i} = \arctan \left(\frac{y_{P_{i+1}} - y_{P_i}}{x_{P_{i+1}} - x_{P_i}} \right) \quad (3.13)$$

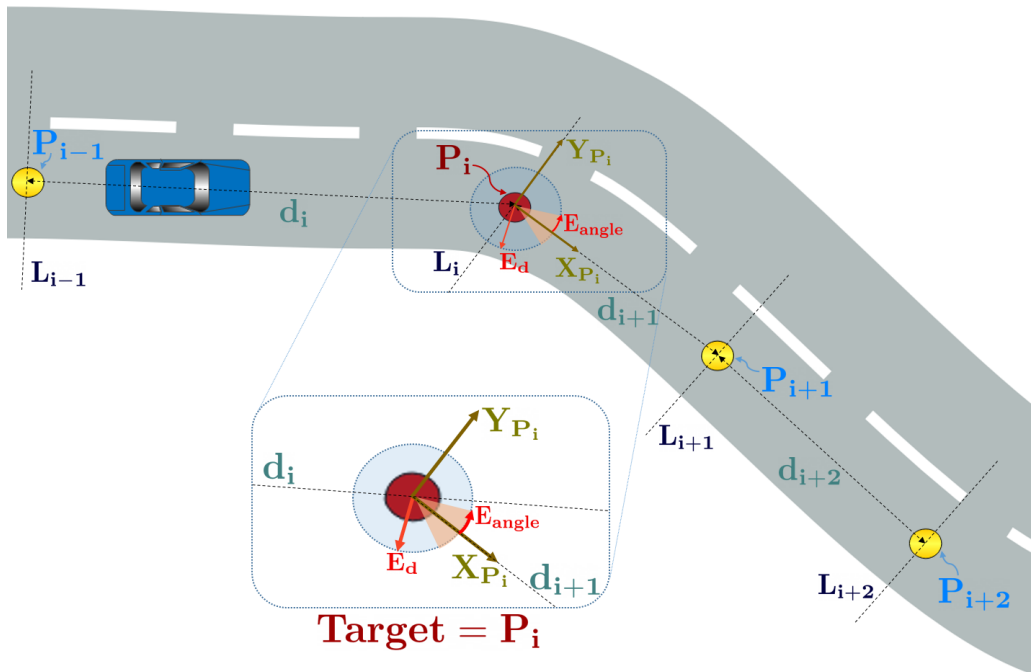


Figure 3.3: Description of NSbSWR target assignment strategy [297].

Accordingly, the waypoint assignment is managed via an algorithm that imposes the respect of the following constraints:

- **Condition 1: Safety-related constraint**

The link between the navigation safety and the waypoint switching rules is definitely strong. As long as the vehicle is far away from its target, the switch should not be accomplished to not deviate from the path given by the sorted waypoints. This primary safety constraint aims to minimize the waypoint following errors and prevents dangerous events. A waypoint is assumed as properly reached only if the vehicle attains the target immediate nearby. In this sense, every defined waypoint is joined with two authorized errors E_d and E_{angle} . An error circle with center at (x_T, y_T) and a radius of E_d may be drawn through these error boundaries (cf. Figure 3.3). The target is updated just when the vehicle crosses the circle borders and the orientation condition is validated:

$$(d \leq E_d) \quad \text{and} \quad (e_\theta \leq E_{angle}) \quad (3.14)$$

where d and e_θ are assessed by equations (3.4) and (3.5).

- **Condition 2: Liveness-related constraint**

Owing to control imperfections, it is not always possible to lead accurately the vehicle towards the target vicinity (the error circle). In such a critical situation, a backup countermeasure must be tackled to carry on the navigation and ensure its liveness. In that case, the local target frame $X_{P_i}Y_{P_i}$ is used. The perpendicular line L_i (Y_{P_i} axis) to the segment relating P_i and P_{i+1} is imposed to guarantee the navigation liveness (cf. Figure 3.3). As soon as the vehicle oversteps L_i and the vehicle coordinate x^{P_i} in $X_{P_i}Y_{P_i}$ implies that $x^{P_i} \geq 0$, the switch to the next waypoint should immediately take place.

Together, conditions 1 and 2 help to construct a safe target assignment strategy for autonomous navigation through waypoints:

Algorithm 1: Target assignment strategy [297]

Require: Waypoint series, vehicle pose, current target P_i .

Ensure : Sequential switch between waypoints.

```

1 if  $(d \leq E_d \text{ and } e_\theta \leq E_{angle}) \text{ or } x^{P_i} \geq 0$  then
2   -Switch to the newt waypoint  $P_i := P_{i+1}$ .
3   -Redefine  $E_d$  and  $E_{angle}$  associated to the new target.
4   -Designate a new local coordinate system  $X_{P_i}Y_{P_i}$ .
5   -Update the vehicle configuration w.r.t the new  $X_{P_i}Y_{P_i}$ .
6 end

```

3.1.3/ SAFETY GUARANTEES FOR TARGET REACHING

As explained earlier, the introduced waypoint assignment strategy uses a nominal strategy to evaluate the error values E_d and E_{angle} to switch between waypoints. From this sight, a well-studied selection of these parameters is mandatory, since they permit reaching the assigned target with proper conditions to reach. Even more, the conditions imposed by the chosen E_d and E_{angle} are essential to keep the vehicle into the road boundaries while moving towards the target. To cope with this issue, an analytical method that leads to an accurate definition of the error maximum thresholds, while considering the control law parameters, was presented in [297]. Within the derived boundary errors, the navigation would be safe. The analytical approach (cf. Appendix B) guarantees the control law ability to guide the vehicle to its current target with error values less than or equal to the derived E_d and E_{angle} . The established relationship between the control law parameters and the target configuration ensures the satisfaction of the vehicle kinematic constraints, which enhances the navigation safety.

It is important to notice that the analytical estimation of E_d and E_{angle} , according to [297], assumes that the vehicle initial orientation, denoted θ_{V_0} , to reach the current assigned waypoint is known with a particular range of uncertainty. Nonetheless, the vehicle dynamics and localization while moving towards the target are supposed as precise. This assumption is controversial and cannot hold true in case of highly uncertain navigation environments. To consider all uncertainties impacting the navigation process while defining E_d and E_{angle} , the proposed approach given in what follows has recourse to the RA to ensure an appropriate reaching of the target. Together, the RA-based estimation of error boundaries, the analytical relations (cf. Appendix B) and the target assignment strategy construct a sound risk management level for the NSbSWR framework.

3.2/ REACHABLE SETS COMPUTATION STRATEGY FOR NSBWR

In this section, a validated set integration RA scheme that is based on the interval Taylor method is introduced. Once a waypoint is assigned to be reached, the RA process is triggered to calculate the reachable sets of the navigation towards the designated waypoint

to appropriately assess the maximum uncertainty that may impact the error between the vehicle and the target poses at the arrival time, while introducing the perception and modeling uncertainties. Hence, the evaluated uncertainties in the final arrival states serve to analysis risks about the ability to reach safely the subsequent waypoints. Compared to other RA methods (cf. subsection 1.3.3, page 29), the interval Taylor-based RA provides deterministic results since it does not include any probabilistic prediction. In addition, it uses interval wrappers and does not require any bisection of the system initial states, which offers a valuable simplicity in terms of set-membership calculation and decreases the computational costs [74, 240, 329]. More importantly, the interval Taylor expansion series were known in the literature as an efficient manner to improve the pessimism that characterizes the interval analysis [154].

Despite its advantages in providing accurate RA, the pessimism may lead to the divergence of the interval Taylor method results after few steps from its execution. Chances to obtain sharp enclosures for the reachable space remain very weak, when widths of interval initial conditions are considerable. In fact, tremendous research work has attempted to mitigate the pessimism and improve performances of the set-integration RA approaches. To meet this goal, the interval Taylor expansion was combined with other complex computational geometry techniques in [196]. Similarly, the interval variables were transformed into an affine form to minimize error propagation through interval Taylor models in [181]. Nonetheless, the loss of information caused by this transformation may lead to under-estimate the reachable space. A new line of research dealing with the conservatism impacting bounds of reachable sets using ODE solvers consists in characterizing features of the studied system. For instance, the over-estimated regions from the reachable space were eliminated via a knowledge-based computation of the system invariant sets in [133] and [264]. This direction seems very promising. However, it has targeted very specific physical features of few systems (such as conservation of mass and energy). Therefore, the proposed methods cannot be easily generalized. A more general solution has been introduced in [263]. It exploits redundancy relations between variables to obtain compact reachable sets. Unfortunately, there was no clear and methodological formalization to derive equations of the redundant states.

Obviously, the interval set-integration-based RA should be enhanced further in terms of robustness against pessimism. In this context, an Interval Taylor based Correlation Constrained RA (ITbCCRA) method is introduced in the sequel. The main contribution of this novel Taylor method extension is prohibiting the fast divergence of the induced reachable state space due to pessimism. It uses a passive characterization of correlation to mitigate the pessimism impacts on the solutions of the uncertain ODE system. Hence, validated and tight bounds of the navigation system reachable space are computed.

Obtaining realistic and tight bounds of the vehicle reachable space is essential for the safe reaching of waypoints. A pessimistic estimation of the error boundaries (E_d and E_{angle} (cf. subsection 3.1.2)) through a set-membership methodology would be useless. Conservative and over-estimated values of E_d and E_{angle} will limit the range of possible choices of the waypoints' locations. In order to avoid huge error boundary values, the distance between the sequential waypoints would be reduced. Such separation distances between the waypoints may be not sufficient enough to fulfill the asymptotic convergence of the navigation errors to zero. Otherwise, important values of E_d and E_{angle} cannot guarantee that the vehicle is always navigating inside the road limits. For these reasons the ITbCCRA is presented to solve these issues [4].

The main idea behind the proposed RA solution is to construct a full interval-based model for the navigation system while considering uncertainties propagated into its states, initial conditions, controls and parameters. From this scope, the dynamical uncertain navigation system can be described through a differential equation with the following shape:

$$\begin{cases} \dot{x}(t) = f(x, s, p, t) \\ x(t_0) \in [x_0], \quad s \in \mathbb{S}, \quad p \in \mathbb{P} \end{cases} \quad (3.15)$$

Where $f : \mathbb{R}^n \rightarrow \mathbb{R}^n$ is a non-linear vector-valued function, which defines the evolution of the system's dynamics. Accordingly, x is a finite-dimensional state vector constructed from n interval components $[x_{i=1..n}]$. $x(t_0)$ designates the initial domain, which is assigned to the state vector. \mathbb{S} and \mathbb{P} represent respectively the system control sets and the uncertain domain enclosing the ODE parameters.

Henceforth, reachable sets of system (3.15) during an interval time $[t_0, t_f]$ are denoted by $\mathcal{R}([t_0, t_f]; [x_0])$. Notably, t_0 is the triggering instant of the RA computation process i.e., when a given waypoint is admitted as a current target for the first time. t_f is the satisfaction instant of the waypoint switch conditions by the computed reachable sets (the estimated reachable sets are close enough from the waypoint configurations). Notably, t_f cannot be known posteriorly, but it is depending on the number of the integration steps that must be proceeded until reaching the target. Thus, the system forward reachable sets $\mathcal{R}([t_0, t_f]; [x_0])$ between $[t_0, t_f]$ can be formalized via ODE solutions issued from system (3.15) with particular initial condition $[x_0]$ as:

$$\mathcal{R}([t_0, t_f]; [x_0]) = \left\{ \begin{array}{l} x(\tau), \quad t_0 \leq \tau \leq t_f \\ (\dot{x}(\tau) = f(x, s, p, \tau)) \wedge (x(t_0) \in [x_0]) \wedge (s \in \mathbb{S}) \wedge (p \in \mathbb{P}) \end{array} \right\} \quad (3.16)$$

Indeed, the analytical form of $\dot{x}(t) = f(x, s, p, t)$ is obtained with a slight modification of the tricycle model described in system (3.1):

$$\begin{cases} \dot{x}_V(t) = V \cos(\theta_V) + w_1 \\ \dot{y}_V(t) = V \sin(\theta_V) + w_2 \\ \dot{\theta}_V(t) = V \frac{\tan(\gamma_V)}{l_b} + w_3 \end{cases} \quad (3.17)$$

In accordance with equation (3.17), $(w_1, w_2, w_3)^T$ is the vector of interval-type noises that may affect the process. The inferior and superior bounds of the interval components $w_{i=1..3}$ must enclose all possible states of noises issued from the system error sources e.g., perception, localization and measurement errors. Before proceeding further, it is mandatory to shape a methodological way to quantify uncertainties associated to initial state intervals at t_0 as well as bounds of intervals $w_{i=1..3}$. At this regard, a prior knowledge of these uncertainties is acquired by examining the employed sensing tools features in relation with the measurement conditions during $[t_0, t_f]$. For more details, a comprehensive method to quantify such uncertainties is introduced in section 4.1, page 93.

As already stated, solving the ODE uncertain problem based on the vehicle kinematic model allows forecasting the system reachable regions in space domain. However, the reachability cannot be separated from the controllability notion. Since it is difficult to anticipate all potential control values under uncertain system states, several RA research work assumes that these values remain constant during a specific period. Indeed, if the system

control specifications are ignored, the estimated reachable sets may be erroneous. For the sake of consistency, the proposed ITbCCRA method explores all the possible controls that may be generated under a given situation and with particular uncertain initial states. The min/max bounds of admissible V and γ_V are over-approximated via the interval arithmetic allied with the original single-valued control law. In such a manner, performances of the ITbCCRA are improved by taking into account the variation in the system controls instead of assuming nominal ones.

It is worth reminding that the control variables are generated relatively to the error states relating the vehicle pose and the target. By dealing with set-valued initial states, the interval arithmetic permits to reveal all the admissible controls at every integration step time from $[t_0, t_f]$. Intuitively, the target configuration (x_T, y_T, θ_T) as well as its velocity V_T are assumed as certain. Correspondingly, the error interval functions, with respect to a local reference frame, are obtained by the following equations:

$$\begin{cases} [e_x] = \cos([\theta_V])(x_T - [x_V]) + \sin([\theta_V])(y_T - [y_V]) \\ [e_y] = \sin([\theta_V])(x_T - [x_V]) + \cos([\theta_V])(y_T - [y_V]) \\ [e_\theta] = \theta_T - [\theta_V] \\ [e_{VT}] = \theta_T - [\theta_{VT}] \end{cases} \quad (3.18)$$

Note that $[\theta_{VT}]$ is expressed as follows:

$$\begin{cases} [\theta_{VT}] = \arctan\left(\frac{y_T - [y_V]}{x_T - [x_V]}\right) & \text{if } \bar{d} > \xi \\ [\theta_{VT}] = \theta_T & \text{if } \bar{d} \leq \xi \end{cases} \quad (3.19)$$

Where the distance between the vehicle and the target orientation line is estimated by the uncertain parameter $[d]$:

$$[d] = \sqrt{(x_T - [x_V])^2 + (y_T - [y_V])^2} \quad (3.20)$$

Hence, all possible values of the vehicle linear velocity and its front wheel orientation are given respectively by intervals $[V]$ and $[\gamma_V]$:

$$\begin{cases} [V] = V_T \cos([e_\theta]) + [v_b] \\ [\gamma_V] = \arctan(l_b[c_c]) \end{cases} \quad (3.21)$$

Noticeably, $[v_b]$ and $[c_c]$ are calculated in a set-membership manner by substituting $(e_x, e_y, e_\theta, e_{VT})$ by their interval values $([e_x], [e_y], [e_\theta], [e_{VT}])$ in equations (3.11) and (3.12). The geometric parameter l_b (cf. equation 3.1) is considered as known precisely.

By providing the admissible set-valued controls to the interval Taylor ODE-based solvers, $\mathcal{R}(([t_0, t_f]; [x_0]))$ can be obtained iteratively by finding solutions of system (3.17) at different subsequent instants $t_i \in [t_0 \dots t_f]$. Afterwards, solution sets that are generated at t_{i-1} starting from $[x_{i-1}]$ are assumed as the ODE initial conditions at the next instant t_i . The initial conditions should be updated from iteration to another as follows:

$$\begin{aligned} [x_1] &= f([x_0], s, p, t_0) \\ [x_2] &= f([x_1], s, p, t_1) \\ &\vdots \\ [x_i] &= f([x_{i-1}], s, p, t_{i-1}) \end{aligned} \quad (3.22)$$

It should be noted that $[V]$ and $[\gamma_V]$ must be recomputed according to new initial conditions at each t_i (cf. equations (3.18)-(3.21)). Finally the reachable sets computation process meets its end once bounds of the obtained solution at a given instant t_i satisfies the sequential waypoint switch rules (cf. Algorithm 1). At this stage, the relation $t_f = t_i$ is validated. Let suppose that each set solution of system (3.17) at t_i is denoted $\mathbb{X}_s(t_i)$. Consequently, $\mathcal{R}([t_0, t_f]; [x_0])$ can be defined as:

$$\mathcal{R}([t_0, t_f]; [x_0]) = \bigcup_{t_i=t_0 \dots t_f} \mathbb{X}_s(t_i) \quad (3.23)$$

With regard to the uncertain system (3.17) and equation (3.23), the derived reachable space can provide a valuable information support about all the future sets that may be occupied by the navigation system.

At each integration step, the interval solutions of $[x_{V_i}]$ and $[y_{V_i}]$ are represented geometrically in the space domain by an axis-aligned box of four vertices. This latter must consider also the vehicle geometrical shape. In this respect, the vehicle length and width are considered as known with precision. By acting on the box dimensions, the vehicle future occupancy fields are determined easily. Likewise, the orientation component should also be taken into account for a more accurate representation of the reachable sets in the space domain. Thus, two simple rotations for the obtained box at t_i are realized, where the point C_i ($[mid([x_{V_i}]), mid([y_{V_i}])]$) is the rotation center and $\underline{\theta}_{V_i}$ and $\overline{\theta}_{V_i}$ are respectively the performed rotation angels (cf. Figure 3.4a).

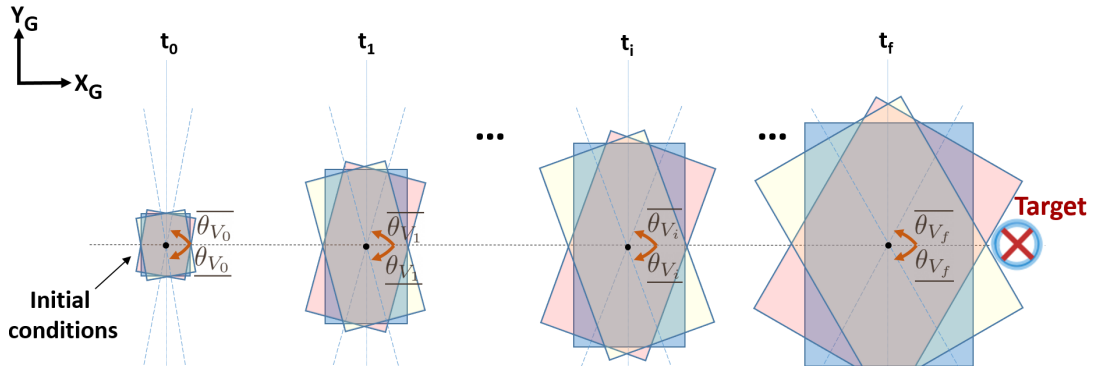
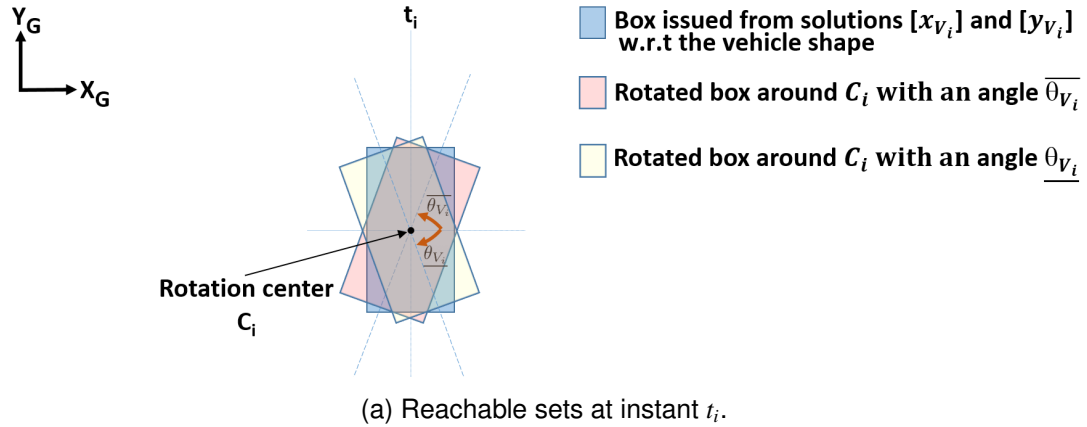


Figure 3.4: Geometrical representation of reachable sets in the space domain.

All the vertices of boxes representing solutions of the uncertain ODE (3.17) and also resulting from the rotational transformations, obtained during $[t_0, t_f]$, are drastically useful to bound the navigation system reachable space. An envelope for the reachable space is extracted using a 2D-convex hull shape [184]. In the computational geometry science, a convex hull associated to a set of points refers to the smallest closed convex polygon that encompasses all these points [26]. It serves to delimit the outer boundary constructed by all the vertices of the reachability boxes. Methods dedicated for boundary formation via such a set-theoretic structure from a set of points are discussed in [178, 243]. In this thesis, the convex hull formation is ensured numerically (cf. Figure 3.5).

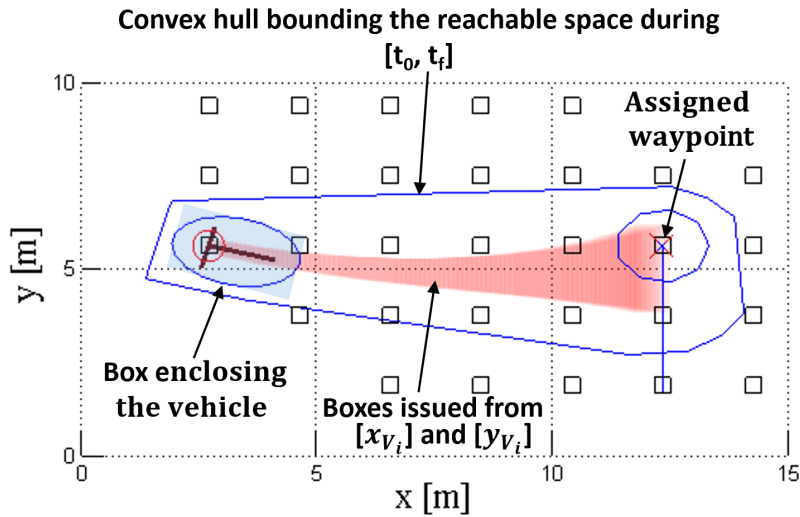


Figure 3.5: Reachable space bounding through convex hull enclosure.

The overall strategy of computing $\mathcal{R}([t_0, t_f]; [x_0])$, while taking into account all uncertainty sources, is illustrated in Figure 3.6. Clearly, the core idea of the proposed method is the employment of the set-membership Taylor expansion series. These interval models are known by their high accuracy and confidence in proceeding numerical integration. The next section is dedicated to detail a novel extension from the interval Taylor approach. It improves the quality of the obtained findings in terms of less pessimism.

3.3/ ITBCCRA METHOD FOR SAFE WAYPOINT REACHING

As already explained, sets reached by the waypoint-based navigation process are obtained by propagating enclosures through Taylor models over discrete time steps. Conventional integration-based RA techniques approximate solution sets for the uncertain studied problem with unknown range of error. Unlike these methods, the interval Taylor concept ensures that the generated sets cannot deviate from its real bounds while containing definitely all possible ODE solutions. In the sequel, a brief reminder about steps of the standard interval Taylor expansion series is depicted in subsection 3.3.1. After that, a novel enhancement for the interval Taylor approach is proposed by characterizing the correlation relating variables that construct the uncertain ODE problem (cf. subsection 3.3.2). Hence, the suggested ITbCCRA scheme reconsiders the interval Taylor-issued solutions to decrease the conservatism.

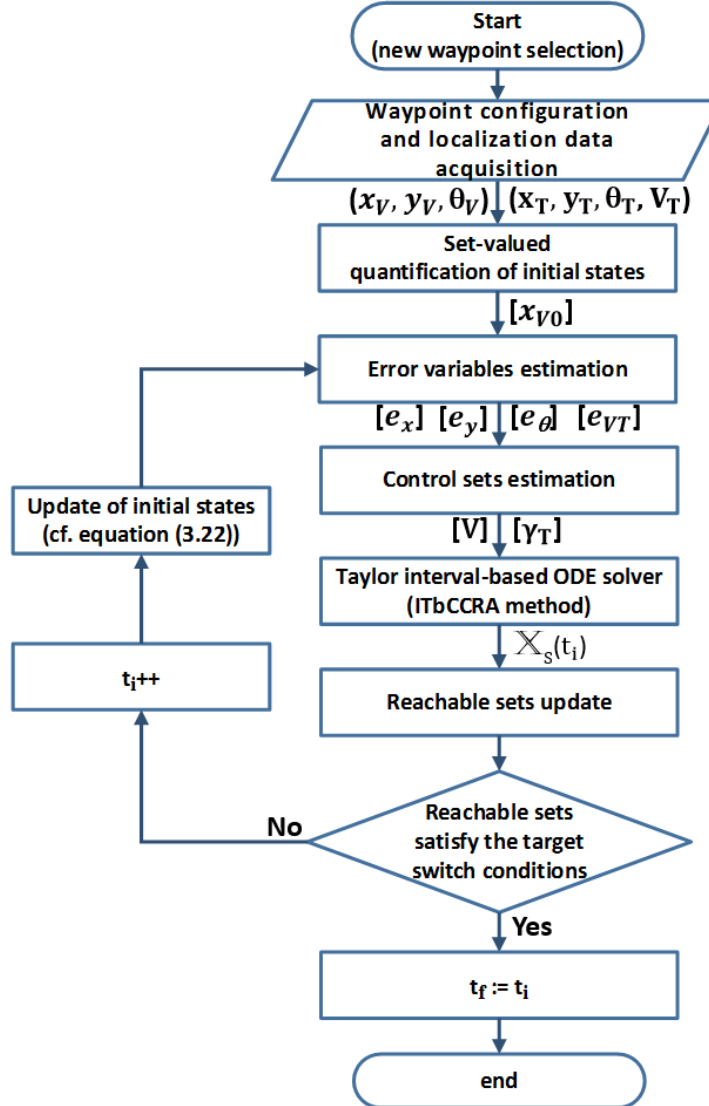


Figure 3.6: Flow chart of the proposed RA process for reaching a given waypoint.

3.3.1/ STANDARD INTERVAL TAYLOR EXPANSION SERIES

Interval Taylor models are designed to enchain solutions resulting from the set-integration process according to a time grid $t_0 < \dots < t_i < \dots < t_f$. Hereinafter, steps that allow finding solutions $\mathbb{X}_s(t_i)$ of system (3.17) at t_i are detailed. In general, Taylor set-integration is initiated by looking for a prior enclosure of the final set-solution at an instant t_i . The prior guess of regions estimated to bound the ODE solutions are not tight enough [240, 241]. Thus, as a second step from the Taylor method, these regions are further refined to obtain the smallest sets bounding the ODE solutions. Accordingly, the prior enclosure, noted $[\hat{x}_i]$, must satisfy the inclusion test described by equation (3.24):

$$\mathbb{X}_s(t) \subset [\hat{x}_i], \quad \forall t \in [t_i, t_{i+1}] \quad (3.24)$$

Various methods have been dedicated in the literature to simultaneously prove the existence/uniqueness of $\mathbb{X}_s(t_i)$ while facilitating the arbitrary guess of $[\hat{x}_i]$. As an approach to

meet this objective, the Picard-Lindelöf theorem is adopted in this stage for its simplicity (see [245] for details). Consider the Taylor integration step $\Delta_{t_i} = t_{i+1} - t_i$. Then, the first guess of $[\hat{x}_i]$ may be derived according to equation (3.25):

$$[\hat{x}_i] = [x_i] + [0, \Delta_{t_i}]f([x_i], [s], p, [t_i, t_{i+1}]) \quad (3.25)$$

Thereafter, the derived prior enclosure is recursively tuned until making sure that:

$$[x_i] + [0, \Delta_{t_i}]f([\hat{x}_i], [s], p, [t_i, t_{i+1}]) \subseteq [\hat{x}_i] \quad (3.26)$$

One way to validate the above inclusion (equation (3.26)) is by diminishing the integration step Δ_{t_i} . Rather, the proposed ITbCCRA method relies on broadening $[\hat{x}_i]$. This permits to proceed with an equally spaced time grid and admit an integration time step size relevantly relative to the real navigation system sampling time.

Once the inclusion condition implied by equation (3.26) is fulfilled, the recursive estimation of $[\hat{x}_i]$ is stopped. As already explained, the estimated prior enclosure $[\hat{x}_i]$ consists of a widely conservative approximation of the final and more compact solution $[x_{i+1}]$.

At this level, efficient techniques to narrow $[x_{i+1}]$ are extremely needed. The over-estimated uncertainty associated to $[\hat{x}_i]$ can be eliminated explicitly by applying the Taylor-based expansion [240]. By joining fundamentals of interval arithmetic with numerical and/or analytical automatic differentiation rules, it is possible to extend the application of common Taylor expansions to sets [203]. For more details about interval-based automatic differentiation, readers are referred to the seminal work reported in [238]. Otherwise, several advanced programming tools can perform the required interval differentiation based on validated formal techniques. As shown in equation (3.27), the over-approximated estimation of $[x_{i+1}]$ is refined with a Taylor expansion of order k . Notably, $[\hat{x}_i]$ is employed to assess the interval remainder r and interval Taylor coefficients $f^{(j)}$.

$$\begin{cases} \mathbb{X}_s(t_i) = [x_{i+1}] = [x_i] + \sum_{j=1}^{k-1} \Delta_{t_i} f^{(j)}([x_i], [s], p, t_i) + r \\ r = \Delta_{t_i} f^{(k)}([\hat{x}_i], [s], p, t_i) \end{cases} \quad (3.27)$$

Where $f^{(j)}$ are interval values obtained numerically as already explained or through the successive partial derivatives of f :

$$\begin{aligned} f^{(0)}([x_i]) &= [x_i] \\ f^{(1)}([x_i]) &= f([x_i]) \\ &\vdots \\ f^{(j)}([x_i]) &= \frac{1}{j} \left(\frac{\partial f^{(j-1)}}{\partial x} f \right) ([x_i]) \end{aligned} \quad (3.28)$$

To recapitulate the earlier discussed steps, the Taylor set-integration method is described in Algorithm 2.

3.3.2/ CORRELATION-BASED OPTIMIZATION FOR INTERVAL TAYLOR METHOD

To over-step the pessimism effects (cf. section 2.4, page 46), a passive characterization of correlation is adopted to avoid divergence of the ODE solutions. The correlation has

Algorithm 2: Standard interval Taylor method

Inputs : t_i , Δ_{t_i} , and $[x_i]$.**Outputs:** $[x_{i+1}]$.

```

1 -Estimate the first guess of  $[\hat{x}_i]$ :
2    $[\hat{x}_i] = [x_i] + [0, \Delta_{t_i}]f([x_i], [s], p, [t_i, t_{i+1}])$ 
3 while  $([x_i] + [0, \Delta_{t_i}]f([\hat{x}_i], [s], p, [t_i, t_{i+1}]) \not\subseteq [\hat{x}_i])$  do
4   | -Enlarge the width of  $[\hat{x}_i]$ .
5 end
6 -Compute interval Taylor coefficients:
7    $f^{(j)}([x_i]) = \frac{1}{j}(\frac{\partial f^{(j-1)}}{\partial x}f)([x_i])$ 
8 -Calculate the remainder term  $r$ :
9    $r = \Delta_{t_i}f^{(k)}([\hat{x}_i], [s], p, t_i)$ 
10 -Calculate solution  $[x_{i+1}]$ :
11    $[x_{i+1}] = [x_i] + \sum_{j=1}^{k-1} \Delta_{t_i}f^{(j)}([x_i], [s], p, t_i) + r$ 

```

been a relevant metric to design several reliability and diagnosis models [128]. The offline characterization of the correlation assigned to nominal system operation is a widespread practice to ensure reliability [99]. Anomalies are detected by comparing the nominal and real progression of the correlation. Intuitively, a system anomaly-free behavior should reflect a smooth progression of correlation [317]. In general, a sudden change in vehicle dynamics is unrealistic in a short time horizon. This assumption holds true for the correlation. Yet, improper correlation evolution can be caused by several anomalies such as erroneous measurements. For instance, trajectories drifts, outliers, erroneous position estimation of map-points are concrete examples of abnormalities that may entail an inappropriate correlation progression of the SLAM-based autonomous driving systems [335]. Likewise, the satellite signal failures are the main cause of several distortions in the correlation properties of the global navigation satellite system receivers [344]. Therefore, constructing process monitoring approaches based on the correlation examination is an emergent direction with promising results [197], [344]. The authors in [346] used the correlation peaks detection as a direct approach to capture/mitigate uncertainties threatening set of cooperative mobile robots while skipping the challenging reconstruction of each agent state estimate. Through the system correlation coefficients experimentally derived in nominal conditions, a natural and systematic detection of noises impacting a neuro-imaging mechanism is performed in [124]. In [46], the correlation analysis helped to face undesired effects (over-fitted/under-fitted estimates) of several abnormalities and chaotic behaviors linked to system's nonlinearity, which may degrade performances of dynamic process monitoring approaches. Even more, relevant degradation patterns (i.e., indicators used in fault prognosis methods for a posterior detection of abnormalities) were extracted through monitoring the run-time correlation behavior of industrial robots in [327].

Hence, the pessimism affecting interval Taylor solutions can be also considered as an anomaly. Thus, a correlation-based optimization for Taylor models is introduced. The correlation that relates the ODE variables is examined to discard over-estimated regions from the reachable space. The pessimism should not cause a major fluctuation in the correlation evolution between two instants t_{i-1} and t_i . By narrowing interval solutions, sharp correlation-constrained results of interval Taylor models are obtained. A realistic transition in the correlation relating successive solutions is reached.

The interest in the correlation as a powerful interpretation tool of a given system hidden structural features is not recent [175]. Several computation approaches of the correlation have been introduced to present meaningful descriptive statistics and highlight systems' intrinsic relationships [247]. For its simplicity and its ability to study dependencies between highly dimensional data, the "Pearson correlation coefficient" is largely used in statistical applied sciences [325]. It inspects the distribution of the data points (i.e., the dispersion of previous samples of a variable in the data-representation space) over time [76]. Based on the data-distribution, the relation (if it exists) that best fits two variables is revealed [232]. At instant t_i and for two variables a and b , this coefficient, designated $COR_{a,b|t_i}$, is estimated as:

$$COR_{a,b|t_i} = \frac{COV_{a,b|t_i}}{\sigma_a \sigma_b} \quad (3.29)$$

Where $COR_{a,b|t_i}$ varies between $[-1, 1]$ to indicate the dependency strength between a and b , $COV_{a,b|t_i}$ is the covariance linking a and b , and σ_a and σ_b are their standard deviations. The evolution in the correlation relating a and b between instants t_i and t_{i-1} , denoted $\chi(a, b)_{t_i|t_{i-1}}$, is estimated by equation (3.30):

$$\chi(a, b)_{t_i|t_{i-1}} = |COR_{a,b|t_i} - COR_{a,b|t_{i-1}}| \quad (3.30)$$

In the sequel, a library describing features of the waypoint-based navigation system correlation evolution is build. It captures maximum values of the correlation evolution under all situations. Due to their important role in describing the navigation system states, the established library characterizes the correlation between the set of variables (x_V, y_V, θ_V) . Afterwards, by using a computation technique for the correlation between interval data, the correlation characterizing the ODE interval solutions is monitored in run-time to refine the interval Taylor performances.

3.3.3/ OFFLINE LIBRARY OF THE CORRELATION EVOLUTION

The main purpose from this offline library is to reveal all possible behaviors of correlation between variables of system (3.17). To fulfil this objective, extensive simulations have been realized for the waypoint-based navigation. Extensive simulation scenarios (with several initial states and final target to reach) have been achieved with various road profiles (curved and straight road segments). In addition, waypoints with wide range of configurations have been selected to reach the vehicle final desired destination. These simulations have been re-executed while incriminating progressively the maximum control velocity permitted for the vehicle. It obliges the navigation control law to generate, as much as possible, large varieties of admissible controls. All adopted maximum velocities are stored in a vector $V_{k=1..m} = [V_1, V_2, \dots, V_m]$, where $V_1 < V_2 < \dots < V_m$. Evidently, varying the driving scenarios, the road conditions and subsequently the waypoint configurations is of utmost importance. To meet confidence requirements and be trusted, the elaborated library must capture all possible transitions in correlation in order to define the closest correlation aspect between variables.

For each realized simulation with different V_k , the variation in correlation relating each possible distinct couple from (x_V, y_V, θ_V) is assessed according to equations (3.29) and (3.30). At each time period $T \in [T_1, \dots, T_n]$, the simulation-issued values of χ_T , associated to every couple of variables, are stored. Technically speaking, for a given couple (a, b) , $COR_{a,b|T}$ is computed by means of several previous samples of a and b . Otherwise, the

offline simulations are carried out without any injection of uncertainties in navigation dynamics to derive correct reference values of the variation in correlation. Since the offline extraction of correlation reference values is taken place without uncertainty injection, an efficient filtering process is needed in the run-time. In that way, a precise comparison is possible between the online correlation features and the offline references. In this context, an Extended Kalman Filter (EKF) is used for this purpose.

After executing all simulations with $V_k \in [V_1 \dots V_m]$, maximum values of the variation in correlation relating every couple from the stated variables are picked up, whatever was the value of γ_V . Only these maximum reference values will be later exploited in the narrowing phase. Admitting the largest trajectory of evolution in correlation independently to γ_V will guarantee that tightened enclosures will still containing all possible solution sets. Let denote by Υ_{V_k} the vector of the memorized reference values, which are issued from simulations executed with a particular V_k as a maximum velocity. Then, Υ_{V_k} can be written as:

$$\Upsilon_{V_k} = \begin{pmatrix} \max_{T \in [T_1, \dots, T_n]} \chi(x_V, y_V)_T \\ \max_{T \in [T_1, \dots, T_n]} \chi(x_V, \theta_V)_T \\ \max_{T \in [T_1, \dots, T_n]} \chi(y_V, \theta_V)_T \end{pmatrix} \quad (3.31)$$

In such a way, the final data-base provided by the established library can be presented as $\Upsilon = [\Upsilon_{V_1} \dots \Upsilon_{V_m}] \in R^{(3 \times m)}$.

3.3.3.1/ CORRELATION COMPUTATION FOR INTERVAL-VALUED VARIABLES

At this level, the acquired knowledge about the correlation evolution over time is exploited to introduce an optimization/correction step for the standard interval Taylor method. In order to proceed a narrowing phase, it is mandatory at first to define a correlation assessment technique, which may handle appropriately interval data.

Typically, the correlation coefficient estimates only the dependency between standard single-valued variables. Only few research work has tackled the correlation computation for interval data [166]. Unfortunately, the proposed methods are computationally cumbersome and inadequate for critical real-time applications. In this thesis, a symbolic description of intervals, named the Vertices Transformation (VT) method, is employed to perform a simple correlation estimation for interval-valued variables [7], [9], [123]. Let denote by X^I an interval data matrix gathering N observations of q interval-valued variables $[x_{i|i=1..q}]$:

$$X_I = \begin{pmatrix} [\underline{x}_1(1), \overline{x}_1(1)] & \dots & [\underline{x}_q(1), \overline{x}_q(1)] \\ \vdots & \ddots & \vdots \\ [\underline{x}_1(N), \overline{x}_1(N)] & \dots & [\underline{x}_q(N), \overline{x}_q(N)] \end{pmatrix} \quad (3.32)$$

A straightforward manner to estimate the exact correlation for interval variables is to calculate this parameter for all points enclosed in the interval samples. Nevertheless, only few points can be incorporated in the correlation assessment for practical issues. Vertices have great capacities in facilitating the worst-case analysis on interval plants. In the literature, vertices have been used to extend several complicated statistical approaches to handle interval observations [1, 6]. In this thesis, vertices are exploited to permit the application of the common approach of estimating the correlation (cf. equation (3.29)).

Geometrically, interval-valued variables can be depicted in the data-representation space through hyper-rectangles. These latter are constructed with 2^q vertices, which are the inferior/superior endpoints of intervals. Consequently, an equivalent-single-valued matrix for X_I , denoted X_H , is extracted. X_H encompasses all X_I vertices and includes $N \times 2^q$ rows and q columns. Thus, X_H is formalized as:

$$X_H = \left(\begin{array}{cccc} \left(\begin{array}{ccc} \underline{x}_1(1) & \cdots & \underline{x}_q(1) \\ \vdots & \ddots & \vdots \\ \overline{x}_1(1) & \cdots & \overline{x}_q(1) \end{array} \right) \\ \vdots \\ \left(\begin{array}{ccc} \underline{x}_1(N) & \cdots & \underline{x}_q(N) \\ \vdots & \ddots & \vdots \\ \overline{x}_1(N) & \cdots & \overline{x}_q(N) \end{array} \right) \end{array} \right) \quad (3.33)$$

For a better understanding of the proposed transformation, simple examples in dimensions 2 and 3 for the VT application are illustrated in Figure 3.7.

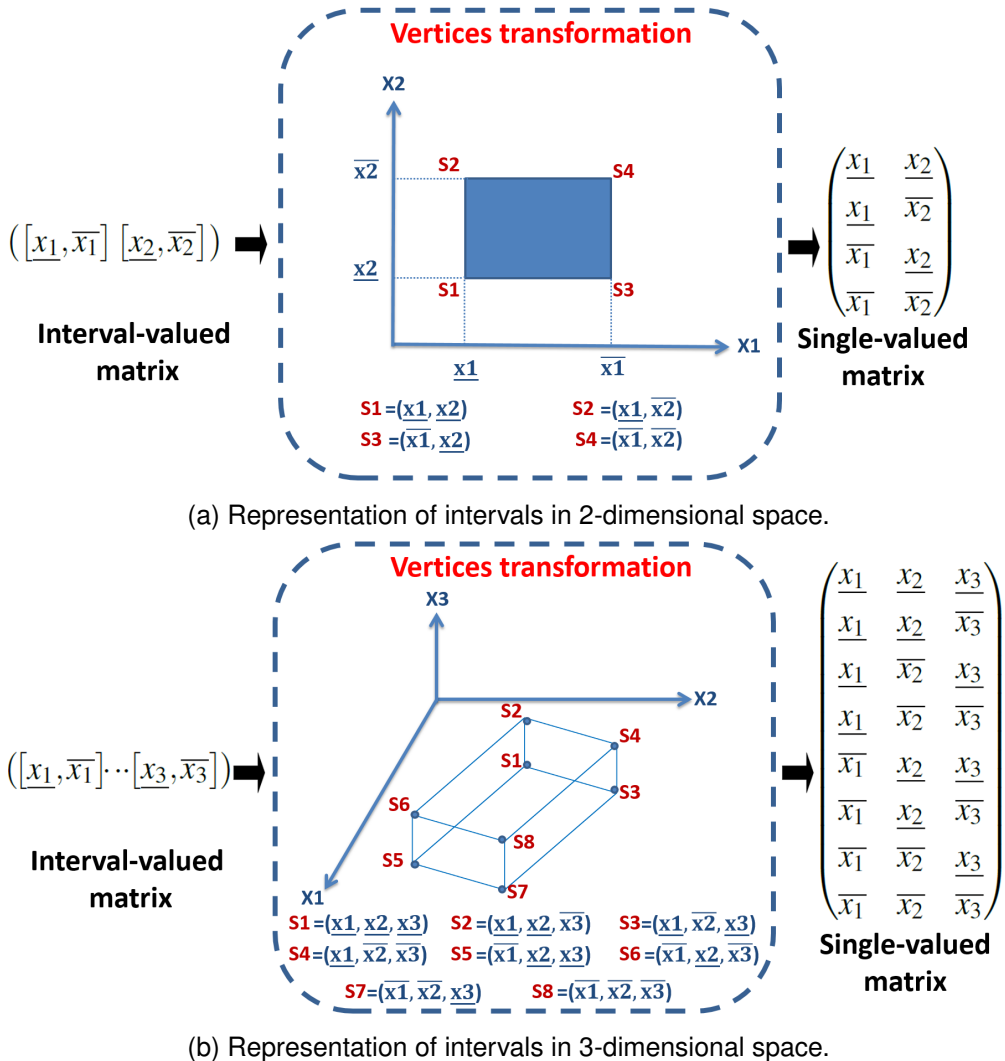


Figure 3.7: Vertices technique in dimensions 2 and 3 for number of observations $N = 1$.

Let denote by $N_{X_H} = N \times 2^q$ the number of samples included in X_H according to the VT. Hence, X_H has the following form:

$$X_H = \begin{pmatrix} x_1(1) & \cdots & x_q(1) \\ & \ddots & \\ x_1(N_{X_H}) & \cdots & x_q(N_{X_H}) \end{pmatrix} \quad (3.34)$$

The VT is actually the backbone part from the statistical correction step, which is joined to the standard Taylor expansion series. Henceforth, all the needed to assess the correlation between interval variables is to determine the single-valued equivalent matrix X^H of the interval samples. Then, equations (3.29) and (3.30) can simply handle the obtained X^H .

Undoubtedly, the pessimism affecting the ODE solutions will badly change the normal evolution of correlation between variables. On the one hand, with interval analysis, all variables are dealt without correlation assumptions, which may lead to dramatic pessimism as explained in section 2.4, page 46. Accordingly, some correlation relations characterizing the system will be lost or under/over-valuated by reason of the “dependency effect” (cf. section 2.4, page 46). On the other hand, the pessimism-related to the “wrapping effect” (cf. section 2.4, page 46) is unpredictable since it can impact separately all or a part of the concerned system interval variables. Consequently, the deviation in widths of the ODE solutions due to the pessimism may invoke important change in the system correlation states. Hence, to enhance performances of the interval Taylor expansion series, the proposed method consists in narrowing recursively interval components of $[x_{i+1}] = ([x_{v_{i+1}}], [y_{v_{i+1}}], [\theta_{v_{i+1}}])^T$. Alone sharp bounds of solutions are able to maintain the proper and real correlation properties.

To assess the evolution in correlation, which is outlined by the interval solutions at t_i , the VT is practiced. As soon as equivalent matrices representing each couple from $([x_{v_{i+1}}], [y_{v_{i+1}}], [\theta_{v_{i+1}}])$ are arranged, the evolution in correlation can be easily evaluated by equations (3.29) and (3.30). For each distinct couple, the interval with the largest width is concerned with iterative narrowing. Narrowing is aborted only when the evolution in correlation, resulting from the tightened solutions, does not exceed the reference maximum values provided by the offline library. Access to the adequate data from the established library is ensured by selecting statistical references recorded within the closest V_k to the actual admissible interval velocity $[V]$ ($V_k \simeq \text{mid}([V])$). Thus, narrowing is ended once the following conditions are satisfied:

$$\begin{cases} \chi([x_V], [y_V])_{t_{i+1}|t_i} \leq \max_{\forall T | V_k \simeq \text{mid}([V])} \chi(x_V, y_V)_T \\ \chi([x_V], [\theta_V])_{t_{i+1}|t_i} \leq \max_{\forall T | V_k \simeq \text{mid}([V])} \chi(x_V, \theta_V)_T \\ \chi([y_V], [\theta_V])_{t_{i+1}|t_i} \leq \max_{\forall T | V_k \simeq \text{mid}([V])} \chi(y_V, \theta_V)_T \end{cases} \quad (3.35)$$

For more details, Algorithm 3 summarizes how to derive sharp enclosures for the ODE problem, denoted $[\tilde{x}_{i+1}]$, starting from results of the standard interval Taylor method.

The introduced step may be considered as a data-driven validation of solutions $[x_{i+1}]$. A more realistic evolution of the uncertainty into the reachable sets is obtained thanks to statistical constraints implied on the progress of correlation. Note that solutions $[\tilde{x}_{i+1}]$ are neither underestimated nor overestimated, since they are validated through the navigation system historic proprieties.

Algorithm 3: ITbCCRA method: Optimized interval Taylor extension

Inputs : t_i , Δ_{t_i} , and $[x_i]$.
Outputs: $[\tilde{x}_{i+1}]$.

- 1 -Estimate $[x_{i+1}]$ via the standard interval Taylor method.
- 2 -Search for the closest value of V_k , where $V_k \simeq \text{mid}([V])$.
- 3 -Load offline reference values Υ_{V_k} corresponding to the selected V_k .
- 4 **for** each couple $([x_{V_{i+1}}], [y_{V_{i+1}}])$, $([x_{V_{i+1}}], [\theta_{V_{i+1}}])$ and $([x_{V_{i+1}}], [\theta_{V_{i+1}}])$ **do**
- 5 **repeat**
- 6 -Apply the vertices technique.
- 7 -Calculate the correlation relating the interval variables (see equation (3.29)).
- 8 -Estimate the progression in correlation $\chi_{t_{i+1}|t_i}$ (see equation (3.30)).
- 9 -Proceed one narrowing step for the largest interval.
- 10 **until** Conditions from system (3.35) are satisfied
- 11 **end**
- 12 -Return $[\tilde{x}_{i+1}]$.

According to the ITbCCRA novel extension of interval Taylor method, a reachability framework is integrated into the waypoint-based navigation system. The architecture of the whole developed framework is illustrated in Figure 3.8.

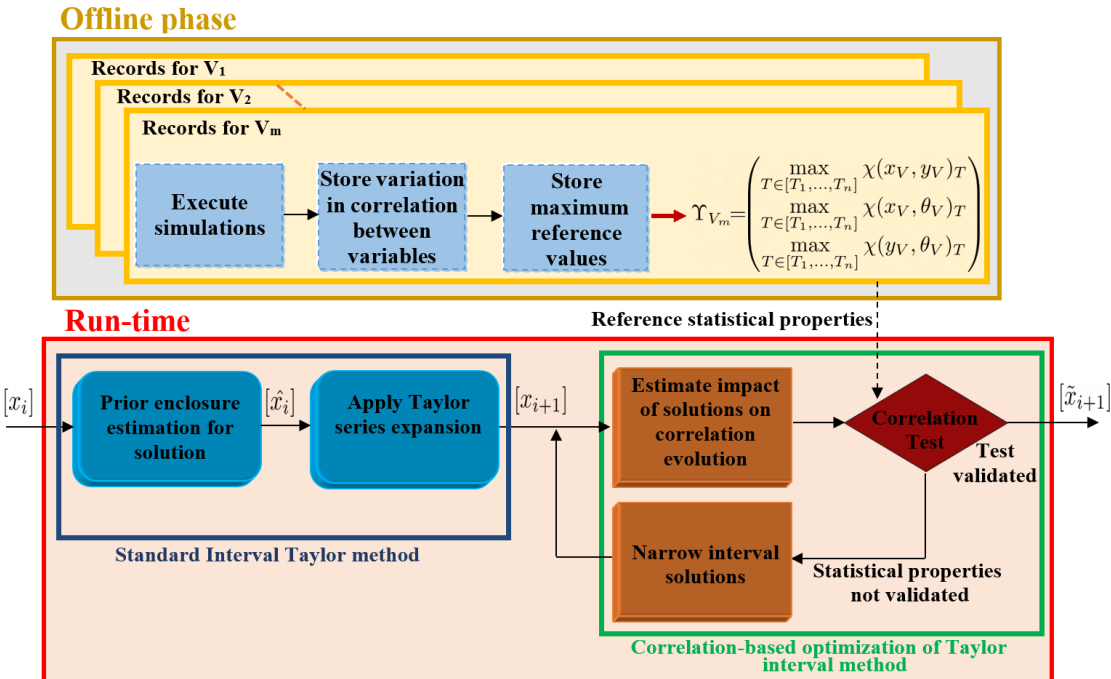


Figure 3.8: Reachability computation via ITbCCRA for NSbSWR.

3.3.3.2/ COMPLEXITY ANALYSIS

The computational performances of the ITbCCRA-based safety verification layout for NSbSWR is discussed in this part. In fact, the complexity issue is toughly linked to three

principle steps from the proposed extension of interval Taylor method:

- **Complexity of the standard interval Taylor method:** The computational cost of a single integration step from the standard interval Taylor method (cf. equations (3.27) and (3.28)) is $O(k^2)$ [240]. Hence, the overall computational complexity of the interval Taylor expansions applied between the interval time $[t_0, t_f]$ is $O(\alpha k^2)$, where α is the number of the proceeded integration time steps. Since a constant time integration step $\Delta_{t_i} = t_{i+1} - t_i$ is used, so $\alpha = \frac{t_f - t_0}{\Delta_{t_i}}$. Note that a second order expansion is sufficient to achieve the reachability computation. Thanks to the proposed correlation-based validation step, the integration accuracy is not influenced by setting ($k = 2$).
- **Complexity of the correlation assessment for interval-valued variables:** Due to the VT method simplicity, there is no excessive additional computational complexity resulting from the correlation evaluation for interval data. For each couple of variables, the VT computational cost is $O(8 \times N)$, where N is the number of the observation samples. Further, the evolution of the correlation can be characterized with a fixed and small number of continuously updated samples N .
- **Complexity of the interval narrowing phase:** Let assume β the narrowing step for a given interval variable ($[a] := [\underline{a} + \beta, \bar{a} - \beta]$). Although the narrowing computational cost is unpredictable, few iterations are proceeded to accomplish this step, especially when β is carefully chosen (neither small nor huge value of β).

According to the analysis above, there is no complications arising from the computational performances of the ITbCCRA method. Furthermore, readers should pay attention to an important issue related to the computational analysis. An apparent advantage from the flexibility offered by the NSbSWR is removing the complexity problems. As soon as a target is assigned via the Algorithm 1, the navigation can be carried out with initial values of E_d and E_{angle} . Intuitively, these provisional values are obtained based on the analytical analysis depicted in Appendix B (by only considering the maximum error of the initial conditions of the vehicle position and orientation). Thus, there is more available time to carry on the RA. Once the reachable space prediction is completed, the temporary fixed E_d and E_{angle} can be updated to take into account the uncertainty propagation into the navigation system.

3.3.4/ ITbCCRA SIMULATION-BASED VALIDATION WORK

To demonstrate the ITbCCRA scheme interest in ensuring the NSbSWR safety, the results of an extensive simulation work are exhibited in the sequel. From a technical point of view, the interval computation is proceeded via the numerical package INTLAB (IN- Terval LABoratory). This interval-based computing environment is selected due to its high portability with Matlab, its provable performances, rigorous results and fast computation [252]. Otherwise, the representation of the navigation system reachable sets in the 2-dimensional space domain is ensured by the Matlab computational geometry toolbox. Mainly, the realized simulations are dedicated to analyze the ITbCCRA limitations in terms of prediction horizon. Quantitative analysis to evaluate the ITbCCRA reliability and consistency via a set of batch simulations is also tackled. It is assumed for all the simulation scenarios presented in this subsection that $V_{max} = 3 \text{ m/s}$, $\gamma_{V_{max}} = 20^\circ$ and $V_T = 1 \text{ m/s}$.

3.3.4.1/ PREDICTION HORIZON OF THE PROPOSED ITbCCRA METHOD

Exploiting the navigation system historical features to face the interval analysis pessimism is expected to improve the ITbCCRA prediction horizon. Nevertheless, the proposed approach is still has limits. The size of boxes wrapping the ODE solutions increases from an iteration to another during the ITbCCRA execution. Based on equation (3.27), the growth of regions bounding the ODE solutions is proved by the following relation that governs the enclosures' widths:

$$wid([x_{i+1}]) = wid([x_i]) + \sum_{j=1}^{k-1} \Delta_{t_i} wid(f^{(j)}([x_j], [s], p, t_i)) + \Delta_{t_i} wid(f^{(k)}([\hat{x}_i])) \geq wid([x_i]) \quad (3.36)$$

Examining the ITbCCRA method limits in terms of prediction horizon is very important. Even after overcoming the pessimism, dimensions of the reachable space will be enormously extended since more and more uncertainty is involved by time in the navigation states. Nonetheless, bounds of the NSbSWR reachable space must ensure always that the vehicle is navigating within the road borderlines. Thus, extensive simulations are elaborated in order to characterize the growth of the ITbCCRA-issued enclosures with respect to the proceeded integration steps and the amount of uncertainties impacting the studied uncertain ODE system (initial conditions, noises $w_{i=1..3}$, etc.). In such a manner, the waypoints' configurations may be adapted for a more relevant and reliable use of the ITbCCRA.

Intuitively, the ITbCCRA prediction horizon is mainly linked to the uncertainty in the vehicle position $([x_v], [y_v])$ and its orientation $[\theta_v]$. Hence, widths' evolution of $([x_v], [y_v])$ and $[\theta_v]$ in function of errors in initial conditions and noises $w_{i=1..3}$ are studied separately hereafter. To start with, let assume that the system reachable states are too large if:

$$wid([x_v]) > W_{x_v} \text{ or } wid([y_v]) > W_{y_v} \text{ or } wid([\theta_v]) > W_{\theta_v} \quad (3.37)$$

$(W_{x_v}, W_{y_v}, W_{\theta_v})$ are thresholds that may be defined according to the geometry and dimensions of the road where the navigation is taking place. From a planning point of view, the choice of $(W_{x_v}, W_{y_v}, W_{\theta_v})$ should ameliorate the selection of waypoint configurations to not emphasize collision risks. Uncertainty boundaries introduced in equation (3.37) must be used to decrease chances of the reachable space expansion behind the road limits after running many cycles from the ITbCCRA. It is worth noting that for the upcoming simulation work to validate the ITbCCRA method, W_{x_v} , W_{y_v} and W_{θ_v} are respectively fixed at 1.5 (m), 1.5 (m) and 30°.

In this sense, let define $d_{ITbCCRA}$ the maximum distance that can be covered by the navigation reachable space during an interval of time $[t_0, t]$ without violating the constraints of equation (3.37) (see Figure 3.9). The distance $d_{ITbCCRA}$ (which is explained in more details below) is used in the sequel to figure out factors governing the growth of the IV reachable space.

For a better characterization of $d_{ITbCCRA}$ (cf. Figure 3.11), it is important to take into account the initial orientation error e_{θ_0} between the target and the vehicle during simulations. For configurations where $e_{\theta_0} \approx 0^\circ$, the distance that will be traveled by the navigation system is close to the Euclidean distance between the vehicle and the target. For values $e_{\theta_0} > 0^\circ$, the distance that should be traveled by the vehicle is more important. The navigation system needs then more time (which means more integration steps for the

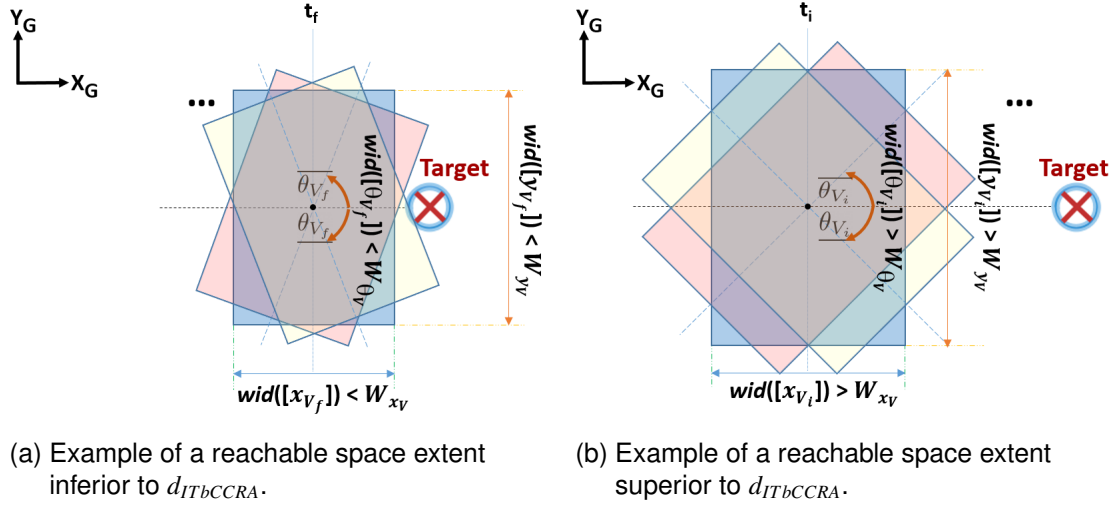
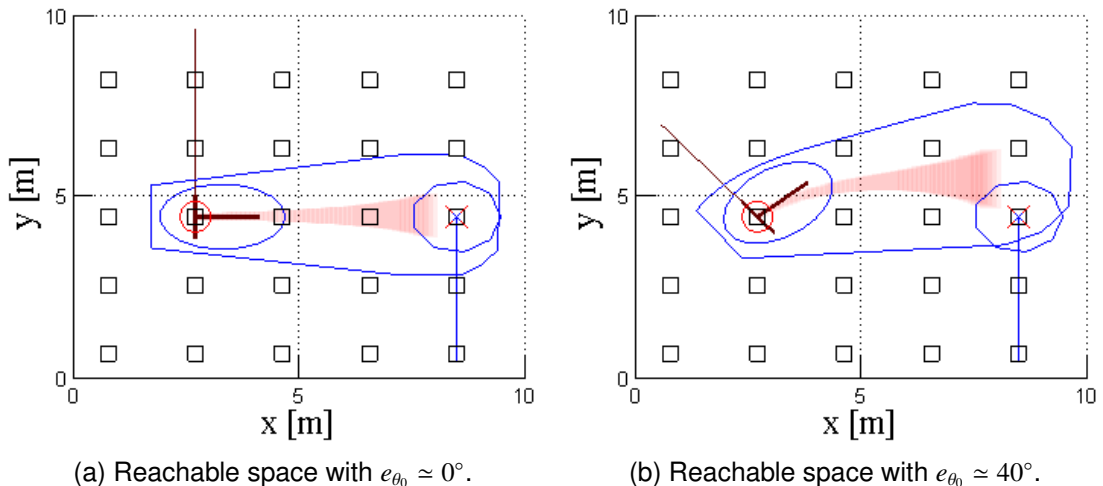


Figure 3.9: Prediction horizon characterization of ITbCCRA method.

reachability computation process) to ensure the convergence of e_θ to zero. In that case, the expansion of the reachable space at the arrival time to the waypoint would be greater. Figure 3.10 illustrates examples of the obtained reachable space from tests conducted with different initial e_{θ_0} values. For both examples ($e_{\theta_0} = 0^\circ, 40^\circ$), bounds of the interval-type uncertainties (in initial conditions and at every iteration) attributed for x_V , y_V and θ_V are respectively $\pm 0.1(m)$, $\pm 0.1(m)$ and $\pm 0.5^\circ$. Although same simulation setups are used while just varying e_{θ_0} , a considerable difference in the growth of the system reachable space in both cases is noticed.

Figure 3.10: Reachable space behavior according to e_{θ_0} .

To proceed the required simulations revealing the ITbCCRA permitted prediction horizon, a waypoint ($x_T = 23 [m]$, $y_T = 5.5 [m]$, $\theta_V = 0^\circ$) is located far away from the vehicle initial position ($x_V = 7.5[m]$, $y_V = 5.5[m]$). This important separation between the vehicle and the assigned target is implied to always force the violation of constraints introduced by equation (3.37). After that, simulations are launched while varying recursively widths of the interval-type uncertainties injected in initial conditions and instantaneous uncertainties (w_1, w_2, w_3) (cf. system 3.17). Since errors impacting (x_V , y_V , θ_V) are mainly linked to the

perception/localization imperfections, the uncertainties attributed to the initial conditions and $w_{i=1..3}$ are set equal. As earlier stated, $d_{ITbCCRA}$ depends also on e_{θ_0} . Correspondingly, simulations are undertaken iteratively within a large range of initial vehicle orientation values to reveal the ITbCCRA prediction horizon under different e_{θ_0} setups.

Each iteration from the executed simulation corresponds to a particular setup of uncertainty injection. During a launched iteration, the reachability computation is aborted once constraints of equation (3.37) are dissatisfied for the first time. Afterwards, the distance covered by the reachable space in the previous cycle from the ITbCCRA is assumed as the relevant value of $d_{ITbCCRA}$ corresponding to the simulated configuration in this iteration.

Among the whole tackled simulations, an example illustrating how to estimate $d_{ITbCCRA}$ is depicted in Figure 3.11. In this example, the initial orientation error between the vehicle and the target is $e_{\theta_0} = 20^\circ$. In addition, bounds of the interval-type uncertainties attributed to (x_V, y_V, θ_V) are respectively $\pm 0.1(m)$, $\pm 0.1(m)$ and $\pm 0.1^\circ$. In fact, $d_{ITbCCRA}$ represents the euclidean distance between the vehicle initial position and the center of the last reachable box, where the constraints in equation (3.37) are still respected. In the delivered example in Figure 3.11, the reachable box drawn within red edges underlines the violation of conditions of equation (3.37) for the first time, since $wid([y_{V_i}]) > W_{y_V}$. Hence, $d_{ITbCCRA}$ is measured between the vehicle position at t_0 and the center of the box drawn within green edges preceding the box in red, where the defined thresholds are exceeded.

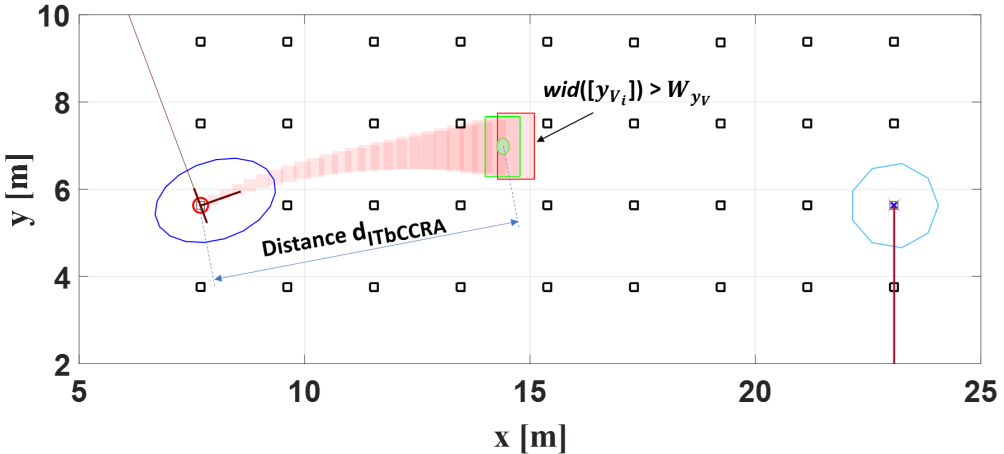
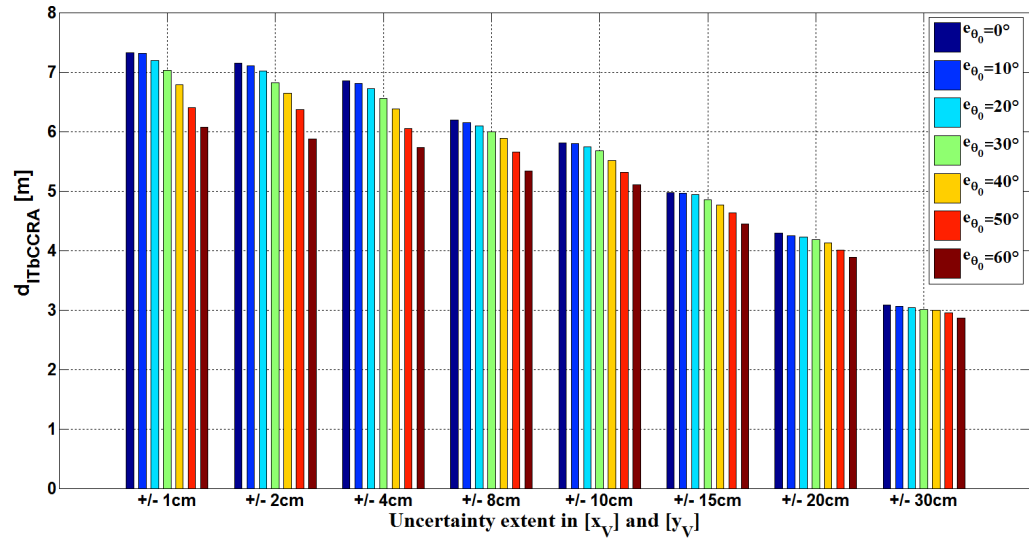
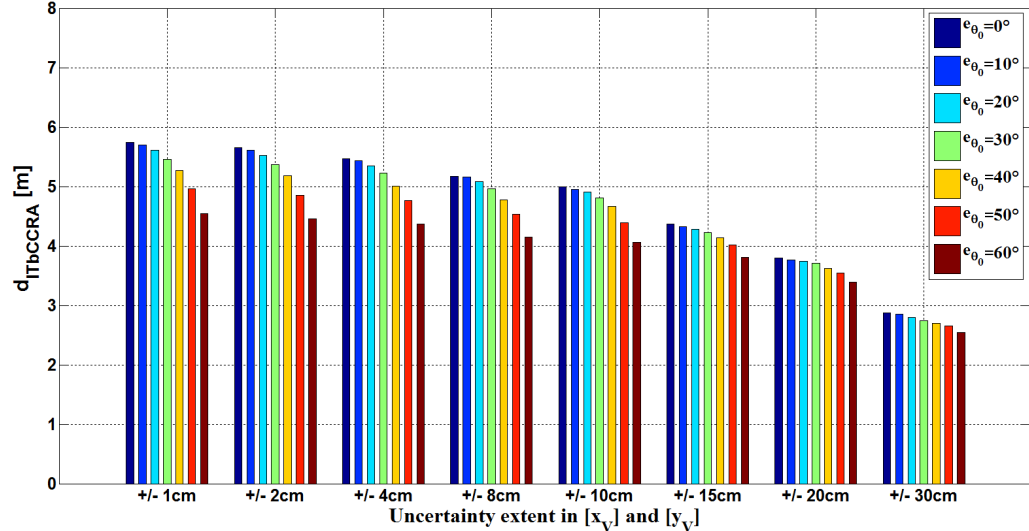


Figure 3.11: $d_{ITbCCRA}$ calculation.

Prediction horizon relatively to uncertainty in vehicle position:

The first test bunches are executed while enlarging progressively the uncertainty extent attributed to the vehicle position $([x_V], [y_V])$ whether for the initial conditions or (w_1, w_2) . In the mean while, the uncertainty extent in $[\theta_V]$ is kept the same. Among a large range of performed simulations with distinct setups and different e_{θ_0} values, a sample of result examples is presented in Figures 3.12a and 3.12b while respectively setting widths of $[\theta_{V_0}]$ and $[w_3]$ to 1° and 2° .

Based on results presented in Figure 3.12a, the more uncertainty attributed to $[x_V]$ and $[y_V]$, the smallest the distance covered by the reachable space before violating equation (3.37). However, the fall in the distance $d_{ITbCCRA}$ in Figure 3.12b, which is entailed by doubling the width of uncertainties impacting $[\theta_V]$, is more important compared to the results of Figure 3.12a. Even through system (3.1), the vehicle position is depending on

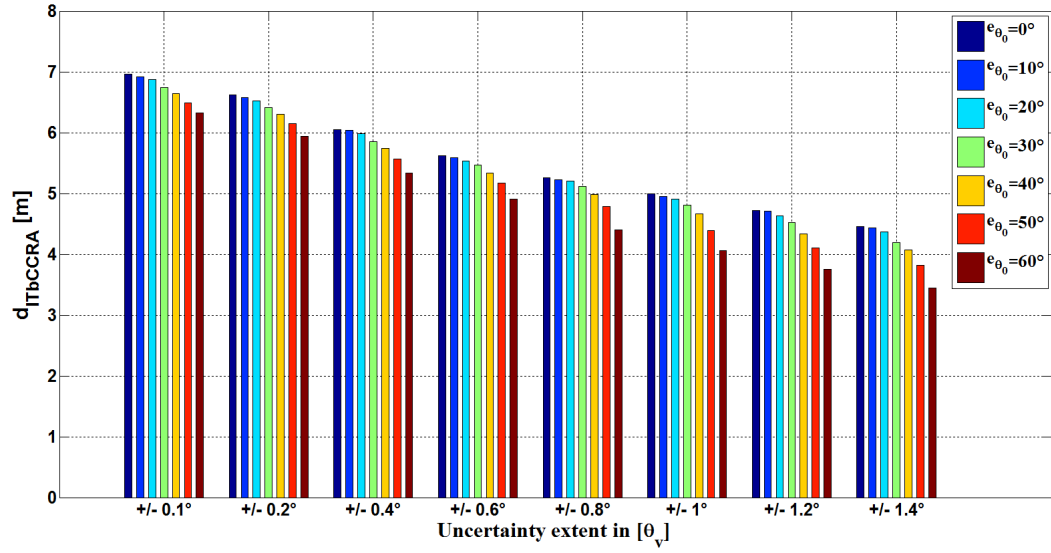
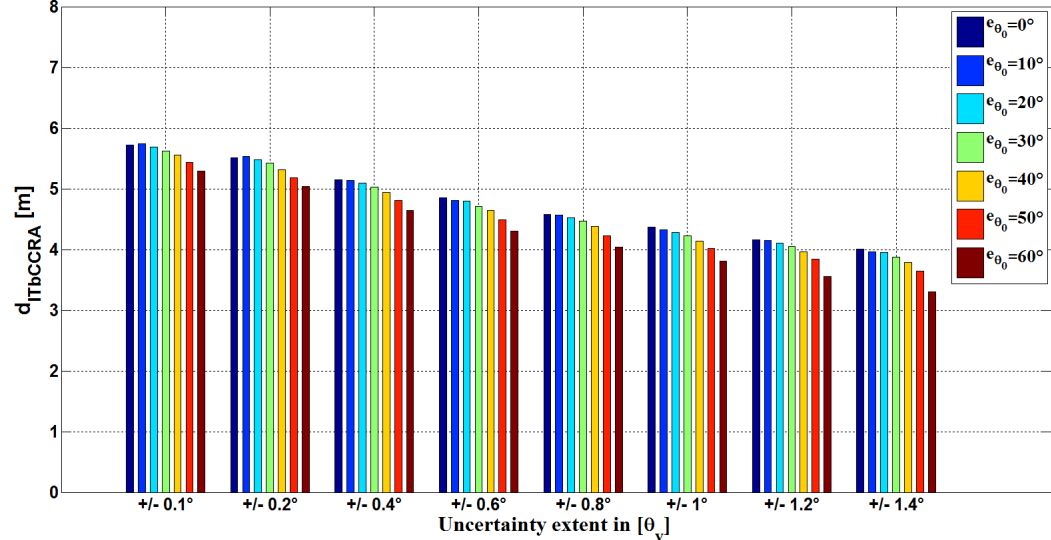
(a) Tests undertaken with uncertainty range attributed to $\theta_V = 1^\circ$ ($\pm 0.5^\circ$).(b) Tests undertaken with uncertainty range attributed to $\theta_V = 2^\circ$ ($\pm 1^\circ$).Figure 3.12: Horizon prediction relatively to uncertainty in position and e_{θ_0} .

its orientation. Correspondingly, more details about the relation between the ITbCCRA prediction horizon and the uncertainty in orientation are provided in the following.

Prediction horizon relatively to uncertainty in vehicle orientation:

At this stage, the amount of uncertainties attributed to $([x_{V_0}], [y_{V_0}])$ and (w_1, w_2) are fixed respectively to 10 cm (cf. Figure 3.13a) and then 15 cm (cf. Figure 3.14). Afterwards, $wid([\theta_V])$ is tuned by varying the uncertainty in vehicle orientation to have more precise idea about the reachability prediction horizon relatively to $[\theta_V]$.

The results shown in Figure 3.14 prove that the error in the vehicle orientation is the most influencing factor on the reachability prediction horizon. Finally, all the horizon prediction tests contribute in defining the ITbCCRA limitations and introducing an uncertainty-aware selection of waypoint locations. Avoiding waypoints' configurations that would violate the assumed constraints is essential to provide strong safety guarantees for NSbSWR.

(a) Tests undertaken with uncertainty range attributed to $x_V, y_V = 20 \text{ cm}$ ($\pm 10 \text{ cm}$).(b) Tests undertaken with uncertainty range attributed to $x_V, y_V = 30 \text{ cm}$ ($\pm 15 \text{ cm}$).Figure 3.13: Horizon prediction relatively to uncertainty in θ_V and e_{θ_0} .

3.3.4.2/ CONSISTENCY OF THE PROPOSED ITbCCRA METHOD

To prove the ITbCCRA consistency¹ through quantitative testes, batch simulations are tackled. The reachable space of a given configuration (of the vehicle and a specific target) is calculated. After that, the vehicle real trajectory is estimated until reaching the chosen target while injecting Gaussian noises into (x_V, y_V, θ_V) .

To more clarify the principle of the proposed batch simulations, two different examples are presented in Figure 3.14. Without injecting uncertainties into the simulated dynamics, the trajectory tracked by the vehicle crosses the center of the reachable boxes as shown in Figure 3.14a. This first simulation validates that the set-membership ITbCCRA

¹Consistency in this context means that the ITbCCRA findings always include all possible trajectories of the ODE solutions regardless of the navigation circumstances and under all uncertainty states.

and the deterministic reaching of the waypoint (within Gaussian noises) are conducted within the same navigation setups. After that, as already said, random noises are injected into (x_v, y_v, θ_v) . The batch simulations aim then to verify whether all the vehicle trajectories induced from executions within Gaussian noises are included into the pre-estimated reachability bounds or not. The magnitude of the injected random noises in each sample time cannot exceed the maximum errors used to define the interval widths in the reachable space computation.

During the batch simulations, important amounts of Gaussian noises are injected into the NSbSWR framework. Under these uncertainties, it is impossible that any robotic system can navigate steadily towards its target. Hence, an EKF is used during the simulations to maintain the stability and smoothness of the NSbSWR trajectories. As shown in Figure 3.14b, the vehicle trajectory after injecting the required stochastic noises is still smooth and enclosed into the ITbCCRA-issued reachable bounds.

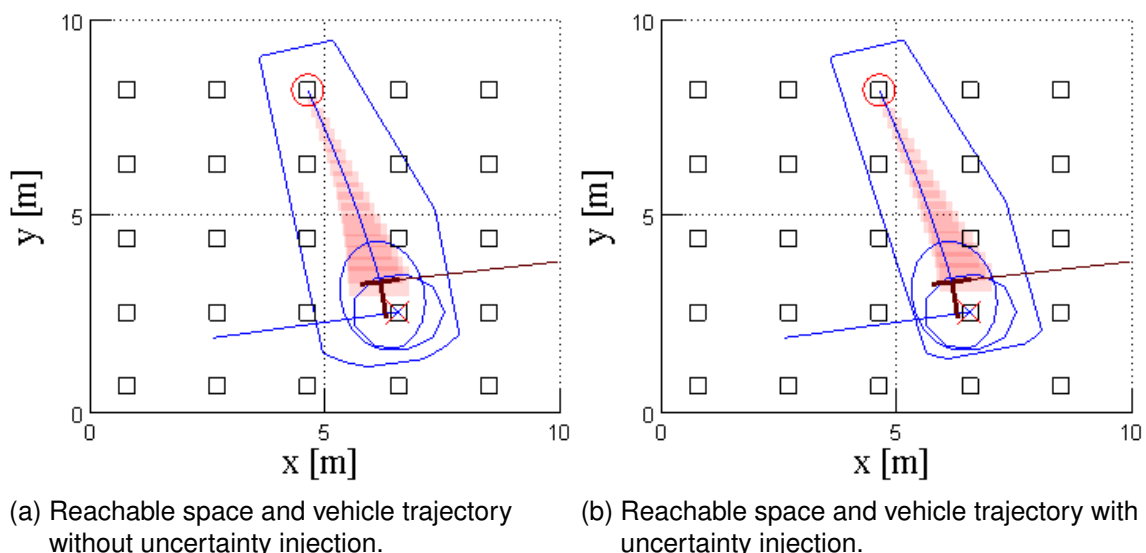


Figure 3.14: Batch simulation principle.

Let consider a first test scenario, where Gaussian uncertainties are injected in the navigation dynamics according to the setups presented in Table 3.1. To estimate the system reachable space within same minimum/maximum values of stochastic uncertainties, bounds of the interval noises attributed to (x_v, y_v, θ_v) at every sample time are respectively $\pm 10\text{cm}$, $\pm 10\text{cm}$ and $\pm 1^\circ$.

Table 3.1: First scenario of batch simulation setups for Gaussian uncertainty injection

Variable	Minimum	Maximum	Mean	Standard deviation
x_v (m)	-0.1	0.1	0	0.05
y_v (m)	-0.1	0.1	0	0.05
θ_v (degree)	-1	1	0	0.5

Including 200 triggered execution, the batch simulation results in the 2-dimensional space are presented in Figure 3.15.

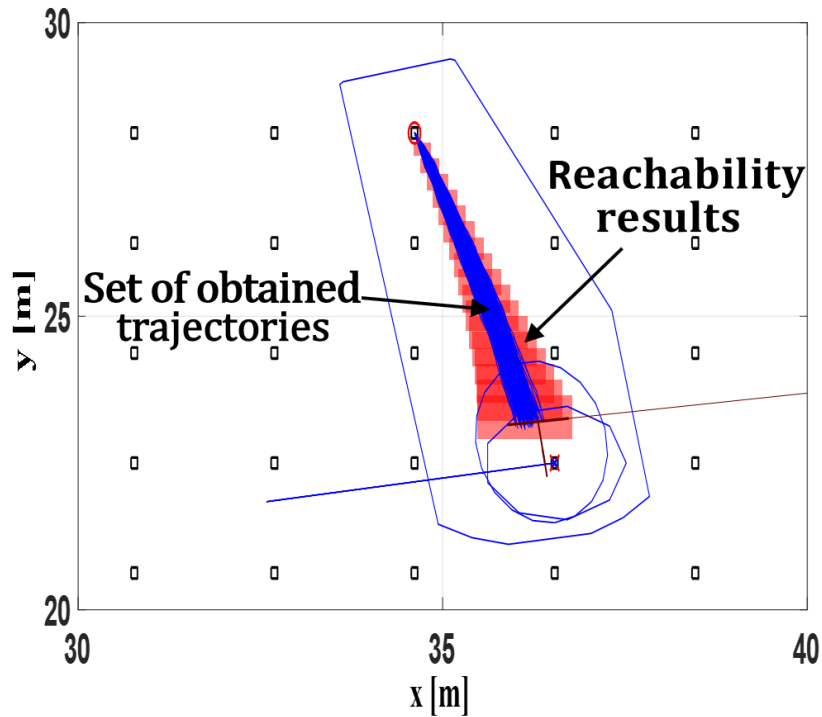


Figure 3.15: First scenario batch simulation results representation in 2D space.

Afterwards, the evolution of (x_V, y_V, θ_V) obtained via batch simulations and their corresponding reachability-issued frames are illustrated in Figures 3.16, 3.17 and 3.18.

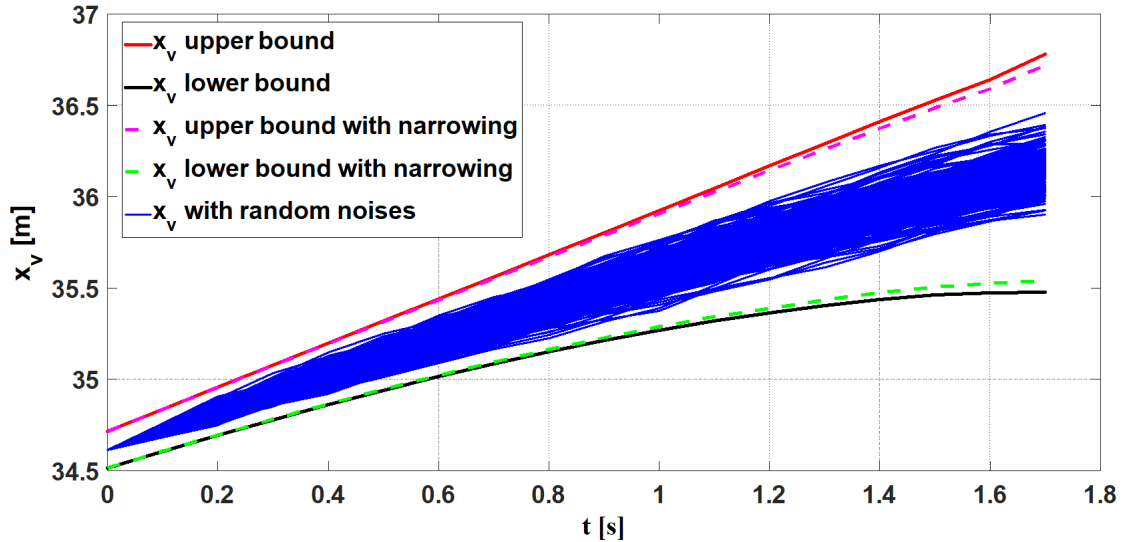


Figure 3.16: Evolution of x_V compared to bounds of the reachable space with/without narrowing (scenario 1).

Obviously, the depicted results show that ITbCCRA-issued bounds enclose perfectly the data obtained via the undertaken batch simulations. Correspondingly, a successful estimation of the NSbSWR reachable state space is then carried out. During the execution of

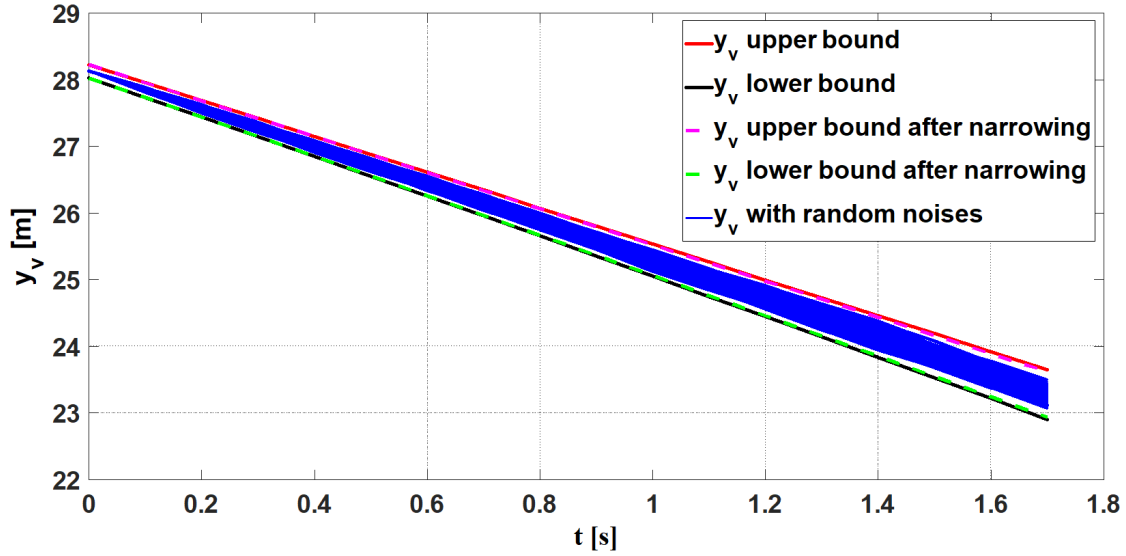


Figure 3.17: Evolution of y_v compared to bounds of the reachable space with/without narrowing with/without narrowing (scenario 1).

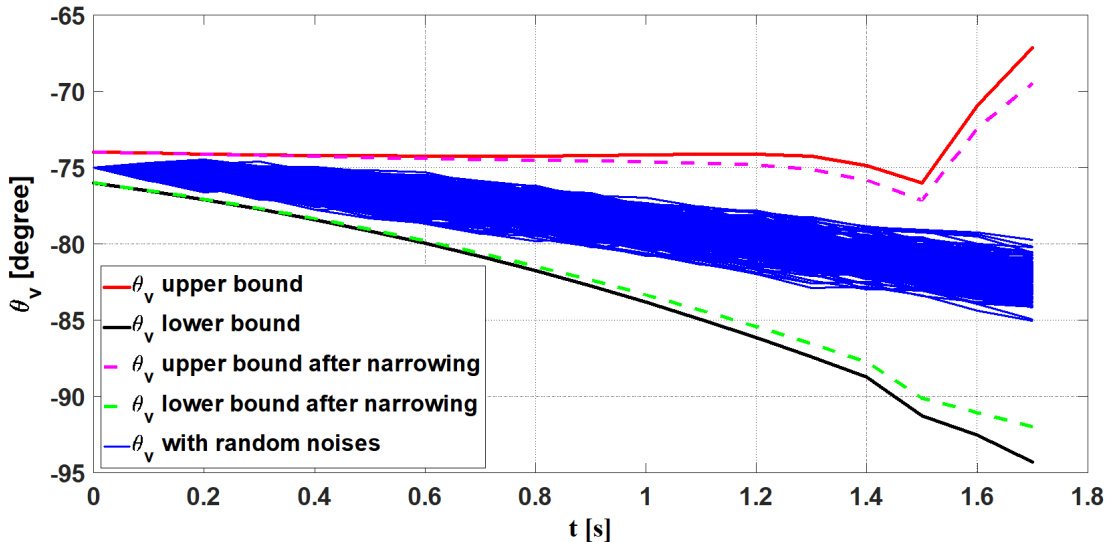


Figure 3.18: Evolution of θ_v compared to bounds of reachable space with/without narrowing (scenario 1).

this simulation scenario, for both states x_v and y_v , there is no notable difference between bounds of the solutions obtained by the standard interval Taylor method and the ITbC-CRA method (within the correlation based narrowing of the ODE interval solutions). In this case, the proceeded correlation-based phase validates the appropriate propagation of the solution enclosures into the uncertain ODE system. Nonetheless, the correlation supervision decreased slightly the extent of uncertainty in solutions of θ_v . The impact of the introduced narrowing phase is more obvious after many steps from the ITbCCRA (starting from instant 1.4s in Figure 3.18).

To interpret in a better way the consistency of the proposed reachability approach, a more critical second test scenario is launched. This time, bounds of the interval uncertainties attributed to (x_V, y_V, θ_V) are respectively $\pm 5\text{cm}$, $\pm 5\text{cm}$ and $\pm 0.5^\circ$. Likewise, Table 3.2 shows the set of appropriate configurations to inject the required stochastic uncertainties into the system variables to perform the batch simulations. For this scenario, since less uncertainties are propagated into the simulated NSbSWR framework, the enclosure of the navigation system reachable space should be tighter. Thus, chances that the noisy states exceed their corresponding interval-based thresholds are stronger.

Table 3.2: Second scenario of batch simulation setups for Gaussian uncertainty injection

Variable	Minimum	Maximum	Mean	Standard deviation
x_V (m)	-0.05	0.05	0	0.025
y_V (m)	-0.05	0.05	0	0.025
θ_V (degree)	-0.5	0.5	0	0.25

Analogously to the realized first scenario, together the ITbCCRA findings as well as the batch simulation results in the 2D space domain of 200 executed simulations are illustrated in Figure 3.19.

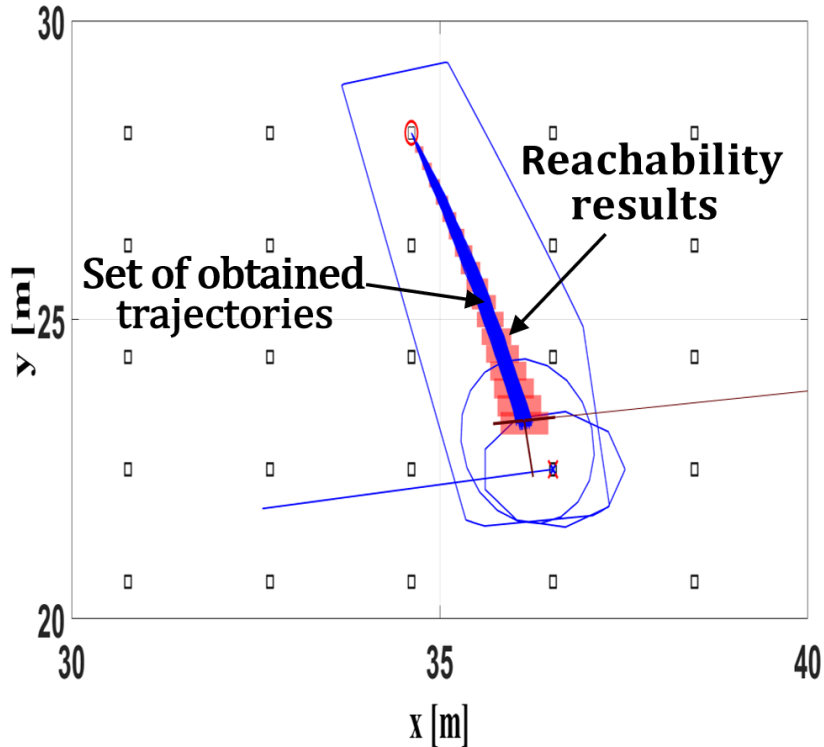


Figure 3.19: Second scenario batch simulation results representation in 2D space.

As expected, the extend of the NSbSWR reachable space in the proposed second test scenario is much tighter. Respectively, the progression of the (x_V, y_V, θ_V) findings over time for both batch simulation and the ITbCCRA method are depicted in Figures 3.20, 3.21 and 3.22. Since the extent of uncertainty in the initial conditions and $w_{i=1..3}$ is tighter,

there is no considerable difference entailed by the narrowing phase for bounds enclosing the system states (x_V, y_V, θ_V).

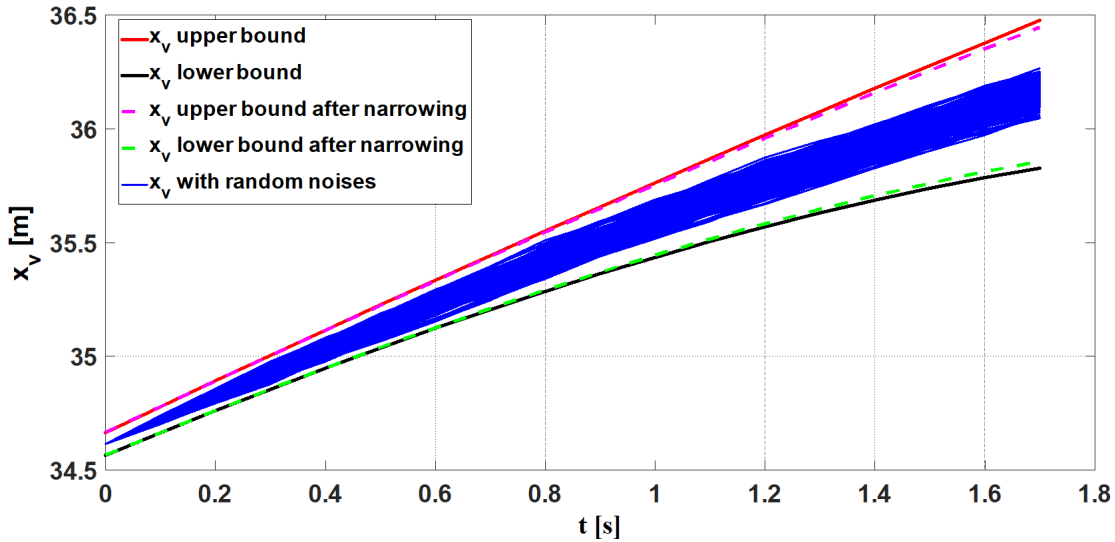


Figure 3.20: Evolution of x_V compared to bounds of the reachable space with/without narrowing (scenario 2).

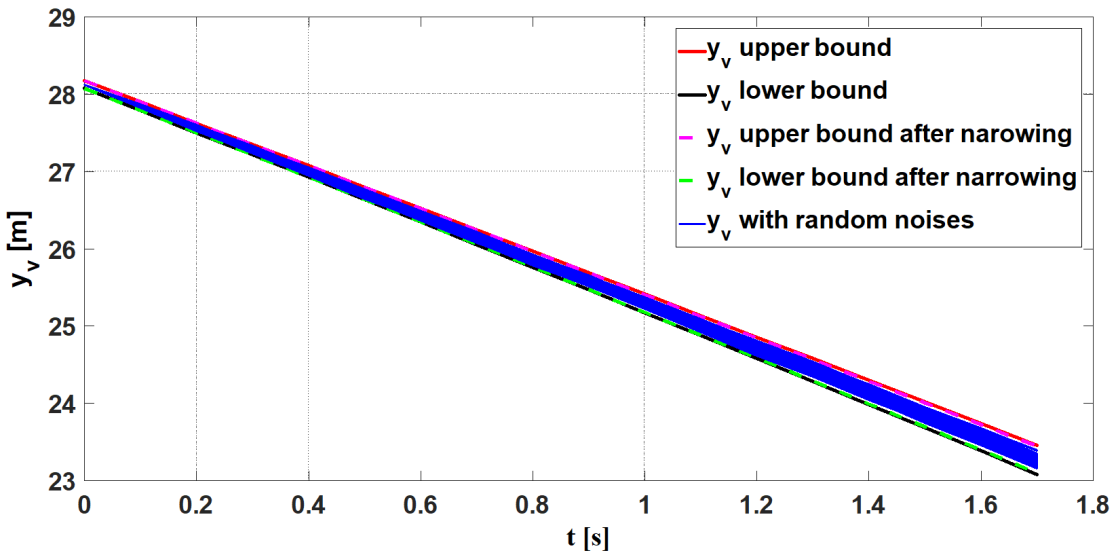


Figure 3.21: Evolution of y_V compared to bounds of the reachable space with/without narrowing (scenario 2).

According to the results of the realized consistency tests (scenario 1 and 2), the simulated uncertain system states, are perfectly enclosed between the set-membership ITbCCRA bounds. These results prove the reliability of the proposed method and its convenience to ensure safety verification for the flexible NSbSWR strategy.

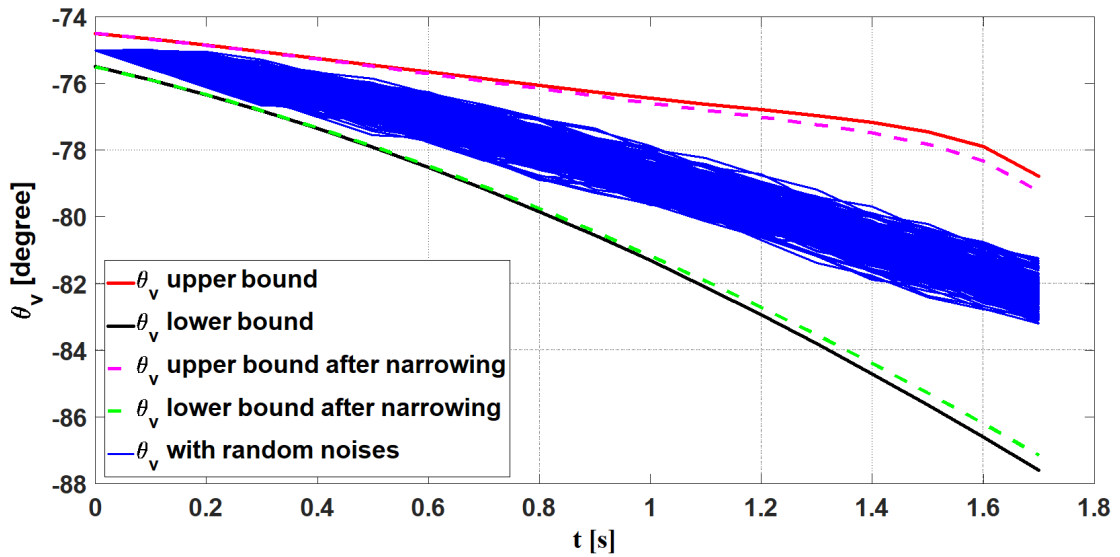


Figure 3.22: Evolution of θ_v compared to bounds of reachable space with/without narrowing (scenario 2).

3.4/ ITBCCRA-BASED RISK ASSESSMENT AND MANAGEMENT

The proposed reachability approach permits to assess all potential risks that threaten the vehicle navigation. More interestingly, it reveals whether or not the vehicle will cross the road limits or collide with other road participants, which is essential for safety assessment. Once detected, collision risks or leaving the road boundaries must be managed. The risk management solution, which is detailed in the sequel, aims to take advantage of the ITbCCRA outputs to ensure that the vehicle maintain a predefined Lower Distance (LD) with the borders or to the obstacles. LD is chosen in order to play as a marginal safety distance to the NSbSWR (cf. Figure 3.23). The remaining of this section is dedicated to explain and validate the suggested ITbCCRA-based risk management layout for NSbSWR.

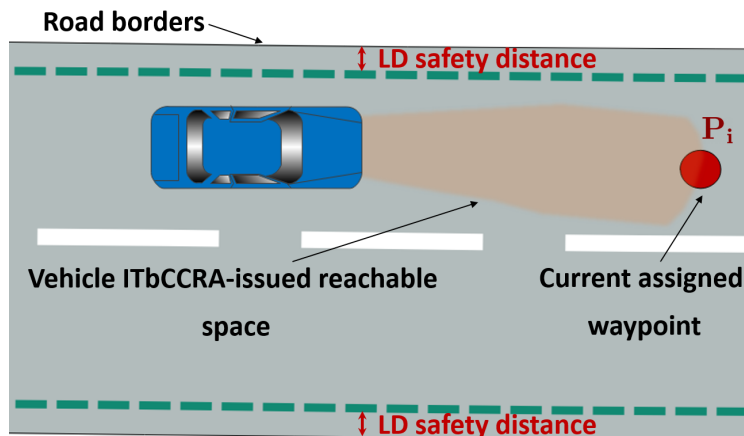


Figure 3.23: ITbCCRA-based risk management principle.

3.4.1/ RISK MANAGEMENT ALGORITHM FOR NSBSWR

Parameters that influence the reachable space evolution may be exploited to guarantee the navigation safety regarding to the uncertainty-induced risks. Hence, the introduced risk management acts on the control parameters to lead the NSbSWR to a safe progression of its reachable space. Let recall that the navigation is ensured through a Lyapunov-based asymptotically stable control law [20, 299]. The control stability is guaranteed for all positive values of parameters included in vector $\mathbf{K} = (K_d, K_l, K_o, K_x, K_{VT}, K_\theta)$. In this context, the control parameter K_θ is the positive parameter, which is related to the vehicle maximum angular velocity. Notably, e_θ is assumed to always converge asymptotically towards zero. Then, through equations (3.10) and (3.12), it is possible to deduce the following:

- For $e_\theta \in]0, \pi/2[$, the term $k_\theta \tan(e_\theta)$ in equation (3.12) is positive. Hence, rising k_θ will deviate the reachable space orientation to the anticlockwise direction (since $\gamma_V = \arctan(l_{bc}) \rightarrow \pi/2$). Contrarily, if k_θ drops to zero then the orientation of the vehicle reachable space will move towards the clockwise direction.
- For $e_\theta \in]-\pi/2, 0[$ and based on the sign of $k_\theta \tan(e_\theta)$, increasing/decreasing the value of k_θ will entail respectively the re-orientation of the vehicle reachable space to the clockwise/anticlockwise direction.

From this scope, one way to satisfy the safety constraints, stay within the road boundaries, and avoid collisions consists of changing slightly the global orientation of the vehicle reachable space (to avoid any risk to go outside the defined safe/free area). As illustrated in Figure 3.24, the direction of the reachable space evolution is given by the line that passes through the center of the initial condition box C_0 and the center C_f of the reached box at instant t_f . As a main assumption to perform the risk management, linking the starting and the arrival point represented respectively by C_0 and C_f is supposed to outline approximately the orientation of the reachable space bounding shape.

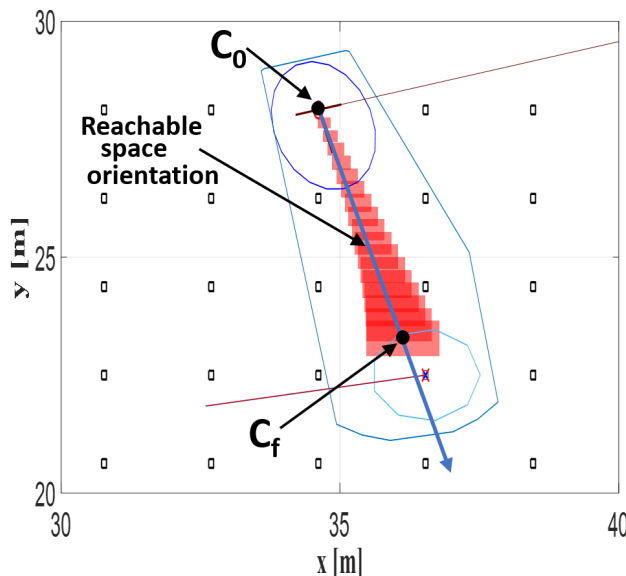


Figure 3.24: Orientation of the bounded reachable space.

As soon as a collision is predicted and starting from its nominal value, a new value of K_θ is selected to manage the risks and guide the navigation system to safe reachable zones. Acting on other control parameters to guarantee a free-collision navigation is possible. Nonetheless, tuning only K_θ relieves the complexity costs of the risk management. Characterizing also the effect of adapting one single parameter is more practical than anticipating the NSbSWR behavior after simultaneously altering several control parameters.

Roughly, the navigation through waypoints and the reachable space calculation via IT-bCCRA should be proceeded through the nominal values of $\mathbf{K} = (K_d, K_l, K_o, K_x, K_{VT}, K_\theta)$. At instant t_f that indicates the end of each reachability estimation cycle (cf. Flowchart 3.6), intersections between the both road boundaries and the navigation system reachable space should be verified. If no intersection is found, the navigation is assumed as safe and the nominal value of K_θ is kept unchanged. In the other case, K_θ is temporally tuned until reaching the current assigned waypoint without having intersection with any undesirable area (in our study, it corresponds to the border of the road).

The new K_θ aims to rotate the reachable space bounded shape around the center C_0 associated to the initial condition domain with an angle θ_R to avoid any collision. The required rotation angle θ_R to the initial unsafe reachable space maybe appropriately determined via the angle between the following lines (see Figure 3.25):

- The line crossing the center C_0 and the point I_1 , which is the closest point from the road boundary (in intersection with the system reachable space) to the convex shape global orientation line.
- The line crossing the center C_0 and the point I_2 . This latter is the most distant point belonging to the convex hull bound (located behind the road margins) from the road segment in intersection with the road borders.

Technically speaking, the road boundaries may be presented as a poly-line that relates points from the road extremities. Hence, points I_1 and I_2 can be determined through fundamental computational geometry algorithms.

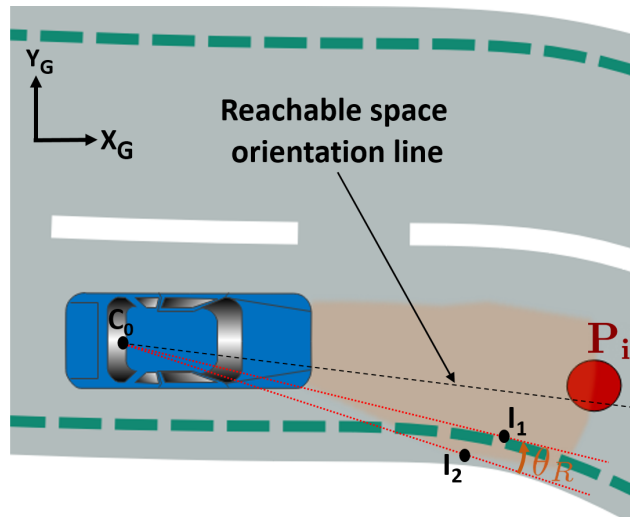


Figure 3.25: θ_R estimation method.

At this stage, it remains to clarify how to select the new value of K_θ once the desired θ_R is estimated. This goal is met by characterizing in offline the effect of increasing/decreasing the nominal value of K_θ on the global orientation of the reachable space bounding shape (cf. Figure 3.24). Through extensive simulations, a large equally spaced values K_θ are applied and the different changes in the reachable space orientation are stored. According to the recorded offline results, the most new suitable K_θ that may achieve the rotation angle θ_R is picked up.

Finally, the whole risk assessment and management strategy that warrants the safe reaching of waypoints under uncertainties is summarized in Algorithm 4.

Algorithm 4: ITbCCRA-based risk management strategy

Require: Waypoint series, vehicle pose, current target P_i .
Ensure : ITbCCRA safety guaranteed navigation through waypoints.

```

1 while NSbSWR process is running do
2   if new waypoint is assigned then
3     -Compute the ITbCCRA-issued reachable space within nominal  $k_\theta$ .
4     -Check collision risks.
5     if no collisions are admitted then
6       repeat
7         -Proceed navigation with nominal  $k_\theta$ .
8       until reaching the assigned waypoint
9     else
10    repeat
11      -Estimate  $\theta_R$ .
12      -Proceed navigation with the adapted  $k_\theta$  based on the offline results.
13    until reaching the assigned waypoint
14  end
15  -Switch to new waypoint  $P_i := P_{i+1}$ .
16 end
17 end

```

3.4.2/ SIMULATION SETUPS AND RESULTS

In this subsection, the proposed risk management performances in terms of collision-avoidance are assessed in presence on uncertainties. Accordingly, an NSbSWR simulation scenario consisting of crossing dangerous road bends is tackled. Evidently, pathway holding on bends and rough road curvature is crucial. Under uncertainties, accidents and road sliding are common in such a driving critical situation. More particularly, the navigation test scene, designed under Matlab, includes two sharp bends. As shown in Figure 3.26, the risk-level of crossing the first road deviation is increased by the presence of another road participant (assumed as a static obstacle). Remarkably, the pathway borders represented in grey color in Figure 3.26 are the concrete road limits. The borders drawn in green are the navigation road boundaries after taking into account the additional safety distance LD. Notably, LD is set to 1 m in this test scenario. To launch the introduced test scenario, the exact initial pose of the navigation system is fixed as follows: $x_V = 7.69$ m, $y_V = 16.87$ m and $\theta_V = -70^\circ$.

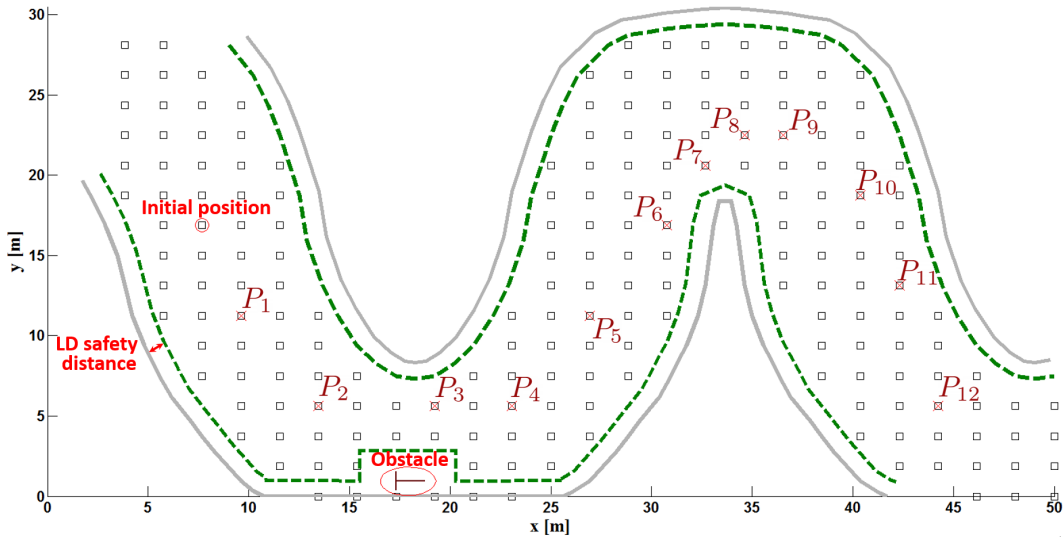


Figure 3.26: Simulation test-scene.

Hence, a set of twelve waypoints are designated to guide the vehicle towards the end of the introduced navigation scene. All positions of the predefined sequential waypoints are given in Table 3.3. It indicates also the orientations of all waypoints, which are determined through equation (3.13). Most importantly, the waypoints designation is accomplished in a manner to assure that the orientation error between the vehicle and its currently assigned target always satisfies: $e_\theta \in]-\pi/2, \pi/2[$ [297]. It is imperative to verify the presence of the target in front of the vehicle to guarantee the navigation stability, smoothness and safety (see Appendixes A and B for details). Otherwise, every waypoint's configuration is joined with specific error values to define its own error circle.

Table 3.3: Waypoints configurations

Waypoint	P_1	P_2	P_3	P_4	P_5	P_6	P_7	P_8	P_9	P_{10}	P_{11}	P_{12}
x_T (m)	9.615	13.46	19.23	23.07	26.92	30.79	32.69	34.61	36.53	40.38	42.30	44.23
y_T (m)	11.25	5.62	5.62	5.62	11.25	16.87	20.62	22.50	22.50	18.75	13.12	5.62
θ_T (degree)	-55.63	0	0	55.63	55.63	62.85	44.27	0	-44.27	-71.12	-75.61	-90

As clear from Figure 3.26, the waypoints' locations are selected in many occasions very close to the road borders in order to invoke critical situations. Besides, the waypoints' poses are defined without any consideration of the previous characterization of the ITbC-CRA prediction horizon (cf. subsection 3.3.4.1). In such a manner, overstepping the road limits by the navigation system is more probable under severe uncertainties.

The remaining part of this subsection focuses on interpreting consequences of adapting K_θ on the Lyapunov function selected for the control law. Besides, attention is paid to analyze changes entailed by the risk management scheme on the convergence rate of the navigation errors (distance to reach the target and e_θ). In such a manner, it is possible to evaluate the ITbCCRA-based risk management performances in ensuring the navigation stability and the safe convergence towards targets. The assessment of the control performances is not the main purpose of this work. For more details about the complete respect of the navigation system kinematic constraints by the adopted control law, readers are referred to [301].

In a first phase, the simulation test designed for NSbSWR is executed without applying the risk management approach proposed in Algorithm 4. The nominal control parameters are maintained all along the navigation run-time. Only the vehicle reachable space is estimated based on the ITbCCRA method to capture potential collisions. The navigation is proceeded with a maximum velocity value $V_{max} = 10 \text{ m/s}$, a maximum front wheel orientation $\gamma_{V_{max}} = 20^\circ$, and a sampling time step equal to 0.02 s . In addition, all the waypoints' velocities are set to $V_T = 5 \text{ m/s}$. Practically, the nominal values of the control parameters associated to vector \mathbf{K} are as follows: $K_d = 0.1$, $K_l = 1.8$, $K_o = 60$, $K_x = 0.4$, $K_{VT} = 0.01$ and $K_\theta = 0.19$. Otherwise, let denote by $P_i|P_{i+1}$ the period of time when the vehicle is traveling starting from the already reached waypoint P_i until reaching the next target P_{i+1} . In particular, $P_0|P_1$ refers to the period corresponding to the travel time between the vehicle initial position and waypoint P_1 . Correspondingly, the extent of interval-type uncertainties injected into the NSbSWR framework to conduct the ITbCCRA method during the different travailing periods $P_i|P_{i+1}$ are detailed in Table 3.4. These extents are attributed to the system initial conditions as well as noises (w_1, w_2, w_3) (cf. equation (3.17)).

Table 3.4: Interval-type uncertainty injection setups

Period	$P_0 P_1$	$P_1 P_2$	$P_2 P_3$	$P_3 P_4$
Uncertainty extent	$(\pm 15\text{cm}, \pm 15\text{cm}, \pm 0.8^\circ)$	$(\pm 15\text{cm}, \pm 15\text{cm}, \pm 1^\circ)$	$(\pm 10\text{cm}, \pm 10\text{cm}, \pm 1^\circ)$	$(\pm 10\text{cm}, \pm 10\text{cm}, \pm 0.5^\circ)$
Period	$P_4 P_5$	$P_5 P_6$	$P_6 P_7$	$P_7 P_8$
Uncertainty extent	$(\pm 15\text{cm}, \pm 15\text{cm}, \pm 0.5^\circ)$	$(\pm 10\text{cm}, \pm 10\text{cm}, \pm 0.5^\circ)$	$(\pm 10\text{cm}, \pm 10\text{cm}, \pm 0.5^\circ)$	$(\pm 10\text{cm}, \pm 10\text{cm}, \pm 0.5^\circ)$
Period	$P_8 P_9$	$P_9 P_{10}$	$P_{10} P_{11}$	$P_{11} P_{12}$
Uncertainty extent	$(\pm 10\text{cm}, \pm 10\text{cm}, \pm 0.5^\circ)$	$(\pm 15\text{cm}, \pm 15\text{cm}, \pm 0.8^\circ)$	$(\pm 15\text{cm}, \pm 15\text{cm}, \pm 1^\circ)$	$(\pm 15\text{cm}, \pm 15\text{cm}, \pm 0.5^\circ)$

Aside from the interval uncertainties to compute the reachable space (cf. Table 3.4), configurations of the stochastic uncertainties injected into the navigation system variables to estimate its real trajectory are depicted in Table 3.5.

Table 3.5: Simulation setups of Gaussian uncertainty injection

Variable	Minimum	Maximum	Mean	Standard deviation
x_v (m)	-0.03	0.03	0	0.01
y_v (m)	-0.03	0.03	0	0.01
θ_v (degree)	-0.02	0.02	0	0.01

Figure 3.27 illustrates the overall results of this first simulation scenario in the 2-dimension space. These results include mainly:

- The navigation system reachable space (issued from the ITbCCRA method) to reach every single waypoint.
- The whole trajectory tracked by the vehicle during the simulation execution.
- The separation between the NSbSWR reachable space and the predefined safety margins to the road borders.

In this context, the thick green segments in Figure 3.27 represent the shortest distance separating bounds of the navigation system reachable space and the road boundaries (from both sides). These segments approve the safety of the navigation towards the next

waypoint. In contrast, the red thick segments underline the regions in intersection with the road safety margins. Accordingly, four potential collisions between the vehicle and the road borders are captured during the simulation run-time. Actually, these collisions are estimated respectively in periods $P_2|P_3$, $P_6|P_7$, $P_7|P_8$ and $P_{10}|P_{11}$.

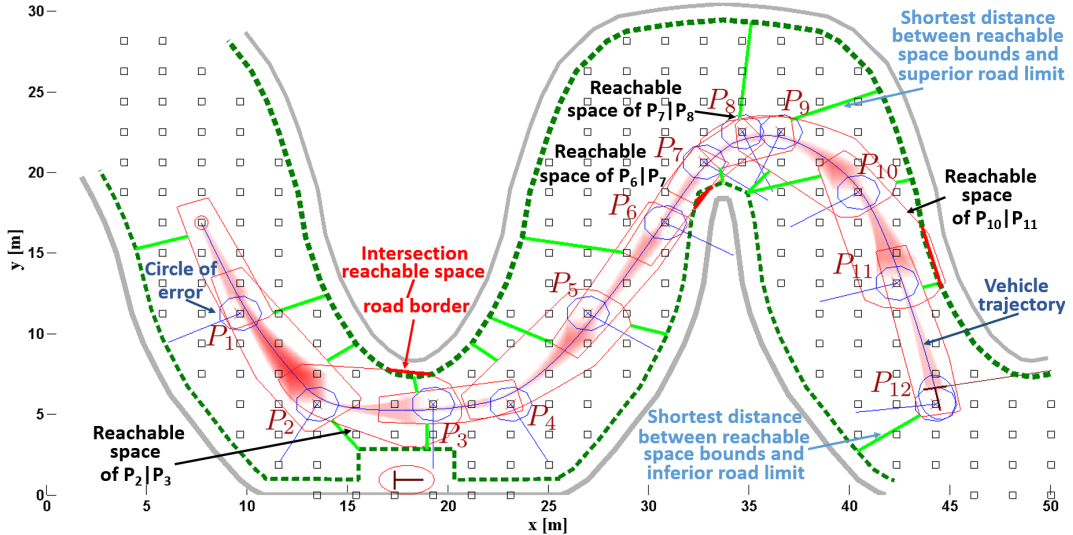


Figure 3.27: NSbSWR simulation results within nominal control parameters.

Based on the above depicted results, the risk assessment step through the ITbCCRA method is succeeded. The estimated reachable space may provide valuable warnings of future in-road hazards. Nevertheless, the control performances of the NSbSWR framework should be also examined. In that regard, the results illustrated in Figure 3.28 are devoted to examine the stability of the adopted control law. As a fact of matter, the controller stability is analyzed based on a convenient Lyapunov function. The analytical formalization of this latter is detailed in Appendix A. According to Figure 3.28, the generated controls for the NSbSWR are able to ensure the asymptotic stability and the convergence to every static target (cf. subsection 3.1.2).

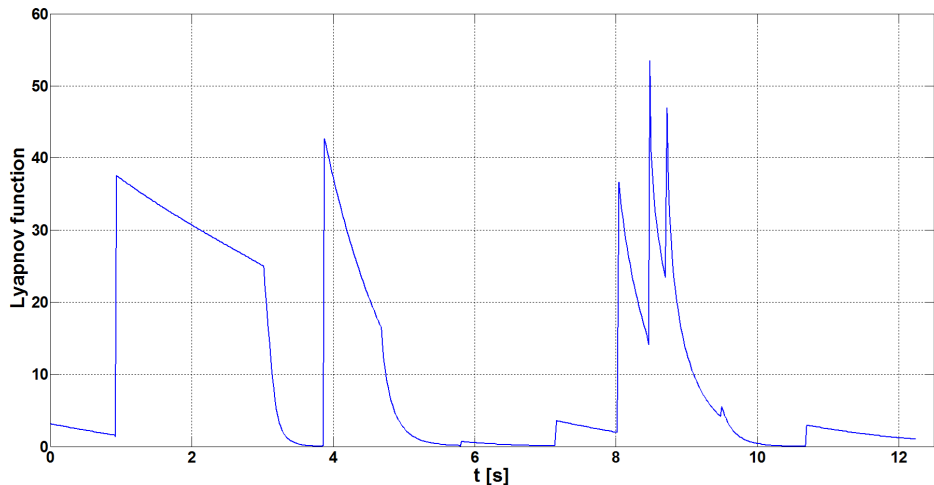


Figure 3.28: Lyapunov function evolution based on proposed control law for NSbSWR.

To evaluate the navigation performances in a more effective way, Figure 3.29 exhibits the evolution of the navigation errors in terms of distance to the target and the difference in orientation between the target and vehicle. Accordingly, the proposed control serves to decrease steadily the mentioned errors to ensure a smooth waypoint reaching. Noticeably, the distance to target never reaches zero since the switch between the sequential waypoints is triggered as soon as the vehicle crosses the circle of error associated to a given target.

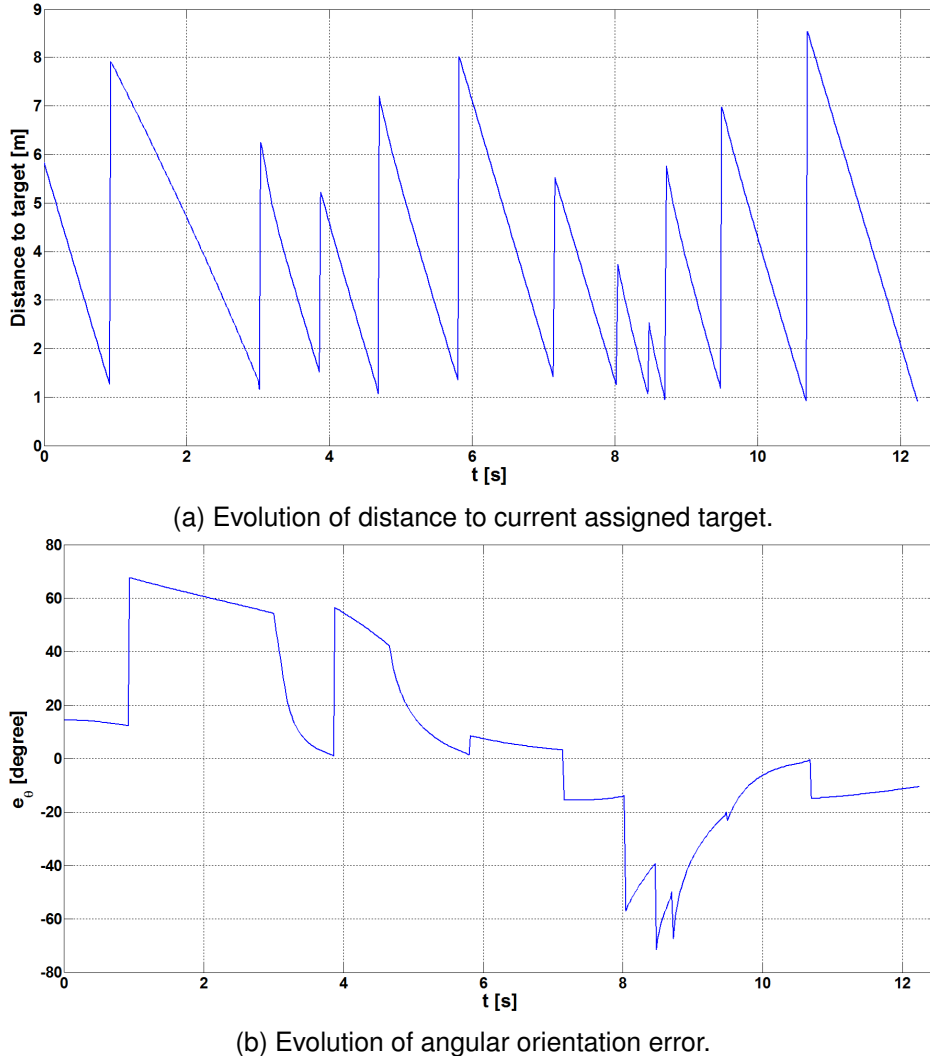


Figure 3.29: Evolution of distance/angular errors.

At this level, a second simulation scenario is realized to test the introduced risk management in terms of safety assurance. As seen in Figure 3.30, all the collision risks are handled by acting on the control parameters (cf. Algorithm 4). The nominal value of K_θ was tuned in three occasions (periods $P_2|P_3$, $P_6|P_7$ and $P_{10}|P_{11}$). The earlier captured collision in period $P_7|P_8$ was systematically mastered since the vehicle changed its trajectory during period $P_6|P_7$. Table 3.6 reveals the applied modification in the control parameters based on the offline results and the re-orientation angle of the initial reachable space.

In respect to the control performances, the evolution of the Lyapunov function presented in Figure 3.31 confirms the navigation asymptotic stability even within the modification in

Table 3.6: Risk management modifications in control parameters

Period	$P_2 P_3$	$P_6 P_7$	$P_{10} P_{11}$
θ_R (degree)	3.34° (anti-clockwise direction)	8.26° (clockwise direction)	3.89° (anti-clockwise direction)
Offline-based adapted value of K_θ	0.143	0.07	0.263

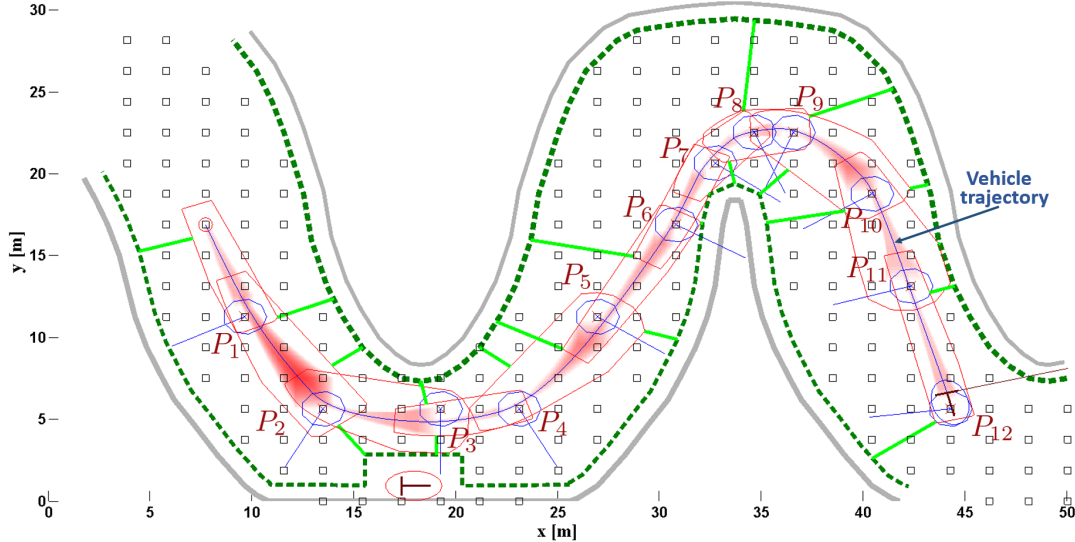


Figure 3.30: NSbSWR simulation results within ITbCCRA-based risk management.

K_θ value. Generally, the same shape of the Lyapunov function evolution is found compared to the results depicted in Figure 3.28. Remarkably, the fall in the Lyapunov function during period $P_6|P_7$ (interval time [7.22s, 8.14s]) is less important. It is worth reminding that this period witnessed the most important change in the control parameters in order to enable the required re-orientation angle θ_R . Despite of this change in the Lyapunov function behavior, the NSbSWR stability is still maintained.

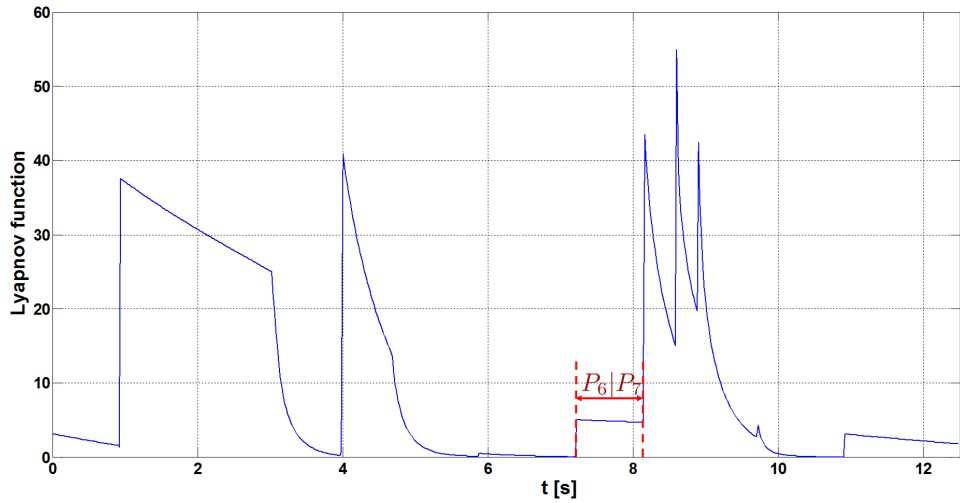


Figure 3.31: Lyapunov function evolution after acting on control parameters.

Finally, consequences of changes in the control parameters should be carefully analyzed

to figure out their effects on the convergence errors. Figure 3.32 shows the evolution of navigation errors (distance and orientation) w.r.t the target. Compared to the first simulation scenario results, the performed changes in k_θ value invoked a slight decrease in the convergence rate of e_θ during $P_2|P_3$ and $P_{10}|P_{11}$. The impacts of the applied modifications on the orientation error e_θ is more obvious during period $P_6|P_7$. Otherwise, the error in terms of final distance to the target is slightly more important than the nominal case during periods $P_6|P_7$ and $P_{10}|P_{11}$.

Through the realized validation work, it can be deduced that the ITbCCRA is quite suitable to ensure safety verification and risk management for the NSbSWR. The adopted Lyapunov-based control law maintains, in a natural way, the navigation stability whatever the value of k_θ (which must be positive). Safety is guaranteed thanks to the proposed solution with a harmless loss of precision in the convergence of the navigation system to its target in worst cases (decrease in the navigation errors convergence rate).

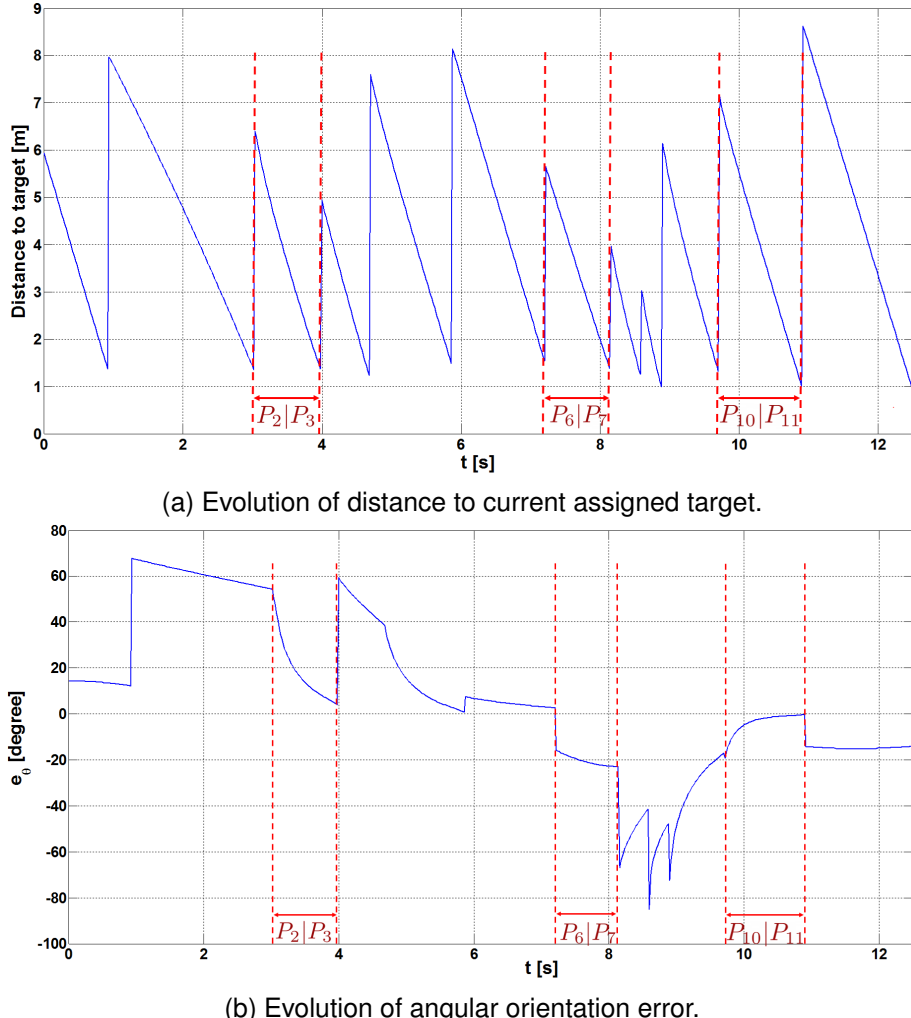


Figure 3.32: Evolution of distance/angular errors with adapted control parameters.

3.5/ CONCLUSION

The Navigation Strategy based on Sequential Waypoint Reaching (NSbSWR) is an emergent flexible navigation trend, which avoids frequent complex trajectories' planning/re-planning. In this chapter, a novel interval-based risk management strategy dedicated for the NSbSWR framework is introduced. Foremost, the suggested risk management enables the explicit consideration of several sorts of navigation uncertainties (uncertainties in modelling, perception, etc.). The interval-based reachability analysis was used for this purpose to provide guaranteed risk assessment. An interval Taylor expansion model is built to solve an uncertain Ordinary Differential Equation (ODE) describing the navigation system. The obtained interval-shaped solutions enclose all possible future trajectories of the NSbSWR framework. Moreover, the correlation between the navigation process variables is characterized to avoid the interval arithmetic pessimism. Hence, an efficient risk assessment based on the navigation reachable space is permitted. In case of collision detection, the control parameters are tuned to influence on the extent of NSbSWR reachable space. The simulation work proved the safety, stability and efficiency of the proposed Interval Taylor-based Correlation Constrained Reachability Analysis (ITbCCRA) solution in handling uncertainties threatening autonomous vehicles.

4

RELIABLE RISK MANAGEMENT FOR SAFE NAVIGATION: APPLICATION TO AN ADAPTIVE CRUISE CONTROL

Following a given road participant is among the most carried out automated driving maneuvers. It represents also a fundamental task from the hierarchy of the majority of intelligent navigation processes. According to the recent survey presented in [282], the interest on the car-following developments has a central role in heading towards reliable and fully autonomous navigation approaches.

Actually, handling all sorts of uncertainties especially for the car-following scenario is substantial. Following a vehicle requires to be close enough to this latter. For this reason, important number of road accidents are occurring during a car-following, which emphasizes the need for efficient anti-collision solutions dedicated for this driving context. The follower motions are controlled in order to adapt the ego-vehicle's velocity to the leader vehicle. In this view, uncertain measurements or error sources related to the complicated composition of modern navigation systems can lead to fatal crashes or undesirable discomfort for passengers during a car-following situation.

Correspondingly, the current chapter inspects how to exploit models and data-driven analysis conducted through the interval analysis in order to make the car-following situation entirely safe. While following a vehicle, not only the safety requirements should be satisfied, but an optimal following behavior is necessary. Accordingly, the light will be focalized also in this chapter on fulfilling the optimality requirements, which are convenient for the car-following scenario.

Under the car-following context, practical solutions devoted to enhance the autonomous navigation reliability through interval analysis-based risk management strategies are introduced. Mainly, all the suggested methods in the present chapter are based on several novel interval-based formalizations for the Time-To-Collision (TTC) risk indicator. Various comparative studies and simulation results are depicted all along this chapter to assess the improvements brought by the suggested different TTC formalizations.

4.1/ NOVEL TTC OVER-APPROXIMATION FOR A CAR FOLLOWING SCENARIO

The use of the TTC as a relevant risk indicator to detect collision probabilities is frequent [56], [349]. Thus, a huge effort has been done to improve methods of the TTC computation over the last years. A comprehensive comparative study between divers one-dimensional and two-dimensional TTC computing algorithms can be found in [144]. The depicted comparison has led to introduce a novel optimized TTC computing procedure in terms of computational complexity. The authors in [257] have considered the employment of point-to-point distances as unrealistic to evaluate the TTC. Alternatively, algorithms computing distances between boxes bounding vehicles have been proposed to derive TTC for complex traffic scenarios. A similar research work, which has modeled vehicles through boxes to estimate TTC for various traffic scenarios, is reported in [308]. To reach an extra-precise TTC approximation, the work proposed in [156] has explored probable accident configurations i.e., the exact points-of-contact of a potential crash between vehicles. The authors in [310] have taken advantage of a relative vehicle motion-based concept to obtain a more precise TTC and diminish the collision warning false alarm rate. Driving intentions of nearby vehicles have been predicted in [328] via an established hidden Markov model in order to enhance accuracy of the TTC estimation.

At the best of our knowledge and after examining the literature, it has been observed according to all our investigations, that the interval analysis has never been used to ameliorate the TTC computation. Consequently, a novel interval-based analytical formalization of this indicator is introduced in the sequel. Further, several improvements will be integrated on the proposed set-membership TTC computation process.

4.1.1/ PROBLEM STATEMENT

Evidently, Adaptive Cruise Control (ACC) systems are designed specially to deal with the car-following driving situation. Even though ACCs have become a mainstream equipment for modern vehicles, proving their correct and comfortable operation is still an open area of research [28]. Although ACCs are assumed to relieve drivers from the arduous driving responsibilities, the human supervision for ACC mechanisms is up to now inevitable.

Let consider two vehicles i and j , which are respectively the leader and the follower (cf. Figure 4.1). The car-following is indeed ensured via an ACC system mounted on the follower vehicle. Let assume that V_i , V_j , p_i and p_j are velocities and vector positions associated respectively to vehicles i and j . In the present case of study, all the navigation dynamics are observed through sensor measurements. In particular, the follower vehicle is equipped with a cyber physical tool, which in charge of measuring the separation distance between both vehicles, denoted d_{ij} . Besides, the ACC host vehicle is supposed to receive instantaneously the V_i value through a Vehicle-to-Vehicle (V2V) communication.

Technically speaking, the ACC should assign at every instant a target set-point to reach. The chosen target allows maintaining a safe reference distance, denoted d_{ref} , from the in-front vehicle. Hence, this section ultimate goal is to define a guaranteed and optimal risk management solution to be implemented on the ACC host vehicle. The designed approach should cope with all the uncertainty sources and all the complexity-issued challenges, which were noticed from the state-of-the-art analysis (cf. section 1.2, page 23).

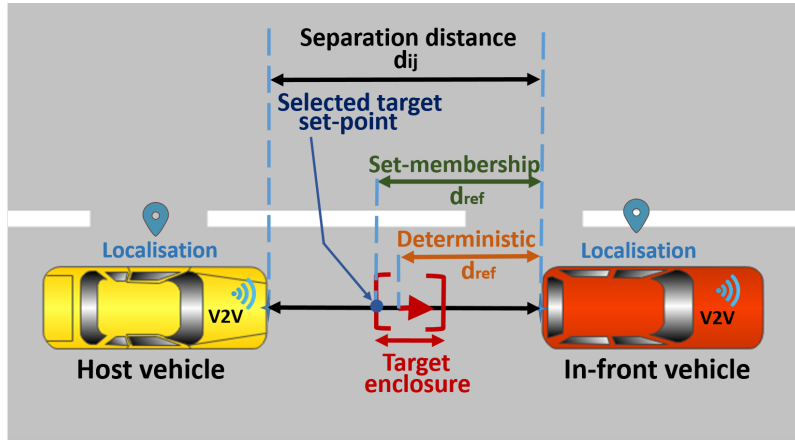


Figure 4.1: Car-following via interval-based ACC system.

Instead of defining d_{ref} in a deterministic manner, the interval analysis is employed to determine an enclosure for d_{ref} to inspect the worst case of risks and uncertainty-induced threats. More precisely, a novel set-membership formalization for the TTC is introduced to perform a reliable risk assessment. Then, the control unit of the ACC-equipped vehicle acts in order to avoid any critical situation based on the evaluated uncertainties and risks. It should be noted that the concerned ACC operation is ensured by the transition between two distinct modes:

- **Cruise control mode:** When there is no another road participant in the ACC-equipped vehicle vicinity, a dynamic target reaching is performed. Indeed, at each control cycle, the selected dynamic target is followed within a pre-defined velocity, which is assigned according to the user preferences.
- **Adaptive cruise control mode:** This mode is triggered once a vehicle is detected in the neighborhood of the follower car. In this case, a well-studied selection of d_{ref} must take place. In addition, d_{ref} should take precautions from the uncertainty impacts as well as any potential dangerous behavior made by the leader vehicle such as a sudden hard braking.

Clearly, the control cruise mode does not include any sever risks. Therefore, focus in this chapter is exclusively oriented towards ensuring safety for the car-following mode, where collision risks are high.

4.1.2/ SET-MEMBERSHIP TTC FORMALIZATION AND ERROR QUANTIFICATION STRATEGY

The TTC is often introduced as the ratio between the distance separating two vehicles and their relative velocity. Rather, the evolution of the follower and leader inter-distance is exploited here to perform more accurate collision prediction. The evolution of the follower and leader spacing distance is exploited at this stage to perform an accurate collision prediction for a car-following scenario. According to the study depicted in [310], the analytical formalization of the TTC based on the model of displacement between vehicles i

and j is expressed as:

$$TTC = -\frac{d_{ij}}{\dot{d}_{ij}} \quad (4.1)$$

where \dot{d}_{ij} is the change rate associated to d_{ij} and described by equation (4.2) (see [310]):

$$\dot{d}_{ij} = \frac{1}{d_{ij}}(p_i - p_j)^T(V_i - V_j) \quad (4.2)$$

However, the TTC formalization, given by equation (4.1) is still sensitive to uncertainties. It is also estimated through observations issued from sensor measurements and inter-vehicle communication. These observations are prone to important latencies. To handle these issues, a TTC interval-based over-approximation is defined. To adequately deal with uncertainties, the interval analysis is employed. With respect to measurement conditions, upper and lower bounds of data are computed.

Before proceeding further, it is necessary to set a sound strategy to acquire a prior knowledge of the uncertainty associated to intervals. Interval widths should be correlated with the environmental conditions emphasizing the uncertainty. In other words, a cause-effect link between uncertainty sources and interval widths is created in order to found a risk management of a high credibility. Accordingly, uncertainties are quantified at every sampling time through the following assumptions, which are made based on a deep knowledge of the navigation system properties. The assumptions below take also into account changes of the surrounding environment.

- At first, the localization inaccuracy is assessed via a signal strength indicator. It shows the satellite masking state and the signal attenuation in the navigation zone. In the run-time, the localization interval measurements should be adapted relatively to the available signal strength indicator. $[P_i]$ and $[P_j]$ are over-approximated relatively to the value indicated by the signal strength indicator.
- The accumulated error impacting the separation distance measurement is considered by an uncertainty range of $\pm x\%$ from the measured value of d_{ij} . The uncertainty extent attributed to $[d_{ij}]$ is based on the confidence interval provided by the manufacturer of the distance measurement device. Hence, the value of x depends mainly on the measurement technology.
- Several imperfections in the vehicular mechanical components (powertrain, combustion engine, torque, etc.) can take place. This can entail a slight difference between the velocity selected by the vehicle control units and the real velocity transmitted by the vehicular mechanical motor. Based on a prior knowledge of properties of the automotive mechanical part, V_i and V_j are assumed to be uncertain with a range of $\pm y\%$.

By turning the single-valued variables of expression (4.1) and (4.2) to intervals thanks to the defined assumptions, an interval-based formalization of the TTC is obtained:

$$\begin{cases} [\dot{d}_{ij}] = \frac{1}{[d_{ij}]}([p_i] - [p_j])^T([V_i] - [V_j]) \\ [TTC] = -\frac{[d_{ij}]}{[\dot{d}_{ij}]} \end{cases} \quad (4.3)$$

Even with the consideration of multiple uncertainty sources, the formalization given by system (4.3) does not consider any sort of communication latency. In several circumstances, communication delays can threaten the navigation safety and slow down the risk management reaction to abrupt in-road hazards. This issue is handled in the sequel.

4.1.3/ MATERIAL CONSTRAINTS-ISSUED UNCERTAINTIES

As early stated, the material constraints imposed by the modern Intelligent Vehicles (IVs) consist mainly of latencies impacting the intra/inter-vehicular¹communication. In accordance with the interval-based handling of uncertainty, the min/max variation of these delays over time should be properly defined. To meet this purpose, root causes and factors influencing the automotive communication delays should be well-analyzed. Based on the carried analysis, the development of an efficient latency-aware in-road risk management for autonomous navigation can be tackled. In this view, the methodology of how to include the latencies of the V2V communication and respectively the intra-vehicular communication into the risk management-level is detailed below.

4.1.3.1/ INTER-VEHICULAR COMMUNICATION RELATED LATENCY

As the vehicles are traveling, observations issued from communication are assumed to be valid only during a short period. These temporary observations unfortunately do not furnish any information about the evolution of the vehicle states over time. Hence the operation of connected vehicles is extremely sensitive to communication latency. Indeed, performances of the communication channel between two connected vehicles depends on the relation ruling the signal strength and vehicles relative location, where one of the vehicles can have a low signal strength or may be out of communication range [68].

Certainly, making connected vehicles aware about the potential latencies that may occur with nearby vehicles should permit a more reliable data exchange and inter-vehicular communication. Without any exception, the existing risk management strategies do not incorporate the communication latency on the risk assessment process. Contrarily to the existing literature, the proposed safety verification method aims to consider uncertainties invoked by communication delays.

Due to the signal interference and disturbances impacting data emission/reception, finding an analytical relation that rules the signal strength and vehicle locations is not evident. Instead, latencies affecting the communication range can be characterized empirically in respect to the velocity of the vehicle broadcasting periodically the required data. At present time, the Dedicated Short Range Communications (DSRC) is the common wireless technology that ensures the vehicular connectivity. The proposed method here pays attention in particular to the delay analysis of the DSRC technology due to its widespread usage in the automotive applications. To meet this goal, the results of a pioneer research work reported in [81] are exploited. The in-field tests carried out in [81] have provided a valuable description of the minimum/maximum variation of the DSRC latencies.

On the one hand, the DSRC latencies have been characterized relatively to the velocity of the connected vehicle transmitting data. Table 4.1 presents the empirically recorded

¹The intra-communication refers to the data exchange inside the IV embedded system via CAN for example. The inter-communication includes interactions between the IV and other vehicles or the infrastructure.

latencies affecting the V2V communication for distinct vehicle velocities during real world driving scenarios according to the study depicted in [81].

Table 4.1: DSRC delays within different speeds

Vehicle speed (m/s)	Minimum latency (ms)	Maximum latency (ms)
9	89.35	89.39
15	93.35	93.84
22	96.10	96.16
31	101.47	101.54

On the other hand, the presence of additional connected vehicles in a same navigation area raises the communication density. When numerous vehicles transmit messages simultaneously, the communication conflicts occurring to reply to data transfer requests provoke supplementary latencies. Thus, for more reliable characterization of the min/max bounds of the DSRC delays, the experimental study conducted in [81] has also quantified latencies issued from the increasing number of connected vehicles present in the close proximity of the communication range. In this sense, Table 4.2 depicts bounds of the DSRC communication delays in function of the number of nearby connected vehicles.

Table 4.2: DSRC delays within distinct number of vicinity vehicles

Neighborhood vehicles number	Minimum latency (ms)	Maximum latency (ms)
10	35.47	35.54
20	50.66	50.70
30	66.63	66.66

It is important to remind that the follower vehicle acquires the V_i value through a V2V communication (more precisely through a DSRC tool). Therefore, the results exhibited in Tables 4.1 and 4.2 are exploited to consider the additional uncertainties in the temporal space that may originate from communication latencies. Henceforth, $[T_{V2V}]$ designates latencies related to the V2V communication. To properly define $[T_{V2V}]$, both the vehicle speed and the number of nearby-connected cars are checked at each sample time to derive the appropriate experimental min/max delays corresponding to these factors.

4.1.3.2/ INTRA-VEHICULAR COMMUNICATION RELATED LATENCY

Especially for large scale automotive Networked Control Systems (NCSs), the data proliferation contributed recently to more important network-induced imperfections. Similar to the inter-vehicle communication delays, an approach to define intervals of the in-vehicular latencies is extremely needed. To bound the latency that may happen during the data propagation through the embedded system of the navigation process, it is indispensable indeed to master all the system timing-properties, including sensors update time and the end-to-end data transfer time through components, etc.

Let denote by $[T_L]$ the constant interval representing the delay of the onboard embedded

system. $[T_L]$ is fixed by the automotive designer at an early design phase of the navigation process. In fact, multiple alternatives are available to pre-estimate $[T_L]$. This is may be accomplished through extensive testing. Otherwise, several advanced computer aided design tools, which perform automotive network simulations, may approximate $[T_L]$ [195]. Differently, $[T_L]$ may also be fixed based on theoretical analytical models [210]. At this stage, bounds of interval $[T_L]$ are supposed to be well-known. Due to the importance of the materials constraints related to the intra-vehicular data traffic, an illustrative example that illustrates how to calculate the data propagation time through an onboard automotive system will be delivered in chapter 5. The communication delays may emphasize unpredictably a given in-road situation criticality. To avoid risks induced from the communication latency in the temporal space, $[T_{V2V}]$ and $[T_L]$ must be subtracted from $[TTC]$. The final TTC interval expression is given as:

$$[TTC] = -\frac{[d_{ij}]}{[\dot{d}_{ij}]} - [T_{V2V}] - [T_L] \quad (4.4)$$

The $[TTC]$ given by equation (4.4) represents the interval to which the exact TTC value belongs. This interval allows incorporating various uncertainties and latencies independently of a particular probabilistic distribution of the noise features, which may change in the run-time. Definitely, the $[TTC]$ over-approximation permits taking precautions against the worst case of uncertainties. Figure 4.2 summarizes the adopted uncertainty quantification strategy used for the set-membership TTC-based risk assessment.

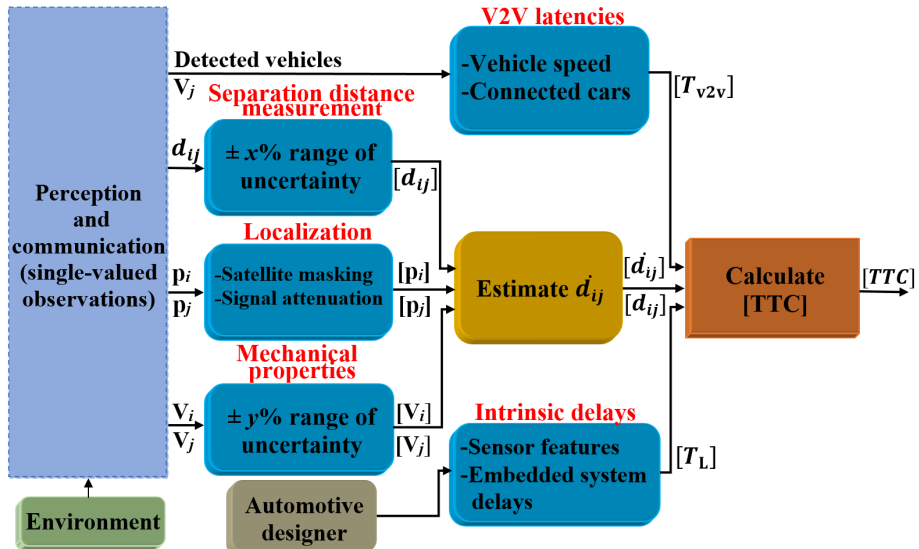


Figure 4.2: Uncertainty assessment strategy for interval-based TTC.

4.1.4/ INTERVAL-BASED/DATA-DRIVEN TTC

Similar to the previously proposed solution to obtain sharper bounds for the reachability space of an IV (cf. subsection 3.3.2, page 63), the car-following behavior is characterized by the correlation that relates variables to eliminate over-estimated uncertainties. It is quite useful to recall that a smooth progression of correlation underlines a correct behavior of the considered system (cf. subsection 3.3.2, page 63). Thus, a correlation-based

narrowing is proceeded to regulate uncertainty amounts assigned to interval measurements. This measure prohibits any divergence from the real progression of correlation. It is also worth reminding that at instant t_k , the dependency between two variables a and b are practically measured through the correlation coefficient $COR_{a,b|t_k}$ (cf. equation (3.29), page 65). The calculation of the correlation factor for interval data is also conducted via the interval vertex-based computation. $[p_i]$, $[p_j]$, $[V_i]$, $[V_j]$ and $[d_{ij}]$ are actually the interval variables that are concerned by the correlation-based narrowing.

Let denote by X_H the obtained equivalent matrix for an interval matrix of $N \times m$ measurements samples, where m is equal five in this case. Note also that $N_{X_H} = N \times 2^m$ is the number of samples included in X_H according to the Vertices Transformation (VT) (cf. subsection 3.3.3.1, page 66). Immediately after constructing X_H , the covariance values of each couple from the system variables ($[p_i]$, $[p_j]$, $[V_i]$, $[V_j]$ and $[d_{ij}]$) must be evaluated. The simplest way to determine the requested covariances is through computing the covariance matrix Σ associated to X_H :

$$\Sigma = \frac{1}{N_{X_H}} X_H^T X_H \quad (4.5)$$

By definition, Σ is a $(m \times m)$ square matrix, which is written as a function of covariances between each pair of variables (x_1, \dots, x_m) as follows:

$$\Sigma = \begin{pmatrix} Var_{x_1} & COV_{x_1, x_2} & \dots & COV_{x_1, x_m} \\ COV_{x_2, x_1} & \ddots & \dots & \vdots \\ \vdots & \vdots & \ddots & \vdots \\ COV_{x_m, x_1} & \dots & COV_{x_1, x_2} & Var_{x_m} \end{pmatrix} \quad (4.6)$$

It is worth noting that the covariance $COV_{x_i, x_j} = COV_{x_j, x_i}$ and Var_{x_i} is the variance of x_i . As shown in equation (4.6), the required covariance values can be easily extracted from Σ . At this stage, the evaluation of correlation $COR_{a,b|t_k}$ can be proceeded for all couple of variables $a, b \in ([p_i], [p_j], [V_i], [V_j], [d_{ij}])$, where $a \neq b$. Thereafter, the width of each interval measurement is narrowed. The interval with the largest width is concerned with iterative narrowing. Quite simple narrowing is proceeded by means of a preselected narrowing step α_i for each interval variable: $([a_i] := [\underline{a}_i + \alpha_i, \bar{a}_i - \alpha_i])$. After that, the VT is practiced. The gap in the correlation $\chi(a, b)_{t_k|t_{k-1}}$ between instants t_k and t_{k-1} is estimated (cf. equation (3.30), page 65). It is also worth mentioning that narrowing is aborted in two conditions:

- **Condition 1:** When $\chi(a, b)_{t_k|t_{k-1}}$ decreases from one iteration to another and suddenly starts to raise; i.e., the interval is narrowed as much as possible. Extra-reduction in the interval width may cause an undesirable modification in the correlation structure.
- **Condition 2:** Once $\chi(a, b)_{t_k|t_{k-1}}$ exceeds the minimum variation of correlation, which is recorded during off-line simulation of a normal system operation.

Finally, Algorithm 5 summarizes the main steps from the optimized TTC over-approximation. Thanks to the proposed interval-based/data-driven method, chances to obtain neither too conservative nor optimistic approximation for the TTC are definitely higher. Likewise, the credibility and consistency of the TTC bounds reached through Algorithm 5 are validated via the navigation system historical properties (correlation features).

Algorithm 5: TTC optimized over-approximation

Inputs : $p_i, p_j, V_i, V_j, d_{ij}, [T_L]$, and α_i .
Output: $[TTC]$.

1 **while** Navigation process is running **do**

2 -Estimate $[T_{V2V}], [d_{i,j}], [V_i], [V_j], [p_i]$ and $[p_j]$.

3 **repeat**

4 -Apply the VT method (cf. subsection 3.3.3.1, page 66).

5 -Estimate the covariance matrix Σ .

6 **for** each couple of variables between t_k and t_{k-1} **do**

7 -Calculate $COR_{a,b|t_k}$ (see equation (3.29), page 65).

8 -Estimate $\chi(a, b)_{t_k|t_{k-1}}$ (see equation (3.30), page 65).

9 -Narrow interval data if needed:

10 $[a_i] := [a_i + \alpha_i, \bar{a}_i - \alpha_i]$

11 **end**

12 **until** Condition 1 or 2 is satisfied for all couples

13 -Calculate the $[TTC]$ (see equation (4.4)).

14 **end**

By consequence, these bounds may play as certain inferior/superior safety margins in the context of set-membership risk management strategy.

4.1.5/ INTERVAL-BASED RISK MANAGEMENT DEPLOYMENT INTO ACC

As previously stated, the overall set-membership risk assessment developments proposed in this section are indeed dedicated to monitor ACC. The interval-based TTC formalization joined with the correlation analysis are employed to enhance the safety assurance for an ACC designed according to a multi-controller architecture introduced in [19]. Figure 4.3 presents the designed ACC architecture that includes two main parts:

- **Data acquisition and risk assessment:** First, data received from the navigation environment are transformed to intervals according to the measurement conditions. Then, they are narrowed based on the correlation analysis performed on intervals. By referring to the system statistical properties, the compact interval measurements produced by the heuristic narrowing phase allow to assess in a guaranteed and optimal way the situational in-road risk through the TTC over-approximation.

Consider $[\tilde{T}]$ the required time to travel the reference distance $[d_{ref}]$. An important parameter that should be addressed while fixing $[\tilde{T}]$ and respectively $[d_{ref}]$ is the ACC-equipped vehicle time to full breaking. Under a dangerous situation as the in-front vehicle hard breaking, the follower vehicle needs a short period of time $[T_{bre}]$ to stop completely after breaking. According to [253], $[T_{bre}]$ may be determined through equation (4.7):

$$[T_{bre}] = [V_j]/[a] \quad (4.7)$$

Note that a consists of the vehicle deceleration rate. For simplicity, $[a]$ is assumed to be as a constant interval. Afterwards, interval parameters $[\tilde{T}]$ and $[d_{ref}]$ should satisfy the

relations given below:

$$\begin{cases} [\tilde{T}] = [T_{bre}] + [T_{min}] \\ [d_{ref}] = [\tilde{T}] \times ([V_i] - [V_j]) \end{cases} \quad (4.8)$$

Where $[T_{min}]$ is a predefined temporal minimum safety distance. This latter permits maintaining a desired minimum security distance between vehicles according to their relative velocity. The follower navigation is supposed safe in that condition where d_{ref} is exploited to assign the target set-point. This distance ensure indeed a safer TTC between vehicles in a short term. Finally, the selected target set-point is reached thanks to a control unit. Due to its high stability and flexibility, the control law presented in chapter 3 is adapted here to reach a dynamic target (cf. subsection 3.1.1, page 52).

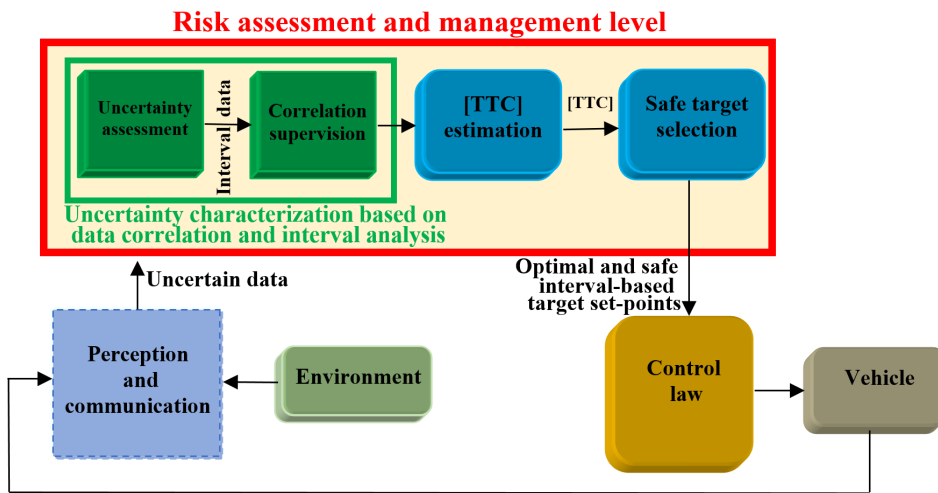


Figure 4.3: Architecture of proposed interval analysis-based ACC.

4.1.6/ SIMULATION SETUPS AND RESULTS

In an effort to validate the proposed risk management, the simulation work is tackled in the sequel. In this context, a 2D Matlab highway navigation simulator is developed to play as a test environment for the car-following scenario. In addition, due to its high portability with Matlab, the INTLAB package is trusted to ensure the required interval arithmetic computation [252]. The developed environment uses a model of a freeway-road segment as a test scene to conduct the required simulation. Notably, all motions of the vehicles involved in the validation work are simulated at ever sample time based on the widely known tricycle kinematic model. In accordance with the operation principle of the developed ACC system, the interval-based target assignment strategy combined with the correlation-based narrowing for interval data are implemented in the proposed navigation architecture to ensure the follower-car safety. Seemingly, the leader is assumed to be freely guided into the highway according to a dynamic target reaching strategy.

Otherwise, a Gaussian noise is injected into measurements to conduct the validation work. The different setups adopted for the overall simulation are kept simple as much as possible. It aims to facilitate the interpretation of the quantitative results obtained from the methods introduced in this section. The main setups implicated in the established simulation are presented in Table 4.3.

Table 4.3: Simulation setups

Configuration	Default setting
Time sampling step	0.1 (s)
Sensors update time	0.01 (s)
Leader maximum velocity	22 (m/s)/ 79.20 (km/h)
Follower maximum velocity	23 (m/s)/ 82,80 (km/h)
Follower in-vehicular delay	0.025 (s)
Minimum security distance	3 (m)
Uncertainty range $\pm x\%$ (cf. subsection 4.1.2)	$\pm 1\%$
Uncertainty range $\pm y\%$ (cf. subsection 4.1.2)	$\pm 0.5\%$

In a first place, the role of the correlation analysis in delivering sharper bounds of the TTC based on the system statistical properties is assessed. For this aim, the over-approximated TTC values according to the expression given by equation (4.4) are recorded all along the simulation run-time. Findings of the TTC computation process with/without proceeding the narrowing phase are simultaneously exhibited in Figure 4.4a to compare both interval results. This first test scenario serves not only to reveal the reduced quantity of uncertainty amounts attributed to intervals by the proposed heuristic narrowing, but it tends also to evaluate the consistency and correctness of the obtained TTC set-membership approximations. In this context, Figure 4.4b presents the evolution of the exact TTC values over time i.e., single-valued TTC results obtained through equation (4.1) in a deterministic manner (there is no use of the interval arithmetic) and without injecting any type of noise into measurements. These exact values are regarded as reference results since they reflect the certain state of situational risk. Thus, the exact findings are compared to results of the proposed interval-analysis/correlation-based TTC computation process (see Figure 4.4b).

Based on the results presented in Figure 4.4, the whole obtained outcomes show almost an identical global evolution of the TTC parameter, except the difference in the uncertainty-level. Indeed, the established simulation starts with an initial separation distance of 9.5m between the host vehicle and the ahead car. After that, the ACC-equipped approaches steadily to the leader. In the meantime, the TTC indicator begins to fall progressively due to the decrease in the distance separating both vehicles. In a few seconds, the separation distance and respectively the TTC results are roughly maintained stable since the ACC process imposes the stationary respect of the required reference distance.

As clear from Figure 4.4a, the correlation analysis applied on interval-data has effectively reduced the uncertainty extent into the TTC over-approximation. In comparison with the results reached without narrowing, performances of the risk management-level have been largely optimized by exploiting the navigation process historical features. In average, the TTC interval over-approximation has been tightened with a range of 60.40%. Such a reduction in the uncertainty impacts on the risk assessment is valuable and leads to a more efficient handling of potential threats. Much more significantly, all over the simulation run-time, TTC bounds derived according to the suggested method may be considered as tight frames for the exact TTC evolution (cf. Figure 4.4b). In that respect, it can be concluded that the produced inferior and superior uncertainty margins of the TTC are properly determined via the adopted risk evaluation strategy.

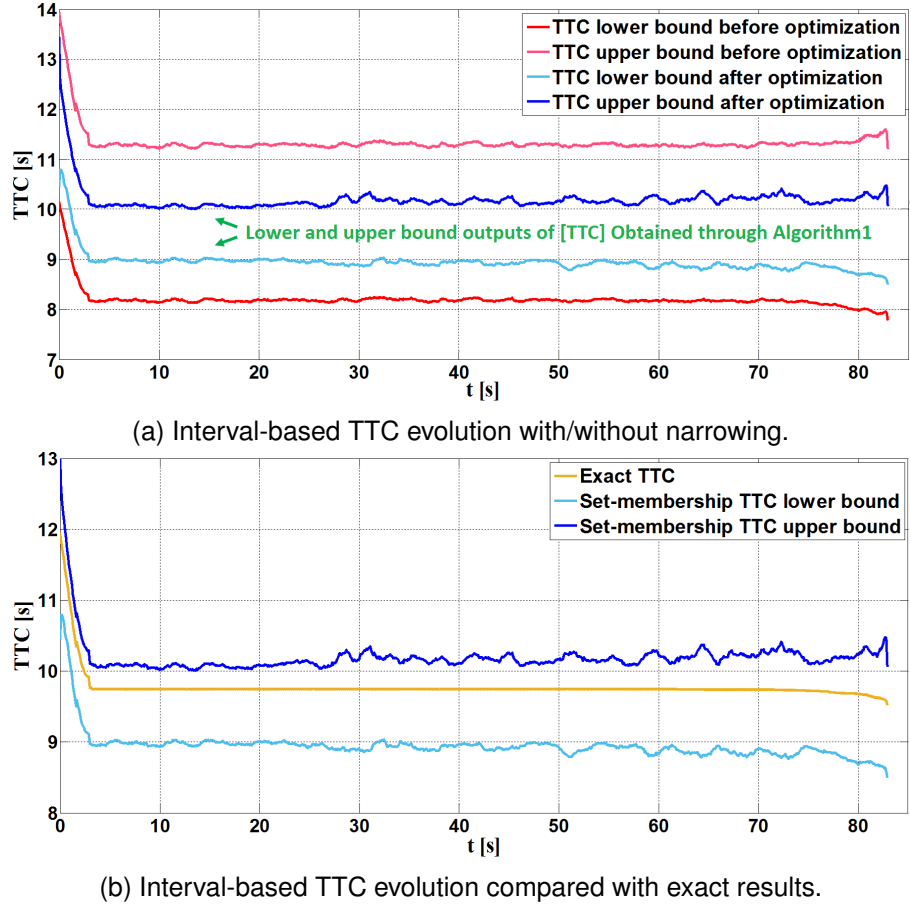


Figure 4.4: Interval-based/data-driven TTC enclosures.

To interpret in a better manner the suggested method capacities in dealing with uncertainties, a second test scenario is devoted to inject much more severe uncertainties in the simulated navigation dynamics. More precisely, these important uncertainty amounts have been implied at distinct periods (P_1, P_2, P_3 and P_4) from the simulation. Indeed, uncertainties of 0.03 m/s, 0.06 m/s, 0.12 m/s and 0.18 m/s have been respectively injected during these periods into V_i . In practice, similar amounts of uncertainties may take place because of an erroneous data transmission via the V2V communication or faulty sensor measurements. Results recorded during this test are illustrated in Figure 4.5.

This time, the results of the non-interval TTC formalization (cf. equation (4.1)) estimated under uncertainties are compared with findings of the proposed set-membership risk assessment technique. With respect to the vehicle's relative velocity, Table 4.6 depicts the error in the reference distance obtained by each method based on to the real d_{ref} that must be kept between vehicles.

Summing the whole results, the simulations proves the introduced risk management efficiency. The uncertainty-induced risks have been completely mastered or at least notably mitigated. Unlike the existent approaches in the literature, the introduced interval-based characterization of uncertainty does not imply any probabilistic calculation or linearization.

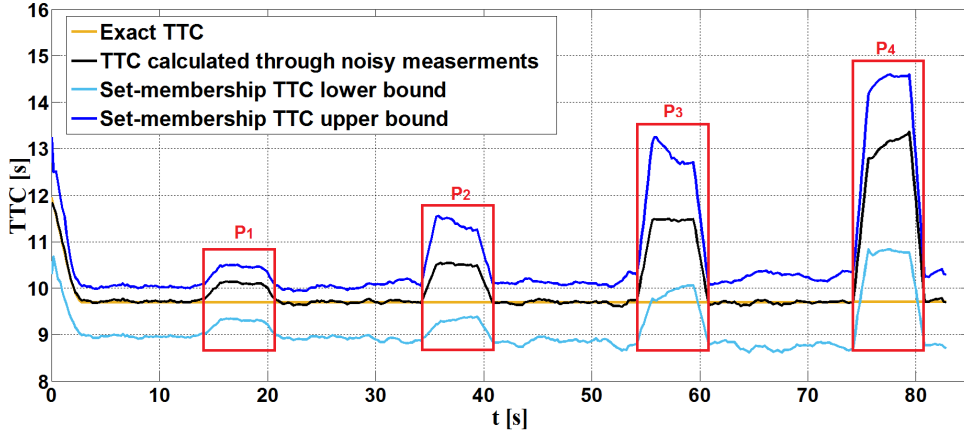


Figure 4.5: Interval-based TTC results with high uncertainty injection.

Table 4.4: Error impacting d_{ref}

	P_1	P_2	P_3	P_4
Average of error in d_{ref} for deterministic computing (m)	-0.385	-0.631	-1.435	-2.753
Average of error in d_{ref} for set-membership computing (m)	+0.324	+0.171	-0.319	-0.833

4.2/ ENHANCED CORRELATION ESTIMATION FOR INTERVAL-DATA

As explained previously in subsection 4.1.4, the correlation properties are used to minimize the uncertainty extent into the interval observations. The VT approach permits also deriving an equivalent sample matrix for the interval one (cf. subsection 3.3.3.1, page 66). After that, as a key component from the proposed optimization strategy, the covariance between system variables are assessed using a covariance matrix (cf. equation (4.5)). As soon as the required covariances are obtained, the correlation that relates variables may be approximated. Nonetheless, the suggested correlation characterization method for interval data suffers from several drawbacks:

- To evaluate the covariance between interval variables in a simple manner, the method introduced in subsection 4.1.4 uses the maximum likelihood estimator (cf. equation (4.5)). This latter, known also as the Sample Covariance Matrix (SCM) in the computational statistics literature, is relevant only for Gaussian data [190], [206]. When data alter to be non-Gaussian, the SCM becomes useless.
- Under the absence of a simple full interval method for correlation assessment, the VT is used for this reason. Especially if widths of interval observations are important, the use of vertices (end-points of intervals) to calculate the correlation may turn the observations into impulsive samples. Hence, the correlation estimation may be degraded by the loss of local stationarity in the data distribution. Consequently, a

regression technique for the impulsive observations is needed before proceeding the covariance/correlation estimation.

- As illustrated in subsection 4.1.4, the proposed method to shrink the interval TTC bounds exploits the correlation features of the navigation system. However, the occurrence of successive outliers might corrupt the historical features that describe the navigation system dynamics. This can discredit the suggested method consistency. Misleading results can be outputted and may invoke the failure of the risk management layout.

To overcome the disadvantages of the formerly suggested method, a more reliable way to proceed the interval-based correlation analysis is presented in this section. The robustness of the correlation assessment for interval data against outliers is improved via advanced statistical methods. Although the employment of those techniques is mainstream in the data analysis, they have never been applied before as pre-processing procedures for the set-membership computation. The proposed enhancements have a great practical importance for the accuracy and confidence of the set-membership results.

4.2.1/ SAMPLES UPDATE

For a given couple of variables (a, b) , $COV_{a,b}$ is computed by means of several previous samples of a and b . In that regard, the work reported in [258] proved that the number of samples used during the covariance computation has a great impact on the results. By increasing the sample size to take into account the new incoming data describing the system operation in run-time, the obtained covariance values may be saturated under the influence of the large number of older samples. For this reason, the evaluation of the covariance/correlation in our case of study should always be done with a fixed number of samples rather than an increasing sample size. At each sampling period, the collected observations are updated with the newly incoming data, and the oldest samples are excluded. In such terms, the sample size influence on the correlation assessment is prohibited [258]. The fixed number of the examined observations must be well selected. A large number of samples will lead to saturation and the correlation-based detection of anomalies will become less sensitive to the instantaneous changes in the navigation dynamics [258].

4.2.2/ SAMPLE MATRIX CENTERING

The covariance between variables is determined by examining the collected samples. However, different units and scales can be used for the observations. The scaling-related ambiguity can be avoided simply via standardization. Sample centering is a common practice that guarantees the correctness of the statistical analysis [33], [316]. For every variable, samples are rearranged by subtracting their sample mean. At first, the mean

value $M_{i=1..m}$ and the standard deviation $\sigma_{i=1..m}$ of each column from X_H are calculated:

$$\begin{cases} M_i = \frac{1}{N_{X_H}} \sum_{k=1}^{N_{X_H}} x_i(k) \\ \sigma_i^2 = \frac{1}{N_{X_H}} \sum_{k=1}^{N_{X_H}} (x_i(k) - M_i)^2 \end{cases} \quad (4.9)$$

The centralized matrix $X_c = [X_{c_1}, \dots, X_{c_m}]$ is then constructed by taking into account the calculated M_i and σ_i of each column of the initial dataset X_H :

$$X_{C_i} = X_{H_i} - \frac{M_i}{\sigma_i} \quad (4.10)$$

The resulting matrix is constructed from the observations of the same dispersion and mean values. Thus, the samples collected in X_C are independent of the scale and the unit defined by the measurement channels. Remarkably, the use of centring as a pre-processing step is not imperative, but heavily recommended for a more reliable distributional analysis of data.

4.2.3/ ROBUST EVALUATION OF COVARIANCE MATRIX

As already stated, the SCM is not sufficiently reliable in the presence of outliers and impulsive measurements. Alternative covariance computation structures, which are joined with more advanced statistical techniques, have been introduced in the literature to handle this issue [34, 58, 60]. Various probabilistic data classifiers were developed to distinguish between significant and erroneous measurements to perform an outlier-free sample estimate [96]. Only significant data participate in the sample covariance estimation. However, in some cases, regular observations may be excluded from the covariance estimation. In addition, the most suitable probability function fitting the distribution of the studied samples must at first be determined [48]. Another way to mitigate the outlier effects is to inspect the density of the data distribution over time [164]. Indeed, outliers, aberrant values and noise disperse the real geometrical distribution of data. Since it describes how variable attributes are spread out from their average value, the variance associated to data samples has been used to derive regression techniques [151], [326]. According to the mean-variance optimization theory, data distribution is adjusted to minimize the global variance of data. In this context, several variance majorization/minimization algorithms have been put into practice to reduce the fluctuation in data variances.

To improve the study of the correlation between interval data, an alternative estimator for the covariance matrix is used instead of the SCM. The adopted technique explores the distributional features of observations in the data representation space. Contrary to the conventional SCM estimator, observations have not the same relevance in the robust covariance estimation. Every observation is weighted to prohibit its deviation from the global distribution presented by most data. The re-weighted robust covariance matrix associated to $X_H = [x_1, \dots, x_m] \in R^{(N_{X_H} \times m)}$, named Σ_{robust} , is expressed as follows:

$$\Sigma_{robust} = \frac{\sum_{i=1}^{N_{X_H}-1} \sum_{j=i+1}^{N_{X_H}} \omega(i, j)((x(i) - x(j))(x(i) - x(j))^T)}{\sum_{i=1}^{N_{X_H}-1} \sum_{j=i+1}^{N_{X_H}} \omega(i, j)} \quad (4.11)$$

where the weight terms $\omega(i, j)$ are written as:

$$\omega(i, j) = \exp\left(-\frac{\beta}{2}(x(i) - x(j))^T \Sigma^{-1}(x(i) - x(j))\right) \quad (4.12)$$

Note that β is a smoothing constant used to calibrate the rearrangement of the data distribution. The criterion of optimality related to the selection of β are detailed in [251]. The weight expression (equation (4.12)) ensures a moderate sample arrangement, where the weight drops down as a given observation gets more distant from the sample average. The majority of methods in the literature have suffered from masking effect problems; i.e., only a limited number of outliers can be detected and suppressed. Unlike these methods, the proposed robust covariance estimation is efficient regardless of the number of existing outliers. The relevance of the adopted method was demonstrated in [251] through extensive tests on numerous well-known datasets. The robust estimation of the covariance matrix for interval data can be summarized in Algorithm 6:

Algorithm 6: Robust covariance matrix estimation

Inputs : N, m, X .

Output: Σ_{robust} .

```

1 -Update  $X$  (cf. subsection 4.2.1).
2 -Construct the interval data matrix  $X_I$ .
3 -Apply the vertices technique.
4 -Standardize/center  $X_H$  (cf. equations (4.9) and (4.10)).
5 -Calculate the standard covariance matrix  $\Sigma$ .
6 for  $i = 1$  to  $N_{X_H} - 1$  do
7   for  $j = i + 1$  to  $N_{X_H}$  do
8     -Calculate  $\omega(i, j)$ :
9      $\omega(i, j) = \exp\left(-\frac{\beta}{2}(x(i) - x(j))^T \Sigma^{-1}(x(i) - x(j))\right)$ 
10    -Calculate  $\Sigma_{robust}$ :
11    
$$\Sigma_{robust} = \frac{\sum_{i=1}^{N_{X_H}-1} \sum_{j=i+1}^{N_{X_H}} \omega(i, j)((x(i) - x(j))(x(i) - x(j))^T)}{\sum_{i=1}^{N_{X_H}-1} \sum_{j=1}^{N_{X_H}} \omega(i, j)}$$

12  end
13 end

```

Algorithm 6 ensures in a natural way error mitigation and regression by fitting the data distribution. Accordingly, the introduced correlation characterization of interval data is resistant to outliers and less sensitive to impulsive disturbances. Then, the developed ACC simulator is used to evaluate the role of the covariance robust estimation and the proposed statistical steps in guaranteeing a satisfactory level of accuracy. Attention is paid here particularly to the correlation that relates $[V_i]$ and $[V_j]$. This correlation value has a qualitative impact on the performances of the studied ACC system. It is important to recall that the correlation factor varies between $[-1, 1]$ to indicate the dependency strength between variables. The ACC adapts the follower velocity to the leader in order to maintain the required safety distance and to ensure the navigation stability. Hence, it is important to maintain a steady and smooth evolution of the correlation between $[V_i]$ and $[V_j]$. In this view, the results of the correlation values for couple $([V_i], [V_j])$ narrowed according to the correlation analysis proceeded based on the SCM approach and the proposed

robust covariance estimation are recorded. In addition, multiple outliers are injected in the samples of both variables. The evolution of the correlation based on both approaches are then compared with the correlation assessed with the exact values of V_i and V_j , where no uncertainty is injected. The obtained results are illustrated in Figure 4.6.

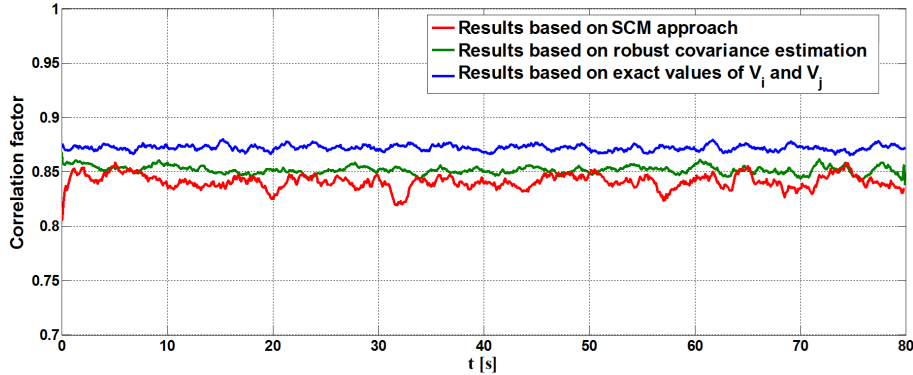


Figure 4.6: Correlation assessment for interval variables $[V_i]$ and $[V_j]$.

Obviously, the robust covariance estimation contributes strongly to narrowing the interval widths of measurements with a better impact on the correlation evolution. Compared to the SCM-based approach, the findings of the robust covariance estimation is closer to the exact results. Furthermore, the re-weighted arrangement of the data distribution ensured by the robust covariance computation leads to a smoother correlation progression.

4.3/ SECOND-ORDER VS. FIRST ORDER INTERVAL TTC

Designing high fidelity models for dynamic systems and IVs in particular is not trivial. It requires in fact the involvement of all the influencing parameters and physical quantities into the studied system model. On the other hand, applying several simplifications on models for practical aims is common. In this view, model reduction is among reasons that stand behind modeling errors.

Given that the analytical formalization of the previously proposed interval-based TTC includes few simplifications, this section tends to analyze the interval-based/data-driven modeling strategy in dealing with the model reduction-related errors. A higher-order model to estimate the TTC is suggested. It describes in a better way the evolution of vehicle motions for the car-following scenario. Henceforth, the first order TTC interval model refers to the formerly proposed model (cf. section 4.1). Respectively, the high-order model joined with the correlation analysis, introduced in the current section, is denoted in the sequel by the interval second TTC model. From an analytical standpoint, the second-order interval TTC model is a quadratic interval polynomial i.e., the polynomial coefficients are in the shape of intervals. This is indeed the first utilization of the interval polynomial to cope with safety verification and uncertainty characterization for IVs [5, 8].

In what follows, the second order interval TTC formalization is detailed. Then, the selected method to find roots of polynomials with perturbed coefficients is explained. Finally, consequences of the up-grade in the set-membership model formalization from the first to the second order are studied through simulations. The analysis of the first and

second order interval-based TTC results should reveals both of the interval analysis and the correlation role in covering and compensating the modeling errors.

4.3.1/ SECOND ORDER INTERVAL-BASED TTC FORMALIZATION

By building on the vehicles' separation distance model, one more additional parameter can be derived to describe the evolution of interactions between vehicles. In addition to equation (4.2), the variation of the change rate in the separation distance between vehicles, denoted \ddot{d}_{ij} is expressed as:

$$\ddot{d}_{ij} = \frac{1}{d_{ij}}(V_i - V_j)^T(V_i - V_j) - \dot{d}_{ij}^2 \quad (4.13)$$

For clarification, \ddot{d}_{ij} is obtained by deriving equation (4.2). By putting together equations (4.2) and (4.13), it has been proven in [310] that a more accurate TTC value can be approximated from both vehicles motion equations. By excluding the assumption that \ddot{d}_{ij} is always equal to zero, the relation linking d_{ij} , \dot{d}_{ij} and \ddot{d}_{ij} is given by the following polynomial:

$$d_{ij} + \dot{d}_{ij}TTC_{O2} + \frac{1}{2}\ddot{d}_{ij}TTC_{O2}^2 = 0 \quad (4.14)$$

Actually, equation (4.14) represents the analytical formula of the desired higher-order model. When $\ddot{d}_{ij} \neq 0$, the TTC_{O2} consists of the second-order TTC value, which is reached by solving the polynomial equation (4.14) [8]. Hereafter, TTC_{O1} is used to refer to the TTC value given formerly by the first-order model underlined by equation (4.4).

Indeed, the established model indicates instants of any collision manifestation with the condition that both vehicles maintain their current velocities. In the case where the polynomial expression has multiple roots, only a single value should be held from the set of roots. Hence, the appropriate value assigned to TTC_{O2} pinpoints the instant of the first potential collision. Consequently, it matches the first time that the separation distance between vehicles would be zero. According to this understanding, TTC_{O2} is determined in the following manner. Whenever $\ddot{d}_{ij} = 0$ or no root is found for equation (4.14), the reduced model is used and TTC_{O2} is assumed to be equal to TTC_{O1} . Once two real positive roots are obtained, the root of the lower value is selected. When a single root is positive and the other one is negative, the positive one is admitted. A couple of negative roots can be also found. In such a case, the root with the closet absolute value should be selected since it represents the most recent interaction between vehicle motions.

Accordingly, the following system is obtained by extending equation (4.14) to handle interval-data:

$$\begin{cases} [TTC_{O1}] = -\frac{[d_{ij}]}{[\dot{d}_{ij}]} \\ [d_{ij}] + [\dot{d}_{ij}][TTC_{O2}] + \frac{1}{2}[\ddot{d}_{ij}][TTC_{O2}]^2 = 0 \end{cases} \quad (4.15)$$

Let consider $[\mathfrak{R}]$ the selected polynomial root of equation (4.14). In an identical manner to the deterministic case detailed above, $[\mathfrak{R}]$ is the root corresponding to the first collision

interval time. To properly define $[\mathfrak{R}]$, note that the absolute value of an interval variable $[x]$ is calculated as:

$$|[x]| = \text{abs}([x]) = \max(|\underline{x}|, |\bar{x}|) \quad (4.16)$$

Similarly, to compare two distinct intervals $[x_1]$ and $[x_2]$, the following relation is used:

$$\bar{x}_1 < \underline{x}_2 \implies [x_1] < [x_2] \quad (4.17)$$

Eventually, by taking into account the communication latencies, the interval-based final formalization of the second-order TTC adopted in this section is defined as:

$$[\text{TTC}_{O2}] = [\mathfrak{R}] - [T_{V2V}] - [T_L] \quad (4.18)$$

More precisely, the set-membership second-order model is reduced and equation (4.4) is used to define $[\text{TTC}_{O2}]$ solely if $[\mathfrak{R}] = \emptyset$ or $[\ddot{d}_{ij}] = 0$:

$$[\text{TTC}_{O2}] = [\text{TTC}_{O1}] - [T_{V2V}] - [T_L] \quad (4.19)$$

4.3.2/ SOLVING QUADRATIC INTERVAL POLYNOMIAL

An important research work has been devoted to solve interval polynomials. However, the majority of the proposed strategies are cumbersome and time-consuming [102], [339]. Another part from the literature focused in providing simpler and faster approaches to find the interval roots [106]. Nonetheless, only a prior guess for regions enclosing the exact roots have been estimated by these approaches.

Instead of the aforementioned solutions, the adopted method herein counts on interpreting the combination given by endpoints of the interval coefficients. It allows the determination of all possible framing boundaries functions associated to the quadratic interval polynomial. Correspondingly, sharp bounds for roots are obtained rapidly without being affected by the pessimism effects. Hence, let assume that the quadratic interval polynomial can be written as:

$$P([x]) = [\underline{a}]x^2 + [\underline{b}]x + [\underline{c}] \quad (4.20)$$

Indeed, the adopted method is based on the reformulation of the polynomial throughout its boundary functions, such as $P([x]) = [\underline{P}([x]), \bar{P}([x])]$. Initially, eight distinct real functions can be distinguished directly through bounds of $[\underline{a}]$, $[\underline{b}]$ and $[\underline{c}]$:

$$\begin{cases} f_1 = \underline{a}x^2 + \underline{b}x + \underline{c}; & f_2 = \underline{a}x^2 + \underline{b}x + \bar{c} \\ f_3 = \underline{a}x^2 + \bar{b}x + \underline{c}; & f_4 = \underline{a}x^2 + \bar{b}x + \bar{c} \\ f_5 = \bar{a}x^2 + \underline{b}x + \underline{c}; & f_6 = \bar{a}x^2 + \underline{b}x + \bar{c} \\ f_7 = \bar{a}x^2 + \bar{b}x + \underline{c}; & f_8 = \bar{a}x^2 + \bar{b}x + \bar{c} \end{cases} \quad (4.21)$$

Based on the interpretation of the dominant term of $P([x])$, one can deduce that $\underline{P}([x])$ is framed by (f_1, f_2, f_3, f_4) . Respectively, it is quite clear that functions (f_5, f_6, f_7, f_8) are enclosures of $\bar{P}([x])$. Otherwise, it is important to notice that:

$$\begin{cases} f_1 \leq f_2; & f_3 \leq f_4 \\ f_6 \geq f_5; & f_7 \geq f_8 \end{cases} \quad (4.22)$$

To simplify the notation, let suppose that $P_1 = f_1$, $P_2 = f_3$, $P_3 = f_8$ and $P_4 = f_6$. Consequently, it can be deduced that:

$$\underline{P}(x) = \begin{cases} P_1 = \underline{a}x^2 + \underline{b}x + \underline{c}, & \text{if } x \geq 0 \\ P_2 = \underline{a}x^2 + \bar{b}x + \underline{c}, & \text{if } x \leq 0 \end{cases} \quad (4.23)$$

and

$$\overline{P}(x) = \begin{cases} P_3 = \bar{a}x^2 + \bar{b}x + \bar{c}, & \text{if } x \geq 0 \\ P_4 = \bar{a}x^2 + \underline{b}x + \bar{c}, & \text{if } x \leq 0 \end{cases} \quad (4.24)$$

In such a manner, systems (4.23) and (4.24) permit together to simplify the original interval problem. Because $P_{i=1..4}$ are non-interval real functions, solving the interval polynomial is from right now feasible via standard real arithmetic. Figure 4.7 depicts illustrative examples of quadratic interval polynomials presented through their boundary functions.

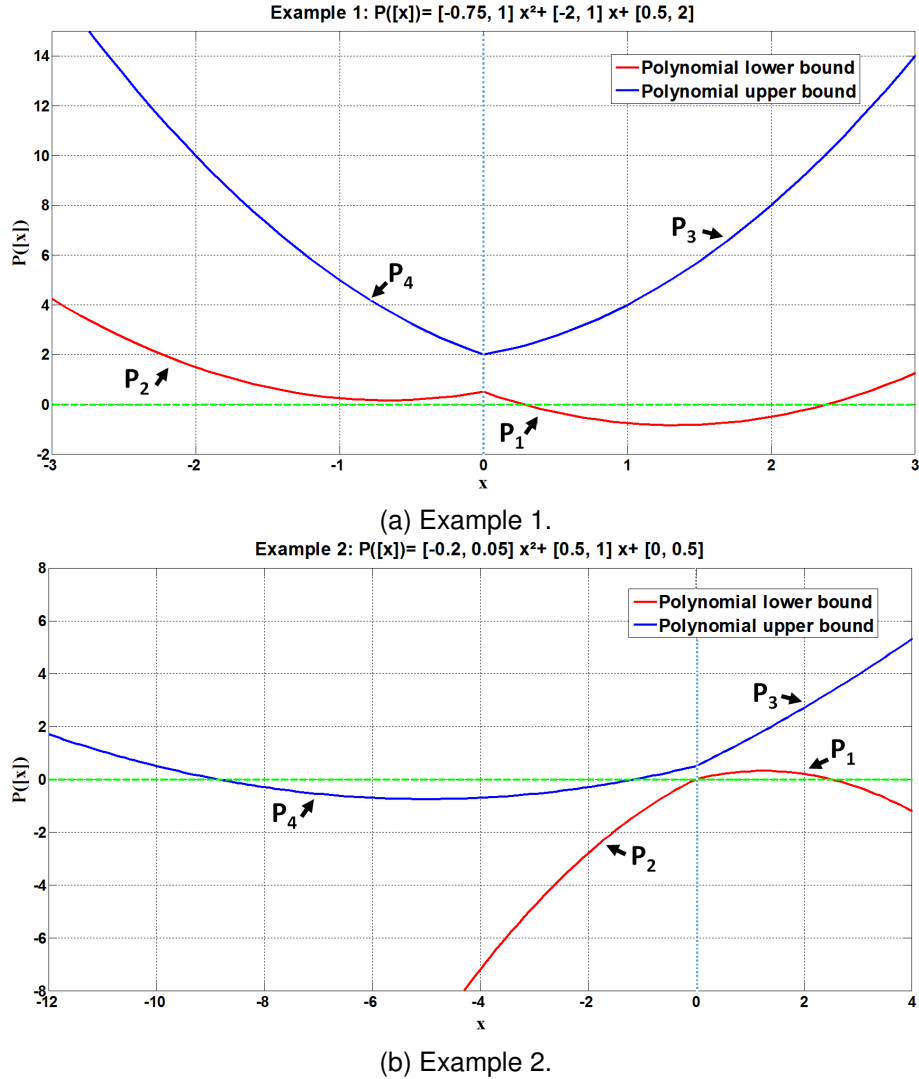


Figure 4.7: Examples of quadratic interval polynomials.

At this stage, it remains to look for sets satisfying $\underline{P}([x]) \leq 0 \leq \overline{P}([x])$ to solve the problem. Hence, a simple algorithm introduced in [130] and [131] is adopted to define the interval roots in function of the real solutions of $P_{i=1..4}$. All roots of $P_{i=1..4}$ must be calculated

through an interval analysis-based approach. Indeed, several theoretical and numerical methods are available to isolate roots of real polynomials while considering rounding errors. As soon as all the interval roots of every P_i are obtained, they must be arranged in a list L . Multiple interval roots should be entered twice into L . Few instruction must be followed to properly arrange elements of L . It is important to notice that P_1 and P_2 enclose $P([x])$ exclusively when $x \geq 0$ (cf. equation (4.23)). Consequently, each negative root or part of a root issued from P_1 and P_2 should be eliminated from L . In a similar way, positive roots or parts of roots originated from P_3 and P_4 should be discarded. Besides, there are few exceptions that must be considered. Notably, a double root is found at $x = 0$ for (P_1, P_2) when $\underline{c} = 0$ and respectively for (P_3, P_4) if $\bar{c} = 0$. For both cases, this root must be added only once to L . In addition, in some cases, degenerate infinite intervals should be placed in L . According to [130], $-\infty$ should be inserted into L when equation (4.25) is satisfied:

$$\underline{a} < 0 \vee (\underline{a} = 0 \wedge \bar{b} > 0) \vee (\underline{a} = 0 \wedge \bar{b} = 0 \wedge \underline{c} \leq 0) \quad (4.25)$$

Seemingly, $+\infty$ is placed in L in the following case:

$$\underline{a} < 0 \vee (\underline{a} = 0 \wedge \underline{b} > 0) \vee (\underline{a} = 0 \wedge \underline{b} = 0 \wedge \underline{c} \leq 0) \quad (4.26)$$

Afterwards, let consider $[S_i] = [\underline{S}_i, \bar{S}_i]$ the intervals remaining in L . The set of intervals $[S_i]$ must be sorted in a way that $\underline{S}_i \leq \underline{S}_{i+1}$. Let denote by n the number of intervals held in L (six interval roots in maximum). At the last stage from the interval root determination algorithm, the final solution is obtained relatively to n . Table 4.5 recapitulates the algorithm outcome according to possible values of n . Unlike the non-interval polynomials, quadratic interval polynomials may have as a maximum three roots (see Figure 4.7).

Table 4.5: $P([x])$ interval roots relatively to n

List length	Interval roots
$n = 0$	\emptyset
$n = 2$	$[\underline{S}_1, \bar{S}_2]$
$n = 4$	$[\underline{S}_1, \bar{S}_2], [\underline{S}_3, \bar{S}_4]$
$n = 6$	$[-\infty, \bar{S}_2], [\underline{S}_3, \bar{S}_4], [\underline{S}_5, +\infty]$

Finally, the required steps to solve an interval polynomial are summarized in Algorithm 7.

Algorithm 7: Solving interval polynomial

Require: $[a]$, $[b]$ and $[c]$

Ensure : Solve $P([x]) = [a]x^2 + [b]x + [c]$

- 1 -Designate $P_{i=1..4}$ (see equations (4.23) and (4.24)).
- 2 -Find interval roots of $P_{i=1..4}$.
- 3 -Place results in L .
- 4 -Add infinite entries $\pm\infty$ to L , if needed (cf. equations (4.25) and (4.26)).
- 5 -Sort the interval elements in L ($\underline{S}_i \leq \underline{S}_{i+1}$).
- 6 -Find out the length of L to determine roots of $P([x])$ (cf. Table 4.5).

Given the nature of the model describing the TTC evolution for a car-following scenario, the interest has been only given in this section to solve a quadratic interval polynomial. Remarkably, Algorithm 7 can be extended to deal with interval polynomials regardless to their degrees. Full details about this issue can be found in [131].

4.3.3/ SIMULATION RESULTS AND DISCUSSION

To compare performances of the second and first order interval TTC models, Algorithm 7 is integrated into the already established car-following simulation framework. Accordingly, the control architecture of the follower vehicle may adapt the reference distance from the in-front vehicle based on the worst case of hazard assessed either through $[TTC_{O1}]$ or $[TTC_{O2}]$. The simulation setups shown in Table 4.3 are kept the same.

As illustrated in Figure 4.8, $[TTC_{O1}]$ and $[TTC_{O2}]$ are both tightened via the iterative narrowing. Narrowing reduced the initial uncertainties attributed to $[TTC_{O1}]$ with an average rate of 60.30%. Seemingly, the average reduction in the uncertainty extent of $[TTC_{O2}]$ is around 65.79 %.

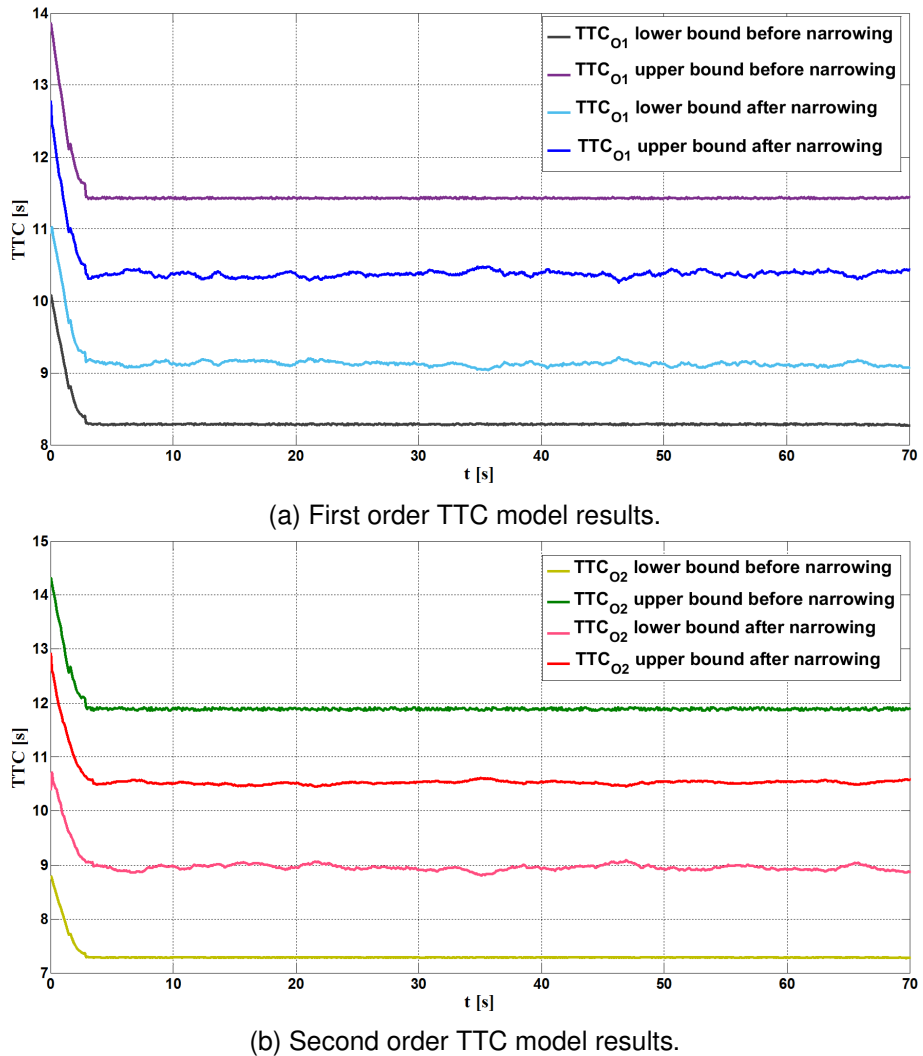


Figure 4.8: $[TTC_{O1}]$ and $[TTC_{O2}]$ evolution before/after narrowing.

After narrowing, the average widths of $[TTC_{O1}]$ and $[TTC_{O2}]$ all along the simulation execution time are respectively around 1.25s and 1.58s . With respect to these results, one can deduce that the second-order set-membership TTC formalization is quite more pessimistic than the first-order interval model. It may be presumed that this fact is caused by the “dependency effect”, which is emphasized by the model up-grade. The multiple

appearance of several interval variables in the expression of the interval polynomial coefficients accentuates the “dependency effect” (cf. equations (4.3), (4.13) and (4.15)).

Respectively, Figure 4.9 compares the TTC narrowed interval results with the exact TTC_{O1} and TTC_{O2} . Once again, it is worth to remind that the exact results (TTC_{O1} and TTC_{O2}) are estimated without injecting any sort of noises in the simulation dynamics. The depicted results demonstrate consistency of the interval-based modeling allied with the correlation analysis. For the whole time, both the $[TTC_{O1}]$ and $[TTC_{O2}]$ enclose tightly the exact results. However, bounds of $[TTC_{O1}]$ are notably the sharpest enclosures for the exact values. Definitely, the decision making for autonomous navigation is more reliable with less uncertainties.

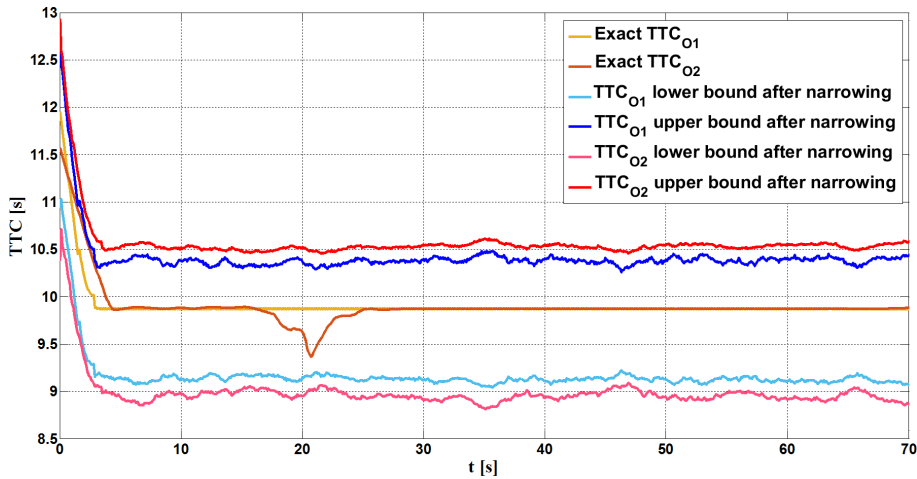


Figure 4.9: TTC_{O1} and TTC_{O2} enclosures compared with exact results.

Due to its simplicity, the first-order interval model is more computationally effective than the higher-order model. At every sample time during simulations, about of $0.09s$ as an average additional time is required to solve the interval polynomial to assess $[TTC_2]$.²

As obvious from simulations, the first-order TTC interval model permitted to master the uncertainty-issued risks with more compact results. Consequently, combining the interval-arithmetic with the correlation analysis can be regarded as an efficient methodology to compensate modeling errors. Without any need for complicated and time consuming models, the proposed modeling approach is convenient especially to perform risk management for IVs since it compromise between accuracy and simplicity. All along the remaining of this chapter, the first-order interval formalization of the TTC is admitted for the risk management instead of the second-order model.

4.4/ COMBINATION OF INTERVAL ANALYSIS/STOCHASTIC RESULTS

The final purpose of this chapter is to integrate uncertainty-robust risk management into ACC while guaranteeing safety and optimality. At this stage, a combined stochastic/interval-based policy to define the TTC and respectively d_{ref} is presented [3]. The idea of merging intervals with stochastic methods has been indeed poorly stud-

²The simulations are conducted on an Intel i5 Processor with 3.5 GHz and 16 GB memory.

ied in the literature. The motivations and steps to manage risks based on a combined stochastic/interval-based policy are detailed in the following subsections:

4.4.1/ MAIN MOTIVATIONS

It was demonstrated that correlation-based interval narrowing (cf. section 4.1) discarded around 64% of overestimated uncertainties. Nevertheless, the obtained results remained too conservative. Despite the heuristic narrowing of the interval data, the suggested approach is still pessimistic due to the initial exaggerated uncertainty assignment for intervals. Definitely, the pessimism would impact the choice of d_{ref} . Even though the interval analysis are guaranteed and the obtained bounds are validated through the system historical properties, sharper bounds for the min/max safety margins are needed.

For highway or urban driving areas, the spacing between vehicles should be minimized to avoid the traffic distribution and congestion. In this context, the conservatism impacts would be more important in a larger scale. For instance, an optimal control for platoons is unfeasible via the proposed method. Maintaining a conservative separation distance between vehicles is not efficient for platoon formation. In fact, problems related to traffic jams and road congestion are getting currently more attention in the literature due to the exponential increase in the number of vehicles in-roads. In rural or urban regions, the expansion in the world population is entailing an extra-load on both public and individual transport means. Referring to the predictions presented in [201], around 70 million of connected vehicles will be present in the worldwide roads soon by the year 2023. Later in the year 2030, the total number of vehicles (intelligent and common vehicles) in the entire world roads is expected to exceed 2 billion vehicle.

Accordingly, it is mandatory to improve the proposed interval-based risk management utility by decreasing the spacing between vehicles while ensuring safety. Herein, the utility (or the optimality) means estimating the different states of the navigation while getting closer to the reality to define properly the safety measures. Besides, the proposed interval-based uncertainty assessment is highly sensitive to changes in measurement conditions. From a safety point of view, it is advisable to take more caution in case of bad measurement conditions. However, the continuous change in the environmental factors, which are taken into account to quantify uncertainties, may cause the degradation of other important aspects of the navigation process. For instance, the environmental changes may entail an irregular evolution of the spacing between vehicles, which leads to large jerk values. By definition, the jerk consists of the longitudinal acceleration oscillations [255]. Under these oscillations, a non-smooth and abrupt change in the vehicle motion take a place due to the repeated bounding between acceleration/deceleration.

One way to face the pessimism effects of the set-membership computation is to combine the interval analysis with stochastic approaches. Several approaches have been introduced in the control engineering literature that merge interval analysis and probabilistic methods [93], [198]. However, a clear and methodological layout to merge the results of the distinct approaches has never been defined.

Thus, a relevant policy to combine the interval analysis with stochastic methods is proposed in the sequel to overcome pessimism and to ensure the navigation stability and passengers comfort. Since it is based on the credibility assessment of results, the proposed method may be seen as a reliability-oriented merging model for the set-membership/stochastic findings.

4.4.2/ CONFIDENCE METRICS FOR MERGING INTERVAL-BASED AND STOCHASTIC RESULTS

To optimize the car-following impact on the traffic flow, an interval-based/stochastic target selection for ACC is introduced. In this view, an Extended Kalman Filter (EKF) is used to estimate the states of vehicles. Correspondingly, the vehicle motions are represented in the following model:

$$\begin{cases} x_{k+1} = f(x_k, u_k) + w_k \\ z_k = h(x_k) + v_k \end{cases} \quad (4.27)$$

where x_k , z_k and u_k are respectively the vehicle state vector, the observed state and the control input, and w_k and v_k are respectively the process noise and the measurement noise. The evolution of the system states and the observations are estimated respectively thanks to f and h .

Optimal uncertainty characterization implies neither underestimating nor overestimating the uncertainty affecting the navigation. Respectively, the arbitrary merging of set-membership/stochastic findings may raise the error rate in final estimates. Subsequently, both approaches should be relevantly merged according to a confidence weighting strategy. In fact, the consistency check of the uncertainty evaluation has been rarely studied. Mostly, the existing contributions rely on a simple comparison with true ground results, which are not always available in reality.

In the following, two confidence evaluation metrics are introduced to decrease the non-overlapping ratio of the set-membership and stochastic methods. Notably, the interval analysis results are guaranteed, so the consistency assessment is restricted for the EKF.

4.4.2.1/ CUMULATIVE DISTRIBUTION-BASED CONFIDENCE ASSESSMENT

Roughly, the stochastic filtering is carried out by propagating the covariance of the system parameters through a particular model. Nevertheless, the way the covariance is propagated is not further verified. Mainly, the system non-linearity and non-Gaussianity of parameters are the origins of the inexact covariance propagation over time [345].

Consequently, a metric evaluating the accumulated error in the propagated covariances is put forward. It is inspired from confidence-weighted learning practiced by several classification approaches [85], [88]. These methods are usually conjoined with the probability estimation of correct classification. The cumulative error rate in the estimates is frequently assessed through the Cumulative Distribution Function (CDF) [291]. Notably, the CDF estimation is widely used for evaluating novel filtering techniques and developing several statistical normality tests [205], [311].

Indeed, the CDF examines the data distribution via the Gauss error function, named erf . It represents the probability that an estimated variable may be greater than a certain value. Intuitively, the CDF may be interpreted to judge whether the EKF estimates have been over/under-estimated.

Consider a Gaussian distribution with a standard deviation and a mean, noted respectively σ and μ . Actually, $x_{i=1 \dots j}$ is a set of j states estimated by the EKF at instant t_k . The

CDF associated to a given state is expressed by:

$$\forall i = 1 \dots j, \quad CDF|_k(x_i) = \frac{1}{2} * (1 + erf(\frac{x_i - \mu_i}{\sigma_i * \sqrt{2}})) \quad (4.28)$$

Afterwards, a reliability metric, denoted $\xi_{CDF|k}$, is derived based on the CDF concept. It characterizes the global error in the covariance propagation into the EKF at instant t_k :

$$\xi_{CDF|k} = mean[CDF|_k(x_1), \dots, CDF|_k(x_j)] \quad (4.29)$$

4.4.2.2/ REDUNDANT MODELING-BASED CONFIDENCE ASSESSMENT

As a model-based estimator, the EKF uses a motion model to predict transitions in the vehicle states. Then, it is susceptible to severe modeling imperfections due to common practices, as linearization and discretization. Accordingly, a redundant modeling is proposed to capture the EKF errors. Through deviations between both models, a relevant trust estimation for the EKF performances is derived. For the sake of credibility, the back-up model should be analytically different from the original one. Despite their dissimilarity, a correct filtering should be approved by a great similarity in the predictions of distinct models. The mismatch between models is exploited to assess the filtering quality.

In practice, a tricycle kinematic-based motion model is adopted for the EKF. Similarly, a back-up motion model using the road curvature as a predictive variable is selected to apply our confidence assessment method [313]. After that, the vehicle's traveled distance between successive instants t_{k-1} and t_k , denoted Δ_d , is predicted by both models. Δ_d presents the relative transition in the navigation dynamics between a past state and a current one. For the back-up model, Δ_d is determined by equation (4.30) [313]:

$$\Delta_d = \frac{CR_0(k) - CR_0(k-1)}{CR_1(k-1)} \quad (4.30)$$

where $CR_1(k-1)$ is the corresponding curvature change rate, and $CR_0(k-1)$ and $CR_0(k)$ are respectively the vehicle's local curvature at instants t_{k-1} and t_k . Notably, the road curvature is measured in the run-time by cyber physical systems. Finally, an error rate between both models, denoted by ξ_m , is obtained to report the filtering confidence. Figure 4.10 illustrates the EKF modeling reliability assessment principle.

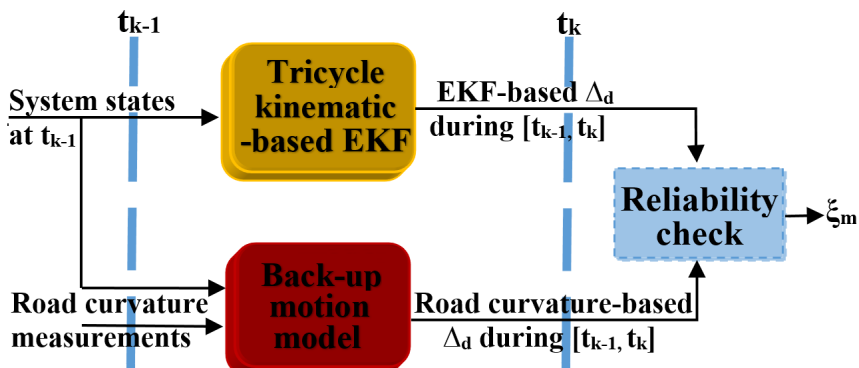


Figure 4.10: Reliability check for EKF modeling performances.

4.4.3/ INTERVAL-BASED/STOCHASTIC RISK MANAGEMENT FOR ACC SYSTEM

The interval-based/stochastic uncertainty handling and confidence weighting are exploited to monitor ACC. An adaptive target assignment is introduced to maintain a reference distance from the leader. This distance must ensure a safe TTC between vehicles in a short term. Hence, $[TTC_1]$ and $[d_{ref1}]$ denote the intervals issued from the over-approximation without narrowing. $[TTC_2]$ and $[d_{ref2}]$ are intervals obtained through the correlation-based optimization step. Similarly, TTC_{EKF} and d_{EKF} designate the TTC and d_{ref} obtained through the EKF outputs.

Since the EKF results are uncertain, it is not possible to use a formal model to combine the results of the interval-based and stochastic approaches. Instead, the convergence rate between both approaches is interpreted. Especially in case of a conflict between the outputs of both approaches, the results are heuristically combined based on the confidence level of the EKF findings.

The proposed method in this section creates a sort of complementarity between the set-membership and stochastic approaches. The interval-based method defines the min/max safety thresholds. Once the EKF estimations are out of regions determined via the interval analysis, the filter findings are merged with the interval-based results to compensate inaccuracy. The EKF results contribute also to improving the optimality. Accordingly, an adaptive algorithm is adopted herein to ensure a safe and optimal target selection by treating the following cases:

- **Case1:** $d_{EKF} \in [d_{ref1}]$

When d_{EKF} is jointly enclosed inside $[d_{ref1}]$ and $[d_{ref2}]$ ($[d_{ref2}] \subset [d_{ref1}]$). It means that the EKF outputs agree with the set-membership results. Looking for optimality, the target is assigned through d_{EKF} to reduce pessimism.

- **Case2:** $d_{EKF} \notin [d_{ref1}]$

In this case, the EKF outputs diverge away from the largest bounds obtained by the interval analysis. Thus, the worst risk case is admitted by re-initializing the initial EKF states and selecting $\overline{d_{ref1}}$ to determine the target.

- **Case3:** $d_{EKF} \in [d_{ref1}]$ and $d_{EKF} \notin [d_{ref2}]$

This is the most confusing situation. The EKF outputs are not entirely diverging, but they are far away from correlation-issued bounds. Consequently, the results are merged based on a confidence assessment process (see subsection 4.4.2) without over/under-estimating uncertainties.

The result combination in case 3 at instant t_k is achieved by reducing the gap between d_{EKF} and $mid([d_{ref2}])$. This latter is denoted by $\Upsilon = |d_{EKF} - mid([d_{ref2}])|$. Hence, the new adaptive value of d_{ref} , noted d_{adap} , is defined as follows:

$$d_{adap} = \begin{cases} d_{EKF} - (\xi_{CDF|k} + \xi_m) \times \Upsilon, & \text{if } d_{EKF} > mid([d_{ref2}]) \\ d_{EKF} + (\xi_{CDF|k} + \xi_m) \times \Upsilon, & \text{if } d_{EKF} < mid([d_{ref2}]) \end{cases} \quad (4.31)$$

Equation (4.31) ensures the closeness of the results to the true values, which are represented by the interval regions validated via the statistical system properties. Eventually, the merge results are fixed based on the inaccuracy range indicated by the confidence metrics associated to the EKF. Finally, Figure 4.11 depicts the follower target generation principle.

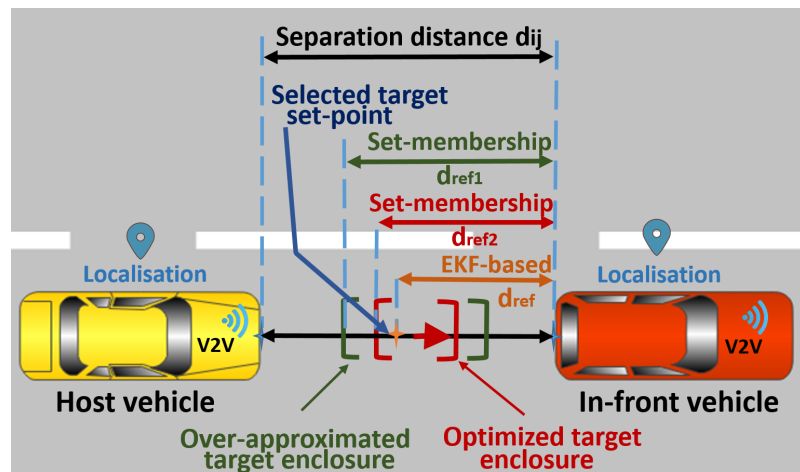


Figure 4.11: Suggested ACC principle.

Afterwards, all the required steps to put in practice the proposed interval-based/stochastic approach are recapitulated in what follows:

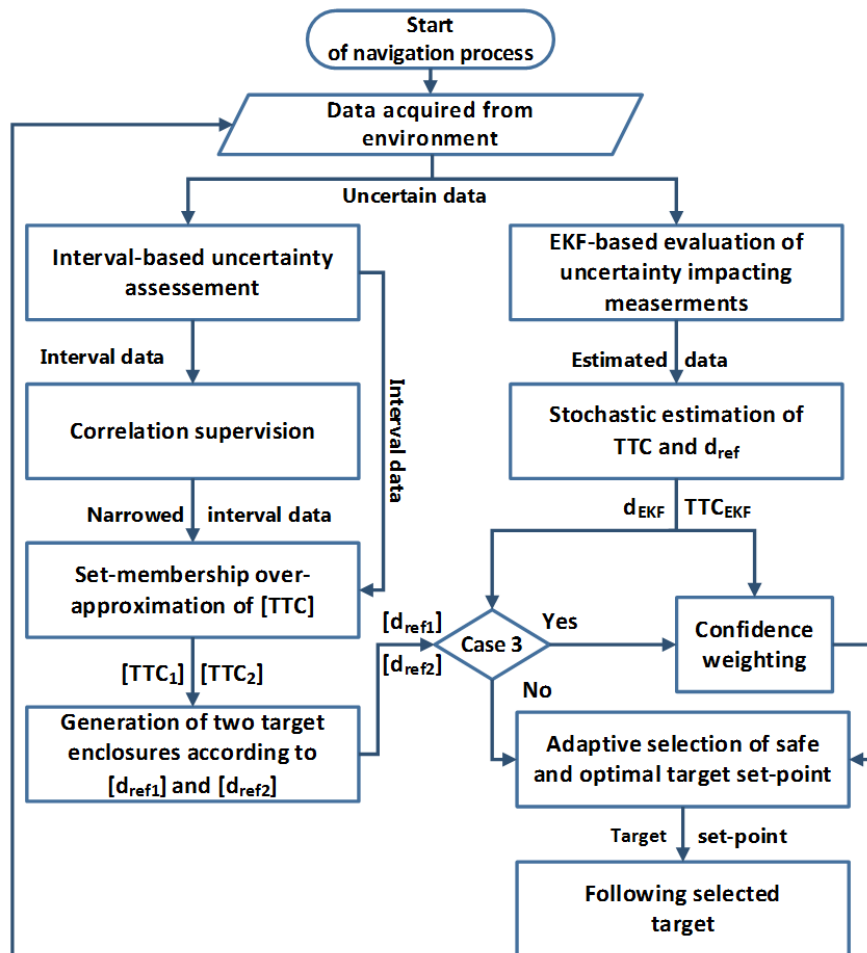


Figure 4.12: Flowchart of target set-point generation strategy.

On the other hand, Figure 4.13 presents the designed ACC architecture. By examining the EKF findings and these enclosures, the adaptive algorithm selects an optimal and safe target, which is finally reached by the control unit with a desired orientation and velocity.

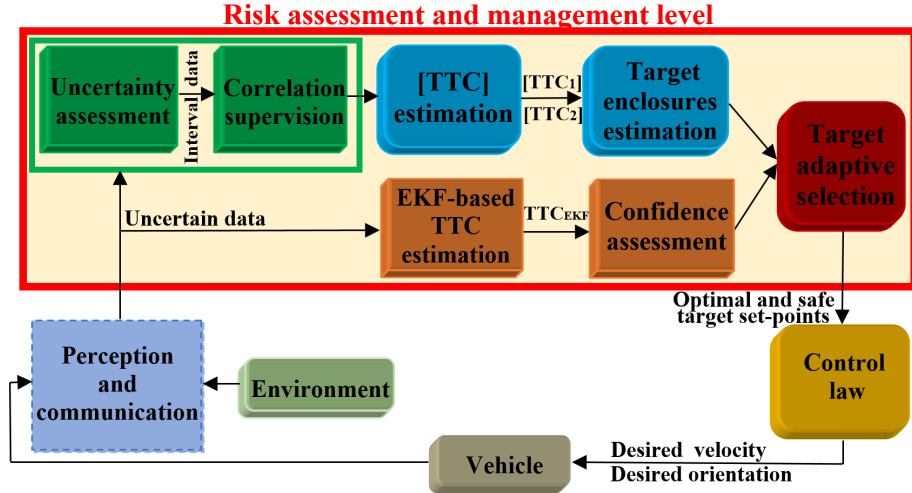


Figure 4.13: Set-membership/stochastic ACC architecture.

4.4.4/ SIMULATION RESULTS

In the following test scenario, the d_{ref} results according to different formalizations are analyzed (see Figure 4.14). These results are compared first with the exact d_{ref} values, which are calculated without injecting any noise in measurements. The results show a fall in the uncertainty extent due to the correlation analysis. The average width of $[d_{ref2}]$ is around 0.985 (m). Such an uncertainty marge is still considerable, which proves the need to overcome the pessimism of the proposed interval-based approach.

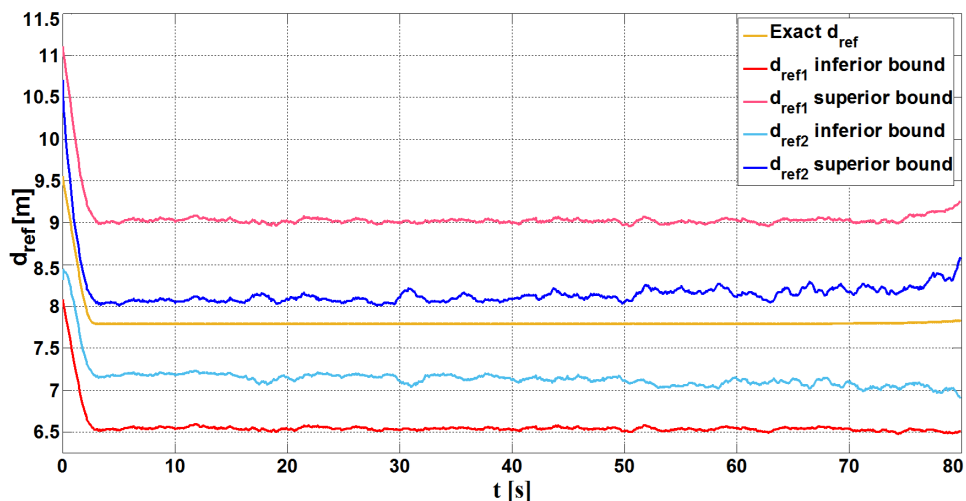


Figure 4.14: d_{ref} evolution.

Next, the combined interval-based/stochastic approach advantages in compromising between safety and optimality are evaluated. As shown in Figure 4.15, d_{EKF} and d_{adap} are coincident, since d_{EKF} is almost enclosed inside $[d_{ref2}]$. Therefore, the filtering quality is validated. The confidence weighting (case 3 in subsection 4.4.3) is not proceeded. In terms of optimality, the gain in the spacing between vehicles by assuming d_{adap} rather than $\overline{d_{ref2}}$ reaches 1.33 (m) as a maximum and an average of 0.349 (m) in each control cycle.

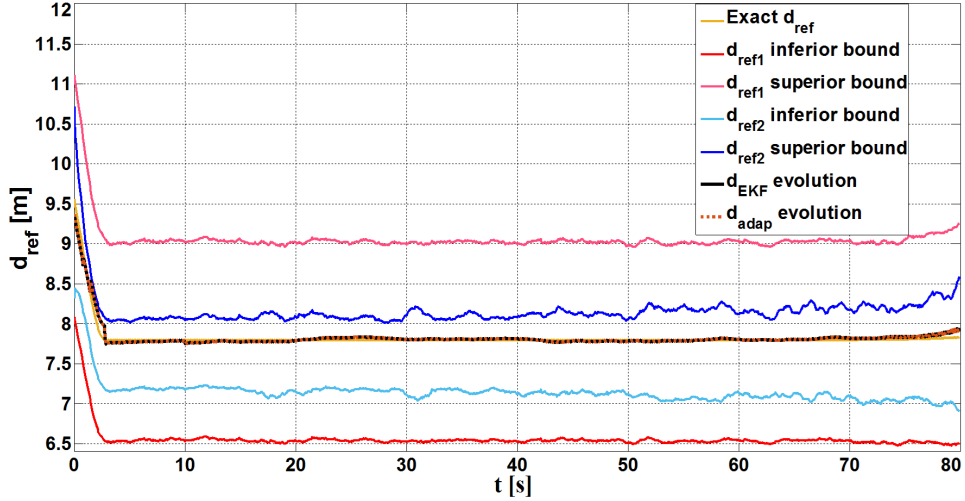


Figure 4.15: d_{ref} evolution for EKF correct behavior.

To comprehensively validate the proposed approach, the next simulation scenario is carried out with an improper conditioned EKF due to an imperfect characterization of initial states and noise features. Such problems entail definitely poor performances in handling severe uncertainties. Then, additional uncertainty amounts, which may reach 0.12 m/s (around 0.55% of the real value), are incorporated in the measurements of V_i at P_1 , P_2 and P_3 . The obtained results are depicted in Figure 4.16.

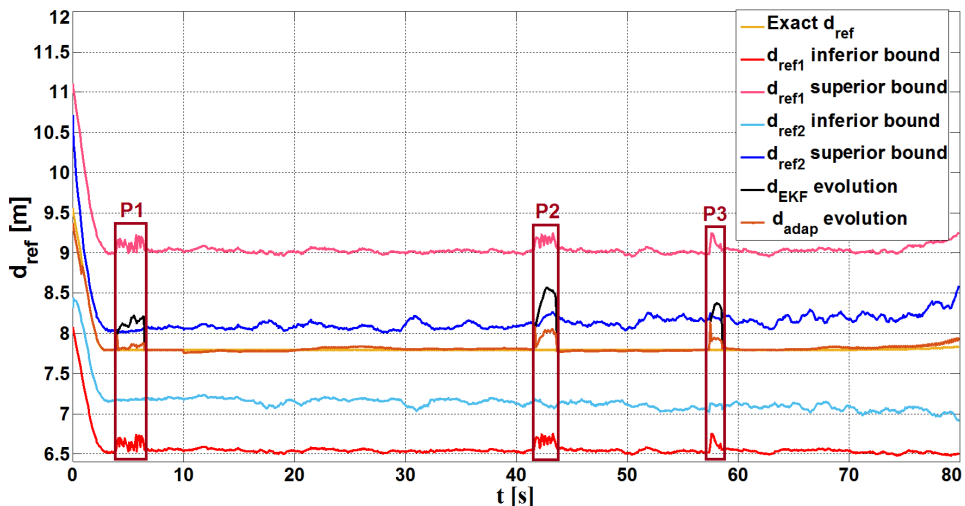


Figure 4.16: d_{ref} evolution for EKF imperfect behavior.

The confidence weighting to merge the EKF and the set-membership results is extensively applied at P_1 , P_2 , and P_3 . Table 4.6 illustrates the error in the reference distance given by each method relative to the exact d_{ref} .

Table 4.6: Error impacting d_{ref}

	P_1	P_2	P_3
Average error impacting d_{EKF} (m)	0.322	0.613	0.476
Average error impacting d_{adap} (m)	0.033	0.178	0.121
Maximal error impacting d_{EKF} (m)	0.423	0.774	0.575
Maximal error impacting d_{adap} (m)	0.080	0.255	0.151

Compared to the EKF, the combined risk management guarantees navigation safety and optimality. Uncertainty-induced risks are mastered with particular optimization in spacing between vehicles. The set-membership/stochastic car-following ensures a strongly safe navigation, by depending not only on the filtering process, but also on the interval safety margins. In such a way, the EKF approach inaccuracy has been compensated and the pessimism of the proposed interval-based safety verification layout has been decreased.

4.5/ CONCLUSION

This chapter presented guaranteed solutions to handle uncertainties and risks endangering Intelligent Vehicles (IVs) during car-following situations. As an approach to meet safe and reliable autonomous navigation in the car-following context, a novel set-membership strategy to assess situational risk through the Time-To-Collision (TTC) computation was introduced. This new concept of the set-membership TTC combines the best features of the interval-based modeling of uncertainty evolution and the data-driven/correlation-based analysis of the system historical properties. Unlike the existing risk management and uncertainty handling methods, the defined strategy to quantify uncertainties and errors in the navigation dynamics relies on a careful consideration of sever new emergent challenges such as Vehicle-to-Vehicle (V2V) communication latencies and automotive embedded system delays. Further, several enhancements for the statistical process devoted to calculate the correlation for interval data were applied. For more relevant data analysis via the correlation assessment, robust statistical instructions were exploited to interpret the structure and distribution of the interval-type data. Compared to the standard estimation of covariance/correlation, the simulation results proved the efficiency of the adopted statistical procedures in analyzing the system historical features, even under the presence of outliers. Nonetheless, the proposed interval-based schema for risk management may be too conservative due to the pessimism. In an effort bridge this gap, the interval-based modeling was combined with the stochastic characterization of uncertainty. Hence, a methodological merge between the two proposed approaches has been performed based on several reliability and confidence oriented metrics. The carried out simulations demonstrated that the combined approaches high ability in ensuring safety, robustness against uncertainty and satisfying requirements of optimal navigation.

5

MATERIAL CONSTRAINTS-RELATED RELIABILITY ISSUES: FAULTS AND ON-BOARD COMMUNICATION DELAYS

In previous chapters, guaranteed navigation approaches and risk management schema have been introduced. These latter are high level software solutions targeting the navigation safety assurance. Nonetheless, once these strategies are well defined, it is important to handle material constraints related to the on-board equipments, where the high level navigation algorithms are deployed. Although the high level approaches are sufficiently reliable, the Intelligent Vehicle (IV) safety is still tightly linked to the proper operation of its embedded system. This issue is emphasized by the deep complexity of modern IV embedded systems, where several strict material constraints must not be violated. Hence, increasing the high level software awareness of the IV material constraints is now required more than ever. As a complementary contribution for the already proposed work in previous chapters, the material aspects related to IVs internal composition/communication are considered in this chapter in a more detailed manner.

Despite the high level algorithms capacities in mastering uncertainties, the measurement errors may exceed the normal rate due to fault occurrence at the material level. Correspondingly, the high level uncertainty handling approaches must be reinforced by a fault detection layer. Side by side, the diagnosis and uncertainty handling approaches should collaborate to ensure robustness to uncertainties and faults.

Aside from faults, intra-communication latencies are another important sort of material constraints imposed by the IV on-board composition. Such delays may slow down reactions made by the IV high level safety verification techniques. In chapter 4, an intra-communication latency aware risk management for IVs was presented. However, there was no clear strategy permitting to quantify and characterize such delays. In this view, the current chapter is dedicated to deal with the mentioned material constraints, which are faults and intra-vehicular delays.

Indeed, a fault may be defined as an anomaly that entails a deviation in the system behavior compared to its expected performances. In the literature, faults are usually classified according to their origins, such as sensor faults, actuator faults and component faults [115]. Differently, faults can be categorized also as permanent (failures that touch the computational/functional capacities of the system) or intermittent (wiring and connectors imperfections) [278]. Intuitively, it is mandatory to prohibit faults from interrupting the control instructions and modifying randomly the system input/output features. Ac-

cordingly, an interval-based diagnosis method, which has a great compatibility with the already proposed risk management approaches, is detailed in the first part of this chapter. Thus, threats induced from uncertainty and faults are simultaneously handled by the introduced navigation architecture (cf. subsection 5.1.3). The computational complexity and the overall performances of the interval-based diagnosis are discussed and evaluated through simulations.

Afterwards, the second part of this chapter is devoted to present a Response Time Analysis (RTA)-based algorithm permitting to characterize the variation of the intra-vehicular communication latencies. A proof of concept of this algorithm is presented by conducting experiments on an industrial automotive system within a diagnosis context. The evaluation of the diagnosis messages transmission time is indeed crucial, since the violation of the on-board diagnosis hard deadlines can be destructive. The main advantage of the suggested RTA method is the characterization of the minimum and maximum potential delay that may impact a given intra-vehicular message. Hence, the proposed method has a wide application in the benefits of the diagnosis and the risk management strategies (especially the set-membership approaches).

5.1/ INTERVAL-BASED DIAGNOSIS FOR RELIABLE IVs

For any automated process, diagnosis is a central part from the abnormal event management level. In particular, seeking for the most appropriate approach to monitor IVs is essential. This should be achieved with respect to the IV nature and specific features. Besides, the selection of the relevant diagnosis approach for a given IV depends on the manner of extracting the required knowledge about the system to report its correct/incorrect functioning. According to this understanding and in order to discuss each category pros and cons, the existing diagnosis approaches are reviewed in the sequel.

5.1.1/ DIAGNOSIS-RELATED WORK

Through a deep examination of the literature, the diagnosis methods may be classified into the different categories detailed in below. For each category, several examples of fault detection methods are delivered.

- The physical redundancy is a simple approach that duplicates the hardware material to obtain certain feed-backs about the state of the diagnosed system. In case of conflicts between each material outcomes, the final diagnosis decision is made according to a predefined arbitration scheme, such as the limit checking or the majority voting approaches [115]. Despite its reliability and simplicity, the material redundancy is definitely expensive and impractical for a whole navigation system.
- A large part from the diagnosis approaches consists of a qualitative procedures. The main purpose of any qualitative diagnosis is to present a logical formalization of the causal relation between faults and their corresponding symptoms. Intuitively, these qualitative models conduct a diagnosis operation without any need for mathematical procedures. Instead, they rely on a symbolic description for the process distinct operation modes. This allows to detect and localize failure sources by a simple examination of the diagnosed system measured outputs. In that sense, this

methodology can be also categorized as a knowledge-based diagnosis. The expert system is the most known qualitative diagnosis approach in the literature [321]. It consists of transforming the human expertise to a rule-based reference data-set. The diagnosis decisions are directly made via a knowledge-based set of rules. The fault tree analysis is also another qualitative diagnosis method that has been largely adopted for various systems [295]. Faults are detected thanks to a logical tree-based graphical representation of the studied system events. The evaluation of a given situation via this approach is done by propagating the primary events through the layers of the constructed tree by means of logic operators. To conclude, the major advantage of the qualitative approaches is the simplicity of handling a large number of events/symptoms in short periods of time. However, such qualitative methods are system specific and cannot be generalized easily.

- Aside from the qualitative strategies, another diagnosis direction has paid attention to the quantitative methods. In a first step, developing a fault-self-aware system in this case is met by carrying out a system identification phase. A mathematical description, which may be built on a statistical or non-statistical formulation, is requested to succeed this step. This description should reveal the system inherent operational features and/or the analytical redundancy between variables. Afterwards, the mathematical description of the system behavior may be joined with a set of physical principles to derive quantitative information, known in the literature as residual or signature. In a such a way, the quantitative diagnosis produces a sort of fault indicators by interpreting the system parameters and measurable data. Owing to the simplicity of the state estimation techniques and since faults generally invoke changes in the state variables, the use of observers as non-statistical fault detectors was mainstream in the literature. Several varieties of early fault detection methods were developed based on the sliding observer, adaptive observer, unknown input observer, etc. [91]. The parity equation approach is another non-statistical diagnosis technique that captures faults starting from the conventional system state space representation. Thus, the state model is arranged to highlight the analytical parity relations, where parity means the redundancy between variables [272]. Through a sort of a residual structuration, faults are detected and easily isolated, since simple separable fault signature can be deduced from the parity space. Without any use of statistics and joined with a residual generation phase, the Fuzzy logic and neural networks have been also used for diagnosis purposes [163], [186]. As obvious, the non-statistical quantitative diagnosis approaches are relying on models, learning approaches or analytical redundancy to generate residuals. For the sake of simplicity and to leverage the residual generation, a large number of quantitative diagnosis approaches have recourse to statistics. The partially least squares, the support vector machine and the statistical pattern classifiers are among these techniques. Instead of concentrating on the analytical redundancies, static and/or dynamic historical relations between the measurable variables are assessed through statistical descriptive metrics [115]. The use of the statistical quantitative diagnosis approach is becoming more popular recently in many application fields. Since they skip the modeling or learning phase, these approaches are more quick and less demanding computationally than the rest of diagnosis strategies.

In particular, the Principle Component Analysis (PCA) is the more widespread statistical quantitative fault detection and identification technique. It ensures anomaly detection regardless to the type and source of fault (sensor, actuator, materiel, etc.). This fact

discards the need to a large expertise about the diagnosed system and the probable faults that may impact it. Instead, failures are easily captured by examining the considered system inputs and outputs [218]. Additionally, the PCA method scales down the measurement dimensionality. It arranges the available data into principle and residual components [182]. Therefore, only the meaningful and influenceable part of data is kept to check the system correct operation. As a data-driven approach, the PCA avoids the complicated system modeling phase. For all its stated advantages, the PCA is highly recommended to ensure diagnosis for autonomous systems and especially IVs.

With time, the PCA has been adapted in several ways to be convenient for various applications. Thus, a multitude of new PCA extensions have been formulated [191]. The classical PCA relies on linear projection of data towards a new space of a reduced dimensionality, which facilitates the data interpretation. With accordance to this reasoning, a new PCA extension was developed to reveal the non-linear dependencies between variables [315]. One of the concerns that preoccupied researchers during the last years is overcoming the missing data problem while conducting a PCA-based analysis. Evidently, the PCA process may be aborted due to missing run-time data and measurements. The iterative PCA has been proposed to face such an issue by initially choosing random data to fill gaps in incomplete databases [216]. Through a recursive test of the variances of data, the inserted values are adjusted until reaching a minimum of convergence towards an appropriate density of the variance [215]. Several researches agree that relying on the static dependencies between variables is not enough to carry out sound data-based procedures [86]. From this scope, the dynamic PCA has been introduced to capture the latent dynamic variation in the correlation relating variables [294]. Independent Component Analysis (ICA) is another statistical component inspection approach. It has been introduced not only for dimensionality reduction, but also to ensure component separation [41]. Usually, ICA is used to distinguish between several sources of signals while discarding noises [230].

As a fact of matter, all the stated PCA extensions may only handle single-valued data. From a practical point of view, several cases require processing interval-type data to avoid loss of information and overstep data inaccuracy. It has been proved also that performing diagnosis in a bounded error context, to consider measurements variability's, boosts the accuracy and sensitivity to faults [55], [287]. Correspondingly, the standard PCA is adapted in the following to take into consideration uncertain/erroneous measurements.

5.1.2/ VERTICES PRINCIPLE COMPONENT ANALYSIS (VPCA) DIAGNOSIS

Since it belongs to the data-driven approaches, the PCA reliability is tightly related to the measurements accuracy. To face the PCA vulnerability to uncertain data, this section presents a PCA extension permitting to proceed failure analysis with interval-type data. Such an extension is expected to enhance the sensitivity to faulty data. In the following, all the required steps to apply this method are detailed.

5.1.2.1/ VPCA IMPLICIT MODEL AND DIMENSIONALITY REDUCTION STEP

The PCA interval extension transforms the measurements from single-type to interval-type data. Hence, the Vertices Transformation (VT) is used to construct a new single-valued matrix (cf. subsection 3.3.3.1, page 66). Due to the use of the Vertex-based

computation, the proposed extension is called VPCA. Indeed, the VPCA is composed from two fundamental phases. The first step is proceeded in offline to characterize the system nominal functioning through statistics. Let suppose that the system is described through its interval-valued variables, inputs and outputs. Accordingly, interval-data matrix, constructed from N samples of m interval measurement, is obtained. It is worth reminding that a second single-valued matrix $X \in [N \times 2^m, m]$ may be produced via the VT to substitute the initial interval matrix (cf. subsection 3.3.3.1, page 66). Henceforth, let note by N_1 , the new number of samples in X (number of rows in X), where $N_1 = 2^m \times N$.

The VPCA offline phase consists of building an implicit data-driven model for the statistical dependencies between the system variables. This implicit model do not only characterize the system correct operation, but also serves to split the data representation space into principle and residual components for dimensionality reduction aims. To distinguish between the significant and non-significant components, the calculation of the covariance matrix Σ , which is associated to X , is necessary (cf. equation (4.5), page 99). The VPCA procedure uses also the matrix $P = [p_1, p_2, \dots, p_m] \in R^{(m \times m)}$, which is the eigenvector matrix of Σ , to capture statistical features of the system nominal functioning. Afterwards, fulfilling a linear transformation into another data representation space is required:

$$T = XP \quad \text{and} \quad X = TP^T \quad (5.1)$$

where $T = [t_1, t_2, \dots, t_m] \in R^{N_1 \times m}$. Then, different statistical analysis, which are applied on Σ and P , permit to determine the real number of the system principle components, denoted l . A correct estimation of l is decisive for succeeding the VPCA-based fault detection. A wrong reduction in the dimension of the data representation space induces definitely misleading diagnosis results. Reader is referred to [292] for a detailed comparison between approaches allowing to recognize l . In this stage, the Variance of the Reconstruction Error (VRE) method is adopted to explore this parameter [123]. Initially, the mean value of variance between the system variables is estimated for all $l \in [1, \dots, m - 1]$. Finally, the value of l that corresponds to the lowest possible variance is admitted. The identification of l allows immediately to decompose P and T . Henceforward, (\hat{P}, \hat{T}) and (\tilde{P}, \tilde{T}) indicate the principal and the residual spaces associated to P and T . Equations (5.2) and (5.3) designate dimensions of the principle/residual components:

$$P = \begin{bmatrix} \hat{P}_{[m \times l]} & \tilde{P}_{[m \times (m-l)]} \end{bmatrix} \quad (5.2)$$

$$T = \begin{bmatrix} \hat{T}_{[m \times l]} & \tilde{T}_{[m \times (m-l)]} \end{bmatrix} \quad (5.3)$$

It is worthy to point that the initial data-set can be represented in the following shape thanks to the latest decomposition of the system components:

$$X = \hat{P}\hat{T}^T + \tilde{P}\tilde{T}^T = \hat{X} + \tilde{X} \quad (5.4)$$

Finally, the VPCA implicit model within its both principle and residual parts (\hat{C}, \tilde{C}) is revealed by the expressions below:

$$\hat{C} = \hat{P}\hat{P}^T \quad \text{and} \quad \tilde{C} = \tilde{P}\tilde{P}^T = (I_m - \hat{C}) \quad (5.5)$$

Since the VPCA implicit model extraction is an offline step, the expansion in the dimension of the data-set X via the VT method does not bring any computational complications.

5.1.2.2/ VPCA STATISTICAL/THRESHOLD-BASED FAULT DETECTION STEP

The remaining steps from the VPCA technique are dedicated for the run-time. The VPCA exploits in fact the realized implicit model to capture faults. In that case where the newly incoming data from measurement tools show an enormous change in the dependencies between variables, a fault occurrence is admitted. The deviation between the system nominal and run-time behaviors is assessed through a statistical index generation step. In this context, various expressions for the PCA-dedicated indexes have been proposed in the literature (see Table 5.1). For each statistical index, there is also a well-defined threshold value that must not be exceeded by the index during a system anomaly-free operation. Table 5.1 presents the most known indexes/thresholds used within the PCA.

Table 5.1: PCA-based fault detection step: indexes/thresholds

Index	Index expression	Threshold expression
Squared Prediction Error (SPE)	$x(k)(I - \tilde{P}\tilde{P}^T)x(k)^T$	$\delta_\alpha^2 = g \chi_{h,\alpha}^2$
Squared weighted error	$x(k)(\tilde{P}\tilde{\Lambda}^{-1}\tilde{P}^T)x(k)^T$	$\mathcal{T}_{H,\alpha}^2 = \chi_{(m-l),\alpha}^2$
Hotelling index	$x(k)(\hat{P}\hat{\Lambda}^{-1}\hat{P}^T)x(k)^T$	$\mathcal{T}_\alpha^2 = \chi_{l,\alpha}^2$
Mahalanobis distance	$x(k)(P\Lambda^{-1}P^T)x(k)^T$	$\mathcal{D}_\alpha = \chi_{m,\alpha}^2$

Note that k is the index corresponding to the newly up-coming measurements. Λ consists of the eigenvalue matrix associated to Σ . χ is the chi-square distribution function and α is an empirically predefined freedom degree parameter [123]. Let assume that λ_j are the eigenvalues of Σ . Then, g and h are calculated in function of λ_j as follows:

$$\begin{cases} \theta_i = \sum_{j=l+1}^m \lambda_j^i \\ h = \text{floor}(\theta_1/\theta_2) \\ g = \theta_1/\theta_2 \end{cases} \quad (5.6)$$

In the sequel, the SPE index is adopted to perform the fault detection step because of its low rate of false alarms [1]. As shown in Table 5.1, each new collection of measurements must be verified and pass the threshold-based diagnosis test. However, the measurements are interval-shaped sets to consider measurement errors. In the meantime, the VT should be applied locally on the new measurements acquired at instant k . Hence, as illustrated in Figure 5.1, the estimation of the SPE index is repeated 2^m time to verify every row from the obtained VT-induced matrix.

Compared to the generalized PCA method, the use of the VT in run-time entails an increase in the required number of SPE index-based tests that must be accomplished to monitor the concerned system. To reach a final diagnosis decision, the highest value recorded for the SPE index among the 2^m obtained values at the instant k is retained. Such a choice reinforces the VPCA sensitivity to faults. In other words, the VPCA permits to approve or disapprove the system correct behavior regarding to the most critical situation of uncertainty.

In terms of real time computational constraints, the 2^m index values may be calculated based on a concurrent computing strategy (hardware or software concurrency) [42]. In

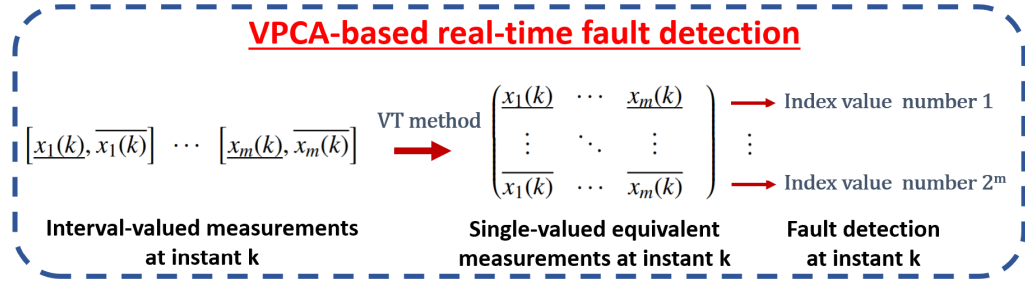


Figure 5.1: VPCA-based run-time fault detection principle.

case of the sequential computation, the VPCA-based fault detection process must satisfy the following constraint:

$$\Delta_{VPCA} \leq \frac{\Delta_{Sys}}{2^m} \quad (5.7)$$

Where Δ_{VPCA} is the VPCA diagnosis task sampling time and Δ_{Sys} is the monitored system sampling period.

5.1.2.3/ VPCA FAULT ISOLATION STEP

In presence of faults, succeeding a diagnosis mission requires imperatively to isolate the anomaly source (faulty variable or parameter). To meet this goal and ensure the fault localization, the VPCA takes advantage of the statistical redundancies between the system components. Through the dependency relations captured via the system implicit model, the VPCA fault localization step assumes that every variable may be erroneous. Then, it triggers a sort of reconstruction operation for the whole system variables (one by one). Let suppose that X_R is the reconstructed vector associated to one variable from the initial data-set matrix. Hence, $R = 1 \cdots m$ refers to the index of the variable concerned by the reconstruction. Besides, Ξ_R represents the matrix that indicates the reconstruction direction. At a given instant k , the principal part from X_R , denoted \hat{X}_R , is estimated through the relations described by equation (5.8):

$$\begin{cases} \hat{X}_R = G_R X \\ G_R = I_m - \Xi_R (\tilde{\Xi}_R^T \tilde{\Xi}_R)^{-1} \tilde{\Xi}_R^T \\ \tilde{\Xi}_R = (I_m - \hat{P} \hat{P}^T) \Xi_R \end{cases} \quad (5.8)$$

After proceeding the reconstruction phase, a fault localization index denoted A_{SPE_R} is employed. Using the reconstruction-induced data, the A_{SPE_R} expression at an instant k is given by equation (5.9):

$$A_{SPE_R}(k) = \frac{SPE_R(k)}{\delta_\alpha^2(k)} \quad (5.9)$$

It is worth noting that the $SPE_R(k)$ is computed through the same formalization of the SPE index utilized in the fault detection phase (cf. Table 5.1). By checking the index values for all $R = 1 \cdots m$, a variable is supposed erroneous once the isolation index is lower than 1.

5.1.3/ VPCA-BASED DIAGNOSIS INTEGRATION INTO ADAPTIVE CRUISE CONTROL (ACC) ARCHITECTURE

In previous chapter, a specific ACC architecture was proposed to master efficiently collision risks and uncertainties. The simulation results proved the efficiency of the interval-based risk management. Despite its robustness to uncertainties, the suggested risk management remains sensitive to system deficiencies. Due to failures, the error rate in measurements and in system parameters may overstep the normal level of uncertainty. Thus, both the reliability and safety requirements can be violated. To face such a vulnerability, the proposed VPCA diagnosis method is adopted to ensure robustness against faults. It permits to report the system state while considering the most critical level of uncertainty that impact measurements. Hence, the VPCA is exploited to surveil the previously introduced ACC system (cf. subsection 4.1.5, page 100). The set of variables (p_i , p_j , V_i , V_j and d_{ij}) are selected to characterize the system. After the integration of the VPCA diagnosis scheme into the risk management layer, the ACC control architecture is illustrated in Figure 5.2.

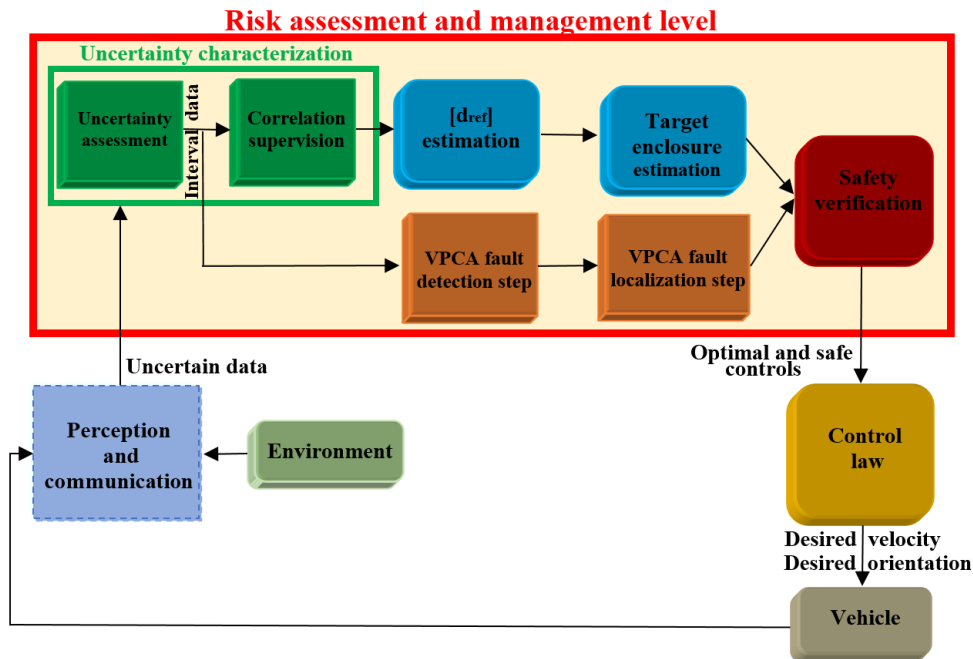


Figure 5.2: Interval-based ACC fault aware control architecture.

Most of the existent IVs risk management strategies neglect the probability of fault occurrence and focus only on uncertainty in measurements and driving behaviors. Thus, the proposed interval-based ACC architecture aims to present a fault-aware safety verification layer, which simultaneously detects faults and discards uncertainties. The interval-based computation guarantees a particular robustness to uncertainties of both the diagnosis and risk management components. Even more, the reliability and safety are increased due to the considerable mutuality between the diagnosis and uncertainty handling approaches.

The sound relation between the interval-based handling of uncertainties and diagnosis permits to distinguish easily between faults and uncertainty. The employed statistical threshold (associated to the SPE index) serves to decide whether the uncertainty level

is acceptable or it is sufficiently high to admit a system failure. As soon as a fault is identified, warnings are transmitted to the risk management layer. Thus, the worst case of risk is approved and the ACC functioning is aborted.

5.1.4/ DIAGNOSIS RESULTS

The simulation work is tackled at this stage to prove the VPCA efficiency in capturing and locating faults. As already stated, the VPCA initial step consists of constructing an implicit model for the navigation system to explore its inherent features. Interval samples corresponding to variables $[p_i]$, $[p_j]$, $[V_i]$, $[V_j]$ and $[d_{ij}]$ are stored and transformed to single-valued data-set via the VT. Evidently, the stored data describe the ACC system fault-free operation. Besides, matrix centering (see subsection 4.2.2, page 105) is practiced on the obtained data-set for more relevant and confident statistical analysis. Note that the VPCA implicit model in the current simulation work is built through an interval data-set with a dimension of 2000×5 , which corresponds to a single-valued data set of 64000×5 (since $N_1 = 2^m \times N = 2^5 \times 2000 = 64000$).

Afterwards, the number of principle components is determined through the VRE method. The computation results of the variables' accumulated variance for $l \in [1 \dots 4]$ are shown in Figure 5.3. As clear from the results, the minimum variance of the system variables is associated to $l = 4$. Henceforth, the system implicit model (see equation (5.5)) can be exploited in the fault detection and localization phases.

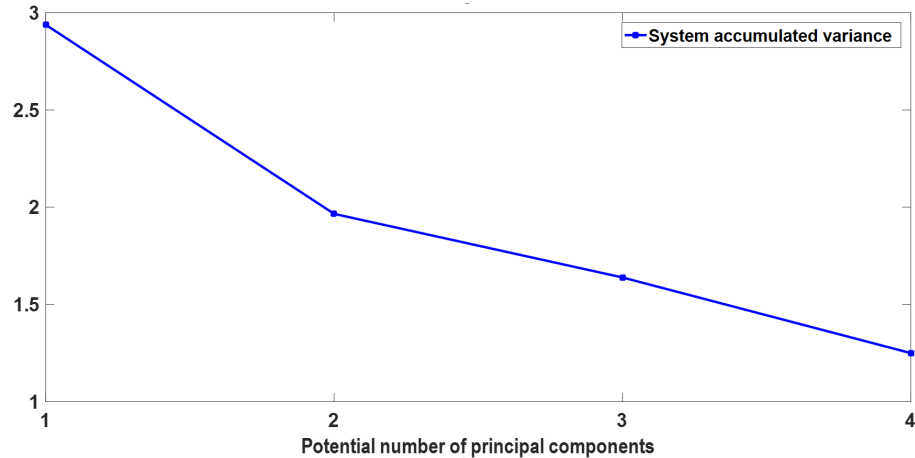


Figure 5.3: Number of principle components-based on VRE method.

A test scenario is then proceeded to judge the VPCA abilities in fault detection. Three faults of different magnitudes are injected in the communication-issued data (attribute of the V_i variable) during distinct periods of the simulation run-time (respectively between $[100s..130s]$, $[400s..420s]$ and $[500s..560s]$ (cf. Figure 5.4)). During these periods, the error rate in the data attributed to V_i varies between 10 and $15m/s$. Aside from the fault injection periods, random Gaussian uncertainties are injected into the overall navigation dynamics. The transformation of single data to interval measurements in run-time is achieved according to the uncertainty quantification assumption presented in subsection 4.1.2, page 94.

The results of this test according to the explained configuration of fault injection are illustrated in Figure 5.4. As obvious, the SPE index has succeeded the fault detection step. The index exceeded its threshold three times during the whole fault injection periods. Despite that the VPCA takes into account the most critical situation of uncertainty distribution, there are no false alarms triggered during the test. This means that the proposed risk management architecture is able to distinguish successfully between faults and uncertainties. Hence, the validation work proves the VPCA sensitivity to faults and its robustness against false alarms.

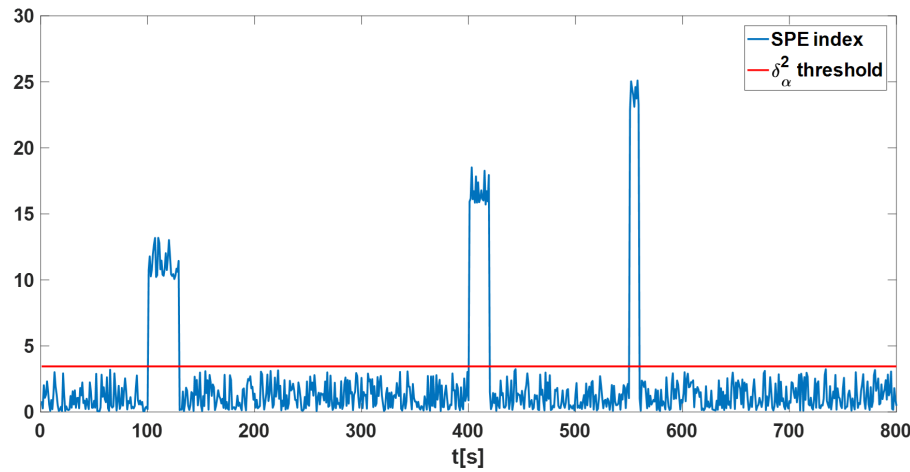


Figure 5.4: SPE index-based fault detection.

Finally, Figure 5.5 depicts the fault localisation results for the first instant when a fault occurrence is approved. The A_{SPE_R} test shows a localisation index lower than 1 for the variable V_i , which confirms that the communication tool providing the leader velocity is the fault source. Accordingly, the efficiency of all the VPCA diagnosis steps have been demonstrated.

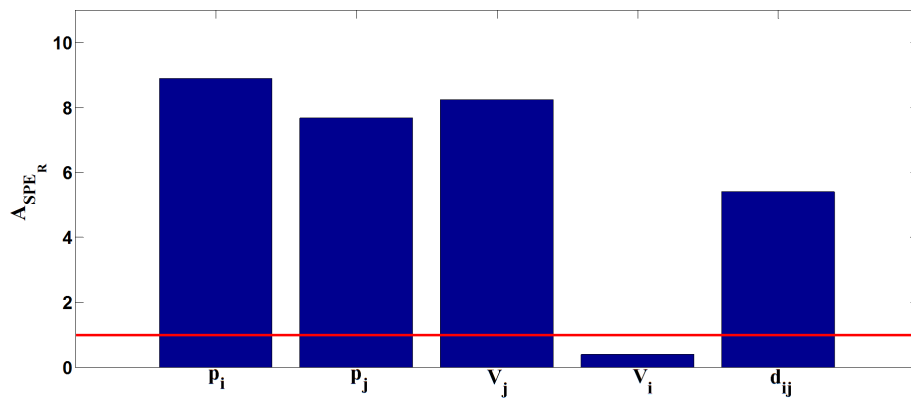


Figure 5.5: Fault localisation.

5.2/ RTA FOR INTRA-VEHICULAR LATENCY CHARACTERIZATION

As already explained, delays manifestation into the IV embedded layout is an alarming issue that threatens safety of autonomous navigation processes. Thus, it is primordial to found risk management and diagnosis approaches with great awareness of such latencies in regard to their role in warranting operational safety.

To characterize data propagation delays through the navigation system embedded architecture, a large range of professional software tools are available in the automotive market. CANoe, CANalyzer, SymTA/S and Rubus-ICE are among the advanced engineering software solutions that may assure latency analysis and intra-vehicular network simulation [32, 98, 277]. However, these commercial software tools are most of the time non-free products. Besides, they do not provide facilities to evaluate performances of the risk management and safety verification levels. Moreover, a large expertise is required to master the establishment of latency analysis through these advanced tools. As an alternative for the time-wasting and challenging use of the professional tools, interest is given in the sequel to Response Time Analysis (RTA) algorithms.

5.2.1/ RTA PRINCIPLE AND RELATED WORK

Generally, RTA are analytical models permitting the approximation of the end-to-end data transmission time through embedded systems. Since every communication protocol posses particular schedulability features, the RTA inspects major concerns as satisfying temporal constraints and meeting hard-deadlines for the studied embedded system [103]. To master all timing characteristics of a given process, RTA examines the communication triggered events and data flows. It verifies also the temporal dependencies between the system different components [211]. The first application of the RTA for intra-vehicular communication protocols was carried out by Tindell seminal research work in 1995 [289]. Due to the on-going interest in boosting the RTA theories, more potent models are nowadays available to perform timing analysis for in-vehicular systems. Hence, latest versions of RTA models consider mainly:

- **Message maximum transmission time:** It underlines the largest period of time needed to broadcast a single frame from a message. The calculation of such a period is accomplished with respect to the communication payload and more importantly to the transmission time of one bit. Evidently, these two parameters vary depending on the communication protocol employed to enable the communication between the different components of the navigation system. For instance, the maximum possible payload of CAN frame is 8 bytes.
- **Maximum release jitter:** By definition, the jitter delays consists of the time interval extended between the message generation instant (due to a particular event) and the moment of its queuing.
- **Queuing delays:** Indeed, the intra-vehicular communication is governed through a set of priority rules defined by the automotive designers. Regarding to its criticality, a specific priority value is attributed to every possible message. According to this fact, a message can be blocked temporarily until delivering other higher priority messages. Otherwise, queuing delays may be noticed when the communication channel is not available until accomplishing an already initiated transfer of

a lower priority message. As a consequence, both higher and lower priority messages queuing block-time should be considered to present correct estimation of the end-to-end transmission latencies.

Indeed, a multitude of statistical RTA-based approaches were proposed to calculate a message transmission delays. These methods are efficient in performing RTA while filling gaps caused by incomplete information about the configurations and composition of the considered Networked Control System (NCS) [337]. In a different way, several RTA models used probabilities to explore the system response times [119]. From this perspective, the probabilistic reasoning allowed standard RTA to predict events such erroneous data exchange [261]. Otherwise, the authors in [266] have recourse to Taylor series expansion to cope with RTA modeling imperfections. For an accurate estimation of the embedded system delays and response times, RTA models should be comprehensive. All probable data transmission scenarios and occurrence of unpredictable events must be examined. From this scope, the RTA-based algorithms introduced in [209] have attempted to integrate several Hardware and Software technical issues into their models.

Hereafter, the RTA models are exploited for the first time in the benefit of the in-road risk management strategies. Conventionally, RTA models provides reliability guarantees during an early design phase of a given embedded system to prohibit any unacceptable violation of on-board communication deadlines [10]. Unlike the research line that relied on statistical or stochastic RTA models, focus in this thesis is put on deterministic approaches to bound the navigation system response times. Certain thresholds of the minimum and maximum possible temporal delays that may occur during the data propagation through the IV embedded system are sought. From this perspective, RTA findings may serve as a useful information-support to avoid slow reactions of the risk management and safety assurance levels against any potential hazard.

5.2.2/ RTA MODEL FOR INTERVAL TIME OF CAN RESPONSES

As explained, RTA is adopted to deliver bounds of possible latencies that may happen into the embedded structure of a navigation system. In particular, the introduced RTA algorithms are dedicated for NCSs where the CAN bus is the communication support. Every exchanged data between components must pass through the CAN before reaching its final destination.

Technically, CAN is an event-triggered/multi-master serial communication bus [118, 235]. During the past several decades, CAN has dominated the intra-vehicular communication and the worldwide car-manufacturing domain. Due to its cost-efficiency and reliability, CAN has been also the main on-board communication middleware for most robots and modern intelligent navigation systems. A complete description of the CAN features and technical aspects may be found in [165].

It should be well-noted that the ultimate concern of this section is to proceed RTA for risk management purposes. Attention should be paid exclusively to the suggested methodology that stands behind the estimation of the minimum and maximum delays affecting the intra-vehicular communication. The CAN is only an automotive communication protocol, which is selected to present an example of particular RTA case of study. However, the proposed approach may be extended and applied on other different protocols. For this reason, the CAN technical configurations and characteristics will not be intensively

discussed in the sequel. When necessary, readers will be referred to the appropriate references in order to find the required information about CAN.

The first step from the proposed method to define bounds of the CAN-based intra-vehicular communication delays is to distinguish all the intervening nodes, tasks and data flows presented in the considered case of study. In fact, a node refers to an ECU or a sub-entity from the whole NCS, which is connected to the communication bus. It is important to notice that a finite number of tasks are implemented on each vehicular node. Every task is in charge of several well-defined functionalities. According to the network messages schedule, the manifestation of some specific events triggers the transmission of particular collection of messages through the CAN bus towards a destination task. In contrast to methods introduced in the literature, the adopted RTA algorithm incorporates component local analysis to obtain precise message transmission-time. It means that even factors that may slow down a message instance and transmission during the task execution are also examined. In this view, all the timing properties of elements included in the data diffusion process should be considered. Technically, a data flow refers to the set of elements involved in the data transmission starting from the transmitter task, up to recipient task. Therefore, CAN response time prediction is tackled relatively to the point-pointed flows in the studied system. Consider an embedded system of a modern IV, which is constructed from a network of n nodes. To simplify the notation, let suppose that each single node, denoted $N_{h=1..n}$, executes a finite number of tasks. Similarly, every task associated to N_h is denoted by $\Gamma_{h,i}$. Figure 5.6 gives a simple example of a node representation according to the proposed notation.

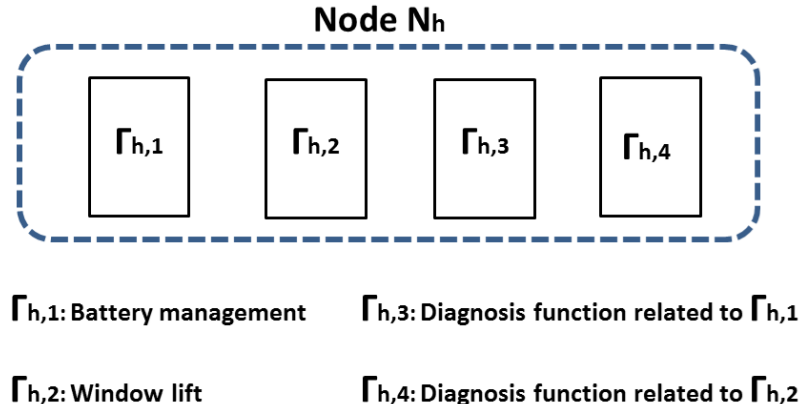


Figure 5.6: Node modeling for RTA purposes.

Afterwards, let note by $S_{h,j}$ a particular message stream that assembles the series of messages, which are initiated starting from a particular source task. It is important to note that one task may definitely transmit more than one stream. In that case, if we adopt the notation of $S_{h,j}$, it is impossible to distinguish between the set of streams transmitted by the considered task. For this reason, it is unavoidable to attribute to each stream a particular number j . In addition, since a node can include several tasks, it is worth mentioning that a stream message is assigned to a specific task instead of a node. In this sense, a flow φ_c consists of the overall path that conjoins message streams and tasks involved in the data propagation from a source to a final destination task. For a better understanding, Figure 5.7 clarifies the concept of data flows.

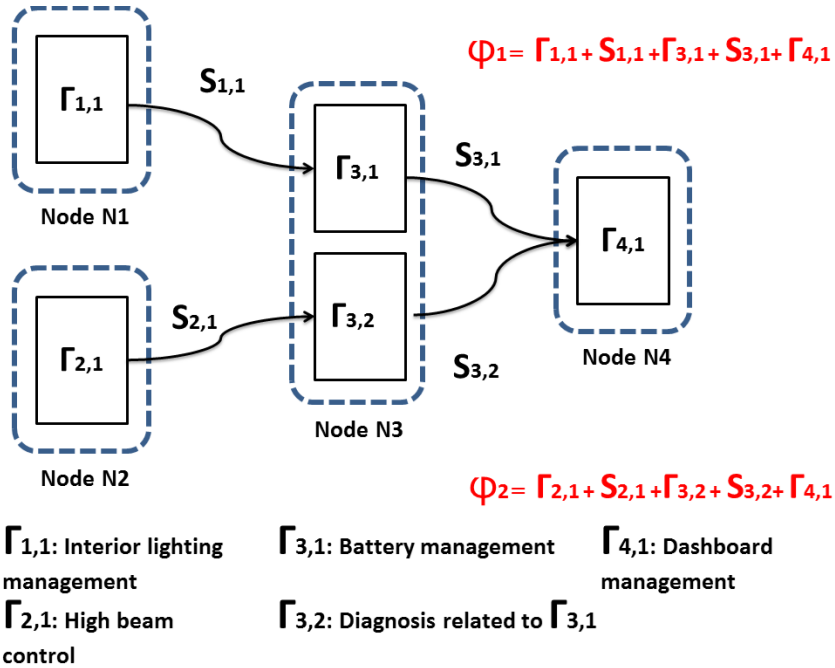


Figure 5.7: Data flows modeling.

In the aim to fulfill the RTA modeling, let define the following assumptions:

- Every task $\Gamma_{h,i}$ has a well-defined maximum execution time. This latter is denoted as $C_{h,i}^{task}$.
- Every message stream $S_{h,j}$ is featured by a maximum duration to deliver the message. This maximum period is denoted in the sequel by $C_{h,j}^{message}$. Note that the $C_{h,j}^{message}$ value does not consider any interference induced from other messages that may allocate the CAN-bus.

Indeed, $C_{h,i}^{task}$ and $C_{h,j}^{message}$ play an important role in defining the final response time of the CAN-based network. Let assume that $m_{h,j}$ is a CAN frame (message) initiated by the node N_h . Conventionally, a frame refers to the numeric form (represented by bits) of a message transmitted over CAN. Since RTA here is applied for one CAN frame message, there is no significant difference between a frame and message in the proposed model. Each frame from the CAN protocol possess a unique identifier (*ID*). There are actually two distinct types of frames, which are the standard CAN frame of 11 bits *ID* and the extended CAN frame format of 29 bits *ID*. The model introduced in this section to apply RTA focuses on the message length. The number of bits included in the message is decisive to approximate the maximum transmission time for a given message. Hence, the maximum transmission time for a 11 bits *ID* frame is given by equation (5.10):

$$C_{h,j}^{message} = (55 + 10 \times lm_{h,j}) \times \tau_{bit} \quad (5.10)$$

Respectively, the calculation of the maximum transmission time associated to a 29 bits *ID* frame is feasible through equation (5.11):

$$C_{h,j}^{message} = (80 + 10 \times lm_{h,j}) \times \tau_{bit} \quad (5.11)$$

Where $Im_{h,j}$ is the number of data bytes incorporated in a message and τ_{bit} is the amount of time needed to deliver one single bit from a CAN frame. τ_{bit} is indeed fixed according to the considered CAN-based network baudrate and its speed.

It is important to notice that the use of equations (5.10) and (5.11) to count the maximum transmission time for a CAN frame is very common by the automotive community. To be entirely trusted, these equations have been validated and revised through many studies [171]. These equations rely on estimating in worst cases the maximum number of bits that may a CAN frame include. Besides, the number of additional bits inserted in the CAN frame due to the so-called bit stuffing mechanism is considered. The bit stuffing is based on inserting a complementary bit after transmitting five bits of the same polarity. This additional bit of opposite polarity follows the five homogeneous bits to prevent the signal synchronization loss. Accordingly, one stuffing bit per four original bits can take place in worst cases, in fields where the bit stuffing is allowed. Note that a CAN frame is constructed basically from a “Data Bytes” field that includes the message content. It incorporates also other fields required to ensure the correct transmission of data (ID, error detection, etc.). Consequently, without counting the content of the “Data Bytes” field, the 55 and 80 used respectively in equations (5.10) and (5.11) represent the maximum theoretical number of bits involved in the rest of fields in the case of a 11 bits and 29 bits ID frames.

Thereafter, a Worst Case Response Time (WCRT) must be calculated for every single message stream to eventually obtain the global end-to-end response-time for the whole flow. Let admit that $R_{h,j}$ is the WCRT of a specific message $m_{h,j}$ induced from a stream $S_{h,j}$. As already stated, not only the CAN frame transmission time delay should be taken into account, but also the maximum release jitter and the queuing block time. Correspondingly, equation (5.12) allows to estimate $R_{h,j}$:

$$R_{h,j} = J_{h,j} + C_{h,j}^{message} + W_{h,j} \quad (5.12)$$

where:

- $J_{h,j}$ presents the maximum queuing jitter [73]. $J_{h,j}$ is indeed regarded as the main source of variability in the CAN message transmission delays. In reality, this parameter is tightly linked to the processing capacities of the node initiating the message transmission. As soon as an event occurs in the node-level and implies to send a message, this latter is queued by a software task implemented on the node on-chip CAN controller. Hence, the longest duration extended from the instant of the initiating event occurrence until the message being queued is then related to the node own clock. In the sequel, it is assumed that every node from the CAN network is characterized by a known value of maximum release jitter.
- $W_{h,j}$ is the message queuing delay. As already explained, multiple messages can be prepared in the same time for transmission through the CAN. The authors in [73] and [171] have presented the required algorithms that permit to estimate $W_{h,j}$. These algorithms tackle all potential scenarios with regard to CAN bus blocking time entailed by both higher and lower priority sets of messages.

After all, the notion of priority concerns not only messages, but also tasks implemented on the same on-chip CAN controller. In this context, the WCRT of a predefined priority task may be estimated through equation (5.13):

$$R_{h,i} = I_{h,i} + C_{h,i}^{task} \quad (5.13)$$

Note that $I_{h,i}$ is the interference time caused by the set $hp(h, i)$, which gathers all tasks of a priority higher than $\Gamma_{h,i}$. This issue is discussed with more details in [171], where recursive algorithms to calculate $I_{h,i}$ are provided.

Once again, it is important to recall that the WCRT evaluation of a message starts from the instant of the initiating event to the instant of the message reception by the recipient task. From this viewpoint, the complete WCRT corresponding to a φ_c is calculated by summing all the response times of message streams and their source tasks.

Since RTA is used roughly to verify the respect of message deadlines, a considerable literature is available on the approximation of the worst cases of CAN response times. Nonetheless, the best cases of the CAN response times (minimum possible data propagation time through the embedded system) were rarely discussed. With a slight modification in the proposed model to compute the WCRT of a given φ_c , a completely optimistic evaluation of response times may be obtained. The required modifications are detailed in what follows:

- Contrarily to equations (5.10) and (5.11), which are used to predict the maximum transmission time for a CAN frame, the impact of the bit stuffing mechanism should be ignored to obtain the shortest transmission period of a CAN frame. According to [73] and [225], the transmission time for CAN frame without adding the stuffing additional bits is given by equations (5.14) and (5.15) respectively for 11 bits and 29 bits *ID* frames:

$$C_{h,j}^{message} = (47 + 8 \times lm_{h,j}) \times \tau_{bit} \quad (5.14)$$

$$C_{h,j}^{message} = (67 + 8 \times lm_{h,j}) \times \tau_{bit} \quad (5.15)$$

- Both delays $W_{h,j}$ and $I_{h,i}$, defined in equations (5.12) and (5.13), should be neglected by assuming that there is no blocking time entailed from higher or lower priority tasks/messages.

Finally, the introduced RTA model enables to derive an interval time describing the required minimum and maximum duration of any data propagation through CAN-based in-vehicular systems. In contrast to the existing methods that tackle the worst case of response times, the proposed method permits to assess the exchanged data freshness and its validity (cf. subsection 2.2.2, page 40). It allows also to integrate risks of the intra-vehicular communication delays into the in-road risk assessment process (see subsection 4.1.3.2, page 97).

5.2.3/ PROOF OF CONCEPT: APPLICATION ON SMART DISTANCE KEEPING (SDK) SYSTEM

In order to validate the suggested approach in estimating realistic intervals for the in-vehicular systems response times, a high fidelity model of an industrial anti-crash system is employed. On the one hand, this module simulates modern in-vehicular components and measurement devices, which have intensive use in the automotive industry. The model is indeed validated according to the very rigorous and strict industrial specifications¹. On the other hand, the provided model has a great portability with the Hardware-

¹The industrial model was elaborated and validated by a collaboration between Renault Trucks/Volvo SAS and SERMA INGENIERIE under the DIAFORE (Diagnosis for Distributed Functions) project [10].

In-the-Loop (HIL) experimental plants. Hence, the timing delays of the communication may be assessed through a real intra-vehicular communication middleware. Before tackling the experimental setups and the validation phase, the different facilities and safety enhanced functionalities supplied by the industrial anti-crash modeled mechanism, named SDK system, are detailed. Further, the role of every component and the diagnosis layer, which constitute the SDK architecture are described.

More accurately, the SDK is an anti-crash system which is implemented on trucks. It is developed to ensure safety assurance for truck's drivers during highway travels. Based on statics furnished by the French motorways companies organization ASFA (for Association des Sociétés Françaises d'Autoroutes), 18.43% of fatal in-road incidents in France during the year 2011 were in highways [10]. In particular, truck drivers are the most road participants which are concerned by these accidents in this case. The long and exhausting travel distances are factors that emphasize truck drivers distractions and consequently road accidents. In this context, the SDK is developed to assist drivers in coping with hazardous situations in motorways.

The SDK can be regarded as an Adaptive Cruise Control (ACC) system (cf. subsection 4.1.1, page 93). Apart from adjusting the ego-vehicle's velocity to maintain a safe distance from in-front vehicles (see Figure 5.8a), the SDK provides several additional safety assurance services for trucks' drivers. For instance, the SDK warns the driver in case of a sudden lane change performed by other vehicles towards the current lane of SDK-equipped vehicle, as shown in Figure 5.8b. In such a circumstance, the SDK regulates the truck velocity to mitigate crash risks. Threats invoked from unexpected hard breaks of other vehicles are also mastered via the SDK controller. Especially for night time travels, the SDK detects rough curvatures through monitoring the road yaw rate and diminishes the truck speed to avoid sliding risks (cf. Figure 5.8c). As illustrated in Figure 5.8d, the SDK helps to deal with traffic jams and difficult driving situations due to congestion by maintaining a convenient safety distance from in-front objects. Figure 5.8 recapitulates the SDK process facilities to assist truck drivers. It is clear that the SDK provides more driving assistance functionalities to drivers than standard ACCs. The increased number of functionalities raises systematically the intra-communication load. Therefore, it is crucial to study and verify the SDK internal communication latencies.

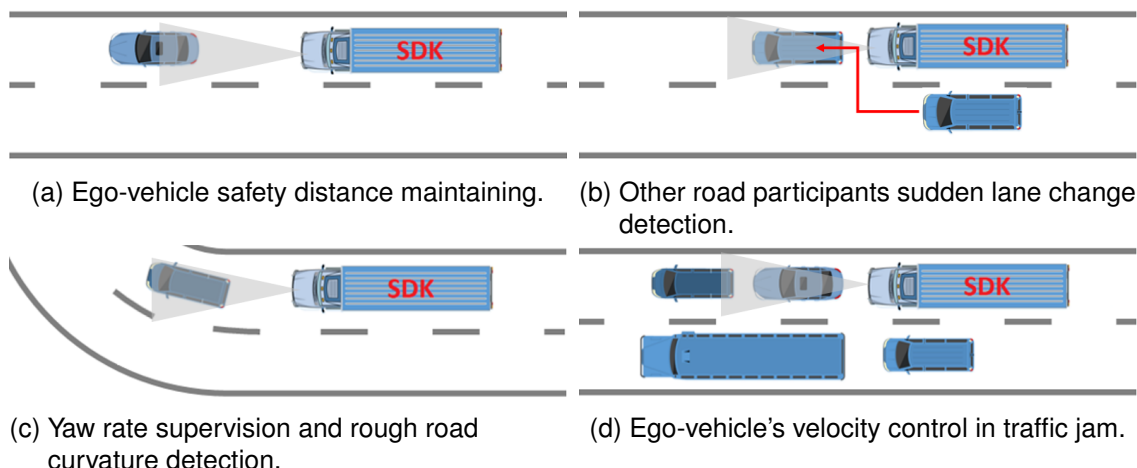


Figure 5.8: SDK capacities in truck drivers assistance.

The whole architecture and composition of the SDK system, which is integrated into trucks embedded systems, is mainly composed from the following components:

- To sense the environment, a radar is mounted on the SDK host truck to capture the relative velocity and the spacing distance from other road participants. A diagnosis task is implemented also into the radar node to detect faulty measurements. Due to interferences, a radar may return unreal measurements, where vehicles are traveling with physically impossible velocities. For this reason, a local diagnosis is indispensable to monitor the radar device.
- The SDK system is indeed reinforced with a “wheel’s ECU”. Note that the SDK is devoted to assist drivers of six-wheel trucks. Hence, six sensors ensure the angular velocity measurement’s of each wheel. Actually, wheels damages are responsible for several highway crashes. One probable trouble related to wheels is the improper tire pressure. It may influence the truck stability and its smooth navigation. To react efficiently against the aforementioned problem, the “wheel’s ECU” checks continuously the difference between the angular velocities of wheels. This node estimates also the truck longitudinal speed through the collected wheels velocities. To monitor sensors implemented on wheels, a task running an analytical redundancy-based diagnosis method is integrated into the “wheel’s ECU” [1].
- The transmission ECU has as a role to determine the truck longitudinal speed based on the crankshaft angular speed. For functional safety verification, the obtained value will be compared later with the measurement provided by the wheel’s ECU.
- The “SDK controller” is the ECU in charge of operational decision making for the overall anti-crash process. A smooth control of the truck while mastering the in-road hazards is ensured by this node. Depending on data provided by the rest of components, the “SDK controller” generates the convenient control-inputs for the fuel injector, the braking system, the engine and the gearbox.
- A decentralized diagnosis is deployed over the truck embedded system. A supervisor node is dedicated to receive local diagnosis reports ensured by the remaining SDK components. The supervisor executes a fault-tolerant control algorithm. It aims to carry on the SDK operation even under presence of faults by exploiting the data redundancy. The SDK functioning is aborted only when no available back-up may be proceeded. For instance, faults affecting the Transmission ECU can be tolerated since the truck angular velocity can be estimated also by the “wheel’s ECU”. The whole fault tolerant control strategy is detailed in [10]. The supervisor final report about the state of the SDK different components is displayed on a Human Machine Interface (HMI) to warn the driver in case of threats.

Remarkably, there are no diagnosis tasks to monitor neither the SDK controller nor the transmission ECU. According to the description of each component, message streams can be classified into: (i) Standard messages to deliver findings of each component towards other nodes, (ii) Diagnosis messages including reports of local diagnosis functions and (iii) Recovery messages to substitute erroneous data and pursuit the appropriate operation of the SDK or to abort its functioning, if necessary. For more clarity, Figure 5.9 schematizes the different data flows and message streams that may be exchanged over the CAN into the SDK system.

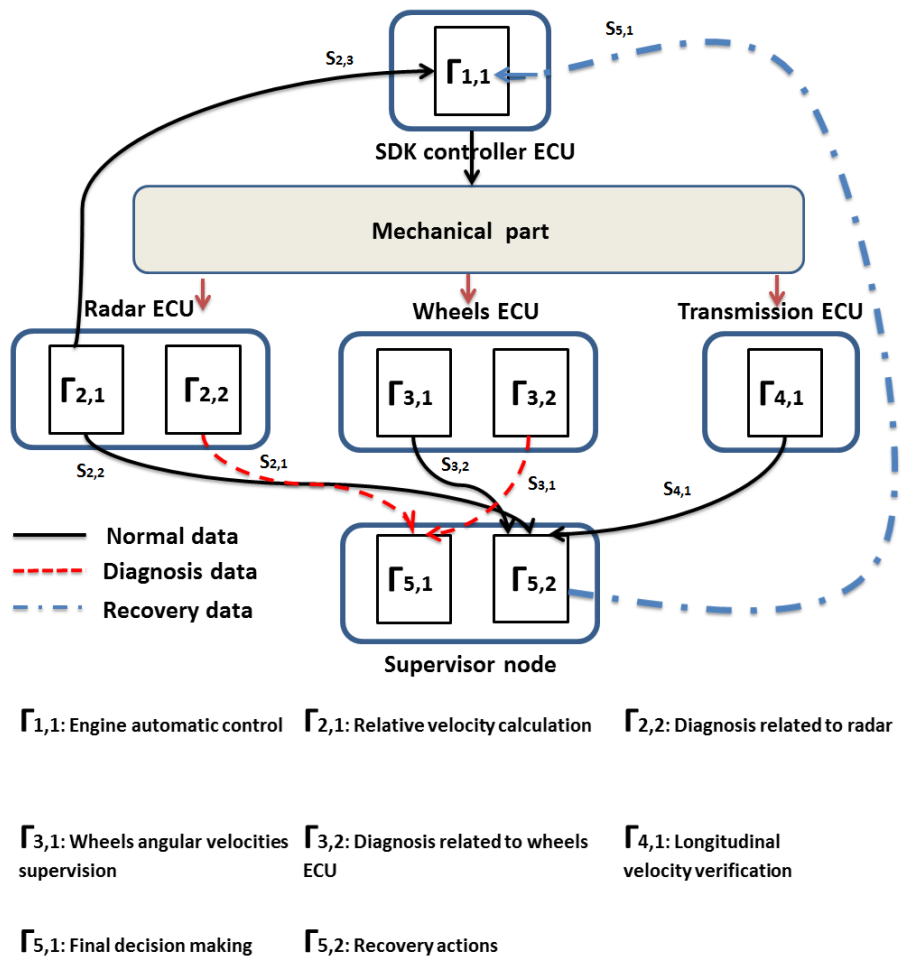


Figure 5.9: SDK data flows.

- $\varphi_1 = \{\Gamma_{5,2} + S_{5,1} + \Gamma_{1,1}\}$ is the data flow devoted to transfer recovery information and enabling/disabling the drive assistance based on the SDK controller decisions.
- $\varphi_2 = \{\Gamma_{2,2} + S_{2,1} + \Gamma_{5,1}\}$ is exclusively responsible for transferring the diagnosis results of the radar device towards the supervisor.
- $\varphi_3 = \{\Gamma_{3,2} + S_{3,1} + \Gamma_{5,1}\}$ is in charge of providing the supervisor by the local diagnosis outcomes generated by the wheels' ECU.
- $\varphi_4 = \{\Gamma_{2,1} + S_{2,2} + \Gamma_{5,2}\}$ is the data flow that delivers the truck longitudinal velocity calculated in run-time by the radar to the supervisor node.
- $\varphi_5 = \{\Gamma_{2,1} + S_{2,3} + \Gamma_{1,1}\}$ provides the SDK controller with the truck longitudinal velocity calculated by the radar.
- $\varphi_6 = \{\Gamma_{3,1} + S_{3,2} + \Gamma_{5,2}\}$ is the data flow that informs the supervisor node by the truck longitudinal velocity calculated by the wheels controller.
- $\varphi_7 = \{\Gamma_{4,1} + S_{4,1} + \Gamma_{5,2}\}$ provides the supervisor with the truck longitudinal speed, which is estimated by the transmission block.

The priority of each message is assigned relatively to how much crucial is its content for the SDK operation and the truck safety. The message priorities are attributed in the following order:

- Messages issued from the supervisor to carry out the recovery process in case of fault occurrence. In view to their importance in enabling/disabling the whole process, these messages have the highest priority-level.
- Messages issued from the radar diagnosis task, since faulty radar measurements will lead the SDK to make wrong and dangerous decisions.
- The diagnosis messages including reports of the wheels and the transmission block controllers.
- The rest of messages are assumed to have the same priority value.

Otherwise, the scheduling policy, which is adopted to define priorities attributed to every task from the SDK nodes, can be found in [10]. It optimizes the schedule by giving the priority for tasks of shortest execution time to diminish the waiting queue. It also takes in account each task relevance and its critical role in ensuring the vehicle safety.

5.2.4/ EXPERIMENTAL CONDITIONS AND EMULATION ENVIRONMENT

To validate the proposed RTA methodology, experiments are tackled in the sequel. Evidently, it is not trivial to carry on the experimental work on real automotive embedded systems in regard to its high cost. The use of the HIL plants to verify behavioral aspects of automotive components has become a conventional phase from the development life cycle of any industrial automotive product [323]. The HIL test is dedicated to construct high fidelity prototypes by interconnecting models of several nodes with real implementation of other nodes. A concrete physical interaction between the simulated components and real automotive sub-entities is generally established through a real communication middleware. It enables the deployment of many executable codes with the possibility to modify some specifications and to test particular behavioral aspects.

At first, the code of the supervisor node, which coordinates between the local diagnosis functions, was implemented on a real electronic board. Afterwards, a CAN-based HIL experimental platform is realized to enable the communication between the trustworthy industrial model of the SDK system and the real supervisor. It is worth mentioning that the truck mechanical behavior and the vehicle dynamics are virtually simulated by the employed model. This model has recourse to physic laws to simulate with high fidelity the evolution of the truck dynamics.

Indeed, the realized HIL test includes two real on-chip CAN nodes that exchange data via a CAN bus. The first electronic board is connected to the computer that runs the simulation of the SDK controller, the Wheels ECU, the Transmission block and the radar. Hence, the first electronic node is responsible for the transmission/reception of messages towards/from the second electronic board that represent the supervisor. Aside from the standard messages broadcasted over CAN, the undertaken test over the HIL plant is based on the injection of several faults that affect the simulated components. At each event, a diagnosis message is triggered. After that, a series of message streams are provoked with accordance to the supervisor decision. Apart from monitoring the whole

SDK system, the supervisor electronic board is linked to a HMI to keep the truck driver up-to-date with the occurring events and informed by any emergency. To proceed the experiments, the HMI is executed on a second computer.

In technical terms, the constructed HIL is composed from two ARM Cortex-M4 electronic boards. The data transmission/reception between both nodes through the CAN protocol is enabled physically through the *SN65HVD230* transceivers. For all the realized test scenarios, the bit rate of the CAN bus was fixed at 500 Kbit/s . Besides, all the messages without exception are of 11 bits *ID*. Otherwise, the connection between each computer with its corresponding electronic board is established based on an Universal Synchronous/Asynchronous Receiver/Transmitter (USART) communication in order to avoid the usage of expensive CAN-bus emulation software. Finally, Figure 5.10 shows the overall experimental HIL platform layout.

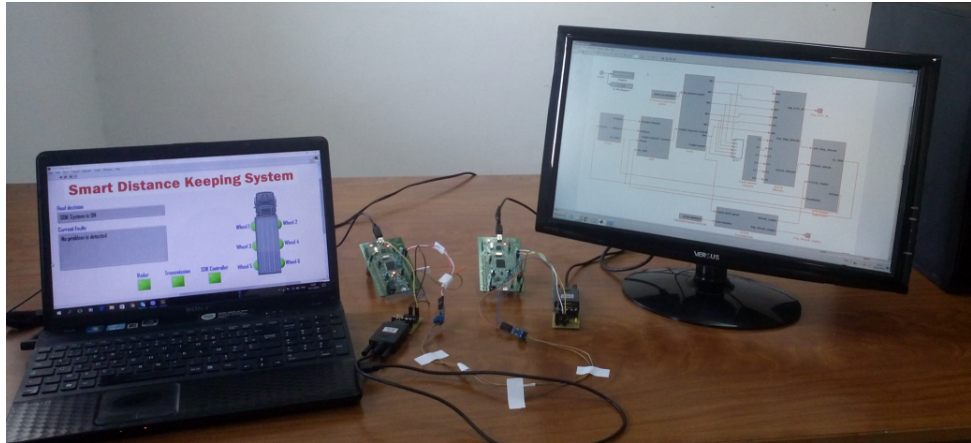


Figure 5.10: HIL platform for realistic experimentations.

In the present case of study, it is very difficult to present complete and precise results due to the industrial property restrictions. However, testes are tackled by triggering message streams after injecting faults in different components from the SDK system. This direction highlights the utility of utilizing the proposed RTA algorithm in the benefit of IV safety verification. Without any doubt, the navigation system is prone to fatal risks in case of important delays in the transmission of diagnosis messages, which are assumed to handle situations of critical failures. In addition, the focus on latency characterization of the diagnosis messages facilitates the interpretation of the experimental results. In contrast to the rest of standard streams, diagnosis messages are event-triggered elements. Hence, increasing the number of injected faults, raises systematically the number of the initiated messages. Consequently the CAN traffic flow is appraised. The more overloaded the CAN bus, the more latency may occur, which permits to conduct test under more critical situations. Finally, both the theoretical as well as the practical results are provided within the realized scenarios to prove the efficiency of the proposed RTA-based approach.

The theoretical minimum and maximum response times of elements in flows φ_1 , φ_2 and φ_3 (flows related to diagnosis and recovery messages) are presented in Tables 5.2, 5.3 and 5.4.

In order to validate the theoretically derived results, the HIL-based experiments are carried out within distinct scenarios of fault injection. For each undertaken scenario, a par-

Table 5.2: Minimum and maximum response times of elements in flow φ_1

Elements in flow φ_1	Minimum response time (ms)	Maximum response time (ms)
$\Gamma_{5,2}$	6.4	7
$S_{5,1}$	0.24	0.36
$\Gamma_{1,1}$	10.2	11
Total (ms)	16.84	18.36

Table 5.3: Minimum and maximum response times of elements in flow φ_2

Elements in flow φ_2	Minimum response time (ms)	Maximum response time (ms)
$\Gamma_{2,2}$	6.6	7
$S_{2,1}$	0.21	0.52
$\Gamma_{5,1}$	9.3	10
Total (ms)	16.11	17.52

Table 5.4: Minimum and maximum response times of elements in flow φ_3

Elements in flow φ_3	Minimum response time (ms)	Maximum response time (ms)
$\Gamma_{3,2}$	4.7	5
$S_{3,1}$	0.21	0.68
$\Gamma_{5,1}$	9.3	10
Total (ms)	15.68	14.21

ticular number of diagnosis messages is transmitted. In such a manner, the number of injected faults in the predefined following scenarios is gradually raised and so is the data traffic through CAN. As a consequence, the elaborated tests involve diverse cases of interferences between message streams and tasks. For each configuration (fault injection scenario), experiments have been repeated several times to obtain more certain measurements of response times. Table 5.5 illustrates the experimental results of the Mean Response Time (MRT) of every flow (φ_1 , φ_2 and φ_3).

Table 5.5: Experimental results

Scenarios	MRT of φ_1 (ms)	MRT of φ_2 (ms)	MRT of φ_3 (ms)
Scenario 1	18.272	17.141	15.176
Scenario 2	18.281	17.356	15.258
Scenario 3	18.309	17.427	15.409
Scenario 4	18.407	17.549	15.639
Scenario 5	18.456	17.670	15.760

Obviously, there is a great convergence between the theoretically and experimentally derived responses times. The MRTs recorded in the realistic HIL are almost compatible with the min/max thresholds of the timing performances provided via the proposed RTA model. Nevertheless, in few occasions, the HIL-driven results exceed slightly the theoretical maximum response times. Such a behavior is noticed only for scenarios 4 and 5, where the bus-load is huge. The insignificant dissimilarity between results of the HIL platform and the RTA algorithm may be explained by the use of the USART communication as an interface between computers and the electronic boards. Although the delays over

the USART communication are very small, they are frequent. Evidently, the proposed RTA model does not consider the USART-related latencies. The variance in the release jitter delays, which is difficult to set with precision, is another reason for the difference between the estimated periods and experimental measurements. Therefore, the small and occasional violation of the predicted response times does not contradict the RTA efficient role in providing valuable informative support about bounds of the intra-vehicular communication latencies.

It should be mentioned that the number of the SDK components is quite small compared to other commercialized automotive processes. Additionally, the realized RTA proof of concept did not cover the entire automotive embedded system. Even though the delays that may take place into the SDK are important, more considerable latencies would happen in a larger scale automotive system. Accordingly, the RTA results emphasize the need to seriously consider the intra-vehicular communication, especially for safety-critical IV components.

5.3/ CONCLUSION

In this chapter, the link between the high level solutions (uncertainty handling, risk management, etc.) and the low level material issues is established. Due to faults, the error rate in measurements can be enormous. Hence, developing fault-aware navigation architectures is essential to warrant the autonomous vehicles full reliability/safety. In this context, an interval-based diagnosis approach, called Vertices Principle Component Analysis (VPCA), is introduced in this chapter. For many reasons, this latter is suitable for autonomous vehicles. Indeed, the VPCA is a data-driven method permitting to avoid the modeling errors increased by the complexity of modern navigation systems. Further, the use of interval analysis for diagnosis allows to detect faults while considering all possible uncertainty sets. It guarantees a high robustness to uncertainty and false alarms, which is a fundamental requirement for automotive diagnosis. Even more, the VPCA integration into the navigation architecture enhanced its performances. According to the simulation results tackled on an Adaptive Cruise Control (ACC) system, the mutual collaboration between the interval-based uncertainty handling and diagnosis ensured a simultaneous robustness to uncertainties and faults.

The high level software of safety critical mechanisms, such as ACC systems, may suffer also from delayed responses to risks due to latencies in the navigation system material middleware. Thus, decisions made by the vehicle risk management layer should be sufficiently aware about such delays. Accordingly, a simple algorithm based on a Response Time Analysis (RTA) model is introduced to quantify these latencies. Since it provides an interval estimation of delays, the suggested method has a great compatibility with the interval-based navigation frameworks previously proposed in this thesis. A proof of concept of the suggested RTA model is presented via experiments on a Smart distance keeping (SDK) system. Compared to a regular ACC, the SDK delivers additional assistance services for truck drivers. Due to its multiples functionalities, the data exchange inside the SDK is important, which emphasize the need for the RTA. The realized experiments proved the proposed RTA efficiency in delivering precise estimation of minimum/maximum intra-communication delays.

GENERAL CONCLUSION AND FUTURE WORK

GENERAL CONCLUSION

All along this Ph.D manuscript, several contributions dealing with autonomous navigation have been proposed. Increasing the navigation system reliability and respectively the in-road safety is the real reason standing behind the employment of the interval analysis. Thus, in an attempt to compensate the navigation information inaccuracy, data is turned into interval sets. Oppositely to the most of the set-membership approaches, the transformation of data to sets (intervals in this context) is not build based on arbitrarily predefined hypothesizes. Instead, a logic causality link between the measurement circumstances and the uncertainty distribution is established. Even more, the statistical properties of the navigation system dynamics are exploited in the aim of mastering in a better way the uncertainty-induced risks. In particular, the existing correlation between the navigation system variables are characterized. The use of the correlation is an intelligent and time-efficient practice to characterize systems' features without important modeling efforts. This direction, which joins the interval analysis-based modeling and the correlation analysis for interval variables, is exploited in this thesis in different use-cases. It contributed to develop reliability-increased risk management schema for distinct navigation scenarios (waypoint reaching and car-following scenarios) as well as a highly fault-sensitive diagnosis for Intelligent Vehicles (IVs).

The first part of this thesis was devoted to examine the autonomous/intelligent navigation-related literature. Chapter 1 had as ultimate objective to reveal the real factors standing behind the IV reliability and safety. According to the state-of-the-art analysis, flexibility, robustness to faults and especially the capacity to predict an important part of the uncertainty potential behaviors are among these factors. More precisely, strengths and weaknesses of the existing navigation approaches as well as the current trends in the development of vehicular risk management layers were reviewed. As a main conclusion from the state-of-the-art analysis, the use of the interval analysis for IVs was judged as very promising relatively to its capacity to enclose all possible trajectories of uncertainty evolution.

Accordingly, chapter 2 was dedicated to explore more details about the interval arithmetic properties. More interestingly, the interval-based engineering practices are overseen in the depth. The scope of the reviewed practices covers the interval-based modeling as well as the interval-based statistical data-analysis. The efforts spent in the research community to enhance both of these practices were highlighted. It has been concluded that the interval-based modeling may carefully consider all possible variation in the model parameters. The interval-based data analysis was found relevant to obtain uncertainty-

aware statics and more confident interpretation of data distribution. In addition, as a major drawback of the interval arithmetic, origins of the interval-based computation pessimism have been discussed.

In the second part, the rest of chapters have been dedicated to explain the different contributions of this thesis. These latter aim to meet the autonomous navigation safety requirements outpointed in the first part of this work.

Chapter 3 proposed a novel risk management strategy for autonomous navigation. This latter improves an already proposed flexible Navigation Strategy based on Sequential Waypoint Reaching (NSbSWR) framework, while taking into account explicitly the different uncertainties in modelling and/or perception that may endanger the navigation safety. NSbSWR is an emergent concept that avoids frequent complex trajectories' planning/replanning. The main contribution of this chapter is to introduce the reachability analysis scheme as a main component from the proposed online risk assessment and management technique to ensure safe autonomous navigation between assigned waypoints. The interval analysis is employed to propagate uncertainties influencing the vehicle's dynamics into the navigation system states. By solving an Ordinary Differential Equation (ODE) with uncertain variables and parameters via an interval Taylor series expansion method, all the vehicle's potential trajectories are revealed. Further, a passive characterization of the correlation that relates the navigation process variables is proceeded in order to eliminate the interval computation conservatism. According to the worst-case analysis of the obtained sharp bounds of the reachable sets, a decision about the navigation safety is made and an appropriate adaptive navigation is performed. The control parameters are tuned in order to lead the navigation system to a collision-free reachable space. The simulations results proved the safety, efficiency and robustness of the overall proposed NSbSWR under uncertainties.

In chapter 4, a novel set-membership/stochastic Time-To-Collision (TTC)-based risk management is suggested to monitor Adaptive Cruise Control (ACC). The application of this latter is suitable for any car-following navigation scenario. The interval analysis has dealt with various uncertainties and latencies threatening navigation safety. Once again, the uncertainty evolution was characterized through the correlation that relates the system states variables. Correspondingly, uncertainty amounts attributed to each measurement, calculated per interval, have been diminished to avoid any undesirable change in the appropriate progression of correlation. The simulation results proved that models, elaborated via interval-based modeling joined with the correlation analysis, can substitute more complex models. It compensates efficiently the modeling errors. Hence, simplifications can be adopted to reduce the risk management computational demands while maintaining an extreme accuracy of outcomes. Furthermore, to provide an appropriate correlation assessment for interval variables, a suitable statistical process was introduced to characterize the historical properties of the navigation system. It includes an outlier rejection technique to avoid the misleading results of the correlation analysis. To better ensure a safe spacing between vehicles, the interval results are merged with (Extended Kalman Filter) EKF findings. In this context, an adaptive algorithm is developed based on a confidence weighting methodology. In such a way, the EKF approach inaccuracy is compensated and the pessimism of the proposed interval-based safety verification layout is decreased. The combined risk management is integrated into the ACC architecture. The simulation results proved this proposition efficiency in handling uncertainties and ensuring safer traffic flow.

Finally, chapter 5 presented two major contributions. First, an interval-based extension for the Principle Component Analysis (PCA) diagnosis method is applied to monitor an ACC. The main particularity from this extension performances is its sensitivity to faults. Also, it is convenient for complicated processes, since it skips the system modeling and relies only on statics. Not only faults can be detected in run-time, but also the failure source is located to facilitate future maintenance procedures. Moreover, the depicted interval-based diagnosis is entirely compatible with the previously proposed risk management solutions. The mutual operation of the interval-based diagnosis and uncertainty handling approaches permits to efficiently distinguish between uncertainties and faults. Chapter 5 also focalized the light on methods permitting to quantify in a methodological manner the delays of data propagation through the IV embedded system. The proposed approach delivers the minimum/maximum possible end-to-end latency of in-vehicular messages. For this reason, the results are very useful to easily make the risk management and the safety critical layers for general IV architectures aware of the communication delays.

PERSPECTIVES AND FUTURE WORK

The different contributions, which are performed in this thesis, may introduce a full interval-based navigation framework. An architecture of this latter has to include different layers, such as uncertainty characterization, risk assessment/management, reachability analysis, diagnosis, etc. Nonetheless, the proposed set-membership risk management solutions should be also applied for more critical maneuvers such as lane changes. The formalization of the interval-based TTC should be extended to cover situation of overtaking vehicles. Besides, obstacle avoidance strategies should be joined to the proposed navigation approaches. Accordingly, the different suggested IV architectures in this thesis may be upgraded to an interval-based multi-controller navigation framework as explained in Figure 6.1. Thanks to its different layers of guaranteed performances, this multi-controller navigation framework would have important capacities in overstepping any potential risk. Not only a high robustness to uncertainty is locally acquired by the IV components due to interval analysis, but also holistic advantages are attained at the global architectural scale. The use of guaranteed approaches to handle uncertainties leads more importantly to a more reliable switch between the IV architecture elementary behaviors (cf. Figure 6.1). Evidently, the IV safety depends on the appropriate management of the interaction between the navigation behaviors. With great capacities in mastering uncertainties and faults, undesired jerking or discontinuities in the system performances are avoided.

Regarding the proposed reachability scheme, it should be enhanced by means of more efficient and automatic adaptive tuning for the control parameters in order to ensure a quick and optimal re-shaping for the vehicle reachable space. Otherwise, the Vertices Principle Component Analysis (VPCA) method can be further improved to enhance more efficiently the IVs reliability. As stated, the VPCA detects and locates faults thanks to the analysis of dependencies relating the system states variables. According to this understanding, valuable recovery data can be extracted through these dependencies in the case of faults occurrence to substitute the affected data by the estimated ones. In such a manner, the recovery data might be useful to avoid aborting the navigation task in case of fault occurrence. It is possible then to carry on the navigation until the next maintenance procedure. In addition, the VPCA should be integrated in a manner permitting to provide

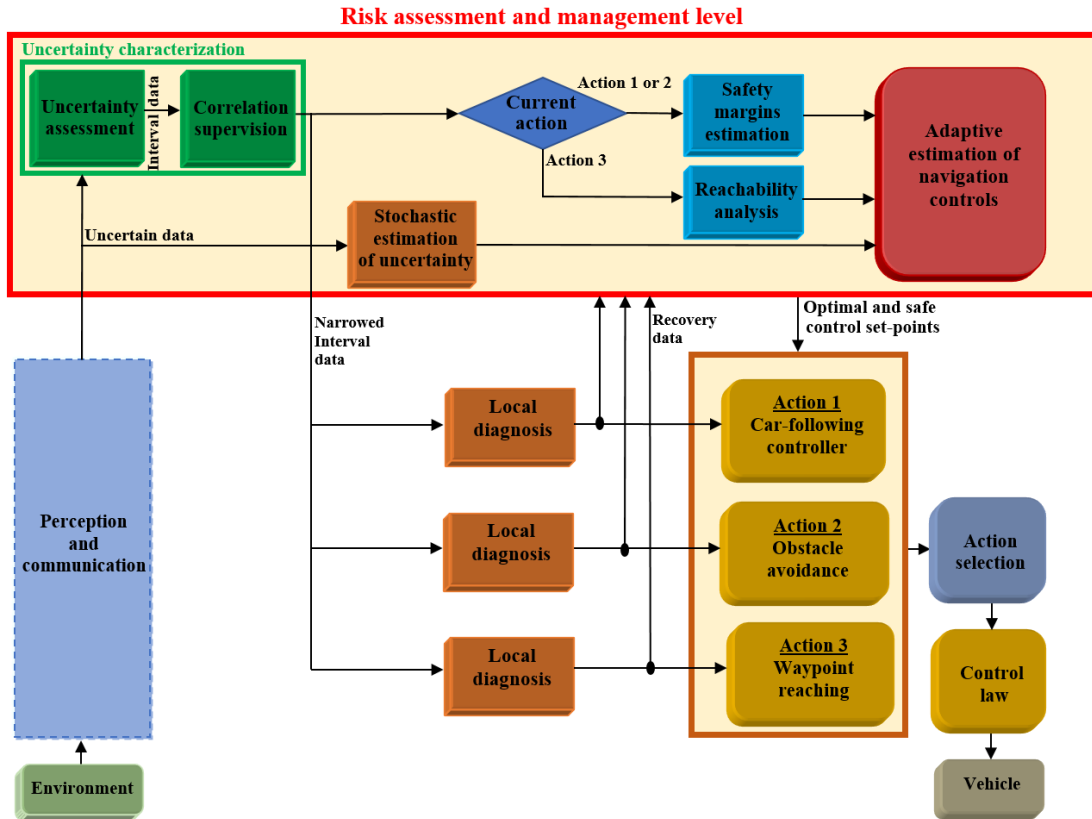


Figure 6.1: Overall view of interval-based reasoning for risk assessment and management of multi-control architecture.

local diagnosis for every controller from the IV interval-based multi-controller architecture. Most of the proposed approaches were validated through an extensive simulation work. Accordingly, the suggested set-membership risk management methods should be integrated in near future on a real vehicle. On the one hand, this step should be tackled according to some engineering practices that includes several overlapping issues, such as reliable implementation of Software components and functional safety of automotive operating systems. On the other hand, the integration of several blocks that perform interval-based computation into real navigation architectures is challenging. Indeed, additional efforts are needed to pick up the appropriate computation packages while dealing carefully with the interval arithmetic issued computational complexity. An interesting target for this implementation work is the VIPALAB (for Véhicule Individuel Public et Autonome) autonomous vehicles, which are provided by the APOJEE company and available in the PAVIN framework (for Plate-forme d'Auvergne pour Véhicules INtelligents) of the Institut Pascal laboratory.



ANNEXES

A

STABILITY PROOF OF CONTROL LAW FOR STATIC/DYNAMIC TARGET REACHING

All the navigation architectures proposed in this thesis use the same control law (cf. subsection 3.1.1). The full demonstration of this controller asymptotic stability, basically presented in [297], is summarized in this appendix. This demonstration is of utmost importance to prove the navigation stability, even within changes in the control parameter K_θ for risk management purposes (cf. section 3.4).

The stability proof of the adopted control law (cf. equations (3.9) and (3.10)) stems from the analysis of the error parameters (e_x , e_y , e_θ) and e_{VT} (cf. equations (3.4) and (3.7)) [297]. By proving the stability of the derivatives of these errors, the control law stability is approved. It is apparent from equations (3.1), (3.2), (3.5), (3.6) that the different derivatives of the aforementioned errors can be expressed as:

$$\begin{aligned}\dot{e}_x &= \cos(\theta_V)(\dot{x}_T - \dot{x}_V) + \sin(\theta_V)(\dot{y}_T - \dot{y}_V) - \sin(\theta_V)(x_T - x_V)\dot{\theta}_V + \cos(\theta_V)(y_T - y_V)\dot{\theta}_V \\ &= -V + e_y\dot{\theta}_V + V_T[\cos(\theta_T)\cos(\theta_V) + \sin(\theta_T)\sin(\theta_V)] \\ &= -V + e_yV\tan(\gamma_V)l_b^{-1} + V_T\cos(e_\theta)\end{aligned}\tag{A.1}$$

$$\begin{aligned}\dot{e}_y &= -\sin(\theta_V)(\dot{x}_T - \dot{x}_V) + \cos(\theta_V)(\dot{y}_T - \dot{y}_V) - \cos(\theta_V)(x_T - x_V)\dot{\theta}_V - \sin(\theta_V)(y_T - y_V)\dot{\theta}_V \\ &= -e_x\dot{\theta}_V - V_T\cos(\theta_T)\sin(\theta_V) + V_T\sin(\theta_T)\cos(\theta_V) \\ &= -e_xV\tan(\gamma_V)l_b^{-1} + V_T\sin(e_\theta)\end{aligned}\tag{A.2}$$

$$\begin{aligned}\dot{e}_\theta &= \dot{\theta}_T - \dot{\theta} \\ &= \omega_T - V\tan(\gamma_V)l_b^{-1} \\ &= \frac{V_T}{r_{ct}} - V\tan(\gamma_V)l_b^{-1}\end{aligned}\tag{A.3}$$

$$\begin{aligned}\dot{e}_{VT} &= \dot{\theta}_T - \dot{\theta}_{VT} \\ &= \frac{V_T}{r_{ct}} - \frac{d}{dt} \left[\arctan \left(\frac{y_T - y_V}{x_T - x_V} \right) \right] \\ &= \frac{V_T}{r_{ct}} - V_T \frac{\sin(\theta_T)(x_T - x_V) - \cos(\theta_T)(y_T - y_V)}{d^2} \\ &\quad - \frac{-V\sin(\theta)(x_T - x_V) + V\cos(\theta)(y_T - y_V)}{d^2} \\ &= \frac{V_T}{r_{ct}} - \frac{V_T e_x \sin(e_\theta)}{d^2} + \frac{V_T e_y \cos(e_\theta)}{d^2} - \frac{e_y V}{d^2}\end{aligned}\tag{A.4}$$

To pursue the proof of stability, it will be assumed henceforward that the target is in front of the vehicle (in regard to its orientation). This assumption implies the following initial conditions related to e_{VT} and e_θ :

$$e_{VT} \in]-\pi/2, \pi/2[\quad \text{and} \quad e_\theta \in]-\pi/2, \pi/2[\quad (\text{A.5})$$

In the sequel, it will be proved that equations (3.9) and (3.10) ensure always the asymptotic stability of the differential errors (\dot{e}_x , \dot{e}_y , \dot{e}_θ , \dot{e}_{VT}), as long as equation (A.5) is satisfied. To this end, a Lyapunov-driven analysis is proceeded [161].

Proof. *In order to demonstrate the proposed control stability based on a Lyapunov method, let consider the following candidate Lyapunov function V_L :*

$$\begin{aligned} V_L &= \frac{1}{2}K_d d^2 + \frac{1}{2}K_l d_l^2 + K_o [1 - \cos(e_\theta)] \\ &= \frac{1}{2}K_d d^2 + \frac{1}{2}K_l d^2 \sin^2(e_{VT}) + K_o [1 - \cos(e_\theta)] \end{aligned} \quad (\text{A.6})$$

As clear from equation (A.6), the suggested V_L function depends only on the evolution of the subsequent parameters:

- The error e_θ between the vehicle and target orientations (cf. equation 3.4).
- The distance d between the target and the vehicle (cf. equation 3.5).
- The distance d_l from the vehicle position to the target line. This latter consists of the line that passes from the target with the same orientation of the target θ_T (cf. Figure A.1). Indeed, d_l is explicitly linked to the line of flight and sight associated to a given target.

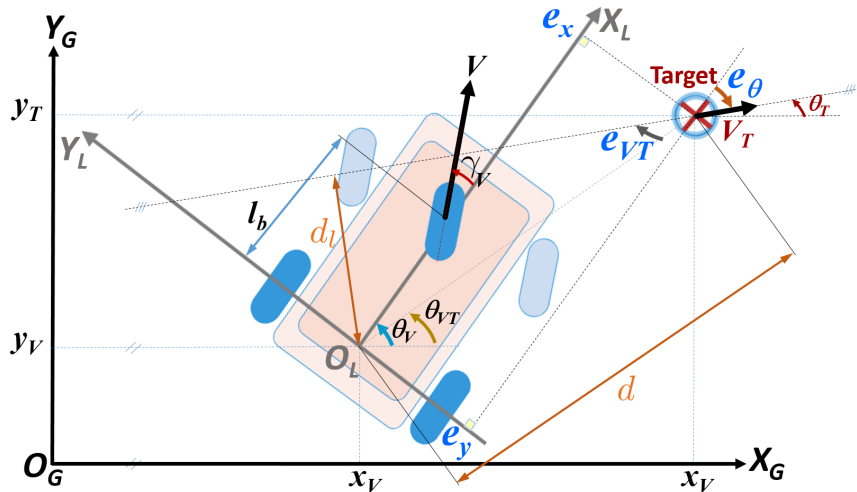


Figure A.1: Vehicle/target parameters used for control law proof of stability.

It is important to outline that the candidate Lyapunov function V_L is positive-definite as far as the assumed initial conditions, given by equation (A.5), hold true [161]. V_L can be expressed also as a function of e_x and e_y as follows:

$$V_L = \frac{1}{2} (e_x^2 + e_y^2) [K_d + K_l \sin^2(e_{VT})] + K_o [1 - \cos(e_\theta)] \quad (\text{A.7})$$

To warrant the system stability, \dot{V}_L must be imperatively negative-definite [161]. Through the derivative of equation (A.7) and thanks to equations (B.9), (B.10), (A.3), (A.4), (3.9) and (3.10), the following expression of \dot{V}_L is obtained:

$$\begin{aligned} \dot{V}_L &= (e_x \dot{e}_x + e_y \dot{e}_y) [K_d + K_l \sin^2(e_{VT})] + K_l d^2 \sin(e_{VT}) \cos(e_{VT}) \dot{e}_{VT} + K_o \sin(e_\theta) \dot{e}_\theta \\ &= (e_x [e_y V c_c - V + V_T \cos(e_\theta)] + e_y [V_T \sin(e_\theta) - e_x V c_c]) [K_d + K_l \sin^2(e_{VT})] \\ &\quad + K_l d^2 \sin(e_{VT}) \cos(e_{VT}) \left[\frac{V_T}{r_{ct}} - \frac{V_T e_x \sin(e_\theta)}{d^2} + \frac{V_T e_y \cos(e_\theta)}{d^2} - \frac{e_y V}{d^2} \right] \\ &\quad + K_o \sin(e_\theta) \left(\frac{V_T}{r_{ct}} - V c_c \right) \end{aligned} \quad (\text{A.8})$$

Then, the substitution of equation (3.9) in (A.8) yields:

$$\begin{aligned} \dot{V}_L &= [-e_x v_b + V_T e_y \sin(e_\theta)] [K_d + K_l \sin^2(e_{VT})] + K_o \sin(e_\theta) \left[\frac{V_T}{r_{ct}} - V_T \cos(e_\theta) c_c - v_b c_c \right] \\ &\quad + K_l \sin(e_{VT}) \cos(e_{VT}) \left[d^2 \frac{V_T}{r_{ct}} - V_T e_x \sin(e_\theta) - e_y v_b \right] \\ &= [e_y (K_d + K_l \sin^2(e_{VT})) - e_x K_l \sin(e_{VT}) \cos(e_{VT})] V_T \sin(e_\theta) \\ &\quad + \frac{V_T}{r_{ct}} [d^2 K_l \sin(e_{VT}) \cos(e_{VT}) + K_o \sin(e_\theta)] - V_T K_o \sin(e_\theta) \cos(e_\theta) c_c \\ &\quad - v_b [e_x (K_d + K_l \sin^2(e_{VT}))] - v_b [e_y K_l \sin(e_{VT}) \cos(e_{VT}) + K_o \sin(e_\theta) c_c] \end{aligned} \quad (\text{A.9})$$

Afterwards, equation (A.10) may be derived directly by inserting equation (3.8) in the first and last terms of equation (A.9) and factorizing the common terms:

$$\begin{aligned} \dot{V}_L &= V_T \sin(e_\theta) [K_d e_y - K_l d \sin(e_{VT}) \cos(e_\theta)] + \frac{V_T}{r_{ct}} [d^2 K_l \sin(e_{VT}) \cos(e_{VT}) + K_o \sin(e_\theta)] \\ &\quad - v_b [K_d e_x + K_l d \sin(e_{VT}) \sin(e_\theta) + K_o \sin(e_\theta) c_c] - V_T K_o \sin(e_\theta) \cos(e_\theta) c_c \end{aligned} \quad (\text{A.10})$$

Lastly, let substitute equations (3.11) and (3.12) in (A.10). It holds that:

$$\begin{aligned} \dot{V}_L &= -K_x [K_d e_x + K_l d \sin(e_{VT}) \sin(e_\theta) + K_o \sin(e_\theta) c_c]^2 \\ &\quad - V_T K_o K_\theta \sin^2(e_\theta) - V_T K_o K_{VT} \sin^2(e_{VT}) \leq 0 \end{aligned} \quad (\text{A.11})$$

Based on equation (A.11), the studied system is definitely stable under the condition that equation (A.5) holds true. \dot{V}_L needs to be negative-definite in order to ensure the asymptotic stability of the proposed control law (cf. equations (3.9) and (3.10)). Hence, let consider the two distinct following cases:

- The first case is when $\dot{V}_L = 0$ and $V_T > \xi$. Since $K > 0$, it is apparent that e_x , e_θ , e_{VT} are equal to zero to satisfy equation (A.11). Accordingly, based on equations (3.6), (3.7) and (A.5), d shall be equal to zero ($e_x = e_y = 0$). Hence, $\dot{V}_L = 0$ when $V_T > \xi$ so long as $(e_x, e_y, e_\theta) = (0, 0, 0)$.

- The second case is when $V_T = \xi$ (ξ represents a constant ($\xi \approx 0$)). The initial assumption is identical. Thus, the second and third terms of equation (A.11) are equal to zero whereas $V_T = \xi$. Besides, $r_{ct} \rightarrow \infty$ in that case where $V_T = \xi$ (quasi-static case) (cf. Subsection 3.1.1). As a result, the first term of \dot{V}_L is equal to zero whenever:

$$K_d e_x + K_l d \sin(e_{VT}) \sin(e_\theta) + K_o \sin(e_\theta) c_c = 0 \quad (\text{A.12})$$

Substituting equation (3.12) with $r_{ct} \rightarrow \infty$ in equation (A.12), the expression given by equation is A.13 derived:

$$\begin{aligned} 0 &= K_d e_x + K_l d \sin(e_{VT}) \sin(e_\theta) + \tan(e_\theta) [K_d e_y - K_l d \sin(e_{VT}) \cos(e_\theta)] \\ &\quad + K_o \sin(e_\theta) \left[K_\theta \tan(e_\theta) + \frac{K_{VT} \sin^2(e_{VT})}{\sin(e_\theta) \cos(e_\theta)} \right] \\ &= K_d [e_x + e_y \tan(e_\theta)] + K_o K_\theta \frac{\sin^2(e_\theta)}{\cos(e_\theta)} + K_o K_{VT} \frac{\sin^2(e_{VT})}{\cos(e_\theta)} \end{aligned} \quad (\text{A.13})$$

Further, the use of equation (3.8) in (A.13) implies that:

$$K_d d \frac{\cos(e_{VT})}{\cos(e_\theta)} + K_o K_\theta \frac{\sin^2(e_\theta)}{\cos(e_\theta)} + K_o K_{VT} \frac{\sin^2(e_{VT})}{\cos(e_\theta)} = 0 \quad (\text{A.14})$$

As obvious, equation (A.14) consists of quadratic terms. Therefore, by taking into consideration conditions exhibited in equation (A.5), $\cos(e_{VT})$ and $\cos(e_\theta)$ are both strictly positive. Consequently, all the terms depicted in equation (A.14) are positives. These latter have also to be equal to zero ($d, e_\theta, e_{VT} = 0$, and if $d = 0$ then $e_x, e_y = 0$). Hence, from equation (A.14), \dot{V}_L is equal to zero when $V_T = \xi$ and $r_{ct} \rightarrow \infty$, on the assumption that $(e_x, e_y, e_\theta) = (0, 0, 0)$.

To summarize, whether $V_T > \xi$ or $V_T = \xi$, V_L is regularly strictly positive. Similarly, \dot{V}_L is always strictly negative while $(e_x, e_y, e_\theta) \neq (0, 0, 0)$. For this reason, it may be affirmed that the system is asymptotically stable given that the assumed initial conditions of the vehicle (see equation (A.5)) are valid [297].

B

ANALYTICAL GUARANTEES FOR SAFE TARGET REACHING

This appendix presents a brief reminder about the analytical analysis depicted in [297]. It permits the definition of the boundary errors when the navigation system is in the proximity of the target to reach according to the Navigation Strategy based on Sequential Waypoint Reaching (NSbSWR) (cf. subsection 3.1). This issue is essential to select the convenient next target, which may be accurately reached by the vehicle.

The analysis in this Appendix aims to determine appropriately the distance d_i , which refers to a minimum initial separation distance between the vehicle and the assigned target. The desired d_i should simultaneously satisfy the vehicle physical constraints and the navigation errors (d and e_θ) at the instant when the vehicle reaches its assigned target. In other words, a target safe reaching is ensured thanks to a set of established analytical relations between the control parameter \mathbf{K} and the waypoint disposition. For a better understanding of the proposed analytical approach, errors related to e_θ and respectively d are separately studied in the sequel. Let consider t_f the waypoint reaching instant. Mainly, d_i should be chosen long enough to ensure that $(d(t_f) \leq E_d \text{ and } e_\theta(t_f) \leq E_{angle})$.

On the one hand, a sufficient distance d_i must be retained to ensure the monotonous convergence of e_θ to zero. It allows the estimation of the minimum time t_f to fulfil: $e_\theta \leq E_{angle}$. The main idea behind the upcoming analysis is to address the most critical configuration $|e_{\theta_i}| = \pi/2 - \zeta$ (ζ is a positive value ≈ 0). In this situation, the vehicle has initially the maximum possible orientation error relatively to the target i.e., the slowest rate of error convergence. Later, results of less critical configuration $|e_{\theta_0}| \ll \pi/2$ can be interpreted, since the convergence of e_θ is certainly more quick than the studied worst case ($|e_{\theta_i}| \rightarrow \pi/2$). Accordingly, \dot{e}_θ is expressed through equations (3.1)-(3.3) as:

$$\begin{aligned}\dot{e}_\theta &= \dot{\theta}_T - \dot{\theta}_V \\ &= \frac{V_T}{r_{c_T}} - v \frac{\tan(\gamma_V)}{l_b}\end{aligned}\tag{B.1}$$

Then, by substituting equations (3.9)-(3.11) in (B.1):

$$\begin{aligned}\dot{e}_\theta &= - \left[\frac{K_x K_d d}{\cos(e_\theta)} + K_x K_o K_\theta \frac{\sin^2(e_\theta)}{\cos(e_\theta)} \right] \\ &\quad \cdot \left[\frac{K_d e_y}{K_o \cos(e_\theta)} + K_\theta \tan(e_\theta) \right] \\ &= - \frac{K_x (K_d d + K_o K_\theta)}{K_o \cos^2(e_\theta)} \left[K_d d + K_o K_\theta \sin^2(e_\theta) \right] \sin(e_\theta)\end{aligned}\tag{B.2}$$

In order to solve the obtained differential equation (B.2) in a simplistic way, the subsequent notations are adopted:

$$a_1 = K_d d; \quad a_2 = K_o K_\theta; \quad a_3 = \sqrt{(a_1 a_2^{-1} + 1)} \quad (B.3)$$

Hence, the analytic solution of equation (B.2) is written as:

$$\ln \left[\tan \left(\frac{e_\theta}{2} \right) \left(\frac{a_3 + \cos(e_\theta)}{a_3 - \cos(e_\theta)} \right)^{a_3/2} \right]_{e_{\theta_i}}^{e_\theta} = - \frac{K_x a_1 a_2}{K_o} a_3^2 t \Big|_0^t \quad (B.4)$$

Since the objective at this stage is to estimate the necessary time t_f to have an error $e_\theta \leq E_{angle}$, equation (B.4) is represented as:

$$e_\theta = F_\theta(t, \mathbf{K}, e_{\theta_i}) \quad (B.5)$$

where:

$$F_\theta = 2 \tan \left(\frac{e_{\theta_i}}{2} \right) \left[\frac{(a_3 + \cos(e_{\theta_i}))(a_3 - 1)}{(a_3 - \cos(e_{\theta_i}))(a_3 + 1)} \right]^{a_3/2} e^{-\frac{K_x a_1 a_2}{K_o} a_3^2 t} \quad (B.6)$$

F_θ allows to extrapolate e_θ evolution when ($d \ll d_i$) at t_f . Consequently, the required t_f to reach $e_\theta = E_{angle}$ is extracted:

$$t_f = F_\theta^{-1}(E_{angle}, \mathbf{K}, e_{\theta_i}) \quad (B.7)$$

Eventually, the obtained t_f serves then to find out a suitable d_i . Indeed, for all configurations where $e_{\theta_i}, e_{VT_i} < \pi/2$, the maximum distance d_i allowing to reach the target is obtained by setting $e_{VT} = 0$ and $e_\theta = 0$ (straight line to the target). Accordingly, equation (3.11) can be formulated as:

$$v_b = K_x K_d d \quad (B.8)$$

Note that through equations (3.1)-(3.6) \dot{e}_x and \dot{e}_y are written as:

$$\begin{aligned} \dot{e}_x &= \cos(\theta_V)(\dot{x}_T - \dot{x}_V) + \sin(\theta_V)(\dot{y}_T - \dot{y}_V) \\ &\quad - \sin(\theta_V)(x_T - x_V)\dot{\theta}_V + \cos(\theta_V)(y_T - y_V)\dot{\theta}_V \\ &= -V + e_y \dot{\theta}_V + V_T [\cos(\theta_T) \cos(\theta_V) + \sin(\theta_T) \sin(\theta_V)] \\ &= -V + e_y V \tan(\gamma_V) l_b^{-1} + V_T \cos(e_\theta) \end{aligned} \quad (B.9)$$

$$\begin{aligned} \dot{e}_y &= -\sin(\theta_V)(\dot{x}_T - \dot{x}_V) + \cos(\theta_V)(\dot{y}_T - \dot{y}_V) \\ &\quad - \cos(\theta_V)(x_T - x_V)\dot{\theta}_V - \sin(\theta_V)(y_T - y_V)\dot{\theta}_V \\ &= -e_x \dot{\theta}_V - V_T \cos(\theta_T) \sin(\theta_V) + V_T \sin(\theta_T) \cos(\theta_V) \\ &= -e_x V \tan(\gamma_V) l_b^{-1} + V_T \sin(e_\theta) \end{aligned} \quad (B.10)$$

Then, \dot{d} is deduced by joining equations (3.11) and (B.8)-(B.10):

$$\dot{d} = \frac{e_x \dot{e}_x + e_y \dot{e}_y}{d} = -\frac{e_x v_b}{d} = -K_x K_d d \quad (B.11)$$

By a simple integration of equation (B.11), it appears that:

$$\int_{d_i}^d \frac{1}{d} \partial d = \int_0^t -K_x K_d \partial t \Rightarrow d = F_d(t, \mathbf{K}, d_i) = d_i e^{-K_x K_d t} \quad (B.12)$$

As clear from equation (B.12), the convergence of d is dependent on K_x , K_d and t_f . Thus, the appropriate d_i leading to $d = E_d$ at $t = t_f$ is given by:

$$d_i = F_d^{-1}(t_f, \mathbf{K}, E_{dis}) = E_d e^{K_x K_d t_f} \quad (\text{B.13})$$

To conclude, relations (B.5) and (B.13) contribute to define wisely E_d and E_{angle} . The overall analytical method leading to an appropriate selection of d_i while knowing \mathbf{K} and e_{θ_0} is summarized in Figure B.1.

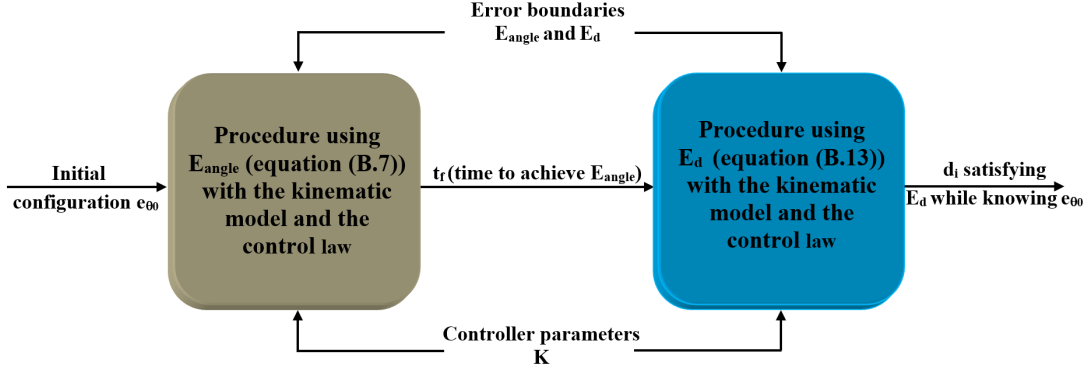


Figure B.1: Analytical method for safe reaching of waypoints [297].

LIST OF MY PUBLICATIONS

- [1] BEN LAKHEL, N. M., NASRI, O., GUEDDI, I., AND SLAMA, J. B. H. **Sdk decentralized diagnosis with vertices principle component analysis**. In *2016 International Conference on Control, Decision and Information Technologies (CoDIT)* (April 2016), pp. 517–522, St. Julian's, Malta.
- [2] BEN LAKHAL, N. M., NASRI, O., ADOUANE, L., AND BEN HADJ SLAMA, J. **Controller area network reliability: Overview of design challenges and safety related perspectives of future transportation systems**. *IET Intelligent Transport Systems* 14 (December 2020), 1727–1739.
- [3] BEN LAKHAL, N. M., ADOUANE, L., NASRI, O., AND SLAMA, J. B. H. **Reliable combined interval-based and stochastic risk management for intelligent vehicles**. *Under review, IEEE Transactions on Intelligent Vehicles* (2021).
- [4] BEN LAKHAL, N. M., ADOUANE, L., NASRI, O., AND SLAMA, J. B. H. **Safe and adaptive autonomous navigation under uncertainty based on sequential waypoints and reliable reachability analysis of state space**. *Under review, Robotics and Autonomous Systems* (2021).
- [5] BEN LAKHAL, N. M., NASRI, O., ADOUANE, L., AND SLAMA, J. B. H. **Analysis of set-membership risk assessment performances**. *Under final evaluation, upcoming as a chapter in Springer LNEE Series book* (2021).
- [6] BEN LAKHAL, N. M., ADOUANE, L., NASRI, O., AND SLAMA, J. B. H. **Interval-based solutions for reliable and safe navigation of intelligent autonomous vehicles**. In *2019 12th International Workshop on Robot Motion and Control (RoMoCo)* (July 2019), pp. 124–130, Poznań, Poland.
- [7] BEN LAKHAL, N. M., ADOUANE, L., NASRI, O., AND SLAMA, J. B. H. **Risk management for intelligent vehicles based on interval analysis of ttc**. *IFAC-PapersOnLine* 52, 8 (July 2019), 338–343. 10th IFAC Symposium on Intelligent Autonomous Vehicles IAV 2019, Gdańsk, Poland.
- [8] BEN LAKHAL, N. M., NASRI, O., ADOUANE, L., AND SLAMA, J. B. H. **Reliable modeling for safe navigation of intelligent vehicles: Analysis of first and second order set-membership ttc**. In *International Conference on Informatics in Control, Automation and Robotics (ICINCO)* (July 2020), pp. 545–552, Paris, France.
- [9] BEN LAKHAL, N. M., ADOUANE, L., NASRI, O., AND SLAMA, J. B. H. **Interval-based/data-driven risk management for intelligent vehicles: Application to an adaptive cruise control system**. In *2019 IEEE Intelligent Vehicles Symposium (IV)* (June 2019), pp. 239–244, Paris, France.
- [10] NASRI, O., BEN LAKHAL, N. M., ADOUANE, L., AND BEN HADJ SLAMA, J. **Automotive decentralized diagnosis based on can real-time analysis**. *Journal of Systems Architecture* 98 (September 2019), 249–258.

BIBLIOGRAPHY

[11] (2016). **Uber to deploy self-driving cars.** available at <https://www.bbc.com/news/technology-37117831>.

[12] (2018). **Tesla was on autopilot in fatal crash.** available at <https://www.bbc.com/news/world-us-canada-43604440>.

[13] (2020). **Google car project.** available at <https://waymo.com/journey>.

[14] (2020). **Self-driving shuttle for passenger transportation.** available at <https://navya.tech/en/solutions/moving-people/self-driving-shuttle-for-passenger-transportation/>.

[15] Abdi, L., et Meddeb, A. (2018). **Driver information system: a combination of augmented reality, deep learning and vehicular ad-hoc networks.** *Multimedia Tools and Applications*, 77(12):14673–14703.

[16] Abhishek, A., Sood, H., et Jeannin, J.-B. (2020). **Formal verification of braking while swerving in automobiles.** In *Proceedings of the 23rd International Conference on Hybrid Systems: Computation and Control*, HSCC '20, New York, NY, USA. Association for Computing Machinery.

[17] Adouane, L. (2005). **Architectures de controle comportementales et reactives pour la cooperation d'un groupe de robots mobiles.** PhD thesis, Universite de Franche-Comte, LAB CNRS 6596.

[18] Adouane, L. (2009). **Orbital obstacle avoidance algorithm for reliable and on-line mobile robot navigation.** *Portuguese Journal Robotica N79, automacao, Selected from International Conference on Autonomous Robot Systems and Competitions.*

[19] Adouane, L. ((2016)). **Autonomous Vehicle Navigation: From Behavioral to Hybrid Multi-Controller Architectures.** Taylor & Francis CRC Press, ISBN: 9781498715584.

[20] Adouane, L. (2017). **Reactive versus cognitive vehicle navigation based on optimal local and global pelc.** *Robotics and Autonomous Systems*, 88:51–70.

[21] Adouane, L. (2017). **Toward fully autonomous vehicle navigation: From behavioral to hybrid multi-controller architectures.** In *2017 11th International Workshop on Robot Motion and Control (RoMoCo)*, pages 85–98, Wasowo, Poland.

[22] Ahiska, K., Ozgoren, M. K., et Leblebiciooglu, M. K. (2018). **Autopilot design for vehicle cornering through icy roads.** *IEEE Transactions on Vehicular Technology*, 67(3):1867–1880.

[23] Aksjonov, A., Nedoma, P., Vodovozov, V., Petlenkov, E., et Herrmann, M. (2019). **Detection and evaluation of driver distraction using machine learning and fuzzy logic.** *IEEE Transactions on Intelligent Transportation Systems*, 20(6):2048–2059.

[24] Alefeld, G., et Mayer, G. (2000). **Interval analysis: theory and applications.** *Journal of Computational and Applied Mathematics*, 121(1):421–464.

[25] Alharbi, M., et Karimi, H. A. (2020). **Probe: Preparing for roads in advance of barriers and errors.** In Arai, K., Bhatia, R., et Kapoor, S., editors, *Proceedings of the Future Technologies Conference (FTC) 2019*, pages 934–957, Cham. Springer International Publishing.

[26] Alshamrani, R., Alshehri, F., et Kurdi, H. (2020). **A preprocessing technique for fast convex hull computation.** *Procedia Computer Science*, 170:317–324.

[27] Althoff, M., et Dolan, J. M. (2014). **Online verification of automated road vehicles using reachability analysis.** *IEEE Transactions on Robotics*, 30(4):903–918.

[28] Althoff, M., Maierhofer, S., et Pek, C. (2021). **Provably-correct and comfortable adaptive cruise control.** *IEEE Transactions on Intelligent Vehicles*, 6(1):159–174.

[29] Amri, M., Becis, Y., Aubry, D., et Ramdani, N. (2015). **Indoor human/robot localization using robust multi-modal data fusion.** In *2015 IEEE International Conference on Robotics and Automation (ICRA)*, pages 3456–3463.

[30] Antsaklis, P. (2020). **Autonomy and metrics of autonomy.** *Annual Reviews in Control*, 49:15–26.

[31] Arkin, R. C. (1990). **The impact of cybernetics on the design of a mobile robot system: a case study.** *IEEE Transactions on Systems, Man, and Cybernetics*, 20(6):1245–1257.

[32] Ashjaei, M., Khalilzad, N., et Mubeen, S. (2018). **Modeling, Designing and Analyzing Resource Reservations in Distributed Embedded Systems**, pages 203–256. Springer International Publishing, ISBN: 978-3-319-72215-3, Cham.

[33] Astivia, O. L. O., et Kroc, E. (2019). **Centering in multiple regression does not always reduce multicollinearity: How to tell when your estimates will not benefit from centering.** *Educational and Psychological Measurement*, 79(5):813–826.

[34] Bagdonavičius, V., et Petkevičius, L. (2020). **A new multiple outliers identification method in linear regression.** *Metrika*, 83(3):275–296.

[35] Barak, S., et Javanmard, S. (2020). **Outsourcing modelling using a novel interval-valued fuzzy quantitative strategic planning matrix (qspm) and multiple criteria decision-making (mcdms).** *International Journal of Production Economics*, 222:1–19.

[36] Barrett, L. (2019). **William Grey Walter**, pages 1–8. Springer International Publishing, Cham.

[37] Bauer, D., Kuhnert, L., et Eckstein, L. (2019). **Deep, spatially coherent inverse sensor models with uncertainty incorporation using the evidential framework.** In *2019 IEEE Intelligent Vehicles Symposium (IV)*, pages 2490–2495, Paris, France.

[38] Behringer, R., et Maurer, R. B. M. (1996). **Results on visual road recognition for road vehicle guidance**. In *Proceedings of Conference on Intelligent Vehicles*, pages 415–420, Tokyo, Japan.

[39] Benzerrouk, A., Adouane, L., Philippe, M., et Andreff, N. (2009). **Multi Lyapunov Function Theorem Applied to a Mobile Robot Tracking a Trajectory in Presence of Obstacles**. In *European Conference on Mobile Robots (ECMR 2009)*, Dubrovnik, Croatia.

[40] Bhatia, N. (1967). **Stability theorems for linear motions with an introduction to Lyapunov's direct method**. *IEEE Transactions on Automatic Control*, 12(5):637–638.

[41] Bi, X., Cao, S., et Zhang, D. (2019). **A variety of engine faults detection based on optimized variational mode decomposition-robust independent component analysis and fuzzy c-mean clustering**. *IEEE Access*, 7:27756–27768.

[42] Bianchi, F. A., Margara, A., et Pezzè, M. (2018). **A survey of recent trends in testing concurrent software systems**. *IEEE Transactions on Software Engineering*, 44(8):747–783.

[43] Bladin, P. F. (2006). **W. grey walter, pioneer in the electroencephalogram, robotics, cybernetics, artificial intelligence**. *Journal of Clinical Neuroscience*, 13(2):170–177.

[44] Bock, F., Siegl, S., Bazan, P., Buchholz, P., et German, R. (2018). **Reliability and test effort analysis of multi-sensor driver assistance systems**. *Journal of Systems Architecture*, 85-86:1–13.

[45] Boldrer, M., Andreetto, M., Divan, S., Palopoli, L., et Fontanelli, D. (2020). **Socially-aware reactive obstacle avoidance strategy based on limit cycle**. *IEEE Robotics and Automation Letters*, 5(2):3251–3258.

[46] Bounoua, W., et Bakdi, A. (2021). **Fault detection and diagnosis of nonlinear dynamical processes through correlation dimension and fractal analysis based dynamic kernel pca**. *Chemical Engineering Science*, 229:116099.

[47] Brambilla, M., Nicoli, M., Soatti, G., et Deflorio, F. (2020). **Augmenting vehicle localization by cooperative sensing of the driving environment: Insight on data association in urban traffic scenarios**. *IEEE Transactions on Intelligent Transportation Systems*, 21(4):1646–1663.

[48] Breloy, A., Ginolhac, G., Pascal, F., et Forster, P. (2016). **Robust covariance matrix estimation in heterogeneous low rank context**. *IEEE Transactions on Signal Processing*, 64(22):5794–5806.

[49] Bridger, M. (2019). **Real Analysis: A Constructive Approach Through Interval Arithmetic**, volume 38. American Mathematical Soc.

[50] Brito, D. N., Pádua, F. L. C., et Lopes, A. P. C. (2019). **Using geometric interval algebra modeling for improved three-dimensional camera calibration**. *Journal of Mathematical Imaging and Vision*, 61(9):1342–1369.

[51] Caruntu, C. F., Lazar, C., et Vargas, A. N. (2017). **Chance-constrained model predictive control for vehicle drivetrains in a cyber-physical framework**. In *2017 International Conference on Engineering, Technology and Innovation (ICE/ITMC)*, pages 1137–1144, Madeira, Portugal.

[52] Chai, C., Zeng, X., Wu, X., et Wang, X. (2019). **Safety evaluation of responsibility-sensitive safety (rss) on autonomous car-following maneuvers based on surrogate safety measurements**. In *2019 IEEE Intelligent Transportation Systems Conference (ITSC)*, pages 175–180, Auckland, New Zealand.

[53] Chandrasekhar Rao, D., Kabat, M. R., Das, P. K., et Jena, P. K. (2018). **Cooperative navigation planning of multiple mobile robots using improved krill herd**. *Arabian Journal for Science and Engineering*, 43(12):7869–7891.

[54] Chang, W., Goswami, D., Chakraborty, S., Ju, L., Xue, C. J., et Andalam, S. (2017). **Memory-aware embedded control systems design**. *IEEE Transactions on Computer-Aided Design of Integrated Circuits and Systems*, 36(4):586–599.

[55] Chatti, N., Guyonneau, R., Hardouin, L., Verron, S., et Lagrange, S. (2016). **Model-based approach for fault diagnosis using set-membership formulation**. *Engineering Applications of Artificial Intelligence*, 55:307–319.

[56] Chen, C., Xiang, H., Qiu, T., Wang, C., Zhou, Y., et Chang, V. (2018). **A rear-end collision prediction scheme based on deep learning in the internet of vehicles**. *Journal of Parallel and Distributed Computing*, 117:192–204.

[57] Chen, L., Ma, N., Wang, P., Li, J., Wang, P., Pang, G., et Shi, X. (2020). **Survey of pedestrian action recognition techniques for autonomous driving**. *Tsinghua Science and Technology*, 25(4):458–470.

[58] Chen, L., Yang, X., Liu, P. X., et Li, C. (2019a). **A novel outlier immune multipath fingerprinting model for indoor single-site localization**. *IEEE Access*, 7:21971–21980.

[59] Chen, M., Herbert, S. L., Vashishtha, M. S., Bansal, S., et Tomlin, C. J. (2018). **Decomposition of reachable sets and tubes for a class of nonlinear systems**. *IEEE Transactions on Automatic Control*, 63(11):3675–3688.

[60] Chen, P., Yang, Y., Wang, Y., Ma, Y., et Yang, L. (2019b). **Robust covariance matrix reconstruction algorithm for time-domain wideband adaptive beamforming**. *IEEE Transactions on Vehicular Technology*, 68(2):1405–1416.

[61] Chen, S. H., Lian, H. D., et Yang, X. W. (2003). **Interval eigenvalue analysis for structures with interval parameters**. *Finite Elements in Analysis and Design*, 39(5):419–431.

[62] Cheng, J., Lu, W., Hu, W., Liu, Z., Zhang, Y., et Tan, J. (2019). **Hybrid reliability-based design optimization of complex structures with random and interval uncertainties based on ass-hra**. *IEEE Access*, 7:87097–87109.

[63] Cheon, H., et Kim, B. K. (2019). **Online bidirectional trajectory planning for mobile robots in state-time space**. *IEEE Transactions on Industrial Electronics*, 66(6):4555–4565.

[64] Chodavarapu, M. M., Singh, V. P., et Devarapalli, R. (2020). **Interval modeling of riverol-pilipovik water treatment plant and its model order reduction.** In Giri, V. K., Verma, N. K., Patel, R. K., et Singh, V. P., editors, *Computing Algorithms with Applications in Engineering*, pages 361–367, Singapore. Springer Singapore.

[65] Claussmann, L., Revilloud, M., Gruyer, D., et Glaser, S. (2020). **A review of motion planning for highway autonomous driving.** *IEEE Transactions on Intelligent Transportation Systems*, 21(5):1826–1848.

[66] Combastel, C., Thabet, R. E. H., Raïssi, T., Zolghadri, A., et Gucik, D. (2014). **Set-membership fault detection under noisy environment in aircraft control surface servo-loops.** *IFAC Proceedings Volumes*, 47(3):8265–8271. 19th IFAC World Congress, Cape Town, South Africa.

[67] Corke, P. (2017). **Robotics, vision and control: fundamental algorithms in MATLAB® second, completely revised**, volume 118. Springer.

[68] Cvjetkovic, M., et Rakocevic, V. (2017). **Relative localisation algorithm for neighbour classification in ad hoc networks of moving robots.** In *Proceedings of the First ACM International Workshop on the Engineering of Reliable, Robust, and Secure Embedded Wireless Sensing Systems*, FAILSAFE’17, page 46–53, New York, NY, USA. Association for Computing Machinery.

[69] Cândido, R. M. F., Hardouin, L., Lhommeau, M., et Mendes, R. S. (2018). **Conditional reachability of uncertain max plus linear systems.** *Automatica*, 94:426–435.

[70] Dadras, S., Dadras, S., et Winstead, C. (2018). **Reachable set analysis of vehicular platooning in adversarial environment.** In *2018 Annual American Control Conference (ACC)*, pages 5568–5575, Milwaukee, WI, USA.

[71] Dahmane, Y., Abdurakhmanov, R., et Adouane, L. (2018). **Stochastic mpc for optimal energy management strategy of hybrid vehicle performing acc with stop&go maneuvers.** *IFAC-PapersOnLine*, 51(9):223–229. 15th IFAC Symposium on Control in Transportation Systems CTS 2018.

[72] Daniel, A., Subburathinam, K., Paul, A., Rajkumar, N., et Rho, S. (2017). **Big autonomous vehicular data classifications: Towards procuring intelligence in its.** *Vehicular Communications*, 9:306–312.

[73] Davis, R. I., Burns, A., Bril, R. J., et Lukkien, J. J. (2007). **Controller area network (can) schedulability analysis: Refuted, revisited and revised.** *Real-Time Systems*, 35(3):239–272.

[74] Dbouk, H., et Schön, S. (2018). **Comparison of different bounding methods for providing gps integrity information.** In *2018 IEEE/ION Position, Location and Navigation Symposium (PLANS)*, pages 355–366, Monterey, CA, USA.

[75] De Iaco, R., Smith, S. L., et Czarnecki, K. (2019). **Learning a lattice planner control set for autonomous vehicles.** In *2019 IEEE Intelligent Vehicles Symposium (IV)*, pages 549–556, Paris, France.

[76] De Leeuw, J. (1983). **Models and methods for the analysis of correlation coefficients.** *Journal of Econometrics*, 22(1):113–137.

[77] De Ryck, M., Versteyhe, M., et Debrouwere, F. (2020). **Automated guided vehicle systems, state-of-the-art control algorithms and techniques.** *Journal of Manufacturing Systems*, 54:152–173.

[78] de Weerdt, E., van Kampen, E.-J., Chu, Q., et Mulder, J. (2012). **Polynomial inclusion functions.** *Reliab. Comput.*, 16:283–307.

[79] Deif, A. (1991). **The interval eigenvalue problem.** *Journal of Applied Mathematics and Mechanics*, 71:61–64.

[80] Desrochers, B., et Jaulin, L. (2016). **A minimal contractor for the polar equation: Application to robot localization.** *Engineering Applications of Artificial Intelligence*, 55:83–92.

[81] Dey, K. C., Rayamajhi, A., Chowdhury, M., Bhavsar, P., et Martin, J. (2016). **Vehicle-to-vehicle (v2v) and vehicle-to-infrastructure (v2i) communication in a heterogeneous wireless network – performance evaluation.** *Transportation Research Part C: Emerging Technologies*, 68:168–184.

[82] DeLaTorre, G., Rad, P., et Choo, K.-K. R. (2020). **Driverless vehicle security: Challenges and future research opportunities.** *Future Generation Computer Systems*, 108:1092–1111.

[83] Dhibi, K., Fezai, R., Mansouri, M., Kouadri, A., Harkat, M., Bouzara, K., Nounou, H., et Nounou, M. (2020). **A hybrid approach for process monitoring: Improving data-driven methodologies with dataset size reduction and interval-valued representation.** *IEEE Sensors Journal*, 20(17):10228–10239.

[84] Ding, W., Li, X., Yang, H., An, J., et Zhang, Z. (2020). **Utilizing statistical information for interval analysis: A method for analyzing the interval uncertainty of line-of-sight measurement error of space-borne observation platforms.** *IEEE Access*, 8:67868–67886.

[85] Djuric, N., Grbovic, M., et Vucetic, S. (2015). **Chapter 7 - distributed confidence-weighted classification on big data platforms.** In Govindaraju, V., Raghavan, V. V., et Rao, C., editors, *Big Data Analytics*, volume 33 of *Handbook of Statistics*, pages 145–168. Elsevier.

[86] Dong, Y., et Qin, S. J. (2018). **A novel dynamic pca algorithm for dynamic data modeling and process monitoring.** *Journal of Process Control*, 67:1–11.

[87] Douzal-Chouakria, A., Billard, L., et Diday, E. (2011). **Principal component analysis for interval-valued observations.** *Statistical Analysis and Data Mining: The ASA Data Science Journal*, 4(2):229–246.

[88] Dredze, M., Crammer, K., et Pereira, F. (2008). **Confidence-weighted linear classification.** In *Proceedings of the 25th International Conference on Machine Learning*, ACM, pages 264–271, Helsinki, Finland.

[89] Drezet, H., Colombel, S., et Avenel, M. (2019). **Human-man interface concept for autonomous car.** In *2019 IEEE International Conference on Consumer Electronics (ICCE)*, pages 1–5, Las Vegas, NV, USA.

[90] Driggs-Campbell, K., Govindarajan, V., et Bajcsy, R. (2017). **Integrating intuitive driver models in autonomous planning for interactive maneuvers.** *IEEE Transactions on Intelligent Transportation Systems*, 18(12):3461–3472.

[91] Du, D., Yang, Y., Zhao, H., et Tan, Y. (2020). **Robust fault diagnosis observer design for uncertain switched systems.** *International Journal of Control, Automation and Systems*, 18:3159–3166.

[92] Duchaud, J., Hlioui, S., Louf, F., Ojeda, J., et Gabsi, M. (2015). **Modeling and optimization of a linear actuator for a two-stage valve tappet in an automotive engine.** *IEEE Transactions on Vehicular Technology*, 64(10):4441–4448.

[93] Duong, P. L. T., et Lee, M. (2012). **Robust pid controller design for processes with stochastic parametric uncertainties.** *Journal of Process Control*, 22(9):1559–1566.

[94] Durisic, D., Nilsson, M., Staron, M., et Hansson, J. (2013). **Measuring the impact of changes to the complexity and coupling properties of automotive software systems.** *Journal of Systems and Software*, 86(5):1275–1293.

[95] Díaz Álvarez, J., Risco-Martín, J. L., et Colmenar, J. M. (2016). **Multi-objective optimization of energy consumption and execution time in a single level cache memory for embedded systems.** *Journal of Systems and Software*, 111:200–212.

[96] El-Laham, Y., Elvira, V., et Bugallo, M. F. (2018). **Robust covariance adaptation in adaptive importance sampling.** *IEEE Signal Processing Letters*, 25(7):1049–1053.

[97] Elliott, D., Keen, W., et Miao, L. (2019). **Recent advances in connected and automated vehicles.** *Journal of Traffic and Transportation Engineering (English Edition)*, 6(2):109–131.

[98] Ettl, J., Bernhardt, H., Pickel, P., Remmele, E., Thuneke, K., et Emberger, P. (2018). **Transfer of agricultural work operation profiles to a tractor test stand for exhaust emission evaluation.** *Biosystems Engineering*, 176:185–197.

[99] Etumi, A. A., et Anayi, F. (2016). **The application of correlation technique in detecting internal and external faults in three-phase transformer and saturation of current transformer.** *IEEE Transactions on Power Delivery*, 31(5):2131–2139.

[100] Eun, Y., Park, S.-Y., et Kim, G.-N. (2018). **Development of a hardware-in-the-loop testbed to demonstrate multiple spacecraft operations in proximity.** *Acta Astronautica*, 147:48–58.

[101] Faes, M., et Moens, D. (2020). **Recent trends in the modeling and quantification of non-probabilistic uncertainty.** *Archives of Computational Methods in Engineering*, 27(3):633–671.

[102] Fan, X., Deng, J., et Chen, F. (2008). **Zeros of univariate interval polynomials.** *Journal of Computational and Applied Mathematics*, 216(2):563–573.

[103] Feld, T., Biondi, A., Davis, R. I., Buttazzo, G., et Slomka, F. (2018). **A survey of schedulability analysis techniques for rate-dependent tasks.** *Journal of Systems and Software*, 138:100–107.

[104] Feng, D., Lin, S., He, Z., Sun, X., et Wang, Z. (2018). **Failure risk interval estimation of traction power supply equipment considering the impact of multiple factors.** *IEEE Transactions on Transportation Electrification*, 4(2):389–398.

[105] Feng, D., Rosenbaum, L., Timm, F., et Dietmayer, K. (2019). **Leveraging heteroscedastic aleatoric uncertainties for robust real-time lidar 3d object detection.** In *2019 IEEE Intelligent Vehicles Symposium (IV)*, pages 1280–1287, Paris, France.

[106] Ferreira, J., Patrício, F., et Oliveira, F. (2001). **A priori estimates for the zeros of interval polynomials.** *Journal of Computational and Applied Mathematics*, 136(1):271–281.

[107] Ferson, S., Ginzburg, L., Kreinovich, V., Longpré, L., et Aviles, M. (2002). **Computing variance for interval data is np-hard.** *ACM SIGACT News*, 33(2):108–118.

[108] FOSSEN, T., Pettersen, K. Y., et Nijmeijer, H. (2017). **SENSING AND CONTROL FOR AUTONOMOUS VEHICLES.** Springer.

[109] Fridman, L., Brown, D. E., Glazer, M., Angell, W., Dodd, S., Jenik, B., Terwilliger, J., Patsekin, A., Kindelsberger, J., Ding, L., Seaman, S., Mehler, A., Sipperley, A., Pettinato, A., Seppelt, B. D., Angell, L., Mehler, B., et Reimer, B. (2019). **Mit advanced vehicle technology study: Large-scale naturalistic driving study of driver behavior and interaction with automation.** *IEEE Access*, 7:102021–102038.

[110] Fu, C., Liu, Q., Wu, P., Li, M., Xue, C. J., Zhao, Y., Hu, J., et Han, S. (2019). **Real-time data retrieval in cyber-physical systems with temporal validity and data availability constraints.** *IEEE Transactions on Knowledge and Data Engineering*, 31(9):1779–1793.

[111] Füngfeld, S., Holzäpfel, M., Frey, M., et Gauterin, F. (2017). **Stochastic forecasting of vehicle dynamics using sequential monte carlo simulation.** *IEEE Transactions on Intelligent Vehicles*, 2(2):111–122.

[112] Gamal, I., Badawy, A., Al-Habal, A. M., Adawy, M. E., Khalil, K. K., El-Moursy, M. A., et Khattab, A. (2019). **A robust, real-time and calibration-free lane departure warning system.** *Microprocessors and Microsystems*, 71:1–10.

[113] Gao, X., et Su, D. (2016). **Suppression of a certain vehicle electrical field and magnetic field radiation resonance point.** In *2016 IEEE Vehicle Power and Propulsion Conference (VPPC)*, pages 1–6, Hangzhou, China.

[114] Gao, Y., Yu, P., Dimarogonas, D. V., Johansson, K. H., et Xie, L. (2019). **Robust self-triggered control for time-varying and uncertain constrained systems via reachability analysis.** *Automatica*, 107:574–581.

[115] Gao, Z., Cecati, C., et Ding, S. X. (2015). **A survey of fault diagnosis and fault-tolerant techniques—part i: Fault diagnosis with model-based and signal-based approaches.** *IEEE Transactions on Industrial Electronics*, 62(6):3757–3767.

[116] García-Valls, M., Perez-Palacin, D., et Mirandola, R. (2018). **Pragmatic cyber physical systems design based on parametric models.** *Journal of Systems and Software*, 144:559–572.

[117] Gassmann, B., Oboril, F., Buerkle, C., Liu, S., Yan, S., Elli, M. S., Alvarez, I., Aerrabotu, N., Jaber, S., van Beek, P., Iyer, D., et Weast, J. (2019). **Towards standardization of av safety: C++ library for responsibility sensitive safety**. In *2019 IEEE Intelligent Vehicles Symposium (IV)*, pages 2265–2271, Paris, France.

[118] Ge, X., Ahmad, I., Han, Q.-L., Wang, J., et Zhang, X.-M. (2021). **Dynamic event-triggered scheduling and control for vehicle active suspension over controller area network**. *Mechanical Systems and Signal Processing*, 152:107481.

[119] Gong, H., Li, R., Bai, Y., An, J., et Li, K. (2018). **Message response time analysis for automotive cyber–physicalsystems with uncertain delay: An m/ph/1 queue approach**. *Performance Evaluation*, 125:21–47.

[120] Gu, W., Cai, S., Hu, Y., Zhang, H., et Chen, H. (2019). **Trajectory planning and tracking control of a ground mobile robot:a reconstruction approach towards space vehicle**. *ISA Transactions*, 87:116–128.

[121] Guan, S., Zhang, Z., et Cui, Z. (2020). **Modeling uncertain dynamic plants with interval neural networks by bounded-error data**. *IEEE Access*, 8:9809–9820.

[122] Gueddi, I., Nasri, O., et Ben Othman, K. (2020). **A new interval diagnosis method: Application to the spacecraft rendezvous phase of the mars sample return mission**. *International Journal of Adaptive Control and Signal Processing*, 34(1):42–62.

[123] Gueddi, I., Nasri, O., Benothman, K., et Dague, P. (2017). **Fault detection and isolation of spacecraft thrusters using an extended principal component analysis to interval data**. *International Journal of Control, Automation and Systems*, 15(2):776–789.

[124] Guerrero-Mosquera, C., Borragán, G., et Peigneux, P. (2016). **Automatic detection of noisy channels in fnirs signal based on correlation analysis**. *Journal of Neuroscience Methods*, 271:128–138.

[125] Guo, J., Song, B., He, Y., Yu, F. R., et Sookhak, M. (2017). **A survey on compressed sensing in vehicular infotainment systems**. *IEEE Communications Surveys Tutorials*, 19(4):2662–2680.

[126] Guéguen, H., Lefebvre, M.-A., Zaytoon, J., et Nasri, O. (2009). **Safety verification and reachability analysis for hybrid systems**. *Annual Reviews in Control*, 33(1):25–36.

[127] Haesaert, S., Van den Hof, P. M., et Abate, A. (2017). **Data-driven and model-based verification via bayesian identification and reachability analysis**. *Automatica*, 79:115–126.

[128] Han, R., Wang, S., Liu, B., Zhao, T., et Ye, Z. (2018). **A novel model-based dynamic analysis method for state correlation with ima fault recovery**. *IEEE Access*, 6:22094–22107.

[129] Han, T., Jing, J., et Özgüner, (2019). **Driving intention recognition and lane change prediction on the highway**. In *2019 IEEE Intelligent Vehicles Symposium (IV)*, pages 957–962, Paris, France.

[130] Hansen, E., et Walster, G. W. (2003). **Global optimization using interval analysis: revised and expanded**, volume 264. CRC Press.

[131] Hansen, E. R., et Walster, G. W. (2002). **Sharp bounds on interval polynomial roots**. *Reliable Computing*, 8(2):115–122.

[132] Harkat, M.-F., Mansouri, M., Nounou, M., et Nounou, H. (2019). **Fault detection of uncertain nonlinear process using interval-valued data-driven approach**. *Chemical Engineering Science*, 205:36–45.

[133] Harwood, S. M., Scott, J. K., et Barton, P. I. (2016). **Bounds on reachable sets using ordinary differential equations with linear programs embedded**. *IMA Journal of Mathematical Control and Information*, 33(2):519–541.

[134] Hasenjäger, M., Heckmann, M., et Wersing, H. (2020). **A survey of personalization for advanced driver assistance systems**. *IEEE Transactions on Intelligent Vehicles*, 5(2):335–344.

[135] Hazra, A., Dasgupta, P., et Chakrabarti, P. P. (2016). **Formal assessment of reliability specifications in embedded cyber-physical systems**. *Journal of Applied Logic*, 18:71–104.

[136] He, F., et Zhang, Z. (2020). **Nonlinear fault detection of batch processes using functional local kernel principal component analysis**. *IEEE Access*, 8:117513–117527.

[137] Heffernan, D., Macnamee, C., et Fogarty, P. (2014). **Runtime verification monitoring for automotive embedded systems using the iso 26262 functional safety standard as a guide for the definition of the monitored properties**. *IET Software*, 8(5):193–203.

[138] Heinzler, R., Schindler, P., Seekircher, J., Ritter, W., et Stork, W. (2019). **Weather influence and classification with automotive lidar sensors**. In *2019 IEEE Intelligent Vehicles Symposium (IV)*, pages 1527–1534, Paris, France.

[139] Heo, S., Cha, J., et Park, C. G. (2019). **Ekf-based visual inertial navigation using sliding window nonlinear optimization**. *IEEE Transactions on Intelligent Transportation Systems*, 20(7):2470–2479.

[140] Herrero, D., Villagrá, J., et Martínez, H. (2013). **Self-configuration of waypoints for docking maneuvers of flexible automated guided vehicles**. *IEEE Transactions on Automation Science and Engineering*, 10(2):470–475.

[141] Heß, D., Althoff, M., et Sattel, T. (2014). **Formal verification of maneuver automata for parameterized motion primitives**. In *2014 IEEE/RSJ International Conference on Intelligent Robots and Systems*, pages 1474–1481, Chicago, IL, USA.

[142] Hladík, M., Daney, D., et Tsigaridas, E. (2010). **Bounds on real eigenvalues and singular values of interval matrices**. *SIAM Journal on Matrix Analysis and Applications*, 31(4):2116–2129.

[143] Hladík, M. (2013). **Bounds on eigenvalues of real and complex interval matrices**. *Applied Mathematics and Computation*, 219(10):5584–5591.

[144] Hou, J., List, G. F., et Guo, X. (2014). **New algorithms for computing the time-to-collision in freeway traffic simulation models.** *Computational Intelligence and Neuroscience*, 2014:1–9.

[145] Hu, X., Chen, X., Parks, G. T., et Yao, W. (2016). **Review of improved monte carlo methods in uncertainty-based design optimization for aerospace vehicles.** *Progress in Aerospace Sciences*, 86:20–27.

[146] Hu, X., Zhao, X., et Feng, X. (2019a). **Probabilistic-interval energy flow analysis of regional integrated electricity and gas system considering multiple uncertainties and correlations.** *IEEE Access*, 7:178209–178223.

[147] Hu, Y., Zhan, W., Sun, L., et Tomizuka, M. (2019b). **Multi-modal probabilistic prediction of interactive behavior via an interpretable model.** In *2019 IEEE Intelligent Vehicles Symposium (IV)*, pages 557–563, Paris, France.

[148] Héry, E., Xu, P., et Bonnifait, P. (2019). **Pose and covariance matrix propagation issues in cooperative localization with lidar perception.** In *2019 IEEE Intelligent Vehicles Symposium (IV)*, pages 1219–1224, Paris, France.

[149] Iberraken, D., Adouane, L., et Denis, D. (2018). **Multi-level bayesian decision-making for safe and flexible autonomous navigation in highway environment.** In *2018 IEEE/RSJ International Conference on Intelligent Robots and Systems (IROS)*, pages 3984–3990, Madrid, Spain.

[150] Iberraken, D., Adouane, L., et Denis, D. (2019). **Multi-controller architecture for reliable autonomous vehicle navigation: Combination of model-driven and data-driven formalization.** In *2019 IEEE Intelligent Vehicles Symposium (IV)*, pages 245–251, Paris, France.

[151] Ilea, I., Bombrun, L., Terebes, R., Borda, M., et Germain, C. (2016). **An m-estimator for robust centroid estimation on the manifold of covariance matrices.** *IEEE Signal Processing Letters*, 23(9):1255–1259.

[152] Ingrand, F., et Ghallab, M. (2017). **Deliberation for autonomous robots: A survey.** *Artificial Intelligence*, 247:10–44. Special Issue on AI and Robotics.

[153] Jalal-Kamali, A., et Kreinovich, V. (2013). **Estimating correlation under interval uncertainty.** *Mechanical Systems and Signal Processing*, 37:43–53.

[154] Jaulin, L., Kieffer, M., Didrit, O., et Walter, E. (2001). **Applied Interval Analysis with Examples in Parameter and State Estimation, Robust Control and Robotics.** Springer, London.

[155] Jenelius, E., et Koutsopoulos, H. N. (2018). **Urban network travel time prediction based on a probabilistic principal component analysis model of probe data.** *IEEE Transactions on Intelligent Transportation Systems*, 19(2):436–445.

[156] Jiménez, F., Naranjo, J. E., et García, F. (2013). **An improved method to calculate the time-to-collision of two vehicles.** *International Journal of Intelligent Transportation Systems Research*, 11(1):34–42.

[157] Kalra, N., et Paddock, S. M. (2016). **Driving to safety: How many miles of driving would it take to demonstrate autonomous vehicle reliability?** *Transportation Research Part A: Policy and Practice*, 94:182–193.

[158] Kamel, M. A., Yu, X., et Zhang, Y. (2020). **Formation control and coordination of multiple unmanned ground vehicles in normal and faulty situations: A review.** *Annual Reviews in Control*, 49:128–144.

[159] Katrakazas, C., Quddus, M., Chen, W.-H., et Deka, L. (2015). **Real-time motion planning methods for autonomous on-road driving: State-of-the-art and future research directions.** *Transportation Research Part C: Emerging Technologies*, 60:416–442.

[160] Keung, K. L., Lee, C. K. M., Ji, P., et Ng, K. K. H. (2020). **Cloud-based cyber-physical robotic mobile fulfillment systems: A case study of collision avoidance.** *IEEE Access*, 8:89318–89336.

[161] Khalil, H. K., et Grizzle, J. W. (2002). **Nonlinear systems**, volume 3. Prentice hall Upper Saddle River, NJ.

[162] Khan, M. N., et Ahmed, M. M. (2020). **Trajectory-level fog detection based on in-vehicle video camera with tensorflow deep learning utilizing shrp2 naturalistic driving data.** *Accident Analysis & Prevention*, 142:1–12.

[163] Khelifi, A., Ben Lakhal, N. M., Gharsallaoui, H., et Nasri, O. (2018). **Artificial neural network-based fault detection.** In *2018 5th International Conference on Control, Decision and Information Technologies (CoDIT)*, pages 1017–1022, Thessaloniki, Greece.

[164] Kim, B., et Lee, S. (2013). **Robust estimation for the covariance matrix of multivariate time series based on normal mixtures.** *Computational Statistics & Data Analysis*, 57(1):125–140.

[165] Kim, D.-S., et Tran-Dang, H. (2019). **Communication Using Controller Area Network Protocol**, pages 31–41. Springer International Publishing, Cham.

[166] Kishida, M. (2017). **On computations of variance, covariance and correlation for interval data.** *Mechanical Systems and Signal Processing*, 84:462 – 468.

[167] Klischat, M., et Althoff, M. (2019). **Generating critical test scenarios for automated vehicles with evolutionary algorithms.** In *2019 IEEE Intelligent Vehicles Symposium (IV)*, pages 2352–2358, Paris, France.

[168] Kuestenmacher, A., et Plöger, P. G. (2016). **Model-based fault diagnosis techniques for mobile robots.** *IFAC-PapersOnLine*, 49(15):50–56. 9th IFAC Symposium on Intelligent Autonomous Vehicles IAV 2016, Leipzig, Germany.

[169] Kvasnica, M., Bakaráč, P., et Klaučo, M. (2019). **Complexity reduction in explicit mpc: A reachability approach.** *Systems & Control Letters*, 124:19–26.

[170] Lamiraux, F., Sekhavat, S., et Laumond, J. . (1999). **Motion planning and control for hilare pulling a trailer.** *IEEE Transactions on Robotics and Automation*, 15(4):640–652.

[171] Lange, R., de Oliveira, R. S., et Vasques, F. (2016). **A reference model for the timing analysis of heterogeneous automotive networks.** *Computer Standards & Interfaces*, 45:13–25.

[172] Le Mortellec, A., Clarhaut, J., Sallez, Y., Berger, T., et Trentesaux, D. (2013). **Embedded holonic fault diagnosis of complex transportation systems.** *Engineering Applications of Artificial Intelligence*, 26(1):227–240.

[173] Lee, D. (2017). **Self-drive shuttle bus in crash on first day.** available at <https://www.bbc.com/news/technology-41923814>.

[174] Lee, H., Ra, M., et Kim, W. (2020). **Nighttime data augmentation using gan for improving blind-spot detection.** *IEEE Access*, 8:48049–48059.

[175] Lee, S.-Y. (1985). **Analysis of covariance and correlation structures.** *Computational Statistics & Data Analysis*, 2(4):279–295.

[176] Lee, Y. S., Kim, J. H., et Jeon, J. W. (2017). **Flexray and ethernet avb synchronization for high qos automotive gateway.** *IEEE Transactions on Vehicular Technology*, 66(7):5737–5751.

[177] Lefèvre, S., Vasquez, D., et Laugier, C. (2014). **A survey on motion prediction and risk assessment for intelligent vehicles.** *ROBOMECH Journal*, 1:1.

[178] Leng, Q., Wang, S., Qin, Y., et Li, Y. (2019). **An effective method to determine whether a point is within a convex hull and its generalized convex polyhedron classifier.** *Information Sciences*, 504:435–448.

[179] Li, S., Li, Z., Yu, Z., Zhang, B., et Zhang, N. (2019). **Dynamic trajectory planning and tracking for autonomous vehicle with obstacle avoidance based on model predictive control.** *IEEE Access*, 7:132074–132086.

[180] Li, Z., et Dixon, S. (2016). **A closed-loop operation to improve gmr sensor accuracy.** *IEEE Sensors Journal*, 16(15):6003–6007.

[181] Liao, X., Liu, K., Niu, H., Luo, J., Li, Y., et Qin, L. (2018). **An interval taylor-based method for transient stability assessment of power systems with uncertainties.** *International Journal of Electrical Power & Energy Systems*, 98:108–117.

[182] Liu, G., Liu, Q., et Li, P. (2017). **Blessing of dimensionality: Recovering mixture data via dictionary pursuit.** *IEEE Transactions on Pattern Analysis and Machine Intelligence*, 39(1):47–60.

[183] Lu, W., Shan, D., Pedrycz, W., Zhang, L., Yang, J., et Liu, X. (2019). **Granular fuzzy modeling for multidimensional numeric data: A layered approach based on hyperbox.** *IEEE Transactions on Fuzzy Systems*, 27(4):775–789.

[184] Lubiw, A., Maftuleac, D., et Owen, M. (2020). **Shortest paths and convex hulls in 2d complexes with non-positive curvature.** *Computational Geometry*, 89:101626.

[185] Lyons, D. M., Arkin, R. C., Jiang, S., Liu, T., et Nirmal, P. (2015). **Performance verification for behavior-based robot missions.** *IEEE Transactions on Robotics*, 31(3):619–636.

[186] Ma, H., et Xu, L. (2020). **Cooperative fault diagnosis for uncertain nonlinear multiagent systems based on adaptive distributed fuzzy estimators.** *IEEE Transactions on Cybernetics*, 50(4):1739–1751.

[187] MA, Y., WANG, Y., WANG, C., et HONG, J. (2020). **Nonlinear interval analysis of rotor response with joints under uncertainties**. *Chinese Journal of Aeronautics*, 33(1):205–218.

[188] Maciel, L., et Ballini, R. (2019). **Fuzzy Rule-Based Modeling for Interval-Valued Data: An Application to High and Low Stock Prices Forecasting**, pages 403–424. Springer International Publishing, Cham.

[189] magazine, L. P. (2017). **Navya : le premier taxi autonome en test à paris**. available at https://www.lepoint.fr/automobile/innovations/navya-le-premier-taxi-autonome-en-test-a-paris-08-11-2017-2170613_652.php.

[190] Mahot, M., Pascal, F., Forster, P., et Ovarlez, J. (2013). **Asymptotic properties of robust complex covariance matrix estimates**. *IEEE Transactions on Signal Processing*, 61(13):3348–3356.

[191] Mair, P. (2018). **Principal Component Analysis and Extensions**, pages 179–210. Springer International Publishing, Cham.

[192] Maiti, S., Winter, S., Kulik, L., et Sarkar, S. (2020). **The impact of flexible platoon formation operations**. *IEEE Transactions on Intelligent Vehicles*, 5(2):229–239.

[193] Makridis, M., Mattas, K., et Ciuffo, B. (2020). **Response time and time headway of an adaptive cruise control. an empirical characterization and potential impacts on road capacity**. *IEEE Transactions on Intelligent Transportation Systems*, 21(4):1677–1686.

[194] Marshall, C. J., Roberts, B., et Grenn, M. W. (2019). **Context-driven autonomy for enhanced system resilience in emergent operating environments**. *IEEE Systems Journal*, 13(3):2130–2141.

[195] Marx, S. E., Luck, J. D., Pitla, S. K., et Hoy, R. M. (2016). **Comparing various hardware/software solutions and conversion methods for controller area network (can) bus data collection**. *Computers and Electronics in Agriculture*, 128:141–148.

[196] Maïga, M., Ramdani, N., Travé-Massuyès, L., et Combastel, C. (2016). **A comprehensive method for reachability analysis of uncertain nonlinear hybrid systems**. *IEEE Transactions on Automatic Control*, 61(9):2341–2356.

[197] Meng, S., Tong, C., Lan, T., et Yu, H. (2020). **Canonical correlation analysis-based explicit relation discovery for statistical process monitoring**. *Journal of the Franklin Institute*, 357(8):5004–5018.

[198] Mercader, P., Soltesz, K., et Baños, A. (2017). **Robust pid design by chance-constrained optimization**. *Journal of the Franklin Institute*, 354(18):8217–8231.

[199] Meslem, N. (2008). **Hybrid reachability of continuous dynamical systems by interval analysis : application to the set-membership estimation**. Theses, Université Paris-Est.

[200] Meslem, N., et Ramdani, N. (2018). **Forward-backward set-membership state estimator based on interval analysis**. In *2018 Annual American Control Conference (ACC)*, pages 5161–5166, Milwaukee, WI, USA.

[201] Miglani, A., et Kumar, N. (2019). **Deep learning models for traffic flow prediction in autonomous vehicles: A review, solutions, and challenges.** *Vehicular Communications*, 20:100184.

[202] Moore, R., Kearfott, R., et Cloud, M. (2009). **Introduction to Interval Analysis.** Society for Industrial and Applied Mathematics.

[203] Moore, R. E. (1979). **Methods and applications of interval analysis.** SIAM.

[204] Moore, R. E. (2009). **Interval analysis: differential equations** *Interval Analysis: Differential Equations*, pages 1685–1689. Springer US, Boston, MA.

[205] Mora-López, L., et Mora, J. (2015). **An adaptive algorithm for clustering cumulative probability distribution functions using the kolmogorov–smirnov two-sample test.** *Expert Systems with Applications*, 42(8):4016–4021.

[206] Morales-Jimenez, D., Couillet, R., et McKay, M. R. (2015). **Large dimensional analysis of robust m-estimators of covariance with outliers.** *IEEE Transactions on Signal Processing*, 63(21):5784–5797.

[207] Mouloua, M., et Hancock, P. A. (2019). **Human Performance in Automated and Autonomous Systems, Two-Volume Set.** CRC Press.

[208] Mu, W., Wang, J., et Feng, W. (2017). **Fault detection and fault-tolerant control of actuators and sensors in distributed parameter systems.** *Journal of the Franklin Institute*, 354(8):3341–3363.

[209] Mubeen, S., Mäki-Turja, J., et Sjödin, M. (2015). **Integrating mixed transmission and practical limitations with the worst-case response-time analysis for controller area network.** *Journal of Systems and Software*, 99:66–84.

[210] Mubeen, S., Nolte, T., Sjödin, M., Lundbäck, J., et Lundbäck, K.-L. (2019a). **Supporting timing analysis of vehicular embedded systems through the refinement of timing constraints.** *Software & Systems Modeling*, 18(1):39–69.

[211] Mubeen, S., Nolte, T., Sjödin, M., Lundbäck, J., et Lundbäck, K.-L. (2019b). **Supporting timing analysis of vehicular embedded systems through the refinement of timing constraints.** *Software & Systems Modeling*, 18(1):39–69.

[212] Mullins, G. E., Stankiewicz, P. G., Hawthorne, R. C., et Gupta, S. K. (2018). **Adaptive generation of challenging scenarios for testing and evaluation of autonomous vehicles.** *Journal of Systems and Software*, 137:197–215.

[213] Mänttäri, J., et Folkesson, J. (2019). **Incorporating uncertainty in predicting vehicle maneuvers at intersections with complex interactions.** In *2019 IEEE Intelligent Vehicles Symposium (IV)*, pages 2156–2163, Paris, France.

[214] Müller, J., Gabb, M., et Buchholz, M. (2019). **A subjective-logic-based reliability estimation mechanism for cooperative information with application to iv's safety.** In *2019 IEEE Intelligent Vehicles Symposium (IV)*, pages 1940–1946, Paris, France.

[215] Nakamura, R., Mitsukura, Y., et Hamada, N. (2013a). **Blind restoration of single-channel image using iterative pca.** In *2013 IEEE Conference on Systems, Process Control (ICSPC)*, pages 84–87, Kuala Lumpur, Malaysia.

[216] Nakamura, R., Mitsukura, Y., et Hamada, N. (2013b). **Iterative pca approach for blind restoration of single blurred image**. In *2013 International Symposium on Intelligent Signal Processing and Communication Systems*, pages 543–546, Naha, Japan.

[217] Narayanan, S., Chaniotakis, E., et Antoniou, C. (2020). **Shared autonomous vehicle services: A comprehensive review**. *Transportation Research Part C: Emerging Technologies*, 111:255 – 293.

[218] Nasri, O., Gueddi, I., Dague, P., et Benothman, K. (2015). **Spacecraft actuator diagnosis with principal component analysis: application to the rendez-vous phase of the mars sample return mission**. *Journal of Control Science and Engineering*, pages 1–12.

[219] Nguyen, T., et Au, T. (2019). **A constant-time algorithm for checking reachability of arrival times and arrival velocities of autonomous vehicles**. In *2019 IEEE Intelligent Vehicles Symposium (IV)*, pages 2039–2044, Paris, France.

[220] Ni, B., et Jiang, C. (2020). **Interval field model and interval finite element analysis**. *Computer Methods in Applied Mechanics and Engineering*, 360:1–40.

[221] Nicola, J., et Jaulin, L. (2018). **Comparison of Kalman and Interval Approaches for the Simultaneous Localization and Mapping of an Underwater Vehicle**, pages 117–136. Springer International Publishing.

[222] Nirmala, T., Datta, D., Kushwaha, H., et Ganesan, K. (2011). **Inverse interval matrix: A new approach**. *Applied Mathematical Sciences*, 5(13):607–624.

[223] Noh, S. (2019). **Decision-making framework for autonomous driving at road intersections: Safeguarding against collision, overly conservative behavior, and violation vehicles**. *IEEE Transactions on Industrial Electronics*, 66(4):3275–3286.

[224] Noh, S., et An, K. (2018). **Decision-making framework for automated driving in highway environments**. *IEEE Transactions on Intelligent Transportation Systems*, 19(1):58–71.

[225] Nolte, T., Hansson, H., Norström, C., et Punnekkat, S. (2001). **Using bit-stuffing distributions in can analysis**. In *IEEE Real-Time Embedded Systems Workshop at the Real-Time Systems Symposium*, pages 1–6, London, UK.

[226] Nowak, P., et Stewart, T. C. (2019). **A spiking model of desert ant navigation along a habitual route**. In Matoušek, R., editor, *Recent Advances in Soft Computing*, pages 211–222, Cham. Springer International Publishing.

[227] Ooi, B. Y., Beh, W. L., Lee, W., et Shirmohammadi, S. (2019). **Using the cloud to improve sensor availability and reliability in remote monitoring**. *IEEE Transactions on Instrumentation and Measurement*, 68(5):1522–1532.

[228] Osman, M., Alonso, R., Hammam, A., Moreno, F. M., Al-Kaff, A., et Hussein, A. (2019). **Multisensor fusion localization using extended hfilter using pre-filtered sensors measurements**. In *2019 IEEE Intelligent Vehicles Symposium (IV)*, pages 1139–1144, Paris, France.

[229] Park, J., Abdel-Aty, M., Wu, Y., et Mattei, I. (2019a). **Enhancing in-vehicle driving assistance information under connected vehicle environment.** *IEEE Transactions on Intelligent Transportation Systems*, 20(9):3558–3567.

[230] Park, J. K., et Kim, J. T. (2019b). **Deterministic sensor signal detection technique for static and short-ranged channels using real-valued independent component analysis.** *IEEE Sensors Journal*, 19(15):6214–6225.

[231] Patle, B., Babu L, G., Pandey, A., Parhi, D., et Jagadeesh, A. (2019). **A review: On path planning strategies for navigation of mobile robot.** *Defence Technology*, 15(4):582–606.

[232] Pearson, K. (1920). **Notes on the history of correlation.** *Biometrika*, 13(1):25–45.

[233] Polygerinos, P., Wang, Z., Overvelde, J. T. B., Galloway, K. C., Wood, R. J., Bertoldi, K., et Walsh, C. J. (2015). **Modeling of soft fiber-reinforced bending actuators.** *IEEE Transactions on Robotics*, 31(3):778–789.

[234] Pusse, F., et Klusch, M. (2019). **Hybrid online pomdp planning and deep reinforcement learning for safer self-driving cars.** In *2019 IEEE Intelligent Vehicles Symposium (IV)*, pages 1013–1020.

[235] Qin, H., Yan, M., et Ji, H. (2021). **Application of controller area network (can) bus anomaly detection based on time series prediction.** *Vehicular Communications*, 27:100291.

[236] Qiu, C., Peng, X., Liu, Z., et Tan, J. (2019). **Sensitivity analysis of random and interval uncertain variables based on polynomial chaos expansion method.** *IEEE Access*, 7:73046–73056.

[237] Quaglia, D., et Muradore, R. (2016). **Communication-aware bandwidth-optimized predictive control of motor drives in electric vehicles.** *IEEE Transactions on Industrial Electronics*, 63(9):5602–5611.

[238] Rall, L. B. (1981). **Automatic differentiation-technique and applications.** *Lecture notes in computer science*, 120.

[239] Rall, L. B., et Corliss, G. F. (2001). **Automatic differentiation: point and interval**Automatic Differentiation: Point and Interval, pages 108–113. Springer US, Boston, MA.

[240] Ramdani, N., Meslem, N., et Candau, Y. (2009). **A hybrid bounding method for computing an over-approximation for the reachable set of uncertain nonlinear systems.** *IEEE Transactions on Automatic Control*, 54(10):2352–2364.

[241] Ramdani, N., Meslem, N., et Candau, Y. (2010). **Computing reachable sets for uncertain nonlinear monotone systems.** *Nonlinear Analysis: Hybrid Systems*, 4(2):263–278.

[242] Rao, D. C., Kabat, M. R., Das, P. K., et Jena, P. K. (2019). **Hybrid iwd-de: A novel approach to model cooperative navigation planning for multi-robot in unknown dynamic environment.** *Journal of Bionic Engineering*, 16(2):235–252.

[243] Renold, A. P., et Chandrakala, S. (2017). **Convex-hull-based boundary detection in unattended wireless sensor networks.** *IEEE Sensors Letters*, 1(4):1–4.

[244] Rigatos, G. G. (2012). **Nonlinear kalman filters and particle filters for integrated navigation of unmanned aerial vehicles.** *Robotics and Autonomous Systems*, 60(7):978–995.

[245] Rihm, R. (1994). **Interval methods for initial value problems in odes.** *Topics in Validated Computations*, pages 173–207.

[246] Rizaldi, A., et Althoff, M. (2015). **Formalising traffic rules for accountability of autonomous vehicles.** In *2015 IEEE 18th International Conference on Intelligent Transportation Systems*, pages 1658–1665.

[247] Rodgers, J. L., et Nicewander, W. A. (1988). **Thirteen ways to look at the correlation coefficient.** *The American Statistician*, 42(1):59–66.

[248] Rohn, J. (1993). **Inverse interval matrix.** *SIAM Journal on Numerical Analysis*, 30(3):864–870.

[249] Rohn, J., et Deif, A. (1992). **On the range of eigenvalues of an interval matrix.** *Computing*, 47(3):373–377.

[250] Rohou, S., Jaulin, L., Mihaylova, L., Le Bars, F., et Veres, S. M. (2017). **Guaranteed computation of robot trajectories.** *Robotics and Autonomous Systems*, 93:76–84.

[251] Ruiz-Gazen, A. (1996). **A very simple robust estimator of a dispersion matrix.** *Computational Statistics & Data Analysis*, 21(2):149–162.

[252] Rump, S. (1999). **INTLAB - INTerval LABoratory.** In Csendes, T., editor, *Developments in Reliable Computing*, pages 77–104. Kluwer Academic Publishers, Dordrecht.

[253] Sam, D., Velanganni, C., et Evangelin, T. E. (2016). **A vehicle control system using a time synchronized hybrid vanet to reduce road accidents caused by human error.** *Vehicular Communications*, 6:17–28.

[254] Santoro, R., Failla, G., et Muscolino, G. (2020). **Interval static analysis of multi-cracked beams with uncertain size and position of cracks.** *Applied Mathematical Modelling*, 86:92–114.

[255] Scamarcio, A., Gruber, P., De Pinto, S., et Sorniotti, A. (2020). **Anti-jerk controllers for automotive applications: A review.** *Annual Reviews in Control*, 50:174–189.

[256] Schubert, R., Richter, E., et Wanielik, G. (2008). **Comparison and evaluation of advanced motion models for vehicle tracking.** In *2008 11th International Conference on Information Fusion*, pages 1–6, Cologne, Germany.

[257] Schwarz, C. (2014). **On computing time-to-collision for automation scenarios.** *Transportation Research Part F: Traffic Psychology and Behaviour*, 27:283–294.

[258] Schönbrodt, F. D., et Perugini, M. (2013). **At what sample size do correlations stabilize?** *Journal of Research in Personality*, 47(5):609–612.

[259] Schörner, P., Töttel, L., Doll, J., et Zöllner, J. M. (2019). **Predictive trajectory planning in situations with hidden road users using partially observable markov decision processes.** In *2019 IEEE Intelligent Vehicles Symposium (IV)*, pages 2299–2306, Paris, France.

[260] Sedighi, S., Nguyen, D., et Kuhnert, K. (2019). **Implementation of a parking state machine on vision-based auto parking systems for perpendicular parking scenarios**. In *2019 6th International Conference on Control, Decision and Information Technologies (CoDIT)*, pages 1711–1716, Paris, France.

[261] Shah, M. B. N., Husain, A. R., Aysan, H., Punnekatt, S., Dobrin, R., et Bender, F. A. (2016). **Error handling algorithm and probabilistic analysis under fault for can-based steer-by-wire system**. *IEEE Transactions on Industrial Informatics*, 12(3):1017–1034.

[262] Shalev-Shwartz, S., Shammah, S., et Shashua, A. (2017). **On a formal model of safe and scalable self-driving cars**. *CoRR*, abs/1708.06374.

[263] Shen, K., et Scott, J. K. (2017). **Rapid and accurate reachability analysis for nonlinear dynamic systems by exploiting model redundancy**. *Computers & Chemical Engineering*, 106:596–608.

[264] Shen, K., et Scott, J. K. (2018). **Tight reachability bounds for nonlinear systems using nonlinear and uncertain solution invariants**. In *2018 Annual American Control Conference (ACC)*, pages 6236–6241, Milwaukee, WI, USA.

[265] Shi, Z., et Zhang, F. (2017). **Model predictive control under timing constraints induced by controller area networks**. *Real-Time Systems*, 53(2):196–227.

[266] Shuai, Z., Zhang, H., Wang, J., Li, J., et Ouyang, M. (2014). **Combined afs and dyc control of four-wheel-independent-drive electric vehicles over can network with time-varying delays**. *IEEE Transactions on Vehicular Technology*, 63(2):591–602.

[267] Si, W., Wei, T., et Liu, C. (2019). **Agen: Adaptable generative prediction networks for autonomous driving**. In *2019 IEEE Intelligent Vehicles Symposium (IV)*, pages 281–286, Paris, France.

[268] Siciliano, B., et Khatib, O. (2016). **Springer handbook of robotics**. Springer.

[269] Sinyavskiy, O. Y., Passot, J., et Ibarz Gabardos, B. (2019). **Parallel algorithm for precise navigation using black-box forward model and motion primitives**. *IEEE Robotics and Automation Letters*, 4(3):2423–2430.

[270] Skrčkij, V., Šabanovič, E., et Žuraulis, V. (2020). **Autonomous road vehicles: recent issues and expectations**. *IET Intelligent Transport Systems*, 14(6):471–479.

[271] Slutsky, M., et Dobkin, D. (2019). **Fast implementation of volumetric occupancy grids**. In *2019 IEEE Intelligent Vehicles Symposium (IV)*, pages 750–755, Paris, France.

[272] Song, Y., Zhong, M., Xue, T., Ding, S. X., et Li, W. (2020). **Parity space-based fault isolation using minimum error minimax probability machine**. *Control Engineering Practice*, 95:1–13.

[273] Sontges, S., Koschi, M., et Althoff, M. (2018). **Worst-case analysis of the time-to-react using reachable sets**. In *2018 IEEE Intelligent Vehicles Symposium (IV)*, pages 1891–1897, Paris, France.

[274] Speck, D., Dornhege, C., et Burgard, W. (2017). **Shakey 2016—how much does it take to redo shakey the robot?** *IEEE Robotics and Automation Letters*, 2(2):1203–1209.

[275] Sprunk, C., Lau, B., Pfaff, P., et Burgard, W. (2017). **An accurate and efficient navigation system for omnidirectional robots in industrial environments.** *Autonomous Robots*, 41(2):473–493.

[276] Storck, C. R., et Duarte-Figueiredo, F. (2020). **A survey of 5g technology evolution, standards, and infrastructure associated with vehicle-to-everything communications by internet of vehicles.** *IEEE Access*, 8:117593–117614.

[277] Sun, X., Cai, Y., Wang, S., Xu, X., et Chen, L. (2019). **Optimal control of intelligent vehicle longitudinal dynamics via hybrid model predictive control.** *Robotics and Autonomous Systems*, 112:190–200.

[278] Suwatthikul, J., McMurran, R., et Jones, R. (2011). **In-vehicle network level fault diagnostics using fuzzy inference systems.** *Applied Soft Computing*, 11(4):3709–3719.

[279] Szczerba, R. J., Galkowski, P., Glicktein, I. S., et Ternullo, N. (2000). **Robust algorithm for real-time route planning.** *IEEE Transactions on Aerospace and Electronic Systems*, 36(3):869–878.

[280] Tabernik, D., et Skočaj, D. (2020). **Deep learning for large-scale traffic-sign detection and recognition.** *IEEE Transactions on Intelligent Transportation Systems*, 21(4):1427–1440.

[281] Taheri, H., et Zhao, C. X. (2020). **Omnidirectional mobile robots, mechanisms and navigation approaches.** *Mechanism and Machine Theory*, 153:1–28.

[282] Talal, M., Ramli, K. N., Zaidan, A., Zaidan, B., et Jumaa, F. (2020). **Review on car-following sensor based and data-generation mapping for safety and traffic management and road map toward its.** *Vehicular Communications*, 25:1–30.

[283] Tan, N., Gu, X., et Ren, H. (2019). **Pose characterization and analysis of soft continuum robots with modeling uncertainties based on interval arithmetic.** *IEEE Transactions on Automation Science and Engineering*, 16(2):570–584.

[284] Tang, L., Xiao, Y., et Xie, J. (2020). **Fatigue cracking checking of cement stabilized macadam based on measurement uncertainty and interval analysis.** *Construction and Building Materials*, 250:1–15.

[285] Tang, W., et Daoutidis, P. (2019). **Distributed control and optimization of process system networks: A review and perspective.** *Chinese Journal of Chemical Engineering*, 27(7):1461–1473.

[286] Teoh, E. R. (2020). **What's in a name? drivers' perceptions of the use of five sae level 2 driving automation systems.** *Journal of Safety Research*, 72:145–151.

[287] Thabet, R. E. H., Combastel, C., Raïssi, T., et Zolghadri, A. (2015). **Set-membership fault detection under noisy environment with application to the detection of abnormal aircraft control surface positions.** *International Journal of Control*, 88(9):1878–1894.

[288] Tian, W., Ni, B., Jiang, C., et Wu, Z. (2020). **Transient response bounds analysis of heat transfer problems based on interval process model.** *International Journal of Heat and Mass Transfer*, 148:119027.

[289] Tindell, K., Burns, A., et Wellings, A. (1995). **Calculating controller area network (can) message response times.** *Control Engineering Practice*, 3(8):1163–1169.

[290] Trang, H. T. H., Dung, L. T., et Hwang, S. O. (2018). **Connectivity analysis of underground sensors in wireless underground sensor networks.** *Ad Hoc Networks*, 71:104–116.

[291] Tulsky, A., Gopaluni, R. B., et Khare, S. R. (2016). **Particle filtering without tears: A primer for beginners.** *Computers & Chemical Engineering*, 95:130–145.

[292] Valle, S., Li, W., et Qin, S. J. (1999). **Selection of the number of principal components: the variance of the reconstruction error criterion with a comparison to other methods.** *Industrial & Engineering Chemistry Research*, 38(11):4389–4401.

[293] Van Brummelen, J., O'Brien, M., Gruyer, D., et Najjaran, H. (2018). **Autonomous vehicle perception: The technology of today and tomorrow.** *Transportation Research Part C: Emerging Technologies*, 89:384–406.

[294] Vanhatalo, E., Kulahci, M., et Bergquist, B. (2017). **On the structure of dynamic principal component analysis used in statistical process monitoring.** *Chemometrics and Intelligent Laboratory Systems*, 167:1–11.

[295] Venkatasubramanian, V., Rengaswamy, R., et Kavuri, S. N. (2003). **A review of process fault detection and diagnosis: Part ii: Qualitative models and search strategies.** *Computers & Chemical Engineering*, 27(3):313–326.

[296] Veres, S. M., Molnar, L., Lincoln, N. K., et Morice, C. P. (2011). **Autonomous vehicle control systems — a review of decision making.** *Proceedings of the Institution of Mechanical Engineers, Part I: Journal of Systems and Control Engineering*, 225(2):155–195.

[297] Vilca, J., Adouane, L., et Mezouar, Y. (2015). **A novel safe and flexible control strategy based on target reaching for the navigation of urban vehicles.** *Robotics and Autonomous Systems*, 70:215–226.

[298] Vilca, J., Adouane, L., et Mezouar, Y. (2016). **Optimal multi-criteria waypoint selection for autonomous vehicle navigation in structured environment.** *Journal of Intelligent & Robotic Systems*, 82(2):301–324.

[299] Vilca, J., Adouane, L., et Mezouar, Y. (2019). **Stable and flexible multi-vehicle navigation based on dynamic inter-target distance matrix.** *IEEE Transactions on Intelligent Transportation Systems*, 20(4):1416–1431.

[300] Vilca, J.-M., Adouane, L., et Mezouar, Y. (2013). **Reactive navigation of mobile robot using elliptic trajectories and effective on-line obstacle detection.** *In Gyroscopy and Navigation Journal, Ed. Springer, Russia ISSN 2075 1087*, 4(1):14–25.

[301] Vilca Ventura, J. M. (2015). **Safe and flexible hybrid control architecture for the navigation in formation of a group of vehicles.** PhD thesis. Thèse de doctorat dirigée par Mezouar, Youcef Vision pour la Robotique Clermont-Ferrand 2 2015.

[302] Vogt, P., Lenz, E., Klug, A., Westerfeld, H., et Konigorski, U. (2019). **Robust two-degree-of-freedom wheel slip controller structure for anti-lock braking.** *IFAC-PapersOnLine*, 52(5):431–437. 9th IFAC Symposium on Advances in Automotive Control AAC 2019, Orléans, France.

[303] Vyas, P., Vachhani, L., et Sridharan, K. (2019). **Hardware-efficient interval analysis based collision detection and avoidance for mobile robots.** *Mechatronics*, 62:102258.

[304] Vyas, P., Vachhani, L., et Sridharan, K. (2020). **Interval analysis technique for versatile and parallel multi-agent collision detection and avoidance.** *Journal of Intelligent & Robotic Systems*, 98(3):705–720.

[305] Wang, C., et Matthies, H. G. (2020). **A comparative study of two interval-random models for hybrid uncertainty propagation analysis.** *Mechanical Systems and Signal Processing*, 136:106531.

[306] Wang, C., Wang, J., Shen, Y., et Zhang, X. (2019a). **Autonomous navigation of uavs in large-scale complex environments: A deep reinforcement learning approach.** *IEEE Transactions on Vehicular Technology*, 68(3):2124–2136.

[307] Wang, P., Chen, Y., Wang, C., Liu, F., Hu, J., et Van, N. N. (2019b). **Development and verification of cooperative adaptive cruise control via Ite-v.** *IET Intelligent Transport Systems*, 13(6):991–1000.

[308] Wang, S., Wang, W., Chen, B., et Tse, C. K. (2018). **Convergence analysis of nonlinear kalman filters with novel innovation-based method.** *Neurocomputing*, 289:188–194.

[309] Wang, Y., Mulvaney, D., Sillitoe, I., et Swere, E. (2008). **Robot navigation by waypoints.** *Journal of Intelligent and Robotic Systems*, 52(2):175–207.

[310] Ward, J. R., Agamennoni, G., Worrall, S., Bender, A., et Nebot, E. (2015). **Extending time to collision for probabilistic reasoning in general traffic scenarios.** *Transportation Research Part C: Emerging Technologies*, 51:66–82.

[311] Wei, G., Ling, Y., Guo, B., Xiao, B., et Vasilakos, A. V. (2011). **Prediction-based data aggregation in wireless sensor networks: Combining grey model and kalman filter.** *Computer Communications*, 34(6):793–802.

[312] Wirges, S., Reith-Braun, M., Lauer, M., et Stiller, C. (2019). **Capturing object detection uncertainty in multi-layer grid maps.** In *2019 IEEE Intelligent Vehicles Symposium (IV)*, pages 1520–1526.

[313] Wu, C., Peng, L., Huang, Z., Zhong, M., et Chu, D. (2014). **A method of vehicle motion prediction and collision risk assessment with a simulated vehicular cyber physical system.** *Transportation Research Part C: Emerging Technologies*, 47:179–191.

[314] Wu, J., Luo, Z., Zhang, N., et Zhang, Y. (2015). **A new interval uncertain optimization method for structures using chebyshev surrogate models.** *Computers & Structures*, 146:185–196.

[315] Wu, P., Guo, L., Lou, S., et Gao, J. (2019). **Local and global randomized principal component analysis for nonlinear process monitoring.** *IEEE Access*, 7:25547–25562.

[316] Wu, Y., Wei, H., Chen, X., Xu, J., et Rahul, S. (2020). **Adaptive authority allocation of human-automation shared control for autonomous vehicle.** *International Journal of Automotive Technology*, 21(3):541–553.

[317] Xia, B., Shang, Y., Nguyen, T., et Mi, C. (2017). **A correlation based fault detection method for short circuits in battery packs.** *Journal of Power Sources*, 337:1–10.

[318] Xiang, G., Starks, S. A., Kreinovich, V., et Longpré, L. (2006). **New algorithms for statistical analysis of interval data.** In Dongarra, J., Madsen, K., et Waśniewski, J., editors, *Applied Parallel Computing. State of the Art in Scientific Computing*, pages 189–196, Berlin, Heidelberg. Springer Berlin Heidelberg.

[319] Xie, G., Zeng, G., Liu, L., Li, R., et Li, K. (2016). **High performance real-time scheduling of multiple mixed-criticality functions in heterogeneous distributed embedded systems.** *Journal of Systems Architecture*, 70:3–14.

[320] Xiong, J., Cheong, J. W., Xiong, Z., Dempster, A. G., Tian, S., et Wang, R. (2020). **Hybrid cooperative positioning for vehicular networks.** *IEEE Transactions on Vehicular Technology*, 69(1):714–727.

[321] Xu, X., Yan, X., Sheng, C., Yuan, C., Xu, D., et Yang, J. (2020). **A belief rule-based expert system for fault diagnosis of marine diesel engines.** *IEEE Transactions on Systems, Man, and Cybernetics: Systems*, 50(2):656–672.

[322] Xue, B., Fränzle, M., et Zhan, N. (2020). **Inner-approximating reachable sets for polynomial systems with time-varying uncertainties.** *IEEE Transactions on Automatic Control*, 65(4):1468–1483.

[323] Yang, C., Jiao, X., Li, L., Zhang, Y., et Chen, Z. (2018). **A robust h control-based hierarchical mode transition control system for plug-in hybrid electric vehicle.** *Mechanical Systems and Signal Processing*, 99:326–344.

[324] Yang, C., Liang, K., et Zhang, X. (2020). **Strategy for sensor number determination and placement optimization with incomplete information based on interval possibility model and clustering avoidance distribution index.** *Computer Methods in Applied Mechanics and Engineering*, 366:113042.

[325] Yang, J., Xie, G., Yang, Y., Zhang, Y., et Liu, W. (2019). **Deep model integrated with data correlation analysis for multiple intermittent faults diagnosis.** *ISA Transactions*, 95:306–319.

[326] Yang, L., Couillet, R., et McKay, M. R. (2015). **A robust statistics approach to minimum variance portfolio optimization.** *IEEE Transactions on Signal Processing*, 63(24):6684–6697.

[327] Yang, Q., Li, X., Cai, H., Hsu, Y.-M., Lee, J., Yang, C. H., Li, Z. L., et Lin, M. Y. (2021). **Fault prognosis of industrial robots in dynamic working regimes: Find degradation in variations.** *Measurement*, 173:108545.

[328] Yang, W., Wan, B., et Qu, X. (2020). **A forward collision warning system using driving intention recognition of the front vehicle and v2v communication.** *IEEE Access*, 8:11268–11278.

[329] Yang, X., et Scott, J. K. (2018). **Efficient reachability bounds for discrete-time nonlinear systems by extending the continuous-time theory of differential inequalities.** In *2018 Annual American Control Conference (ACC)*, pages 6242–6247.

[330] Yarinezhad, R., et Hashemi, S. N. (2019). **A routing algorithm for wireless sensor networks based on clustering and an fpt-approximation algorithm.** *Journal of Systems and Software*, 155:145–161.

[331] Ye, F.-F., Yang, L.-H., Wang, Y.-M., et Chen, L. (2020). **An environmental pollution management method based on extended belief rule base and data envelopment analysis under interval uncertainty.** *Computers & Industrial Engineering*, 144:106454.

[332] Yi, X. J., Shi, J., Dhillon, B. S., Mu, H. N., et Hou, P. (2019). **A new availability assessment method for complex control systems with multi-characteristics.** *IEEE Access*, 7:18392–18408.

[333] Yoon, J.-S., Min, B.-C., Shin, S.-O., Jo, W.-S., et Kim, D.-H. (2014). **GA-Based Optimal Waypoint Design for Improved Path Following of Mobile Robot**, pages 127–136. Springer International Publishing, Cham.

[334] Younus, A., Asif, M., Alzabut, J., Ghaffar, A., et Nisar, K. S. (2020). **A new approach to interval-valued inequalities.** *Advances in Difference Equations*, 2020(1):319.

[335] Yu, Z., Zhu, L., et Lu, G. (2020). **An improved phase correlation method for stop detection of autonomous driving.** *IEEE Access*, 8:77972–77986.

[336] Zacchia Lun, Y., D’Innocenzo, A., Smarra, F., Malavolta, I., et Di Benedetto, M. D. (2019). **State of the art of cyber-physical systems security: An automatic control perspective.** *Journal of Systems and Software*, 149:174–216.

[337] Zeng, H., Natale, M. D., Giusto, P., et Sangiovanni-Vincentelli, A. (2010). **Using statistical methods to compute the probability distribution of message response time in controller area network.** *IEEE Transactions on Industrial Informatics*, 6(4):678–691.

[338] Zernetsch, S., Reichert, H., Kress, V., Doll, K., et Sick, B. (2019). **Trajectory forecasts with uncertainties of vulnerable road users by means of neural networks.** In *2019 IEEE Intelligent Vehicles Symposium (IV)*, pages 810–815, Paris, France.

[339] Zhang, M., et Deng, J. (2013). **Number of zeros of interval polynomials.** *Journal of Computational and Applied Mathematics*, 237(1):102–110.

[340] Zhang, W., Zheng, Y., Gao, Q., et Mi, Z. (2019). **Part-aware region proposal for vehicle detection in high occlusion environment.** *IEEE Access*, 7:100383–100393.

[341] Zhang, X., Sun, J., Qi, X., et Sun, J. (2019). **Simultaneous modeling of car-following and lane-changing behaviors using deep learning.** *Transportation Research Part C: Emerging Technologies*, 104:287–304.

[342] Zhao, Y., Deng, Z., et Han, Y. (2020). **Dynamic response analysis of structure with hybrid random and interval uncertainties.** *Chaos, Solitons & Fractals*, 131:109495.

[343] Zhong, K., Han, M., et Han, B. (2020a). **Data-driven based fault prognosis for industrial systems: a concise overview.** *IEEE/CAA Journal of Automatica Sinica*, 7(2):330–345.

[344] Zhong, K., Han, M., Qiu, T., Han, B., et Chen, Y. W. (2020b). **Distributed dynamic process monitoring based on minimal redundancy maximal relevance variable selection and bayesian inference.** *IEEE Transactions on Control Systems Technology*, 28(5):2037–2044.

[345] Zhou, H., Gómez-Hernández, J. J., Franssen, H.-J. H., et Li, L. (2011). **An approach to handling non-gaussianity of parameters and state variables in ensemble kalman filtering.** *Advances in Water Resources*, 34(7):844–864.

[346] Zhu, J., et Kia, S. S. (2019). **Cooperative localization under limited connectivity.** *IEEE Transactions on Robotics*, 35(6):1523–1530.

[347] Zhu, X., Zhang, H., Wang, J., et Fang, Z. (2015). **Robust lateral motion control of electric ground vehicles with random network-induced delays.** *IEEE Transactions on Vehicular Technology*, 64(11):4985–4995.

[348] Zou, D., Tan, P., et Yu, W. (2019). **Collaborative visual slam for multiple agents:a brief survey.** *Virtual Reality & Intelligent Hardware*, 1(5):461–482.

[349] Åsljung, D., Westlund, M., et Fredriksson, J. (2019). **A probabilistic framework for collision probability estimation and an analysis of the discretization precision.** In *2019 IEEE Intelligent Vehicles Symposium (IV)*, pages 52–57, Paris, France.

Abstract:

Huge advancements have been witnessed recently in the field of Intelligent Transportation Systems (ITSs). In particular, a special focus has been dedicated to ensure the safe and reliable operation of Intelligent Vehicles (IVs). This issue is very challenging due to the considerable environmental uncertainties impacting IVs. Besides, the sophisticated architectures of modern IVs have brought new complications and uncertainty sources, such as failures, communication latencies, etc. This Ph.D thesis aims to provide guaranteed navigation strategies i.e., approaches that consider all potential uncertainty states. To meet this goal, the interval analysis is employed. The principle part of this Ph.D contribution concerns the IV architectures and control aspects. First, a reliable reachability scheme is proposed to present strong safety guarantees for a flexible Navigation Strategy based on Sequential Waypoint Reaching (NSbSWR). The risk management proposed for the NSbSWR reveals the vehicle reachable space, while explicitly considering different uncertainties in modelling and/or perception, etc. The reachability analysis is proceeded via an interval Taylor series expansion method. It uses also the system historical features to improve accuracy of the navigation system reachable space. Once a collision risk is detected, the risk management acts on the control parameters to master the critical situation. Then, this thesis tackles the establishment of risk management solutions for a car-following scenario, which is performed by an Adaptive Cruise Control (ACC) system. Instead of an uncertain probabilistic prediction of threats, the suggested solution has recourse to an interval-based conjoint modeling/data-driven characterization of uncertainties. Hence, a novel extension of the Time-To-Collision (TTC) indicator is introduced to carry out the in-road risk assessment with a comprehensive consideration of uncertainties and material constraints. This extension of TTC is improved later by combining the interval-based computation with a stochastic approach for optimality purposes. The second part of this thesis contributions addresses the tight link between the high-level control aspect and hardware one of IVs. To enhance the risk management robustness to the IV material constraints, relevant techniques to quantify intervals of the inter/intra-vehicular communication latencies are presented. These techniques may avoid any inappropriate and slow reactions of the IV risk management to the in-road threats. Even more, an interval-based extension is proposed for the Principle Component Analysis (PCA) diagnosis method to overcome impacts of failures on IVs. The interval-based PCA is integrated into an ACC architecture to provide a fault-aware risk management level. The sensitivity to faults is increased and the system is monitored in respect to the uncertainty worst cases. The mutuality between the interval-based diagnosis and uncertainty handling approaches enabled to simultaneously detect failures and master all uncertainties. Finally, all the interval-based solutions suggested in this thesis have been validated through extensive simulation work and experiments.

Keywords: Intelligent transportation system, Intelligent vehicle, Risk assessment/management, Interval analysis, Intelligent vehicles, Reachability analysis, System statistical features, Material constraints, Interval-based diagnosis.

Résumé :

Le domaine de développement des Systèmes de Transport Intelligents (STIs) a été ces dernières décennies une source de multiples évolutions marquantes. En revanche, il est primordial d'améliorer davantage la fiabilité et la sûreté des systèmes autonomes de navigation ainsi que la sécurité routière. Ceci représente un grand défi vu les considérables incertitudes liées à l'environnement d'évolution des Véhicules Intelligents (VIs). Ces problématiques de fiabilité sont accentuées en raison de la complexité des architectures modernes des VIs. Ainsi, les VIs sont à présent de plus en plus soumis aux défauts, aux latences de communication, etc. Cette thèse de doctorat cherche à présenter des stratégies garanties de navigation (approches qui sont censées tenir compte de toutes les sources d'incertitudes potentielles). Pour ce faire, l'analyse par intervalle est adoptée pour assurer un fonctionnement fiable des VIs. Cette thèse présente deux catégories de contributions. La principale partie des travaux est liée aux architectures de contrôle des VIs. En premier lieu, une méthode d'estimation de l'espace d'atteignabilité des VIs est proposée pour vérifier la sûreté d'une méthode de navigation nommée NSbSWR (pour Navigation Strategy based on Sequential Waypoint Reaching). Le management des risques proposé pour la NSbSWR prédit l'espace atteignable de véhicule en considérant notamment des incertitudes de modélisation ainsi que de perception. L'étude d'atteignabilité est abordée en utilisant les développements de Taylor par intervalles. L'historique de la propagation des incertitudes au sein du système de navigation est exploité afin d'optimiser la précision de l'atteignabilité. Si un danger de collision est détecté en observant l'Espace Atteignable (EA), la méthode proposée agit sur les paramètres de la loi de commande pour éviter les situations critiques. Les travaux de thèse ont portés par la suite sur le développement des solutions du management des risques pour un scenario de suivi des véhicules assuré par un Système de Régulation Adaptative de la Vitesse (SRAV). La solution adoptée rejoint l'arithmétique par intervalles et l'analyse des données. Dans cette optique, une nouvelle extension de l'indicateur de risque TTC (pour Time-To-Collision) est introduite. L'évaluation des risques se manifeste ainsi en considérant plusieurs incertitudes et contraintes matérielles. L'extension ensembliste de la TTC est améliorée ultérieurement en combinant le calcul par intervalles avec une approche stochastique à des fins d'optimisation. Le deuxième volet des contributions de cette thèse vise à renforcer le lien entre l'aspect de commande et l'aspect matériel des VIs. Pour faire face aux contraintes matérielles des STIs, des approches de quantification des intervalles des latences de communication inter/intra-véhiculaire sont proposées. En outre, une extension par intervalles de la méthode de diagnostic par Analyse en Composantes Principales (ACP) est développée pour détecter les défauts affectant un SRAV. La sensibilité aux défauts est améliorée en prenant compte des pires cas d'incertitudes. La mutualité entre les approches de diagnostic et du management des risques permet de détecter simultanément les défauts et d'éliminer les risques liés aux incertitudes. Au final, un travail extensif de simulations et d'expérimentation est abordé pour valider les travaux de cette thèse.

Mots-clés : Systèmes intelligents de transport, Véhicule intelligent, Evaluation/management des risques, Analyse par intervalles, Atteignabilité, Caractéristiques statistiques du système, Contraintes matérielles, Diagnostic par intervalles.